PHARMACOLOGICAL CHARACTERIZATION OF IMPROVED LIGANDS AND PROSTANOID RECEPTORS IN ISOLATED TISSUE PREPARATIONS

A thesis presented by

WAN AMIR NIZAM WAN AHMAD

in fulfilment of the degree of

Doctor of Philosophy

Strathclyde Institute of Pharmacy and Biomedical Sciences

University of Strathclyde

The John Arbuthnott Building

27 Taylor Street

Glasgow G4 0NR

2010

"This thesis is the result of the author's original research. It has been composed by the author and has not been previously submitted for examination which has led to the award of a degree. The copyright of this thesis belongs to the author under the terms of the United Kingdom Copyright Acts as qualified by University of Strathclyde Regulation 3.50. Due acknowledgement must always be made of the use of any material contained in, or derived from, this thesis."

Signed:  *Date:25th February 2010*

ACKNOWLEDGEMENTS

First, I would like to express my sincere gratitude and appreciation to my supervisors, Professor Robert Jones and Professor Roger Wadsworth. They provided the initial inspiration for the project, and have made themselves available to offer support and guidance throughout its completion, and for this, I am extremely grateful.

My sincere gratitude is also extended to all the technical and postdoctoral staff with whom I have had the pleasure of working and socialising with. My work was made easier and more understandable with their help.

I also like to thank all student members of the Cardiovascular Group, past and present. Not only have they been very helpful in providing advice, it has been a genuinely stimulating experience to work alongside such a talented, diverse range of people. The friendship and support of my friends has been constant throughout, and has been much appreciated.

I would also like to thank the Ministry of Higher Education of Malaysia and Universiti Sains Malaysia for the financial support.

I would also like to acknowledge the important role played by my brothers, sisters and Mum and my late Dad.

Finally yet importantly, I would like to thank my beloved wife, Dr Liza Noordin; my lovely kids; Fitri, Fatihah, Fadzli, Farhanah and Fauzan for their encouragement, love, support and patience, without which success would not have been sweet.

RESEARCH OUTPUTS

Wan Ahmad WAN, Jones RL, Wadsworth RM, Woodward DR. Contractile action of Prostaglandin E_2 on rat mesenteric artery. *Proceedings for Scottish Cardiovascular Forum, 10th Annual Meeting, Belfast* (February 2007)

Wan Ahmad WAN, Jones RL, Wadsworth RM, Woodward DR. Characterization of receptors mediating the contractile effects of prostanoids in rat mesenteric artery. *Proceedings for Young Life Scientist Symposium, Glasgow* (July 2007)

Jones RL, Wan Ahmad WAN, Wadsworth RM, Woodward DR. Discrimination of EP_1 and EP_3 prostanoid receptor systems in smooth muscle using ONO-D1-004 and ONO-AE-248. *Proceedings for Young Life Scientist Conference, Glasgow* (July 2007)

Wan Ahmad WAN, Jones RL, Wadsworth RM. Characterization of receptors mediating the contractile effects of prostanoids in rat urinary bladder. *Proceedings for official launch event of Integrative Mammalian Biology Capacity Building Initiative, Glasgow* (March 2008)

Wan Ahmad WAN, Jones RL, Wadsworth RM, Furman BL. Synergism between phenylephrine and prostaglandins in femoral arteries from rats with streptozotocin-induced diabetes. *Proceedings for Scottish Cardiovascular Forum, 12th Annual Meeting, Inverness* (January 2009)

Wan Wan Ahmad, Robert Jones, Roger Wadsworth, Brian Furman. Role of prostanoid EP_3 receptor synergism in femoral arteries from rats with streptozotocin-induced diabetes. *Proceedings for 7th James Black Conference, London* (September 2009)

TABLE OF CONTENTS

ABBREVIATIONS

5-HT	- 5-hydroxytryptamine
AA	- Arachidonic acid
AMI	- Acute myocardial infarction
ANOVA	- Analysis of variance
Ba^{2+}	- Barium
BOO	- Bladder outlet obstruction
Ca^{2+}	- Calcium
$[Ca^{2+}]_i$	- Intracellular calcium
cAMP	- Cyclic adenosine monophosphate
CI	- Confidence interval
ClogP	- Predicted *n*-octanol / water partition coefficient
COX	- Cyclo-oxygenase
CRC	- Concentration response curve
CRTh2	- Chemoattractant receptor-homologous molecule of Type 2 helper T cells
DAG	- Diacylglycerol
df	- Degrees of freedom
DM	- Diabetes mellitus
DP receptor	- Prostaglandin D receptor
DR	- Dose ratio
EC	- Endothelial cells
EC_{50}	- The molar concentration of an agonist that produces 50% of the maximal possible effect of that agonist
EDHF	- Endothelium derived hyperpolarising factor
EDRF	- Endothelium derived relaxant factor
EH	- Essential hypertension
E_{max}	- The maximal response by the contractile agent / agonist attained
EMR	- Equi-effective molar ratio
EP receptor	- Prostaglandin E receptor
FLIPR	- Fluorometric imaging plate reader

FA - Free acid

FP receptor - Prostaglandin $F_{2\alpha}$ receptor

GK - Goto-Kakizaki

GPT - Guinea-pig trachea

HPO - 15-hydroperoxidase

HPT - Hypertension

i.p. - Intraperitoneal

I/R - Ischaemic-reperfusion

IC_{50} - The molar concentration of an antagonist that reduces the response to an agonist by 50%

IOP - Intraocular pressure

IP receptor - Prostacyclin receptor

IP3 - Inositol triphosphate

IsoPs - Isoprostanes

K_b - Equilibrium dissociation constant

KCl - Potassium chloride

K_i - Antagonist dissociation constant

KO - Knockout

NSAID - Nonsteroidal anti-inflammatory drug

pA_2 - The negative logarithm to base 10 of the molar concentration of an antagonist that makes it necessary to double the concentration of the agonist to elicit the original submaximal response

PAH - Pulmonary artery hypertension

pEC_{50} - The negative logarithm to base 10 of the EC_{50} of an agonist

PG - Prostaglandin

PGD_2 - Prostaglandin D_2

PGE_2 - Prostaglandin E_2

$PGF_{2\alpha}$ - Prostaglandin $F_{2\alpha}$

PGHS - Prostaglandin H synthase

PGI_2 - Prostacyclin

PGIS - Prostacyclin synthase

Phe	- Phenylephrine
PIP	- Phosphatidyl inositol phosphate
PKA	- Protein kinase A
PKC	- Protein kinase C
PLA_2	- Phospholipase A_2
PRP	- Platelet-rich plasma
r^2	- Regression correlation coefficient
RFA	- Rat femoral artery
RMA	- Rat mesenteric artery
RUB	- Rat urinary bladder
SMC	- Smooth muscle cells
SS	- Sum-of-squares
STZ	- Streptozotocin
Th2	- Type 2 helper T cells
TP receptor	- Thromboxane receptor
TXA_2	- Thromboxane A_2
TXB_2	- Thromboxane B_2
VSM	- Vascular smooth muscles
WT	- Wild-type
ZF	- Zuckers fatty

ABSTRACT

The demise of the COX-2 inhibitors in treating rheumatoid arthritis has renewed interest in the development of prostanoid receptor antagonists. While data from radio-ligand binding assays remain useful, functional studies on isolated smooth muscle preparations are also valuable. The present study focussed on the characterization of EP_1 and EP_3 receptors and their novel antagonists in the rat mesenteric artery and the rat urinary bladder. Inhibition-curve protocols (based on the Cheng-Prusoff equation) were used in the first instance and data were analysed by the two-site competition equation in combination with the modified F test to assess the presence of two contractile systems.

In agreement with literature, the prostaglandin receptors in guinea-pig trachea mediating contractile responses appeared to be EP_1 and TP, whereas the relaxant response was attributed to the EP_2 receptor. Contractile responses to the TP agonist, U-46619 contractile were prevented by a selective TP antagonist. Equally, the selective EP_1 antagonist, SC-51322 completely antagonised the contractile response to 17-phenyl PGE_2. The EP_2 agonist AH-13205 showed no evidence of partial agonism, and the apparent two site activities are more likely to be explained by the presence of two isomers having different activities.

In the rat mesenteric artery, only contractile prostanoid receptors were demonstrated with equal contributions from EP_1 and EP_3 receptors. The two-site competition model produced a better fit than the one-site model to the inhibition curve of SC-51322 against 17-phenyl PGE_2.

The contractile responses in the rat urinary bladder appeared to be mediated, in part, by EP_1 receptors but other prostanoid receptor contribute and these remain to be elucidated. The possibility of non-competitive behaviour or a hemi-equilibrium state of antagonist-agonist interaction needs to be considered.

The contractile responses to phenylephrine and KCl in the endothelium-denuded rat femoral artery were not modified by streptozotocin-induced diabetes. The phenylephrine response was reduced by the EP_3 antagonist, L-798106 but not by the TP antagonist. COX-inhibitors did not affect the contractile response. These results suggest the involvement of an endogenous facilitator of contractile responses that acts on EP_3 receptors but which is not generated via the COX pathway.

In conclusion, conventional organ bath methodology coupled with the inhibition-curve protocol is useful to assess pharmacological antagonism and to characterize prostanoid receptors in isolated tissue preparations.

CHAPTER ONE

GENERAL INTRODUCTION

Prostanoids comprise prostaglandins (PGs) and thromboxanes (TXs). The first prostanoid receptor antagonist was described in the late 1960s. SC-19220 (Sanner, 1969) inhibited the contractile actions of prostaglandin E_2 (PGE_2) on intestinal smooth muscle preparations by blocking what we now known to be the EP_1 receptor (see later). Since then, the discoveries of other natural prostanoids, prostaglandin D_2 (PGD_2), thromboxane A_2 (TXA_2), prostacyclin (PGI_2) and prostaglandin $F_{2\alpha}$ ($PGF_{2\alpha}$) and their specific receptors have been followed by corresponding developments of receptor antagonists. However, the pace of development quickened in the mid-1990's owing to the isolation and molecular characterization of these prostanoid receptors. These receptors are termed P receptors, with a preceding letter indicating the natural prostanoid to which each receptor is most sensitive - i.e. DP, EP, FP, IP and TP, respectively (Kennedy *et al.*, 1982). Subsequently, single recombinant prostanoid receptors were introduced into carrier cells to produce efficient screening assays, paralleling developments for other receptors systems (e.g. $5\text{-}HT_{1A}$, Albert *et al.*, 1990). Accompanying this trend was the use of combinatorial chemistry to produce many closely related analogues with much greater efficiency than classical synthetic methods. The outcome has been the appearance in the literature of novel antagonists for DP_1 and DP_2 receptors and EP receptors. EP receptors are subdivided into four groups, EP_1, EP_2, EP_3 and EP_4, originally based on their relative sensitivities to a range of selective agonists and antagonists (see later).

While there is a temptation to proceed to *in vivo* testing of specific agents based on data from radio-ligand binding assays, information from functional studies on isolated tissues can be of considerable value. These first-line preparations ought to be robust and reproducible in their responses to prostanoid standard agonists. Preparations containing a single prostanoid receptor are rare; one such preparation is the rabbit ear artery, which only has an EP_2 receptor (Lydford and McKechnie, 1994). Multiple prostanoid receptors can be a disadvantage in characterizing an antagonist, particularly if opposing agonist actions are possible. Thus activation of EP_1 receptors in HEK-293 cells by 17-phenyl PGE_2 functionally antagonized the TP receptor-induced $[Ca^{2+}]_i$ mobilization (Walsh and Kinsella, 2000). On the other hand, multiple receptors do allow one to test the specificity of the antagonist. In addition, rapid responses to the standard agonist are an

advantage in constructing consecutive concentration-response curves. Many tissues in conventional organ baths (e.g. rabbit and guinea-pig aortic rings) exhibit slow responses to potent agonists and it was hoped that the use of thinner tissues in a Mulvany (wire) myograph would rectify this problem (Mulvany and Halpern, 1977).

In the following sections, I shall describe the biosynthesis of the natural prostanoids, the nature of the prostanoid receptors on which they act, and the properties of the currently available agonists and antagonists for these receptors. The receptor / second messenger nomenclature used in the current study conforms to internationally accepted practice (Neubig *et al.*, 2003; Alexander *et al.*, 2008).

1.1 Prostaglandin biosynthesis

Prostanoids are a group of lipid hormone mediators that are derived from C-20 fatty acids, particularly arachidonic acid (AA). They consist of the prostaglandins and thromboxane. AA has two quite different functions in the body. As a component of cell membrane phospholipids, its *cis*-double bonds disorder the hydrophobic core of the membrane. This will influence the fluidity, permeability and the behaviour of embedded proteins. However, of greater interest is its second function, where in response to various physiological and pathological stimuli, this fatty acid is liberated from the internal membranes by the activity of phospholipase A_2 (PLA_2). AA that is liberated will be converted to prostaglandin G_2 and then to prostaglandin H_2 (PGH_2) by the sequential actions of cyclo-oxygenase (COX) and 15-hydroperoxidase (HPO).

PGH_2 serves as a substrate for different prostanoid synthase enzymes, which are responsible for the production of the five principle bioactive prostanoids generated *in vivo*, PGE_2, $PGF_{2\alpha}$, PGD_2, PGI_2, and TX_A. The prostanoids produced by a given cell largely depend on the expression

profile of the individual prostanoid synthase enzyme. This is summarized in Figure 1.1 (redrawn from Hata and Breyer, 2004).

There are currently three known COX isoforms: COX-1, COX-2 and COX-3. The expression of the three COX isoenzymes is differently regulated. COX-1 gene exhibits the features of a housekeeping gene, constitutively expressed in most tissues. COX-2 expression is more tightly regulated and under most normal physiological conditions, it is not expressed. However, under a variety of pathophysiological conditions its expression can be rapidly induced (Scholz, 2003). Hence, it is widely believed that prostanoids (PGs) derived from COX-1 play a role in normal body function, whereas those from COX-2 are associated with a pathological process in the body. COX-3 was discovered later on and has drawn a considerable attention (Hirai *et al.*, 2001). It is a splice variant of the COX-1 gene isolated from canine brain that retains intron 1. Unlike COX-1 and COX-2, this isoenzyme is highly responsive to acetaminophen. However, COX-3 is not expressed in humans and its relevance to human pathophysiological processes remains questionable.

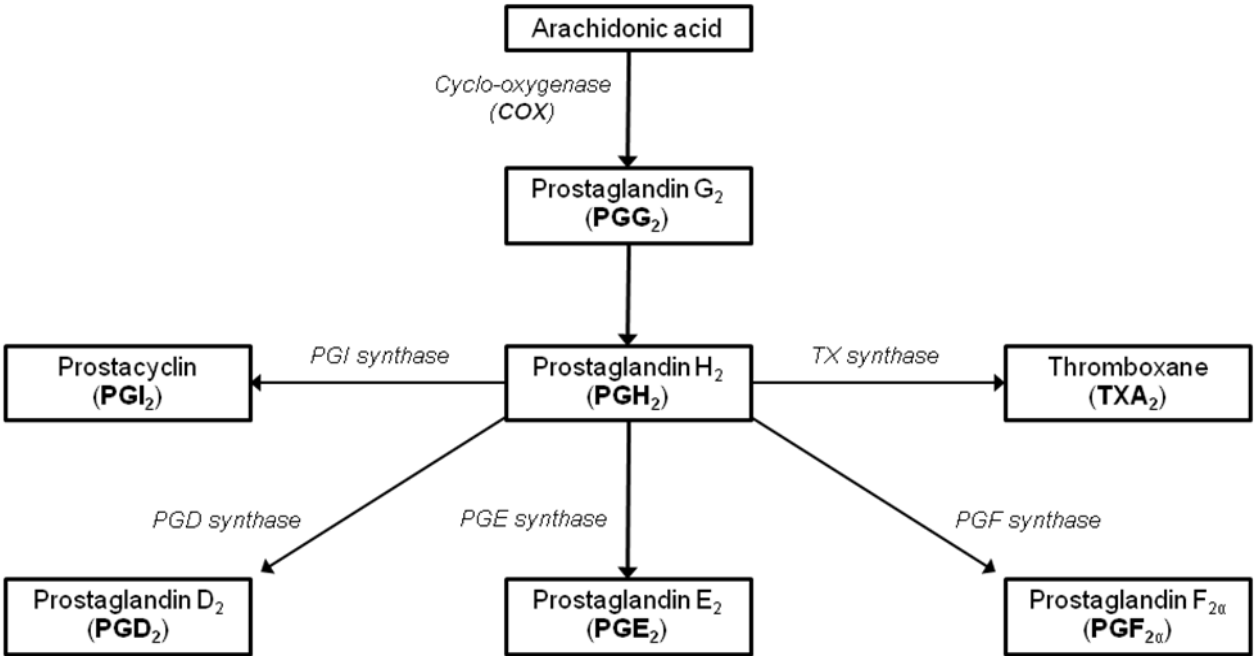

Figure 1.1 Biosynthesis of prostanoids. Redrawn from Hata and Breyer, 2004.

1.2 Molecular biology

An individual gene encodes each prostanoid receptor. The receptors responsive to COX products are evolutionally distinct from the leukotriene receptors of the 5-lipoxygenase pathway (Toh *et al.*, 1995). The first cluster includes EP_2, EP_4, DP and IP receptors, which induce smooth muscle relaxation via activation of adenylate cyclase. EP_1, FP and TP receptors, which cause smooth muscle contraction, form another cluster. On its own, the EP_3 receptor, which usually stimulates smooth muscle contraction, defines the third cluster.

1.2.1 Isoforms

A striking feature of the EP_3 receptor that sets it apart from the other EP receptors is the large number of splice variants generated by alternate splicing of the C-terminal tail. In humans, at least eight EP_3 splice variants have been identified, and multiple splice variants exist for other species. In humans, the TP receptor exists as two alternatively spliced variants, TP_α (placental / platelet) and TP_β (endothelial) (Breyer *et al.*, 2001). Despite the existence of these variants, the mRNAs for both splice variants have been detected in most tissues that express TP receptor including platelets, placenta, vascular smooth muscle, brain, small intestine, and thymus (Raychowdhury *et al.*, 1994; Miggin *et al.*, 2002). Two differentially spliced variants of the FP receptor have been reported (FP_A and FP_B), which differ from each other in C-terminal tail length. Both are coupled to G_q protein but have a different sensitivity to desensitization (Hata and Breyer, 2004). The C-terminal of tail of the FP_A can be phosphorylated by PKC, leading to agonist-induced desensitization and internalization. Generally, prostanoid receptor isoforms exhibit similar ligand responsiveness (Wright *et al.*, 2001).

1.2.2 Signal transduction

The signal transduction pathways of prostanoid receptors have been studied by examining agonist-induced changes in the levels of second messengers (cAMP, free Ca^{2+}, and inositol phosphates), and by identifying G protein coupling by various methods. The first cluster of receptors, which is normally associated with smooth muscle relaxation (EP_2, EP_4, DP and IP), couple via G_s to mediate increase in intracellular cAMP levels (Breyer *et al.*, 2001). The increases in intracellular cAMP were demonstrated after stimulation of the recombinant human EP_2 (Regan *et al.*, 1994), EP_4 (Bastien *et al.*, 1994), DP (Boie *et al.*, 1995) and in IP (Boie *et al.*, 1994) receptors. Similarly, PGD_2 and PGE_1 / PGI_2-responsive receptors have been shown to stimulate the production of cAMP in platelets (Whittle *et al.*, 1978). EP_1, FP and TP receptors couple via G_q of phospholipase C, with subsequent liberation of inositol phosphate (Breyer *et al.*, 2001). The end-result is to elevate Ca^{2+}, leading to muscular contraction. This pathway has been demonstrated in the platelet; the stimulation of TP receptor involved the G_q activation as the primary effector pathway (Arita *et al.*, 1989). The EP_3 receptor, which constitutes the final cluster, has isoforms that inhibit adenylate cyclase through G_i protein; individual isoforms may also couple to G_q and even G_s (Breyer *et al.*, 2001). Figure 1.2 summarizes the signaling modulator involved in each receptor.

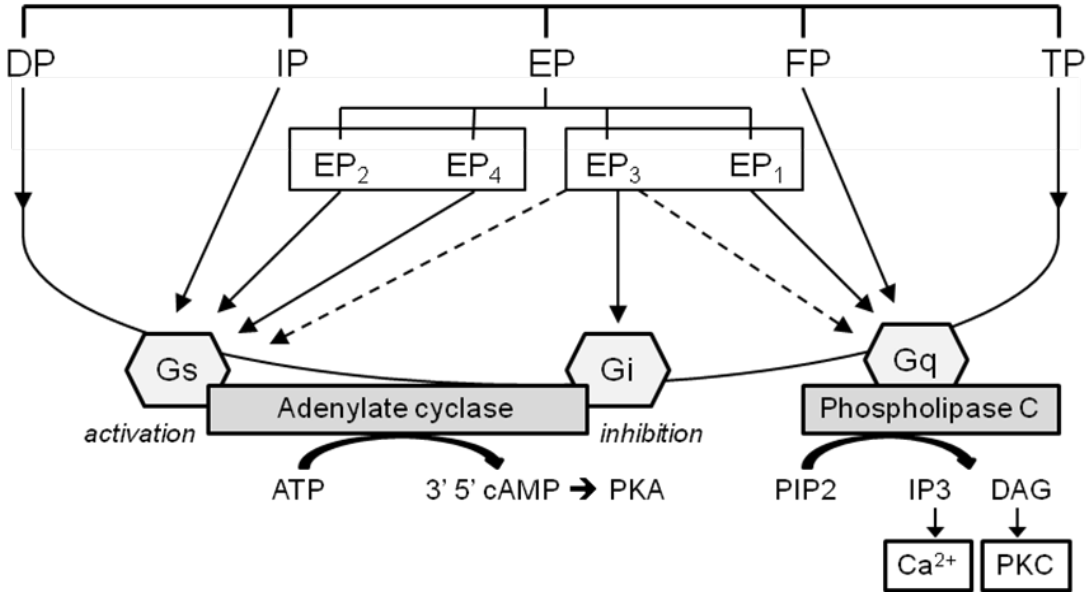

Figure 1.2 Prostanoid receptors, signal transduction and their final effects. Adapted from Wise and Jones, 2000. Broken lines indicate alternative coupling modes of isoforms of the EP_3 receptor.

1.3 Prostanoid receptors classification and distribution

Prostanoids are ubiquitously produced. It is believed that prostanoids work locally in autocrine or paracrine manner. By acting through prostanoid receptor subtypes, these chemical compounds elicit various pharmacological and pathopharmacological reactions in different tissue types. The prostanoid receptor family consists of eight distinct rhodopsin-like receptor proteins, which are classified according to the natural prostanoid ligand that each binds with greatest affinity. The first receptor purified and cloned was the human platelet TXA_2 receptor in 1991 by Hirata *et al*. Since then, homology screening based on amino acid sequence of this receptor was performed in various species. These receptors have been expressed, and their ligand binding properties and signal transductions have been examined. The tissue and cell distribution of the receptors was studied by Northern blot and by *in situ* hybridization analyses of their mRNA expression. Correlation of such knowledge with findings accumulated by pharmacological studies using COX inhibitors and using various prostanoid analogues having agonistic and antagonistic activities helps to define the actions of these receptors. They also help to reveal novel actions of these receptors.

Earlier classification of the prostanoid receptor was based on the study of isolated tissues preparation. Collectively, the receptors have been termed prostanoid DP, EP , FP, IP and TP receptors based on the agonist potencies in functional systems (Kennedy *et al.*, 1982). Further studies subdivided the EP receptor into four subtypes based on their agonist / antagonist specificity and signal transduction, each denoted by a subscript numeral (i.e. EP_1, EP_2, EP_3 and EP_4) (Coleman *et al.*, 1994b). PGD_2 as been identified as a potent agonist at the CRTh2 (chemoattractant receptor-homologous molecule of Type 2 helper T cells) or DP_2 receptor (Hirai *et al.*, 2001). Thus, including DP_2 receptor, the total number of prostanoid receptor subtypes is nine. The original DP receptor is now known as the DP_1 receptor. However, the DP_2 receptor does not contain the characteristic molecular signatures of prostanoid receptors but rather of chemokine receptors (Nagata *et al.*, 1999). This receptor will be not discussed further as it is outside the scope of the current study.

1.3.1 DP_1 Receptor

The DP_1 receptor shows significant sequence identity with IP and EP_2 receptors (Boie *et al.*, 1997). Among the prostanoid receptors, the DP_1 receptor is the least abundant. In humans, on Northern blot analysis, its expression was detected in retina and small intestine. However, human platelets contain functional DP_1 receptor (Giles *et al.*, 1989). DP_1 has been implicated in regulation of immune and skin allergic responses (Angeli *et al.*, 2004). This is correlated with earlier study where PGD_2 induced an asthmatic response in WT-mice but not in DP-KO-mice (Matsuoka *et al.*, 2000).

1.3.2 EP Receptor

The EP receptor family is subdivided into four subtypes: EP_1, EP_2, EP_3, and EP_4. The EP_3 receptor was the first to be cloned (Sugimoto *et al.*, 1994), followed by the EP_1 and EP_4 receptors (Funk *et al.*, 1993; Honda *et al.*, 1993). The EP_2 receptor was later cloned and pharmacologically characterized (Regan *et al.*, 1994). The main endogenous prostanoid that displays the highest potency at receptors of the EP type is PGE_2. It is a major COX product in a number of physiological settings and has by far the largest variety of biological actions. Of the four EP receptors, the EP_3 and EP_4 receptors bind PGE_2 with highest affinity (K_d < 1 nM), whereas the EP_1 and EP_2 receptors bind with lower affinity (K_d > 10 nM, Abramovitz *et al.*, 1994).

PGE_2 usually relaxes isolated vascular preparations and this action is mediated by activation of the EP_2 and / or EP_4 prostanoid receptor subtypes (Narumiya *et al.*, 1999). However, PGE_2 can also activate other prostanoid receptors depending on the vascular preparation examined. In particular, PGE_2 has been shown to activate the EP_3 receptor (Qian *et al.*, 1994; Jadhav *et al.*, 2004) and EP_1 receptor (Jadhav *et al.*, 2004) leading to contraction of vascular smooth muscle.

In some vessels, for example the rat femoral artery, PGE_2 is a weak contractile agent, but exhibits pronounced synergism with strong vasoconstrictors such as phenylephrine (α_1-adrenoceptor agonist) and U-46619 (TP receptor agonist) (Hung *et al.*, 2006).

Correspondingly, PGE_2 elicits vasodilatation and / or vasoconstriction *in vivo* in wild-type animals. A study in EP_2-KO mice showed that intravenous infusions of PGE_2 and sulprostone ($EP_{1/3}$ agonist) raise blood pressure (Kennedy *et al.*, 1999). When fed on a high-salt diet, the EP_2-KO animals developed significant hypertension with concomitant increase in urinary excretion of PGE_2. These results indicate that PGE_2 is produced in the body in response to a high-salt diet and works to negatively regulate the blood pressure via the relaxant EP_2 receptor; dysfunction of this pathway may be involved in producing the salt-sensitive hypertension.

1.3.2.1 EP_1 receptor

The EP_1 receptor was originally characterized as coupling to stimulation of intracellular Ca^{2+}, and little still known about other signal transduction pathways (Hata and Breyer, 2004). The EP_1 receptor is restricted to several organs, such as lungs, stomach and in the kidneys (Breyer and Breyer, 2001).

1.3.2.2 EP_2 receptor

The EP_2 receptor plays a role in uterine implantation and salt-sensitive hypertension, but most importantly is in relaxing vascular and bronchiolar smooth muscle. Human EP_2 receptors are mainly expressed in uterus, lungs and small intestine (Boie *et al.*, 1997, Bastien *et al.*, 1994,

Regan *et al.*, 1994; Breyer *et al.*, 2001). However, Jensen *et al* (2001) showed that the EP_2 receptor could be found in the rat kidneys.

1.3.2.3 EP_3 receptor

The EP_3 receptor is known to have a variety of actions due to its wide tissue distribution. It is highly expressed in the kidneys, uterus, adrenal gland and stomach tissues (Breyer *et al.*, 2001). In brief, it mediates contraction of smooth muscle, including vascular and uterine smooth muscle, enhances platelet aggregation, inhibits lipolysis and gastric acid secretion, and elicits cytoprotection of the gut. The EP_3 receptors have been implicated in febrile responses to pyrogens (Ushikubi *et al.*, 1998).

1.3.2.4 EP_4 receptor

The EP_4 receptor is widely distributed throughout the body and its mRNA has been found to be expressed in almost all mouse tissues examined. Important vasodilator effects of EP_4 receptor activation have been described in venous and arterial beds (Coleman *et al.*, 1994a; Coleman *et al.*, 1994b). A particular role for the EP_4 receptor in regulating the closure of the pulmonary ductus arteriosus has also been suggested by the studies of EP_4-KO mice (Nguyen *et al.*, 1997; Segi *et al.*, 1998).

1.3.3 FP receptor

The FP receptor was originally cloned from human kidneys, uterus, and placental cDNA libraries (Abramovitz *et al.*, 1994). Activation of FP receptor in the cardiovascular system increases systemic blood pressure, partly due to venoconstriction (Ducharme *et al.*, 1968). $PGF_{2\alpha}$, an endogenous FP agonist plays a critical role in mammalian reproduction by inducing luteolysis (Poyser, 1995). It has also been implicated in influencing renal function, regulation of intraocular pressure and in proliferative states such as endometrial carcinoma and cardiac hypertrophy. This reflects the fact that FP receptor expression has been demonstrated in the corpus lustrum, the kidneys, ocular tissues and ventricular myocytes (Hata and Breyer, 2004).

1.3.4 IP receptor

The human IP receptor was first cloned from lung and megakaryote cDNA libraries and has been shown to be expressed in many tissues including the kidneys, liver, lungs, platelets, heart and aorta (Wise and Jones, 2000; Breyer *et al.*, 2001). Activation of the IP receptor has been implicated in vascular homeostasis, because of vasodilatory and antithrombotic effects (see next section). Apart from its vascular effects, the IP receptor has been shown to mediate nociceptive pain during acute inflammation (Murata *et al.*, 1997; Bley *et al.*, 2006). In contrast to the pro-inflammatory effects of this receptor activation in nonallergic acute inflammation, recent studies have suggested that IP receptor signaling suppresses Th2-mediated allergic inflammatory responses. By suppressing the Th2 cell production, lung inflammation is greatly reduced (Takahashi *et al.*, 2002).

1.3.5 TP receptor

The TP receptor is important in modulating cardiovascular function. Stimulation by its endogenous agonists, PGH_2 and TXA_2 leads to shape change and aggregation of blood platelets. Deficiency in TP receptors leads to coagulation defects (Thomas *et al.*, 1998). The TP receptor is also responsible for smooth muscle contraction in various tissues (Eglen and Whiting, 1988). TP receptor signaling has been proposed to play a role in modulating T cell activation. Despite the existence of two variants, the mRNAs for both splice variants have been detected in most tissue that express TP receptor including platelets, placenta, vascular smooth muscle, brain, small intestine, and thymus (Raychowdhury *et al.*, 1994; Miggin *et al.*, 2002).

1.4 Prostanoid receptor ligands

Most of the endogenous prostanoids are prone to be metabolised into inactive compounds. In addition, PGI_2 and TXA_2 are chemically unstable under physiological conditions and their synthetic analogues have usually been used for receptor studies. The structure of synthetic agonists is usually close to the natural agonists, although non-prostanoid agonists exist for EP_3 and IP receptors (Jones *et al.*, 2009). Several routes to prostanoid antagonists have been followed. Some antagonists have emerged by serendipity (SC-19220; Sanner, 1969), while others have been derived from the chemical modification of a partial agonist (EP-045; Armstrong *et al.*, 1985). High throughput screening using cloned receptors is now the dominant route. For functional assays, the additional introduction of chimeric G-protein allows all prostanoid receptors to be investigated through mobilization of $[Ca^{2+}]_i$ using the fluorometric imaging plate reader (FLIPR) technology (Matias *et al.*, 2004; Woodward *et al.*, 2007). In this technique, all 96 wells are stimulated and optically measured simultaneously. Bimaprost has been demonstrated to selectively bind to HEK-293 cells expressing the cloned human ciliary body FP receptor (Sharif *et al.*, 2003).

1.4.1 Selective agonists

Table 1.1 summarizes the prostanoid receptor subtypes and their selective agonists (Jones *et al.*, 2009). Although of considerable pharmacological interest, partial agonists (right-hand column of Table 1.1) are not usually preferred as standard agonists. Table 1.2 listed the K_i value of the agonists used in the current study. Figure 1.3 and 1.4 listed the chemical structure of prostanoid agonists used in the current study.

17-Phenyl-ω-trinor PGE_2 (17-phenyl PGE_2) is a moderately selective EP_1 agonist, and in combination with sulprostone ($EP_3 > EP_1$) it can be used to discriminate between EP_1 and EP_3 receptors. A 6-oxo PGE_1 analogue, ONO-DI-004 also has been reported to be EP_1 selective (Cao *et al.*, 2002; Norel *et al.*, 2004). The prostacyclin analogue, iloprost behaved as a potent partial agonist on the EP_1 receptor (Dong *et al.*, 1986).

Two commonly used EP_2 agonists are butaprost, which is moderately potent, and AH-13205, which has a low potency. However, ONO-AEI-259 is increasingly being used in preference to butaprost, as it is more potent; its selectivity for EP_2 systems is well demonstrated by the studies of Jones and Chan (2005) and Hung *et al.* (2006). CAY-10399, a close relative of butaprost, has a high selectivity on mouse EP_2 receptor with binding K_i value of 2.2 nM; it exhibits much less IP agonism than butaprost (Tani *et al.*, 2001). A non-prostanoid EP_2 agonist, CP-533536 has recently been reported (Cameron *et al.*, 2009).

Sulprostone is a standard agonist used to identify EP_3 receptors as it has the highest affinities for this receptor; it has been demonstrated to be better in controlling post-partum haemorrhage compared with placebo (Poeschmann *et al.*, 1991). However, cardiovascular complications were reported in two patients (Stock *et al.*, 1995), which are likely due to its direct pulmonary

vasoconstrictor action (Qian *et al.*, 1994). Previously, SC-46275 was shown to be the most selective ligand for this receptor (Jones, 2004; Wilson *et al.*, 2004).

A selective agonist has been developed for EP_4 receptor. ONO-AE-329 binds selectively to mouse EP_4 receptor with inhibitory constant (K_i) of 10 nM and to human receptor with K_i of 24 nM (Tsuboi *et al.*, 2002). The non-prostanoid ONO-AP-324 has also been reported to behave as a partial agonist in some preparations (Jones *et al.*, 1998).

PGI_2 has limited use to study IP receptor function due to its unstable nature. Therefore, synthetic agonists such as iloprost, cicaprost, AFP-07 and carbacyclin are commonly used. Cicaprost is the most selective of these agonists (Jones, 2004). Iloprost potently activates the IP receptor but activates the EP_1 receptor as well (Dong *et al.*, 1986). Taprostene behaves as a partial agonist at the IP receptor (Jones and Chan, 2001).

Endogenous TXA_2 is unstable in aqueous solution, being rapidly hydrolyzed to TXB_2, and is therefore not used in receptor binding and signal transduction assays. For that reason, analogues such as U-46619 have been synthesized and most commonly used to probe TP receptor function. Other TP agonists include I-BOP and STA_2. Partial agonists are common, for example CTA_2, PTA_2 and U-44069 (see Jones, 2004).

Selective FP agonists such as fluprostenol and latanoprost-FA have been developed (see Jones, 2004). Fluprostenol could only bind to the FP receptor, indicating the high selectivity of this ligand, with K_i value of 2.7 nM in human receptor.

BW-245C has been widely used as a selective DP_1 agonist.

Table 1.1 Prostanoid receptor agonists for defining antagonist profiles (Jones *et al.*, 2009)

Prostanoid receptor	**Full agonists**		**Partial agonists**
	High selectivity	**Moderate selectivity**	
EP_1	ONO-D1-004	17-Phenyl PGE_2	Iloprost
EP_2	ONO-AE1-259, CAY-10399	Butaprost-FA, CP-533536, 19(R)-hydroxy PGE_2	
EP_3	ONO-AE-248, SC-46275	Sulprostone, MB-28767	ONO-AP-324
EP_4	ONO-AE1-329, tetrazolo PGE_1	(PGE_2)	
IP	Cicaprost	AFP-07, iloprost	Octimibate Taprostone
TP	STA_2, U-46619		CTA_2, PTA_2, U-44069
FP	Fluprostenol, lataprost-FA	Cloprostenol	AL-8810
DP_1	BW-245C	BW A868C	BW-192C86

* FA – free acid

Table 1.2 K_i values (nM) for agonists used in the current study

Ligand	EP_1		EP_2		EP_3		EP_4	
	Human	**Mouse**	**Human**	**Mouse**	**Human**	**Mouse**	**Human**	**Mouse**
U-46619	28,000	>10,000	12,000	>10,000	13,000	>10,000	2,000	>10,000
PGE_2	9.1	20	4.9	12	0.33	0.85	0.79	1.9
17-Phenyl PGE_2		14		>10,000		3.7		1,000
Sulprostone	110	21	>100,000	>10,000	0.35	0.60	7,700	>10,000
ONO-D1-004		150		>10,000		>10,000		>10,000
ONO-AE1-259		>10,000		3		>10,000		6000
Butaprost-FA	28,000		91		1,600		19,000	
AH-13205		>10,000		240		82		>10,000
CP-533535				50				>3,200
CAY-10399		>10,000		92		>10,000		>10,000
ONO-AE-248		>10,000		3,700		7.5		4,200
PGD_2	5,800	10,000	3,000	>10,000	420	280	1,500	>10,000
Cicaprost	>1,300	>10,000	>1,300	1,300	260	170	44	>10,000
Iloprost	11	21	1,900	1,600	56	22	280	2,300
$PGF_{2\alpha}$	550	1,300	960	>10,000	38	75	290	>10,000
Latanoprost-FA	1,800		40,000		6,500		>100,000	

Ligand	DP		FP		IP		TP	
	Human	**Mouse**	**Human**	**Mouse**	**Human**	**Mouse**	**Human**	**Mouse**
U-46619	4,000	>10,000	240	1,000	57,000	>10,000	35	67
PGE_2	310	>10,000	120	100	>10,000	>10,000	29,000	>10,000
17-Phenyl PGE_2		>10,000		60		>10,000		>10,000
Sulprostone	>100,000	>10,000	200	580	>100,000	>10,000	>100,000	>10,000
ONO-D1-004								
ONO-AE1-259								
Butaprost-FA	12,000		>100,000		55,000		20,000	
AH-13205		>10,000		>10,000		>10,000		>10,000
CP-533535								
CAY-10399								
ONO-AE-248								
PGD_2	1.7	21	6.7	47	>100,000	>10,000	6,600	>10,000
Cicaprost	>1,300	>10,000	>1,300	>10,000	17	10	>1,300	>10,000
Iloprost	1,000	>10,000	620	>10,000	11	11	6,500	>10,000
$PGF_{2\alpha}$	860	>10,000	3.2	3.4	>100,000	>10,000	8,700	>10,000
Latanoprost-FA	55,000		2.8		>100,000		16,000	

* Abramovitz *et al.,* (1994); Kiriyama *et al.,* (1997); Suzawa *et al.,* (2000); Tani *et al.,* (2001); Amano *et al.,* (2003)

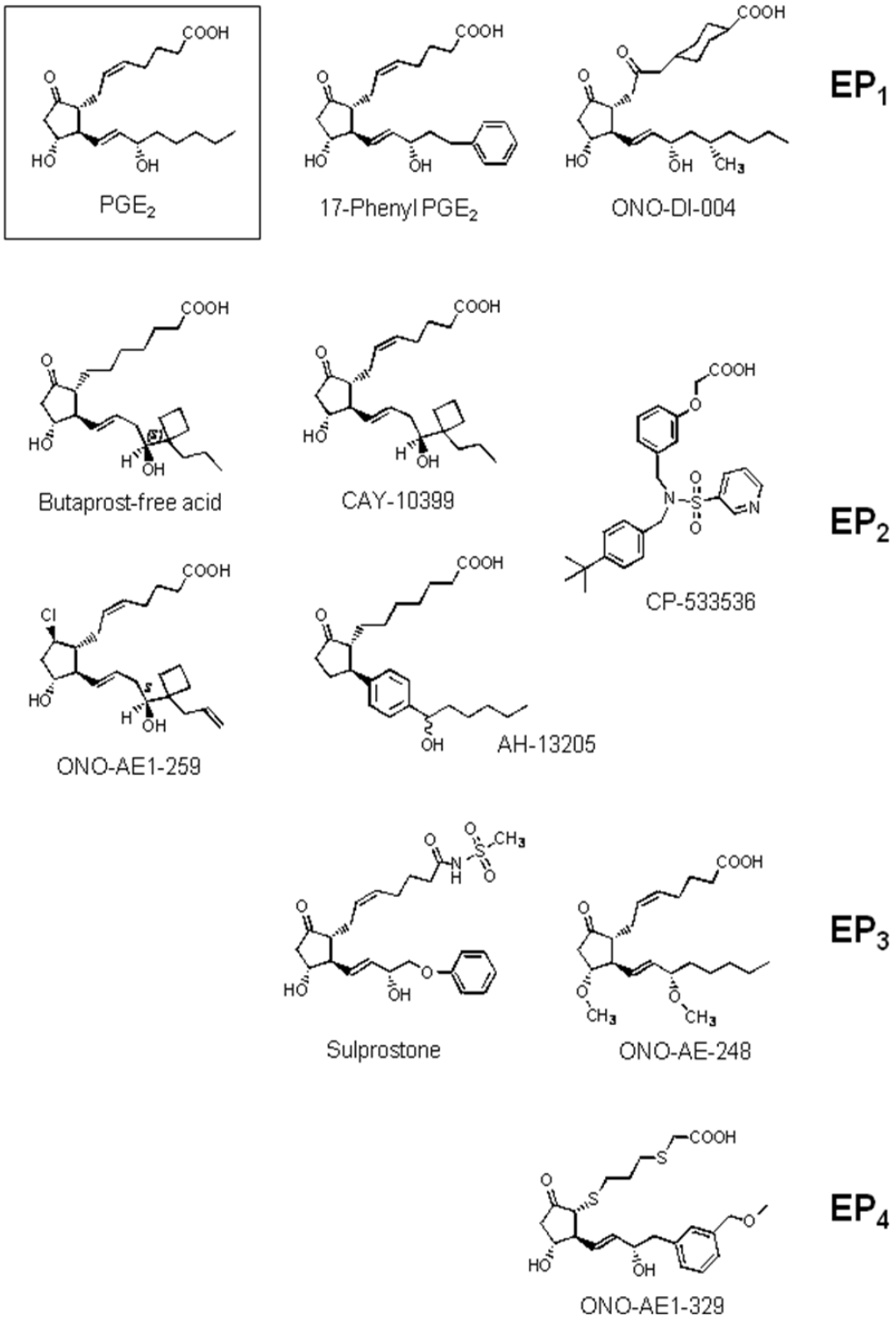

Figure 1.3 Structures of agonists showing selectivity for EP receptor subtypes. The natural agonist PGE_2 is shown in the box. CP-533536 has a non-prostanoid structure.

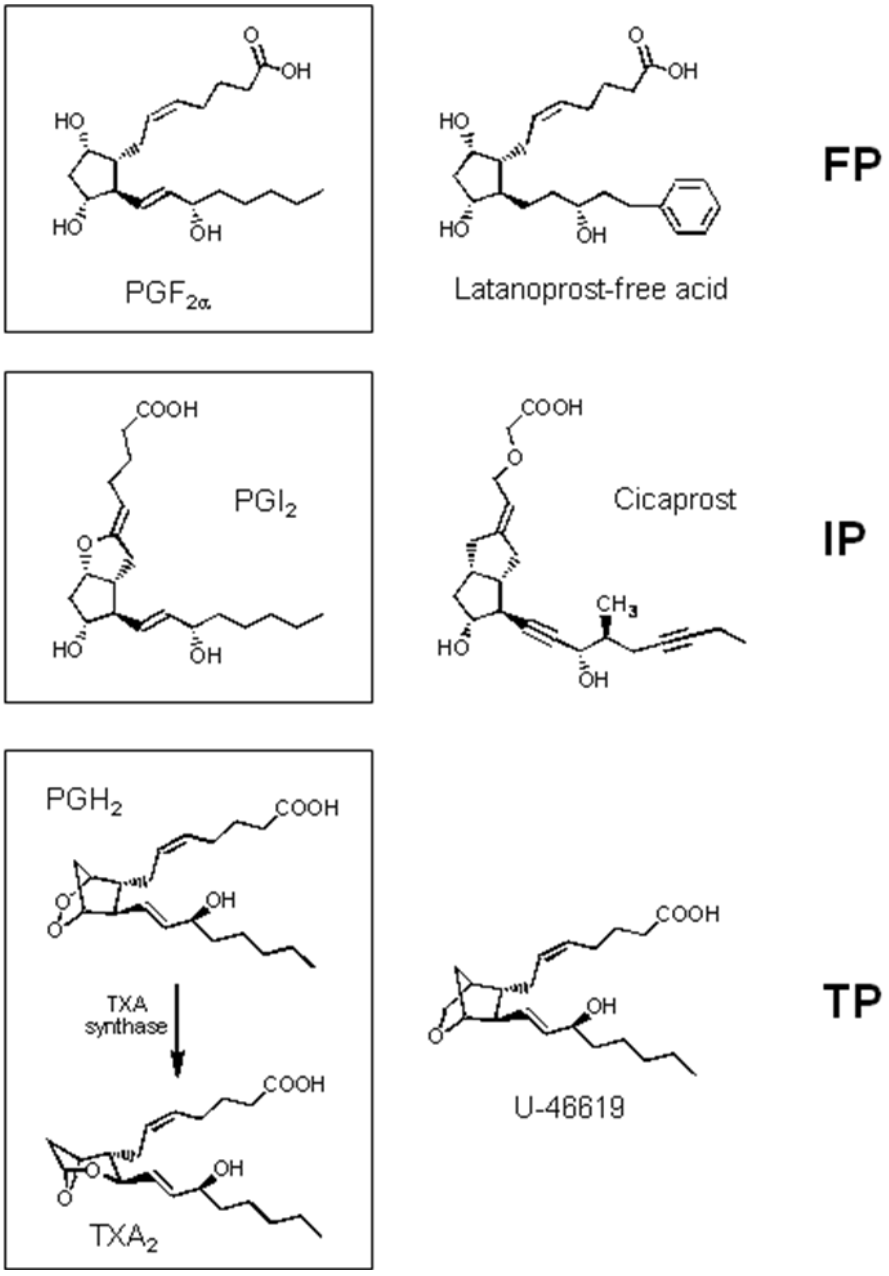

Figure 1.4 Structures of agonists showing selectivity for FP, IP and TP receptors. The natural agonists are shown in the boxes; both PGH_2 and TXA_2 activate the TP receptor.

1.4.2 Selective antagonists

Table 1.3 lists selective prostanoid antagonists that were available for the current studies. Figure 1.5 shows the chemical structure of the selective prostanoid antagonists used in the current study.

Several EP_1 antagonists have been developed. SC-51322 was chosen as the selective EP_1 antagonist in the current study. It antagonised PGE_2 with pA_2 value of 8.1 in guinea-pig ileum assay (Hallinan *et al.,* 1994) and pA_2 of 8.45 in guinea-pig trachea (Hung *et al.*, 2006). A recent EP_1 antagonist developed by the GlaxoSmithKline research group, GW-848687 has been shown to be a competitive antagonist at EP_1 receptor with pA_2 of 9.1 in a recombinant receptor assay (Giblin *et al.,* 2007).

Selective EP_2 antagonists are essentially not available for the current antagonist study.

L-798106 showed high selectivity for EP_3 receptors based on ligand binding assays involving recombinant prostanoid receptors (Juteau *et al.,* 2001). In functional studies, it blocked the action of sulprostone with pA_2 values of 7.82 in guinea-pig trachea (Clarke *et al.*, 2004) and 7.43 – 8.03 in rat femoral artery (Hung *et al.*, 2006) (Table 1.2). L-798106 (known as CM9) has been shown to inhibit PGE_2-induced Ca^{2+} entry in a rat recombinant EP_3 receptor assay, with pK_i value of 7.12 (Jugus *et al.*, 2009). L-826266 is a chloro-analogue of L-798106. In guinea-pig aorta, L-826266 blocked EP_3 agonist-induced contraction with pA_2 value of 7.58 (Jones *et al.,* 2008). Both antagonists had a slow onset of block. This may relate to their high lipophilicity with predicted *n*-octanol / water partition coefficients (ClogP) of 6.9 and 7.4 respectively (ChemAxon freeware). ONO-AE3-240 is reported to be a highly selective EP_3 antagonist (mouse EP_3 K_i = 0.23 nM; Amano *et al.,* 2003), but its structure has not been disclosed.

The TP antagonist available in the current study is BMS 180291 with pA_2 value between 9.2 – 10.0 (Zhang *et al.*, 1996). In the low nanomolar range, BMS-180291 has been reported slowly to reach a steady state, requiring up to 2 h contact in guinea-pig aorta (Jones *et al.*, 2008).

Selective IP receptor antagonists have been documented, but were not available in for the current study. RO-1138452 and RO-3244794 have been shown to selectively bind to human platelet IP receptor and to recombinant IP receptor system (Bley *et al.*, 2006).

Several selective FP receptor antagonists have been studied before, mainly for their effects on myometrium contraction. For example, the non-prostanoid AS-604872 inhibited spontaneous uterine contractions in pregnant rat near term (Cirillo *et al.*, 2007). It has K_i values of 35, 158 and 323 nM for human, rat and mouse rc-FP receptors. Its selectivity for EP_2 receptor was 20-fold and more than 300-fold for other prostanoid receptors. However, no selective FP receptor antagonists were available for the current study.

Table 1.3 Antagonists chosen for use in the current study

Prostanoid receptor	**Antagonists**	**Reported pA_2**	**References**
EP_1	SC-51322	8.45	Hung *et al.*, 2006
	GW-848687	9.1	Giblin *et al.*, 2007
EP_3	L-798106	7.12 – 8.03	Juteau *et al.*, 2001 Clarke *et al.*, 2004 Hung *et al.*, 2006 Jugus *et al.*, 2009
	L-826266	7.58 - 8.35	Clark *et al.*, 2008 Jones *et al.*, 2008
TP	BMS-180291	9.5	Zhang *et al.*, 1996

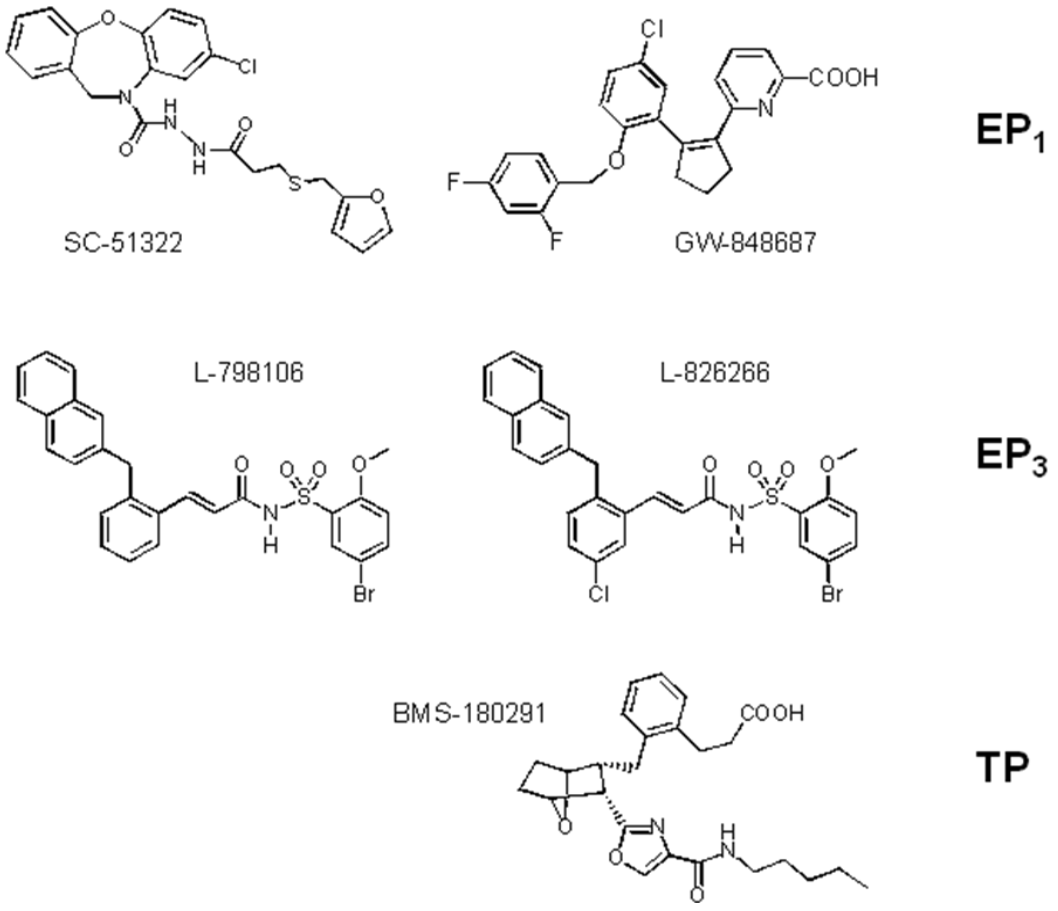

Figure 1.5 Structures of antagonists for EP_1, EP_3 and TP receptors.

1.5 Physiological role of prostanoids in the human body

Prostanoids are presumed to play important roles in a variety of physiological and pathophysiological processes in the body. When induced pathologically, prostaglandins can assume harmful or protective roles. These roles have been studied by use of the knockout (KO) mice. Mice deficient in each prostanoid receptor have been generated by the disruption of each receptor gene by homologous recombination. In the sections below, these roles will be discussed as they relate to the *in vitro* systems studied here.

1.5.1 Heart

Acute myocardial infarction (AMI) is still a leading cause of death in developed countries, and it is usually caused by acute thrombotic occlusion of a coronary artery that has become atherosclerotic. The underlying pathophysiology of AMI is ischemia-reperfusion (I/R) injury of the heart. PGI_2 and its analogues have been reported to attenuate cardiac I/R injury when used exogenously *in vivo* (Narumiya *et al.*, 1999). The proposed mechanisms of protection were because of their inhibitory effects on platelets and neutrophils and ill-defined membrane-stabilizing effects. TXA_2 synthase inhibitors and / or TP antagonists have been reported to reduce myocardial infarct size in animal studies *in vivo* (Xiao *et al.*, 2004). The effects of TXA_2 synthase inhibitors were attributed to enhanced generation of PGI_2 derived from increased availability of its precursor, resulting in inhibition of neutrophil adhesion to endothelial cells. The cardioprotective effects of TP antagonists, however, are variable (Xiao *et al.*, 2001).

Selective COX-2 inhibitors have replaced traditional NSAIDs for many inflammatory conditions. However, the withdrawal of certain COX-2 inhibitors due to increased likelihood of hypertension, myocardial infarction and stroke has cast a shadow over this therapy (Bombardier

et al., 2000; Silverstein *et al.*, 2000; Mukherjee *et al.*, 2001). By inhibition of COX-2, biosynthesis of endogenous PGI_2 is reduced. Hence, the homeostatic response to accelerated platelet-vascular interactions, as in severe atherosclerosis and unstable angina, is abolished (Cheng *et al.*, 2002).

In a study, using IP-KO and TP-KO mice, it was shown that IP receptor deficiency significantly aggravates cardiac I/R injury *in vivo* (Xiao *et al.*, 2004). The IP-KO heart had greater I/R injury when assessed functionally and biochemically. However, the study showed that lack of TP receptors did not significantly alter either the myocardial infarct size *in vivo* or the degree of I/R injury *ex vivo*. This clearly demonstrated that TXA_2 has a small role, if any, in cardiac I/R injury.

It has been shown that up-regulation of COX-2 and increases in PGE_2 synthesis occur in the heart during I/R injury. This result suggested that PGE_2 plays some role in cardiac I/R injury (Calabresi *et al.*, 2003). Another study used EP_4-KO mice to provide direct evidence that EP_4 deficiency significantly aggravates cardiac I/R injury *in vivo* (Xiao *et al.*, 2004). The result showed that endogenous PGE_2 is able to attenuate cardiac I/R injury and that the effect of PGE_2 is mediated by EP_4 receptor. Because there is significant production of PGE_2 during I/R injury and abundant expression of the EP_4 mRNA in the heart, PGE_2 should exert its cardioprotective action by acting directly on the cardiac tissue. Application of an EP_4 agonist significantly reduced the infarct size, thereby providing additional evidence for the involvement of EP_4 receptors.

1.5.2 Thrombosis and haemostasis

It is now understood that atherosclerosis is an inflammation in the intima of large arteries that is triggered by high serum cholesterol and by the complex array interaction of various types of cells

including monocytes / macrophages, endothelial cells (ECs), smooth muscle cells (SMCs), T cells, and blood platelets (Ross, 1999). A variety of substances including cytokines, chemokines, and growth factors are suggested to induce, amplify, and modify this inflammatory process. Involvement of prostanoids in acute inflammation has been well documented based on the finding that aspirin-like NSAIDs are specific COX inhibitors. TXA_2 and PGI_2 are two major prostanoids in the cardiovascular system, being abundantly produced by blood platelets and vascular endothelium, respectively. Previous studies found that TXA_2 and PGI_2 biosynthesis is increased in patients with atherosclerosis (Belton *et al.*, 2000). Urinary levels of TXA_2 and PGI_2 metabolites were elevated in patients with atherosclerosis compared with normal patients. A study by Murata *et al.*(1997) showed that PGI_2 and TXA_2 do not work constitutively in regulation of the systemic circulation, but more likely work on demand in response to local stimuli. The presence of EP_4 receptors on macrophages in atheromatous plaques from human coronary and carotid arteries has been established by immunohistochemistry (Takayama *et al.*, 2002).

Earlier study on human platelets showed that sulprostone enhanced platelet aggregation *in vitro* even at low concentration (4 – 400 nM) (Matthews and Jones, 1993). PGE_2 and the selective EP_3 receptor agonist, AE-248 were shown to potentiate the platelet aggregation induced by U-46619 in WT mice (Ma *et al.*, 2001). In EP_3-deficient mice, both PGE_2 and AE-248 lost this action completely. These results clearly show that the potentiating effect of PGE_2 on platelet aggregation was mediated by EP_3 receptor. In a recent study, DG-041 an EP_3 receptor antagonist has been demonstrated to antagonise the effects of sulprostone on platelet function (Heptinstall *et al.*, 2008). It may be useful in preventing platelet build-up in atherosclerotic lesions.

A study on IP-deficient mice showed that an enhanced thrombotic tendency was observed when endothelial damage was induced (Kobayashi *et al.*, 2004). This finding is consistent with the proposed role of PGI_2 as an endogenous antithrombotic agent. This antithrombotic system is activated in response to vascular injury to minimize its effects (Belton *et al.*, 2000). TP receptor activity has also been shown to have an important role in platelet homeostasis. Activation of TP

receptor lead to platelet aggregation (Arita *et al.*, 1989). Bleeding times were prolonged in TP-KO mice as compared to WT mice (Thomas *et al.*, 1998). Similarly, administration of U-46619 induced a rapid, irreversible platelet aggregation in WT mice but no detectable aggregation of platelets in TP-KO mice.

The balancing act between the opposing effects of PGI_2 and TXA_2 is important to vascular homeostasis. This was demonstrated in the study using apoE-KO mice with deletion of TP or IP receptors as well (Kobayashi *et al.*, 2004). Atherogenesis was significantly accelerated in apoE-KO / IP-KO mice compared with apoE-KO mice. In contrast, TP deficiency suppressed the extent of atherosclerosis. Deposition of human platelets onto damaged rabbit aorta *in vitro* is reduced in the presence of selective TP antagonist, GR-32191 which appears to inhibit aggregation of platelets (Hornby *et al.*, 1989). Similarly, the administration of the TP-receptor antagonist, S-18886 to rabbits strongly inhibited the atherogenic process in both uninjured and injured vessels (Worth *et al.*, 2005). These results suggest that the balance of the PGI_2 and TXA_2 is important for maintaining vascular homeostasis, prevent thrombosis and vasospasm while performing efficient homeostasis.

1.5.3 Hypertension

PGE_2 elicits contractile and / or relaxant responses of vascular smooth muscles *in vitro*. A study in EP_2-KO mice showed that intravenous infusion of PGE_2 and sulprostone ($EP_{1/3}$ agonist) induces hypertension (Kennedy *et al.*, 1999). When fed on a high-salt diet, the EP_2-KO animals developed significant hypertension with concomitant increase in urinary excretion of PGE_2. These results indicate that PGE_2 is produce in the body in response to a high-salt diet and work to negatively regulate the blood pressure via the relaxant EP_2 receptor. The dysfunction of this pathway may be involved in producing the salt-sensitive hypertension.

1.5.4 Pulmonary vasculature

Pulmonary arterial hypertension (PAH) is a condition where there is a continuous high pressure in the pulmonary artery (Farber and Loscalzo, 2004). The average pressure in the normal situation is about 14 mmHg when the person is resting. In PAH, the average is usually greater than 25 mmHg at rest or 30 mmHg with exercise. Early in the disease, as the pulmonary artery pressure increases, thrombotic pulmonary arteriopathy occurs. As the pulmonary pressure continues to rise, plexogenic pulmonary arteriopathy develops. A remodelling of the pulmonary vasculature with intimal fibrosis and replacement of normal endothelial structure characterizes this.

In the human pulmonary arterial smooth muscle, IP and EP_3 receptors have been shown to be responsible for the prostanoid induced relaxation and contraction respectively (Qian *et al.*, 1994; Walch *et al.*, 1999). In PAH, the synthesis of PGI_2 is reduced, whereas the synthesis of TXA_2 is increased (Christman *et al.*, 1992). The relative deficiency of PGI_2 in PAH secondary to reduced PGI_2 synthase activity leads to vasoconstriction, proliferation, thrombosis, and inflammation in the affected vessels (Tuder *et al.*, 1999).

Long-term intravenous PGI_2 has become the most important specific therapy for PAH and associated diseases. However, this therapy is hampered by catheter complications and systemic side effects. Alternatively, inhalation of the PGI_2 analogues, iloprost (Olschewski *et al.*, 2001) and beraprost (Abe *et al.*, 2001) results in pulmonary vasodilation with few systemic side effects.

1.5.5 Kidney function

The role of PGI_2 in regulating renal and glomerular hemodynamics, renin secretion, as well as tubular transport processes has been documented. PGI_2 had a protective role in primary cultures of proximal tubule epithelial cells that were subjected to hypoxia and reoxygenation (Paller and Manivel, 1992). The idea that PGI_2 more than other prostanoids is relevant to the maintenance of renal function stem from various studies. A few studies showed that in recombinant mice lacking the IP receptor there was salt-sensitive hypertension and enhanced renin release following water deprivation (Fujino *et al.*, 2004).

Altered growth responses (proliferation and hypertrophy) contribute to changes in renal function characteristic of various nephropathies. A clear link between renal hypertrophy and changes in renal function has been established (Nasrallah and Hebert, 2005). Cell loss also plays an important role in renal disease progression. There are two distinct forms of cell death, apoptotic and necrotic. In many progressive renal diseases, the primary feature is glomerulosclerosis. Sclerotic glomerulosclerosis is characterized by progressive expansion of the extracellular matrix, which replaces glomerular cells. Apoptotic death in the kidneys is triggered by a disruption of matrix-cell interactions (Sugiyama *et al.*, 1996). Activation of IP receptor in the kidneys has been shown to prevent matrix-induced apoptosis. This prevents the accumulation of the matrix underlying progressive glomerular disease (Nasrallah and Hebert, 2005).

In the kidneys, all four known EP receptors are expressed in different regions (Jensen *et al.*, 1999; Jensen *et al.*, 2001). The natriuretic and diuretic effects of PGE_2 are due to interaction with EP_1 and EP_3 receptors situated on the ascending part of the loop of Henle and the collecting duct system. PGE_2 inhibits arginine vasopressin-stimulated water and sodium transport, thereby increasing water and sodium excretion from the kidneys. The EP_2 receptor is exclusively expressed in the rat kidneys medulla and EP_4 receptor mainly in the medulla. The EP_2 receptor

maintains renal blood flow associated with low-salt states. The EP_4 receptor in the other hand promotes salt excretion in response to a high salt intake (Jensen *et al.*, 1999).

1.5.6 Ductus arteriosus

At birth, mammals including humans undergo a dramatic change in their circulation with the commencement of respiration, i.e., from the fetal circulation system, which shunts the blood flow from the main pulmonary artery directly to aorta via ductus arteriosus, to the pulmonary circulation system in the neonate. This adaptive change is caused by the closure of the ductus and is induced by the withdrawal of the dilator prostaglandins as well as active contraction exerted by increased oxygen tension (Smith, 1998). Elevated oxygen tension also inhibits PGI_2 synthase, which decreases the PGI_2 level in ductus, thus promoting contraction of the ductus arteriosus (Smith *et al.*, 1994).

A study using various synthetic PG analogues suggested that both IP and EP_4 receptors are present in the ductus and cause dilation of this vessel (Smith *et al.*, 1994). PGE_2 is the major prostaglandin that affects tone (Clyman *et al.*, 1980). The other prostanoids play smaller roles (Smith *et al.*, 1994; Smith, 1998). A study using knockout mice showed that disruption of the EP_4 receptor gene resulted in death within three days after birth, due to marked pulmonary congestion and heart failure (Segi *et al.*, 1998). These results suggest a critical role of the EP_4 system in the ductus and suggest that the compensatory mechanism maintains ductus patency not only in the fetal period but also after birth. No abnormality was detected in IP-KO mouse.

1.5.7 Intraocular pressure

Prostaglandins play a role in lowering intraocular pressure (IOP) especially in the case of glaucoma and ocular hypertension. Traditionally, β-blockers are used to lower IOP. FP receptors agonists are currently widely used because they are more effective and have fewer side effects than β-blockers. These agonists exert their effects through activation of FP receptor (Anthony *et al.*, 1998). Latanoprost did not lower IOP in the FP-KO mice (Crowston *et al.*, 2004). In contrast, IOP was reduced in the treated eye of the WT mice. In addition, the potent FP-agonist, tafluprost stimulated production of endogenous prostaglandins through activation of the FP receptor, which in turn act on the EP_3 receptor (Ota *et al.*, 2007). Sulprostone have been shown to decrease IOP in rabbit without any side-effect as compared to ocular irritation and transient increase in IOP caused by PGE_1 and PGE_2 (Waterbury *et al.*, 1990). Allergan Pharmaceuticals, a pharmaceutical company specializing in ophthalmic drugs has an interest in this IOP lowering effect through EP_3 receptors. Allergan Pharmaceuticals supplied novel prostanoid compounds including the selective EP_3 agonist ONO-AE-248 and the EP_3 antagonist L-826266 for use in the current studies.

The selective EP_2 agonists have been shown to have varies in effects on intraocular pressure (Woodward *et al.,* 1993). Butaprost and AH-13205 have a different mechanism from other EP_2 agonists on effect in lowering intraocular pressure (Woodward *et al.,* 1995; Nilsson *et al.,* 2006).

A novel selective EP_4 agonist, PF-04475270 (a pro-drug) has been shown to have an effect of lowering IOP in dogs (Prasanna *et al.*, 2009). The effect was sustainable for a period of time. Further work is in progress by the same author to elucidate the role of lowering IOP by EP_4 agonist in human eye. Recently, a selective EP_2 agonist butaprost has been shown to significantly blunts the detrimental influence of ischemia / reperfusion to the retina (Andrade da Costa *et al.*, 2009).

1.6 Diabetes

1.6.1 Diabetes overview

Diabetes mellitus is an endocrine disease characterized by the lack of insulin production (Type 1) or resistance of the target-organ to insulin (insulin resistance) (Type 2). In early stage of diabetes, the subject usually presents with increased passing of urine (polyuria) and increased water uptake (polydipsia). Weight loss, which was seen in the STZ-rat (see later), is due to an inability to utilise the carbohydrate due to lack of insulin. Instead, the body fat is utilised for the energy.

The effects of diabetes can be examined in various rat models. The Zucker fatty (ZF) rat (Tokuyama *et al.*, 1995) and Goto-Kakizaki (GK) rat (Goto *et al.*, 1976) are both developed by cross-breeding and manifest type 2 diabetes. A more convenient model is the streptozotocin (STZ) induced-diabetic rat (Junod *et al.*, 1969).

1.6.2 Diabetes and endothelium

Endothelium dysfunction has been reported in diabetic people and experimental animals with diabetes (De Vriese *et al*., 2000; Schofield *et al*., 2002; Schalkwijk and Stehouwer, 2005). The dysfunction is caused by the high glucose content in tissues, which triggers a cascade of functional and structural alterations in vascular cells, leading to macrovascular and microvascular diseases (Schalkwijk and Stehouwer, 2005). Diabetes itself also promotes an inflammatory response (Schalkwijk and Stehouwer, 2005), with changes in the ultrastructure and

the function of endothelial cells (Sotnikova *et al.*, 2006). These changes are confined to the endothelial cells and do not affect the smooth muscle cells.

1.6.3 Diabetes and prostaglandins

A hallmark of endothelial dysfunction in diabetes is alteration in the biosynthesis of prostaglandins and oxidative stress products and decreased release and / or bioavailability of nitric oxide (NO) (Tesfamariam *et al.*, 1989; Vanhoutte *et al.*, 2005). The hyperglycaemic state in diabetes alone is the stimulation for productions of prostaglandins (Tesfamariam *et al.*, 1990). In support of this view, there is production of vasoconstrictor prostaglandins other than TXA_2 in rat mesenteric arterial bed as shown by Peredo *et al.* (1999). Endothelial COX, which is upregulated in various pathological conditions including diabetes, is thought to be responsible (Tesfamariam *et al.*, 1989; Ge *et al.*, 1995; Shi *et al.*, 2006; Shi *et al.*, 2007b). In contrast, Peredo *et al.* (2001) showed impairment of prostanoid production in the mesenteric vascular bed of the diabetic rat.

The endogenous prostanoids enhanced by DM have been shown to have synergism with the α_1-adrenoreceptor agonist, phenylephrine through the TP receptor system in the rat femoral artery (Shi *et al*. 2008). However, the possibility of other prostanoid receptor involvement in the rat femoral artery, in particular the EP_3 receptor has not been investigated. There was a pronounced synergism between the EP_3 system and other contraction, accompanied by pronounced synergy with other contractile systems that rely extensively on Ca^{2+} influx through L-type Ca^{2+} channels including phenylephrine (Hung *et al.*, 2006).

1.7 Pharmacological principles

1.7.1 Synergism and its measurement

Synergism occurs when the combination of two or more drugs produces a larger effect than the sum of the effects of each acting alone. This is in contrast to an additive effect, where the combined effect is simply the summation of the components.

In the prostanoid area, synergism between EP_3 and TP contractile systems was demonstrated in rat femoral artery (Hung *et al.*, 2006). On its own, PGE_2 induced a small contraction in the artery. However, strong contraction was seen when the preparation was primed with K^+, phenylephrine or U-46619. Sulprostone also synergised with these strong contractile agents. U-46619 also has a synergistic interaction with adrenaline in human umbilical veins (Errasti *et al.*, 2007). U-46619 at 0.3 nM did not induce contractions but shifted the concentration–response curve for adrenaline to the left without modifying maximal contraction. In comparison, U-46619 at 3 nM increased the maximal response attained by sulprostone in rat femoral artery (Hung *et al.*, 2006). The selective TP receptor antagonist SQ-29548 blocked the potentiating effect of 0.3 nM U-46619.

PGE_2 at high concentration (> 10 μM) has a cross activity on TP receptor, based on binding studies (Dorn *et al.*, 1992). Similarly, other $EP_{1/3}$ agonists also show some TP agonism (Jones *et al.*, 1982; Errasti *et al.*, 2007). For this reason, a TP antagonist was routinely included in the bathing fluid in my studies to prevent potential synergism between the EP and TP contractile systems (see Methods chapter).

1.7.2 Types of antagonism and pA_2 measurement

A receptor antagonist does not provoke a biological response itself upon binding to a receptor, but blocks or reduces the agonist-mediated response. In competitive antagonism, the antagonist binds reversibly to (part of) the agonist binding domain without activating the effector mechanism (Neubig *et al.*, 2003). The antagonism is usually surmountable, that is, a maximum response can still be elicited by increasing the concentration of the agonist. Alternatively, agonist and antagonist can be simultaneously bound to different sites of the receptor; antagonist binding reduces or prevents the action of the agonist with or without any effect on the binding of the agonist. This antagonism is non-competitive; where no amount of agonist can completely overcome the inhibition once it has been established.

pA_2 is defined as the negative log of the concentration of the antagonist required to produce a two-fold shift to the right in the agonist-concentration-effect curve (Neubig *et al.*, 2003). pA_2 is a measure of the affinity constant of an antagonist for the receptor. Binding constants (preferably pK_i) are often given where functional information is not available. pA_2 and pK_i values may not always agree: often the difference is due to processes affecting ligand concentration that are present in intact tissues, but not isolated cells or cell membranes.

The pA_2 value of antagonist can be determined by several experimental protocols. The Schild protocol remains the gold standard for determining the pA_2 of the antagonist. The Schild analysis requires the construction of full concentration-response curves (CRCs) for an agonist in the absence and in the presence of increasing concentrations of antagonist. For the Schild analysis to proceed the antagonism must be surmountable and the log agonist concentration-effect curve should be shifted to the right by the antagonist in a parallel fashion (Arunlakshana and Schild, 1959). The Schild protocol is based on this equation:

$$-\log K_b = \log (DR - 1) - \log B \quad (1)$$

in which DR (= A'/A) represents the ratio between equieffective agonist concentrations, respectively in the presence (A') and in the absence (A) of the concentration B of the competitive antagonist, and the K_b is the equilibrium dissociation constant. In the case of a competitive antagonist with a one-to-one relationship with the receptor, the regression of log (DR – 1) on log B, gives a straight line with slope (Schild slope) = 1 (e.g.: Figure 1.6). The pA_2 is the value of *x*-intercept, which equals the value of – log K_b. Clearly, when the Schild slope is different from unity, the evaluation of the dissociation constant is meaningless. Equation 1 can be re-arranged as follows:

$$-\log K_b = -\log \frac{B}{(DR - 1)} \quad (2)$$

A negative / antilog transformation gives the original Gaddum equation:

$$K_b = B / (DR - 1) \quad (3)$$

Alternatively, the inhibition-curve (Cheng-Prusoff) protocol may be used. The Cheng-Prusoff protocol is derived from enzymatic system study, and describes the interaction between substrate, S and competitive inhibitor, I (Cheng and Prusoff, 1973). This interaction can be expressed by this equation:

$$K_i = \frac{IC_{50}}{1 + \frac{[S]}{K_m}} \quad (4)$$

where K_i is the antagonist dissociation constant, [S] is the fixed concentration of substrate and K_m is the dissociation constant of the substrate. IC_{50} is the concentration of the competitive inhibitor at half-maximal inhibition of the enzyme.

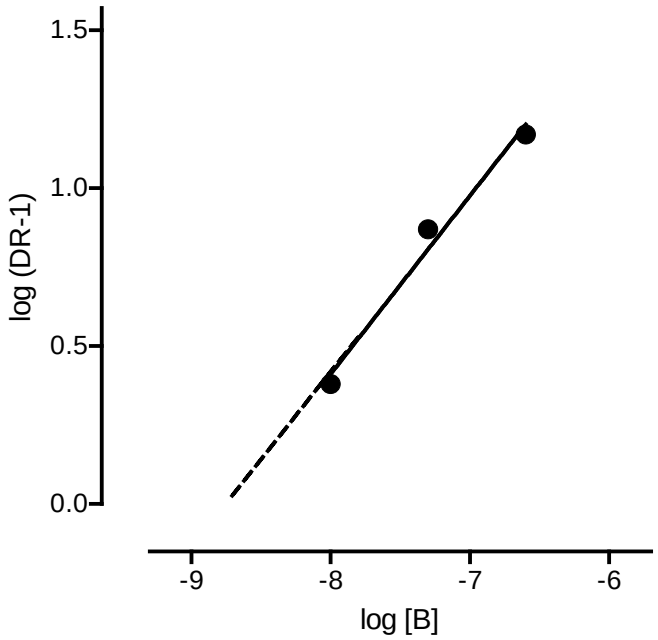

Figure 1.6 An example of a Schild plot. The regression of log (DR – 1) on log B using simulated data, gives a straight line. The pA_2 is the value of *x*-intercept, (8.73) which equals the value of – log K_b.

Similarly, in ligand binding studies, the interaction of the ligand, L and the competitive inhibitor, I can be expressed by the related equation:

$$K_b = \frac{IC_{50}}{1 + \frac{[L]}{K_d}} \quad (5)$$

where K_b is the dissociation constant of the competitor, [L] is the fixed concentration of the (radio) ligand and K_d is the dissociation constant of the (radio) ligand.

Translating equation (5) to functional system gives the interaction between the agonist, A and the competitive antagonist as:

$$K_b = \frac{IC_{50}}{1 + \frac{[A]}{EC_{50}}} \quad (6)$$

where [A] is the fixed concentration of agonist, IC_{50} is the midpoint location parameter in the inhibition curve of the antagonist and EC_{50} is the midpoint location parameter in the agonist curve (Craig, 1993). However, this equation is only valid when the agonist CRC is rectangular hyperbolic in shape, which corresponds to a Hill slope of 1.0 for the logCRC.

Commonly, the CRCs of the agonist in the majority of experiments tend to deviate from a rectangular hyperbola, thus n≠ 1. In the case of n ≠ 1, it is necessary to use a modified form of the Cheng-Prusoff equation (Leff and Dougall, 1993):

$$K_b = \frac{IC_{50}}{\left[2 + \left[\frac{[A]}{EC_{50}}\right]^n\right]^{1/n} - 1} \quad (7)$$

It has been suggested that the best method of analyzing the data from the inhibition-curve protocol is to simultaneously fit the antagonist inhibition curve and the agonist activation curve containing agonist concentrations up to the fixed concentration used in the inhibition curve. Both the agonist and antagonist concentration-effect curves constrained to have the same maximum. The dose-ratio (DR) is then calculated corresponding to the IC_{50} point on the inhibition curve (Lazareno and Birdsall, 1993a). The Gaddum-Schild equation now can be expressed as:

$$K_b = \frac{IC_{50}^*}{\frac{[A]}{EC_{50}^*} - 1} \quad (8)$$

where [A] is the fixed agonist concentration (example, at 100 nM). It should be noted that EC_{50}* will not be the same as true EC_{50} unless the fixed agonist concentration itself produced the maximal response. The IC_{50}* was estimated from an antagonist titration (inhibition curve) in the presence of 100 nM agonist (Figure 1.7B). The agonist concentration causing the same effect (EC_{50}*) is estimated from the agonist titration / CRC (Figure 1.7A).

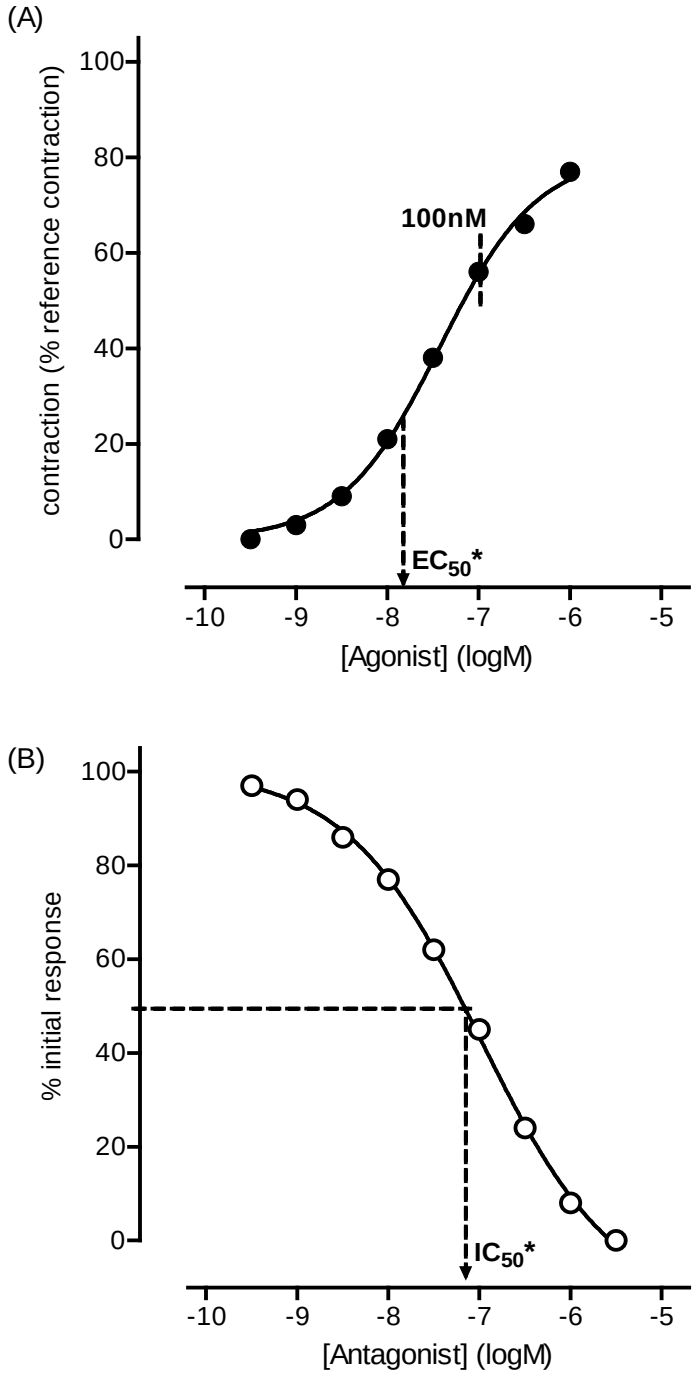

Figure 1.7 The example of basic inhibition-curve protocol used in the current experiments. (A) An agonist curve is first constructed from which the EC_{50}* is obtained. (B) An antagonist inhibition curve is then obtained on the same preparation precontracted with submaximal agonist response (e.g. 100 nM agonist); the IC_{50}* value is obtained.

Another method that was used in the current study, when the inhibition is incomplete is a 'null method' (Lazareno and Birdsall, 1993a). It makes no assumptions about the curves shapes. It is derived from the Gaddum equation (equation 3):

$$K_b = \frac{[B_i]}{\frac{[A_f]}{[A_i]} - 1} \qquad (9)$$

At any level of effect, a horizontal line joining the agonist and antagonist curves defines two concentrations, [A] and [B], i.e. $[A_i]$ and $[B_i]$ such that $[A_f]$ alone has the same effect as $[A_i]$ in the presence of $[B_i]$; so DR in the Gaddum equation above becomes $[A_f]/[A_i]$ (Figure 1.8).

The inhibition-curve protocol and null method were preferred in the current study due to limited availability of the agonists and antagonists, as both are operate over a lower agonist concentration range than Schild protocol. It may also be easier to identify whether two receptors contribute to the measured response using the inhibition-curve protocol.

The inhibition-curve protocol has seen limited use in previous studies of prostanoid antagonists. In a recent study, the properties of two novel IP antagonists, RO1138452 and RO3244794 were studied at the humans rc-IP receptor (Bley *et al.*, 2006). IP receptor antagonism was assessed by the ability of both compounds to block cAMP accumulation stimulated with a fixed-concentration of carbaprostacyclin ($cPGI_2$), a stable PGI_2 analogue. The results were consistent with selective antagonism on IP receptor, but the authors failed to use the modified form of the Cheng-Prusoff equation as described above.

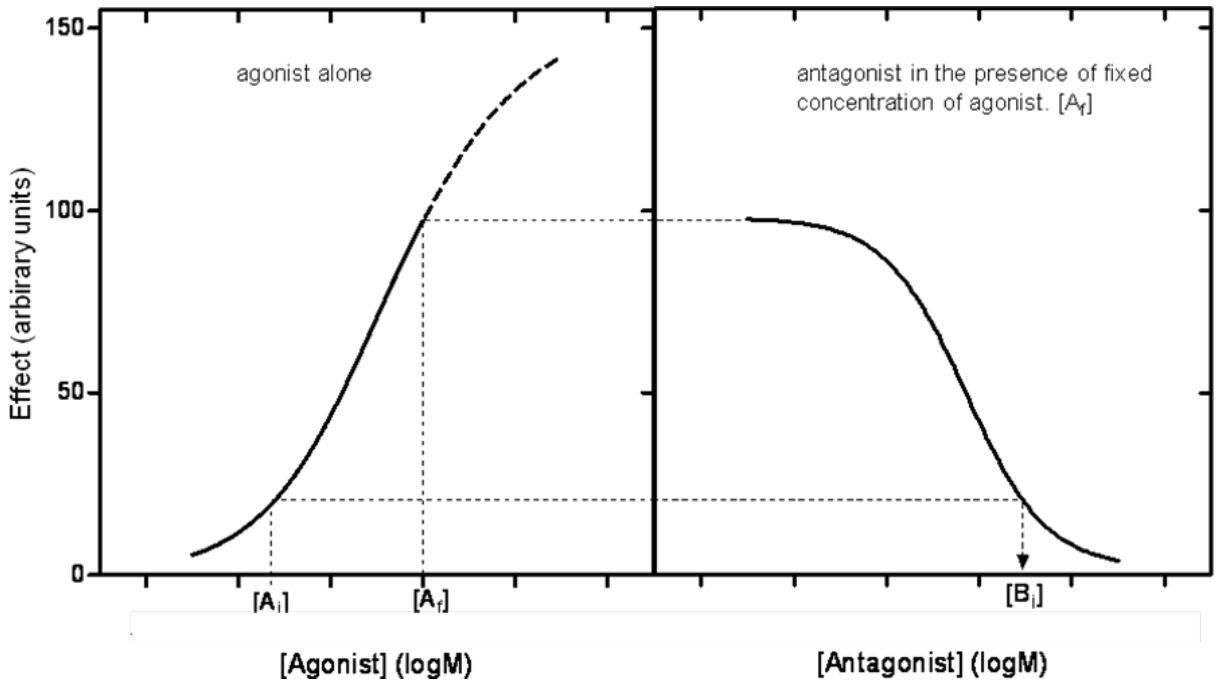

Figure 1.8 A null method for analysing antagonist inhibition curves. The dashed portion of the agonist concentration effect curve indicates data with agonist concentrations greater than the fixed agonist concentration $[A_f]$ used in the inhibition curve and do not contribute to the analysis. At any level of effect, a horizontal line joining the agonist and antagonist curves defines two concentrations, [A] and [B], i.e. $[A_i]$ and $[B_i]$ such that $[A_f]$ alone has the same effect as $[A_i]$ in the presence of $[B_i]$; so DR in the Gaddum equation above becomes $[A_f]/[A_i]$ (redrawn from Lazareno and Birdsall, 1993a).

1.8 Project aims

The main aim of the thesis was to use established and recently developed ligands to explore the nature of prostanoid receptor systems in several biological situations. These included:

1. The relaxant EP_2 system in guinea-pig trachea, with view to explaining why certain validated EP_2 agonists fail to produce their expected activities.

2. The characterization of contractile EP_1 and EP_3 receptors in vascular smooth muscle preparations where these receptors are both present. Published studies on this theme have serious deficiencies where the presence of both receptors has been proposed. It was also considered useful to identify preparations where prostanoid ligands had a rapid onset and offset of action; on-going studies by one of my supervisors had been blighted by the long incubation periods required for some ligands to reach steady-state receptor occupancy.

3. The nature of prostanoid receptors in the mesenteric artery of the rat, in view of the physiological control of the artery being similar to the human counterpart. This preparation may be a good model for pharmacological intervention studies.

4. The nature of contractile prostanoid receptors in the urinary bladder of the rat, in view of the current use of this animal to screen prostanoid ligands for potential as anti-incontinence activity.

5. The role of endogenous prostanoids activating contractile EP_3 and TP receptor systems in controlling vascular sensitivity in the rat streptozotocin model of diabetes. Previous studies on the TP system in the isolated femoral artery from the streptozotocin rat have failed to take into account the possibility of pronounced synergism with endogenous PGE_2 acting via the EP_3 receptor.

A particular focus of the work was the pharmacological utility of novel selective agonists and antagonists for EP_1 and EP_3 receptors. In studying the antagonists, inhibition-curve protocols were explored as an efficient means of establishing the onset kinetics and affinity of each antagonist, and of determining how many receptor types contribute to the agonist action. There has been little use of this type of protocol in the prostanoid receptor area.

CHAPTER TWO

GENERAL METHODS AND MATERIALS

2.1 Tissue isolation

2.1.1 Guinea-pig trachea

Male Dunkin-Hartley guinea pigs (400 - 450 g) were killed by CO_2 inhalation. The cervical trachea identified, removed immediately and dissected. The dissected trachea was pinned down on a Sylgard coated block, immersed in Krebs' solution and cleaned free of surrounding connective and fatty tissue. The trachea was cut into two rings 3 mm wide.

2.1.2 Rat mesenteric artery

Male Sprague-Dawley rats (250 - 350 g) were killed by cervical dislocation. The abdomen was dissected open and the proximal part of the superior mesenteric artery was isolated from the abdominal aorta and tied off. The superior mesenteric artery was dissected out from the surrounding connective tissue. The artery was immersed in Krebs' solution and pinned down on a Sylgard coated block and cleaned free of surrounding fat and connective tissue. Care was taken not to stretch the artery, or to damage the endothelium. The artery was either used the same day or kept overnight at 4º C in Krebs solution (viability as demonstrated by McIntyre *et al.*, 1998). Four ring segments, 3 mm in length, were prepared from each rat.

2.1.3 Rat urinary bladder

Male Sprague-Dawley rats (12 – 14 weeks old, 300 - 400 g) were killed by cervical dislocation and bleeding. The lower abdomen was dissected open, and the urinary bladder was isolated free from the surrounding structures and connective tissue. The whole bladder was excised and transported in oxygenated standard Krebs solution. The bladder was pinned down on a Sylgard coated block, immersed in Krebs' solution, and cleaned of connective tissue (Figure 2.1). The bladder was opened along the midline, and cut into longitudinal strips (7 mm long and 1.5 mm wide) (Maggi *et al.*, 1988; Schneider *et al.*, 2004). The bladder muscle strips were used immediately.

2.1.4 Rat femoral artery

Right and left femoral arteries were obtained from 10 - 12 week old normal or diabetic, male Sprague-Dawley rats (200 - 250 g). The inguinal region was dissected open and the upper section of the femoral artery was isolated and tied off (Figure 2.2). The femoral artery was then gently freed from surrounding tissue by blunt dissection down to first branch of the femoral artery, kept in standard Krebs' solution, and pinned out on a Sylgard coated block (Figure 2.3). After cleaning free of surrounding fat and connective tissue, the artery was cut into rings, measuring 1 - 1.5 mm in length. Artery sections were used immediately. When necessary, the endothelium was removed mechanically from the artery by rolling the intimal surface against a piece of roughened wire slightly thinner than the lumen of the artery. This method has been described in the study of acetylcholine's mechanism of action in cat cerebral artery (Lee, 1982). The removal of endothelium was confirmed by the inability of acetylcholine to relax the artery precontracted with noradrenaline (Furchgott and Zawadzki, 1980; Furchgott, 1983) (See section 6.3.2 for the current experiment).

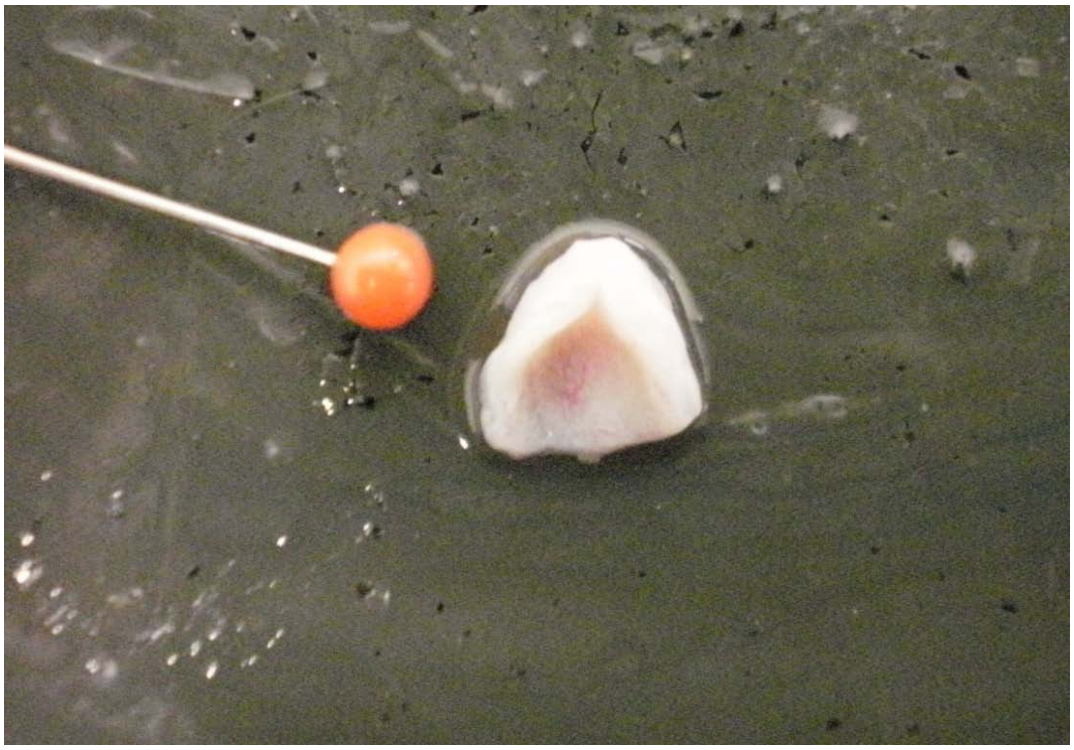

Figure 2.1 Rat urinary bladder after dissection on Sylgard plate.

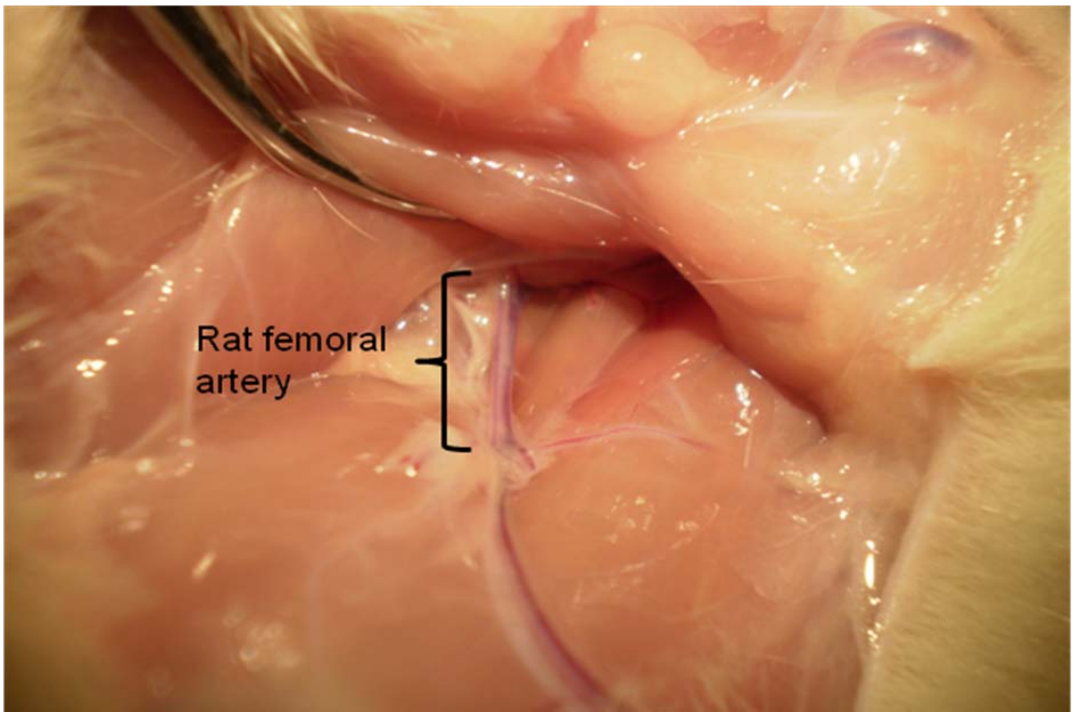

Figure 2.2 Rat femoral artery *in-situ*.

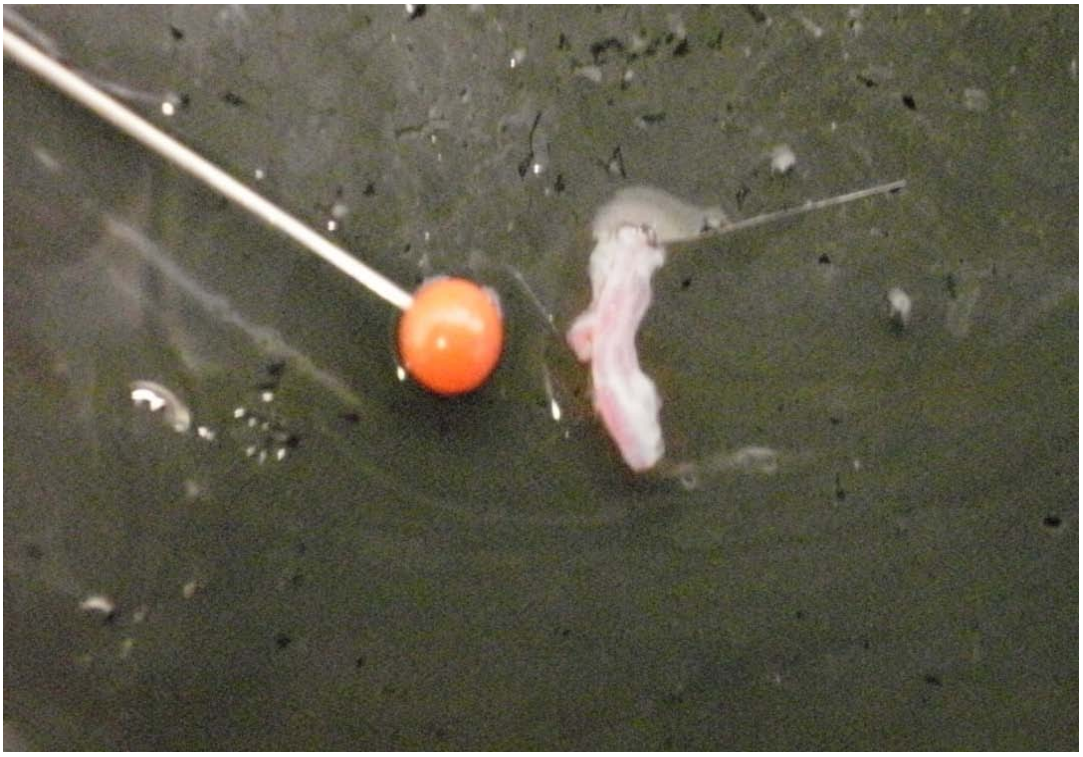

Figure 2.3 Rat femoral artery post dissection on Sylgard plate.

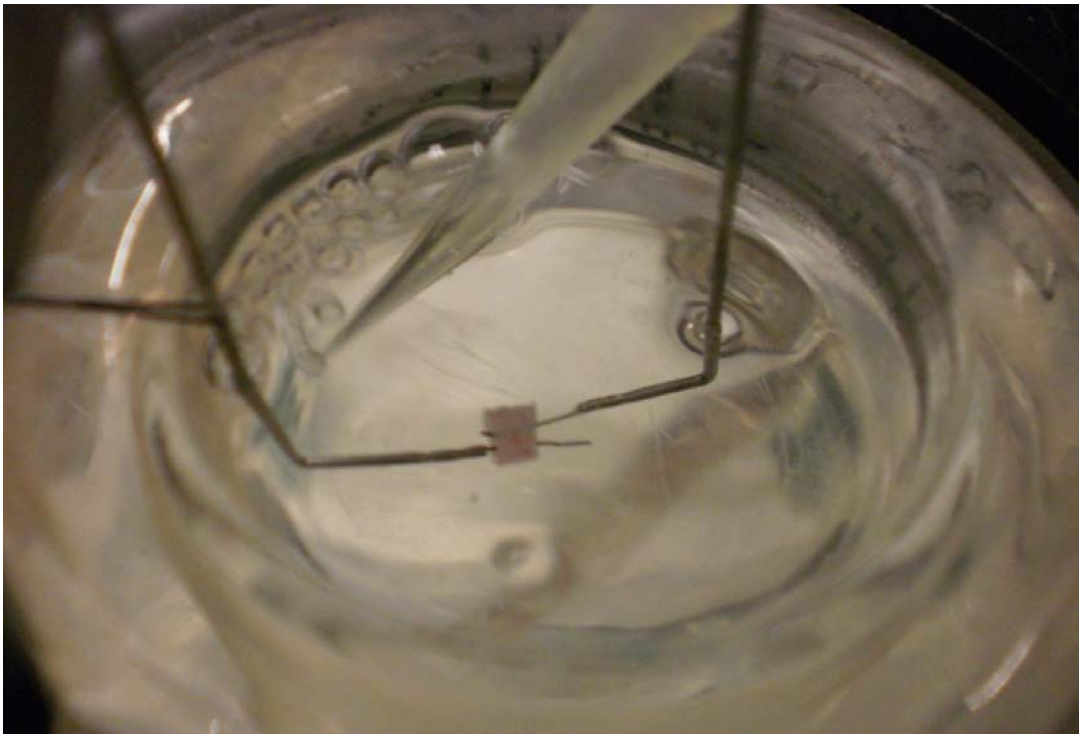

Figure 2.4 Guinea-pig trachea mounted in 10 ml organ bath.

2.2 Wire myograph

2.2.1 Krebs solution

Krebs' solution was prepared fresh on the day of the experiment. The constitution was NaCl 118.4; $NaHCO_3$ 25.0; glucose 11.1; KCl 4.7; $MgSO_4$ 1.2; $CaCl_2$ 2.5 mM, bubbled with 95% O_2 and 5% CO_2 to maintain the pH at 7.4. Where indicated, indomethacin 1 µM was added to bath solution to prevent any influences from endogenous prostanoids (Buus *et al.*, 2000; Chauhan *et al.*, 2003).

2.2.2 Organ bath

2.2.2.1 Guinea-pig trachea

The trachea ring was suspended between two intraluminal stainless steel hooks in Krebs-Henseleit solution aerated with 95% O_2 / 5% CO_2 (pH 7.4) in a conventional organ bath (10 ml) (Figure 2.4). The temperature of the Krebs was thermostatically maintained at 37 ºC using continuous water circulation. Indomethacin 1 µM was added to the Krebs solution to block any influence from endogenous prostaglandin released during the course of the experiment (Undem and Adams, 1988). One hook was fixed while the other was connected to a Grass FT03 isometric force transducer, which in turn was connected to an ADInstruments PowerLab bridge amplifier / digitizer (Chart 5.23 software, sampling rate 400/s). Signals were saved to a Dell laptop computer. Tension was set at 1.5 g, determined from the preliminary experiments as an optimal resting tension, and within range of other published studies (McKenniff *et al.*, 1988; Undem and Adams, 1988; Schlemper *et al.*, 2005). The tracheal rings were allowed to equilibrate for 1 h

with repeated adjustment to ensure the 1.5 g resting tone was maintained. The ring was contracted with increasing concentrations of potassium chloride (KCl) (20, 40 and 60 mM) at intervals of 10 min to indicate tissue viability, and was then washed several times until baseline tone was restored. Any arterial rings not contracted by more than 0.5 g (representing 50% of normal 40 mM KCl response) were excluded from the study. Washout was done manually. The preparations were allowed a further 30 - 40 min to equilibrate. In the contractile studies, the prostanoid agonists were added cumulatively to construct concentration-response curves (CRC). After washout, the preparations were contracted with the agonist to 80% of maximal response (EC_{80}), with the addition of the antagonist once the contraction had stabilised. In the relaxant sequences, histamine was used as the pre-contractile agent. Following pre-contraction, a cumulative dose-response to PGE_2 or other prostanoids (EP_2 agonists) was constructed in the presence of the EP_1 receptor antagonist, SC-51322 (1 µM) and the TP receptor antagonist, BMS-180291 (100 nM).

2.2.2.2 Rat mesenteric artery

Arterial rings were suspended horizontally between two parallel stainless steel prongs in a Danish Myo Technology Model 610 M multichannel myograph for isometric force measurement in an organ bath. The tissue baths (10 ml) contained Krebs-Henseleit solution at 37 °C aerated with 95% O_2 / 5% CO_2 (pH 7.4); washout was done by draining through automatic suction and replacement of bathing solution from a 10 ml pipette. Indomethacin 1 µM was added to bath solution to prevent any influences from endogenous prostanoids as demonstrated in previous studies (Buus *et al.*, 2000; Chauhan *et al.*, 2003). Changes in isometric force were recorded on a Dell laptop computer by use of Chart program (version 5.5.0) and a PowerLab data acquisition system (ADInstruments Ltd, Oxfordshire, UK). The resting tone was set at 1.0 g, determined by preliminary experiment and documented in other studies as optimal resting tension (Massett *et al.*, 1998). Followed a period of equilibration, the arterial rings were contracted by 40 mM of KCl to assess their viability. Any arterial rings not contracted by more than 0.5 g (representing 50% of 40 mM normal KCl response) were excluded from the study. The vessel rings were then

exposed to 10 nM PGE_2, followed by washout. A concentration-response curve was constructed for each prostanoid agonists to determine the maximal response and EC_{50} value. For inhibition curve studies, the arterial rings were precontracted with agonist (at 80% of maximal response; EC_{80}), followed by construction of an inhibition curve for the antagonist. Selective prostanoid receptor antagonists used in the current study included SC-51322 (EP_1), BMS-180291 (TP), and L-798106 (EP_3). In agonist-induced relaxation studies, the preparation was precontracted with phenylephrine followed by a cumulative addition of particular agonist was constructed.

2.2.2.3 Rat urinary bladder

Four bladder muscle strips were tied with cotton thread at each end and suspended in Krebs-Henseleit solution (containing 1 µM indomethacin) aerated with 95% O_2 / 5% CO_2 (pH 7.4) in a conventional organ bath (10 ml) and maintained at 37 °C. The tension signals were relayed from a Grass FT03 force transducer to an ADInstruments PowerLab bridge amplifier / digitizer (ADInstruments Ltd, Oxfordshire, UK) and recorded on a Dell laptop computer by use of Chart program (version 5.5.6). 1 g was set as the resting tension for this preparation, determined by preliminary experiments and has been documented in previous studies (Maggi *et al.*, 1988; Schneider *et al.*, 2004).

The bladder strips were allowed to equilibrate for 1 h, and were challenged twice with carbachol at 100 nM. After washout and an additional 30 min of equilibration, the preparations were exposed to 30 nM PGE_2 for 10 min. In contractile studies, a concentration-response curve was constructed by cumulative addition of the particular agonist. In successive sequences, the vehicle (serving as control) or antagonist at different concentrations was added at least 30 min before the cumulative addition of the agonist. For antagonist studies, the bladder strips were contracted with agonist, followed by construction of an inhibition curve for the antagonist.

2.2.2.4 Rat femoral artery

The arterial rings were mounted using the same technique outlined in Section 2.2.2.2. The resting tone was set at 1.0 g, determined in preliminary experiments. It has also been documented in previous studies (Shi *et al.*, 2007a; Shi *et al.*, 2007b). Reliable contractions to 60 mM KCl were used as an indication of tissue viability. The criteria of exclusion as described in Section 2.2.2.1 were applied. Phenylephrine was used as the precontractile agent. Where applicable, the antagonists used were preincubated for 30 min before cumulative addition of phenylephrine.

2.3 Streptozotocin-induced diabetes

Diabetes was induced with a single dose of streptozotocin (STZ; 60 $mgkg^{-1}$, i.p) after overnight fasting (Pfaffman *et al.*, 1982; Peredo *et al.*, 1999; Burke *et al.*, 2006). Control rats were injected with saline corresponding to the volumes of the STZ vehicle. 72 hours after STZ injection, a blood sample was taken from the tail artery and the fasting blood glucose level was measured using an Ascensia Breeze 2 glucometer (Bayer HealthCare, UK). The cut-off level for fasting blood glucose level to be considered as diabetic was 16 $mmol^{-1}$. Any rat with blood level below 16 $mmol^{-1}$ was excluded from the study and sacrificed. Body weight was measured weekly and rats were kept under optimal conditions and given a normal diet. The rats were decapitated four weeks following the STZ injection. Blood glucose and body weight were measured just before the decapitation. Control rats with non-fasting blood glucose higher than 11.1 $mmol^{-1}$ were excluded from the study. All procedures conformed to Home Office Guidelines. Figure 2.5 summarizes the STZ-induced diabetes protocol in the current study.

2.4 Antagonist protocol and pA_2 estimation

In the current study, the inhibition-curve protocol was preferred to the Schild protocol due to limited availability of the agonists and antagonists and the shorter time period required (Lazareno and Birdsall, 1993b). Basically, the protocol involved initial construction of a concentration-response curve for the agonist. After washout, the preparation was submaximally pre-contracted with agonist (usually at 80% of maximal agonist response, EC_{80}) followed by cumulative addition of the antagonist (Figure 2.6). The experimental data were then fitted separately to construct the antagonist inhibition curve and the agonist activation curve containing agonist concentrations up to the fixed concentration used in the inhibition curve.

From both agonist and antagonist curve, pA_2 (= – log K_b) of the antagonist was estimated using the equation below:

$$K_b = \frac{IC_{50}^*}{\frac{[A]}{EC_{50}^*} - 1}$$

and

$$K_b = \frac{[B_i]}{\frac{[A_f]}{[A_i]} - 1}$$

as been described in detail in General Introduction chapter (section 1.7.2).

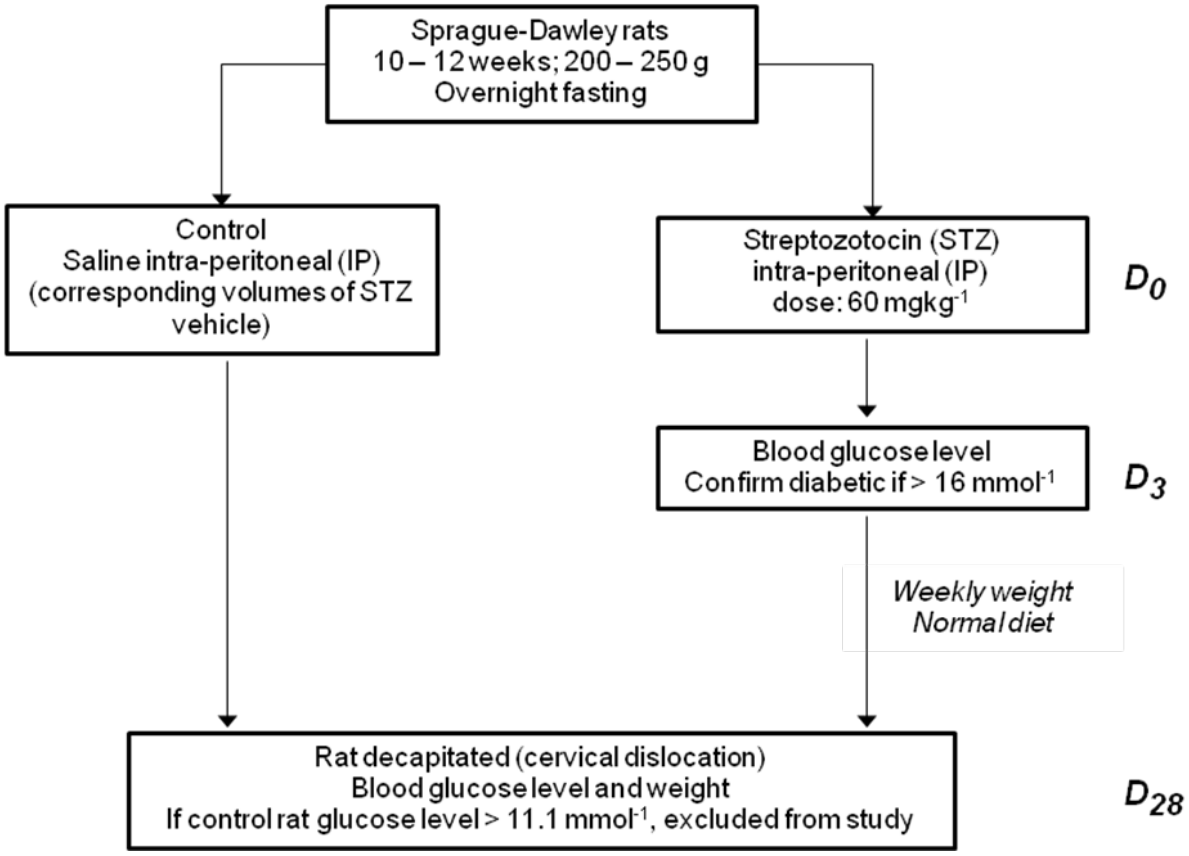

Figure 2.5 The protocol for streptozotocin (STZ)-induced diabetes in rat.

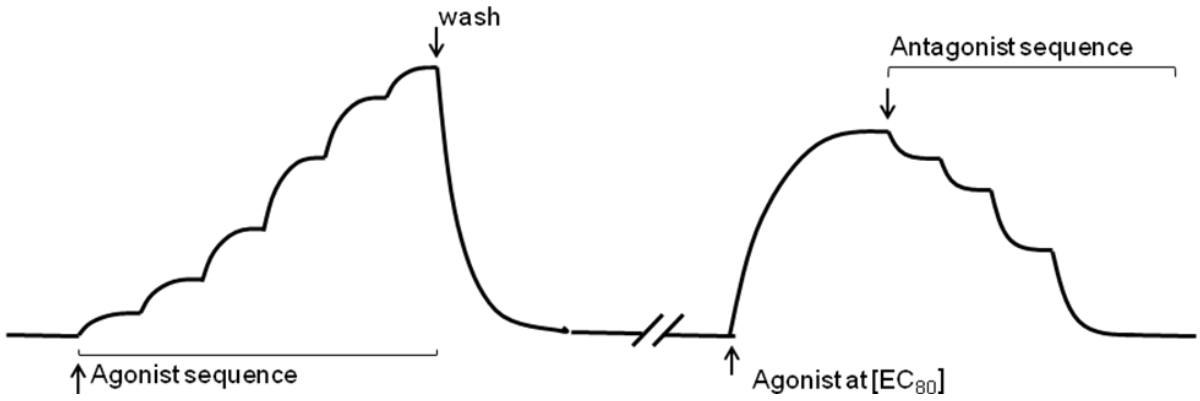

Figure 2.6 Inhibition curve protocol for estimating antagonist affinity.

2.5 Data Analysis

2.5.1 Statistical analysis

Contractile responses were measured as increases in tension (g) above the resting level, and normalized to the second 60 mM K^+ response (K-standard) in the case of rat femoral artery and to the second 100 nM carbachol in rat urinary bladder preparation. Relaxant responses were expressed as a percentage of the established tone induced by a pre-contractile agent. Log concentration-response curves were fitted by sigmoidal curves using GraphPad Prism v4.0 software (GraphPad, San Diego, CA). Where appropriate, the lower asymptote was constraint to zero for contractile agonists and the upper asymptote to 100% for relaxant agonists or antagonists. EC_{50} and IC_{50} values were computed from these curves. Data for individual preparations were used to obtain sigmoidal curve parameters, from which mean $\pm$ SEM were calculated.

Data were analysed by 1-factor and repeated measures 2-factor ANOVA with GraphPad Prism. A pair of means was compared by planned orthogonal contrasts using SuperANOVA software (Abacus Concepts Inc). Planned contrasts represent a robust method of comparing multiple means (Glass and Hopkins, 1996; Bewick *et al.*, 2004). Initially, main effects were assessed for statistical significance by planned (orthogonal) contrasts; individual cell means were then compared as required. Unpaired Student's *t-test* was used to compare two mean values. All tests were two-tailed and the significance level was set at $p < 0.05$.

2.5.2 Two-site competition model

When two components / receptors comprise the response inhibited by the prostanoid, the data fitted by the nonlinear regression analysis (one-site competition equation) using GraphPad Prism will appear to be deviate from the data points. The next step is to fit the inhibition data using the two-site competition equation in GraphPad Prism. The Hill slopes of both sigmoidal components are automatically constrained to 1.0. If the two IC_{50} values are at least a log apart with a narrow and significant 95% confidence interval (CI), then the sum-of-squares (SS) is compare statistically using the modified F test (refer to Motulsky and Christopoulos, 2004). The assumption is based on Null hypothesis that two-site model is better than one-site model in fitting the curves. The two models are compared for goodness-of-fit, with adjusting for difference in the number of degrees of freedom (df), and the F ratio between two models. From F table (Appendix), if $p < 0.05$, we can conclude that the two-site competition equation model fits the data significantly better than the one-site model.

The regression correlation coefficient (r^2-values) for the graph fits in nonlinear regression analysis were also analysed (refer to Motulsky and Christopoulos, 2004). The r^2-values can be obtained from result sheets of the fitted curve with GraphPad Prism. The values range from −1 to 1. A value of 1 implies that a linear equation describes the relationship between *X* and *Y* perfectly, with all data points lying on a line for which *Y* increases as *X* increases. A value of −1 implies that all data points lie on a line for which *Y* decreases as *X* increases. A value of 0 implies that suggests a poor model. The closer the r^2-value to 1, the better the data fitted by the line.

These two-site competition model comparisons with one-site model were applied in guinea-pig trachea, rat mesenteric artery and rat urinary bladder chapters.

2.6 Reagents and chemicals

Table 2.1 lists the reagents and chemicals used in the current experiments.

Table 2.1 Reagents and chemicals used in the current experiments

Agents	**Source**	**Stock**	**Solvent**
17-Phenyl PGE_2 17-phenyl-ω-trinor prostaglandin E_2	Cayman Chemical, USA	10 mM	Absolute ethanol
AH-13205 7-[2-[4-(1-hydroxyhexyl)phenyl]-5-oxo cyclopentyl]heptanoic acid	Cayman Chemical, USA	10 mM	Absolute ethanol
Acetylcholine chloride	Sigma-Aldrich Chemicals, USA	10 µM	Distilled water
BMS-180291 [1s-(*exo*,*exo*)]-2-[[3-[4-[(pentylamino)carbonyl]-2-oxazolyl]-7-oxabicyclo[2.2.1]hept-2-yl]methyl]-benzenepropanoic acid	Bristol-Myers Squibb, USA.	1 mM	Absolute ethanol
Butaprost-FA (±)-15-deoxy-16S-hydroxy-17-cyclo butyl PGE_1	Cayman Chemical, USA	10 mM	Absolute ethanol
Carbachol hydrochloride	Sigma-Aldrich Chemicals, USA	10 mM	Distilled water
CAY-10399 (±)-15-deoxy-16S-hydroxy-17-cyclo butyl PGE_2	Cayman Chemical, USA	10 mM	Absolute ethanol
CAY-10441 (4,5-dihydro-1H-imidazol-2-yl)-[4-(4-isopropoxybenzyl)phenyl]amine	Cayman Chemical, USA	1 mM	Absolute ethanol
CP-533536 2-[3-[N-(4-tert-butylbenzyl)-N-(pyridin-3-ylsulfonyl)aminomethyl]phenoxy]acetic acid	Pfizer, UK	10 mM	Absolute ethanol
GW-848687 6-[2-(5-chloro-2-[(2,4-difluorophenyl)methyl]oxy}phenyl)-1-	GlaxoSmithKline Research & Development, UK	1 mM	Dimethylsulphoxide (DMSO)

Agents	Source	Stock	Solvent
cyclopenten-1-yl]-2-pyridinecarboxylic acid			
Histamine diphosphate	Sigma-Aldrich Chemicals, USA	10 µM	Distilled water
Iloprost 6,9α-methylene-11α,15S-dihydroxy-16-methyl-prosta-5E,13E-dien-18-yn-1-oic acid	Cayman Chemical, USA	10 µM	Absolute ethanol
Indomethacin	Sigma-Aldrich Chemicals, USA	20 mM	Absolute ethanol
Isoprenaline hydrochloride	Sigma-Aldrich Chemicals, USA	100 µM	Distilled water
L-798106 5-bromo-2-methoxy-N-[3-(naphthalen-2-yl-methylphenyl)-acryloyl]-benzene sulphonamide	GlaxoSmithKline Research & Development, UK	10 mM	Dimethylsulphoxide (DMSO)
L-826266 [(2E)-N-[(5-bromo-2-methoxyphenyl)-sulfonyl]-3-[5-chloro-2-(2-naphthylmethyl)phenyl]acrylamide	Dr David Woodward, Allergan Pharmaceuticals, USA	10 mM	Dimethylsulphoxide (DMSO)
Lataprost-FA 17-phenyl-13,14-dihydro prostaglandin $F_{2\alpha}$	Cayman Chemical, USA	10 mM	Absolute ethanol
ONO-AE1-259 11,15-O-dimethyl prostaglandin E_2	Ono Pharmaceuticals, Japan	10 µM	Absolute ethanol
ONO-AE-248 11,15-O-dimethyl-PGE_2	Dr David Woodward, Allergan Pharmaceuticals, USA	10 mM	Absolute ethanol
ONO-DI-004 (17S)-2,5-ethano-6-oxo-17,20-dimethyl PGE_1	Dr David Woodward, Allergan Pharmaceuticals,	10 mm	Absolute ethanol

Agents	**Source**	**Stock**	**Solvent**
	USA		
$PGF_{2\alpha}$ 9α,11α,15S-trihydroxy-prosta-5Z,13E-dien-1-oic acid	Cayman Chemical, USA	10 µM	Absolute ethanol
Phenylephrine hydrochloride	Sigma-Aldrich Chemicals, USA	1 µM	Distilled water
Potassium chloride	Sigma-Aldrich Chemicals, USA	1 mM	Distilled water
Prostaglandin E_2	Cayman Chemical, USA	10 mM	Absolute ethanol
SC-51322 8-chlorodibenz[b,f][1,4]oxazepine-10(11H)-carboxylic acid, 2-[3[2-(furanyl methyl) thio]1-oxopropyl] hydrazine	Biomol International, USA	10 µM	Absolute ethanol
Streptozotocin 2-deoxy-2-(3-(methyl-3-nitrosoureido)-D-glucopyranose	Alexis Biochemical, UK	20 mg/ml	Sodium-Citrate
Sulprostone	Cayman Chemical, USA	5 mM	Absolute ethanol
U-46619 9,11-dideoxy-9α,11α-methanoepoxyprostaglandin $F_{2\alpha}$	Cayman Chemical, USA	10 µM	Absolute ethanol

CHAPTER THREE

GUINEA-PIG TRACHEA

3.1 Introduction

The guinea-pig isolated trachea (GPT) was used in the early part of my PhD study. In view of my lack of laboratory experience, this preparation was considered a suitable starting point to measure agonist and antagonist potency in smooth muscle preparations.

This robust preparation has been widely used in the past to characterize selective β_2-adrenoceptor agonists and for studies on autonomic innervation. The presence of prostanoid receptors in the guinea-pig trachea has been well documented. Activation of EP_1 and TP receptors has been shown to cause a contractile response (Jones *et al.*, 1982; Coleman and Kennedy, 1985; Eglen and Whiting, 1988; McKenniff *et al.*, 1988; Ndukwu *et al.*, 1997). On the other hand, a relaxant effect was demonstrated to be mediated by EP_2 receptor (Gardiner, 1986; Eglen and Whiting, 1988).

Initially, the activities of PGE_2, 17-phenyl PGE_2, sulprostone and U-46619 were investigated. PGE_2 is a prostanoid which activates both contractile and relaxant EP receptors, with weak affinity on the TP receptor (Kiriyama *et al.*, 1997; Abramovitz *et al.*, 2000). 17-Phenyl PGE_2 has a moderate affinity to EP_1, with some activity to EP_3 and minimal to EP_2 (Lawrence *et al.*, 1992; Breyer *et al.*, 2001). Sulprostone has a higher affinity to EP_3 more than EP_1, with some activity on FP receptors (Kiriyama *et al.*, 1997; Abramovitz *et al.*, 2000).

Subsequently, the activities of several EP_2 agonists were investigated. I was particularly interested in AH-13205, which does not show the IOP-lowering activity typical of others EP_2 agonists (Woodward *et al.*, 1995). The intention was to examine the nature of the AH-13205 log concentration-response curve (CRC) to see whether there is any evidence for partial agonism at the EP_2 receptor. Analogously, the ability of AH-13205 to relax under high contractile tone was

investigated; relative to full agonist, a EP_2 partial agonist should show a poorer relaxation when working against higher tone. In addition to PGE_2 and AH-13205, other EP_2 agonists examined were butaprost-FA; CAY-10399 and CP-533535 (Gardiner, 1986; Armstrong, 1995; Kiriyama *et al.*, 1997; Abramovitz *et al.*, 2000; Breyer *et al.*, 2001; Tani *et al.*, 2001; Paralkar *et al.*, 2003; Jones, 2004). CP-533535 has a non-prostanoid structure (refer to Figure 1.3).

Table 3.1 lists the antagonists used in the current study with their respective affinities on the prostanoid receptors. McKeniff *et al.* (1988*)* have demonstrated that the contractile response to U-46619 in guinea-pig trachea is selectively antagonised by the TP antagonists EP-092 and AH-23848. The study also demonstrated that the EP_1 antagonist AH-6809 selectively antagonised the responses to 16,16-dimethyl PGE_2 and $PGF_{2\alpha}$. In the current study, the potent and selective EP_1 antagonist, SC-51322 was used to antagonise the EP_1 effect, while BMS-180291 was used to block the TP receptor (Zhang *et al.*, 1996; Clarke *et al.*, 2004; Hung *et al.*, 2006). Using agonists, direct contraction via EP_3 receptors has not been demonstrated in previous studies on guinea-pig trachea; however EP_3 receptors on parasympathetic nerve endings inhibit transmitter release (Spicuzza *et al.*, 1998; Clarke *et al.*, 2004). In the current study, L-798106, a selective EP_3 antagonist was used to demonstrate whether activation of the EP_3 receptor causes contraction of the tracheal smooth muscle (Clarke *et al*., 2004).

Table 3.1 Antagonists and concentrations chosen for use in the current study.

Antagonists	**Reported pA_2**	**Concentration**	**Expected dose-ratio**	**References**
SC-51322	8.45	1 µM	280	Hung *et al.*, 2006
BMS-180291	9.5 – 9.8	0.1 µM	320 – 630	Zhang *et al.*, 1996
L-798106	7.48 – 7.82	1 µM	30 – 66	Clarke *et al.*, 2004

3.2 Methods

The basic methodology used has been described in detail in Chapter 2. Specific methodological points not discussed previously are addressed below.

3.2.1 Setting up of preparations

The cervical trachea was removed from guinea pig, mounted on myograph as described in Chapter 2. Resting tone was set at 1.5 g, determined from as an optimal resting tension in preliminary experiment, and within range of other published studies (McKenniff *et al.*, 1988; Undem and Adams, 1988; Schlemper *et al.*, 2005). After period of equilibration of 1 hour, viability of the tracheal ring was determined as described in Chapter 2. 1 µM indomethacin was added in Krebs solution throughout the experiment with the tracheal ring.

In the contractile studies, the prostanoid agonists were added to determine the maximal response (E_{max}) with the construction of CRC's. Except when U-46619 used as agonist, 100 nM BMS-180291 was added 30 min before the addition of other prostanoid agonist. Following period of washout, the preparations were subsequently contracted with the agonist to 80% of maximal response (EC_{80}), with the addition of the selective antagonist once the contraction had stabilised (Figure 3.1A).

In the relaxant sequences, 1 µM SC-51322 and 100 nM BMS-180291 were added 30 min before addition of the pre-contractile agent, histamine (see results section). Histamine was chosen (at a concentration corresponding to 30 or 80% maximum response) as it is a non-prostanoid regulator of airways smooth muscle. Furthermore, the contraction produced by histamine is consistent and

does not fade throughout the experimental period. Once the tone is established and stable, PGE_2 or other prostanoids (EP_2 agonists) were cumulatively added to construct cumulative-inhibition curves (Figure 3.1B).

3.2.2 Statistical analysis

Contractile responses were measured as increases in tension (g) above the resting level. The relaxant responses were expressed as a percentage loss of the initial contractile tone developed to the established tone of the contractile agonist or histamine. A variable-slope sigmoidal curve was fitted to log concentration–response data using GraphPad Prism software; the bottom asymptote was constrained to zero for contraction and to 100% for relaxation. Sigmoidal curve parameters were derived from data for individual preparations. Data were further analysed by 1-factor and repeated measures 2-factor ANOVA combined with comparison of selected means by planned (orthogonal) contrasts using SuperANOVA software; all tests were two-tailed and the significance level was set at $p < 0.05$. Where applicable, data were analysed by the two-site competition equation using the modified F test in combination with the r^2-values comparison (refer to Motulsky and Christopoulos, 2004). All data are presented as mean $\pm$ SEM.

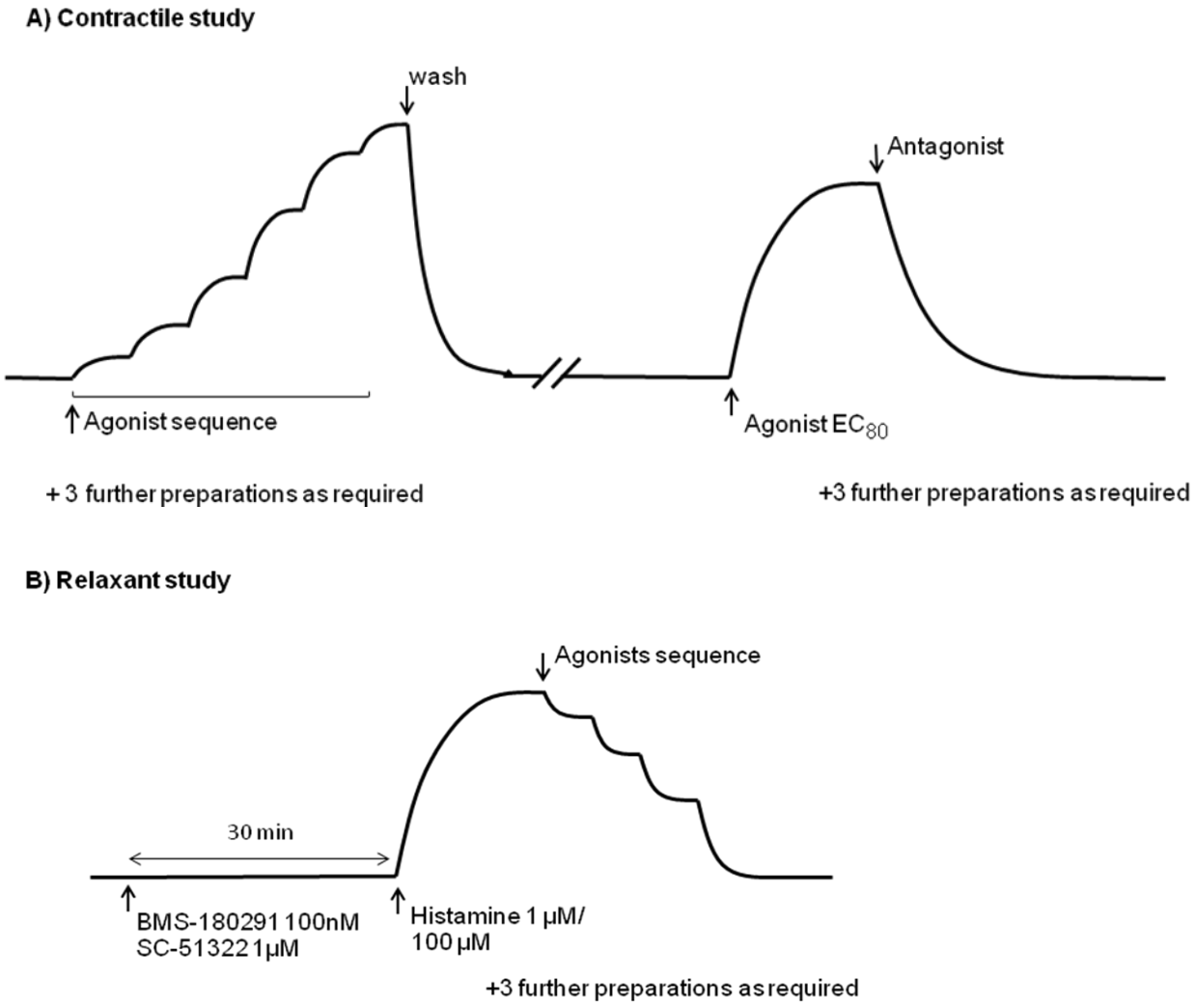

Figure 3.1 Experimental protocols for guinea-pig trachea. A) The protocol used for contractile study. B) The protocol used in relaxant study, where GPT was precontracted with two different concentrations of histamine, corresponding to EC_{30} and EC_{80} of maximal histamine responses.

3.3 Results

3.3.1 Effects of histamine

Histamine contracted GPT in a concentration-dependent manner with maximal response of 2.4 ± 0.2 g and pEC_{50} of 5.32 ± 0.17 (Figure 3.2, n = 4).

3.3.2 Effects of prostanoid agonists

In early part of the study, the effect of U-46619, a selective TP agonist was studied. Increasing concentrations of U-46619 (1 nM – 1 µM) were added cumulatively. Log concentration-responses curve (CRC) was plotted as shown in Figure 3.3 (n = 8). U-46619 contracted the preparation to a maximum response (E_{max}) of 2.8 ± 0.2 g. The pEC_{50} was 7.57 ± 0.07. BMS-180291 at 100 nM completely blocked the established tone.

PGE_2, a non-selective EP agonist was examined in the presence of 100 nM BMS-180291 to block any influence from activation of TP receptors. PGE_2 (1 nM – 1 µM) produced a concentration-dependent contractile response in GPT as demonstrated in Figure 3.4 (n = 4). The maximal response was 1.6 ± 0.1 g with pEC_{50} of 7.76 ± 0.09. Administration of 1 µM SC-51322 to the established tone of PGE_2 reduced the contractile response to resting tension.

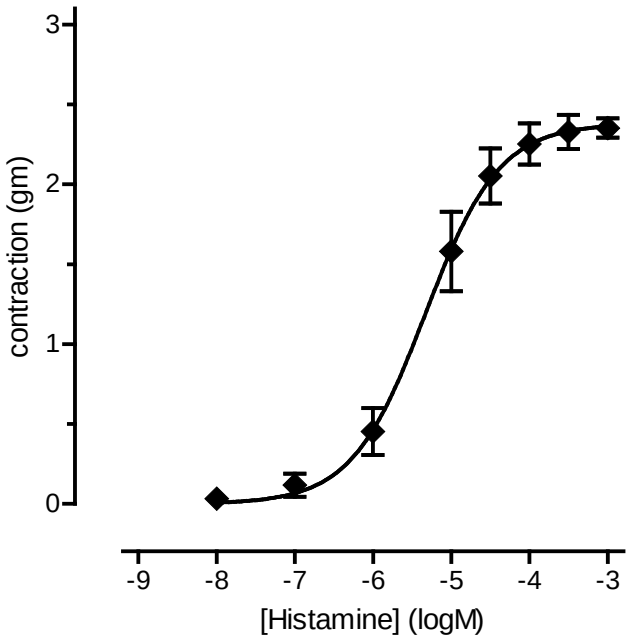

Figure 3.2 Contractile activity of histamine on guinea-pig trachea. Histamine contracted the trachea in concentration-dependent manner (n = 4).

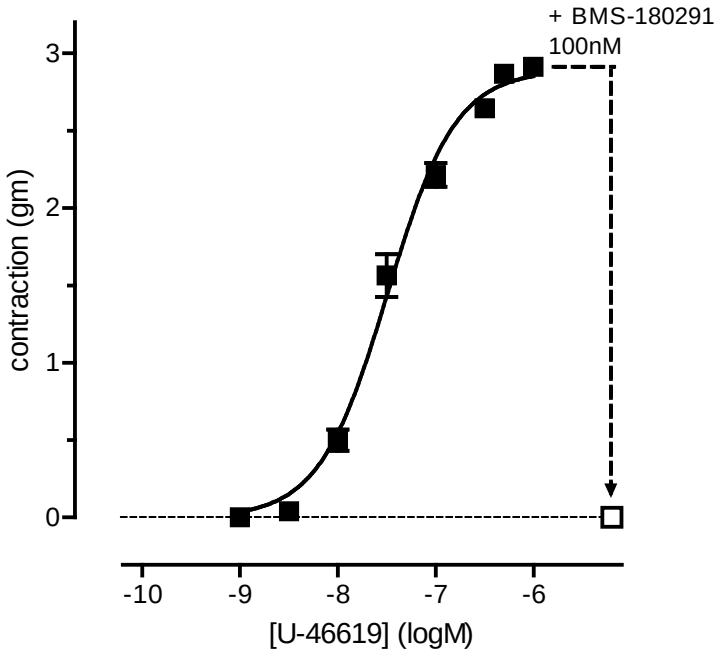

Figure 3.3 Contractile activity of U-46619 on guinea-pig trachea. U46619 (1 nM – 1 µM), a selective TP agonist contracted the trachea in a concentration dependent manner (*n* = 8). 100 nM BMS-180291 completely antagonised the response.

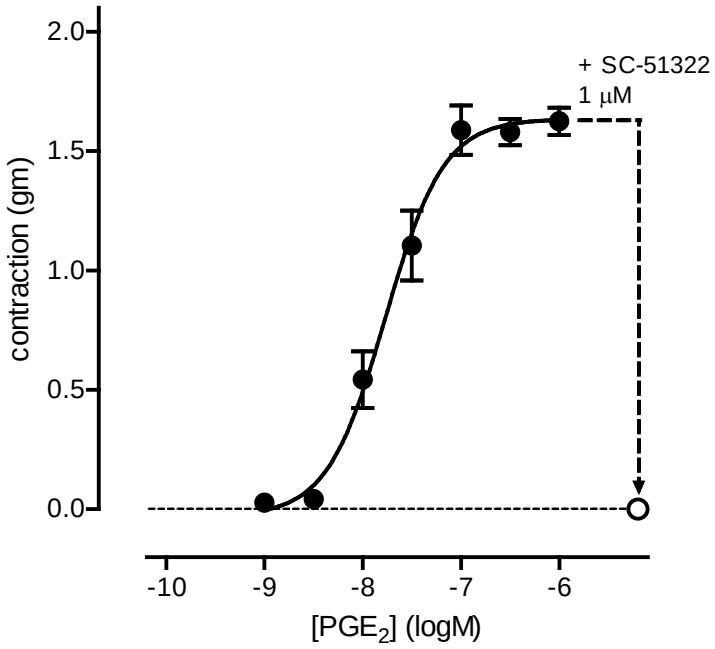

Figure 3.4 Contractile activity of PGE_2 on guinea-pig trachea. PGE_2 (1 nM – 1 μM), a non-selective agonist at EP receptors contracted the trachea in concentration-dependent manner (*n* = 4). 100 nM BMS-180291 was present. 1 μM SC-51322 completely relaxed the tone.

In the presence of BMS-180291, 17-phenyl PGE_2 (1 nM – 1 μM) contracted GPT in concentration-dependent manner with E_{max} 1.5 ± 0.1 g and pEC_{50} 7.63 ± 0.09 (Figure 3.5, *n* = 4). Likewise, the established tone of 17-phenyl PGE_2 was completely inhibited by 1 μM SC-51322.

The effects of sulprostone, (affinity of EP_3 > EP_1, minimal on EP_4 and EP_2) on GPT can be observed as in Figure 3.6 (*n* = 4). Sulprostone (1 nM – 1 μM) produced a contractile response in dose-dependent manner with E_{max} of 2.3 ± 0.2 g and pEC_{50} of 7.88 ± 0.05. SC-51322 at 1 μM abolished the established tone by 100 nM sulprostone. In contrast, L-798106 at 1 μM had no effect on the 100 nM sulprostone-induced tone.

The contractile effects of the agonists used are summarized in Table 3.2.

The selectivity of SC-51322 on GPT using the inhibition-curve protocol is demonstrated in Figure 3.7. SC-51322 inhibited the established tone of 10 nM 17-phenyl PGE_2 in concentration-dependent manner. At 1 μM, SC-51322 completely blocked the 17-phenyl PGE_2 contraction. At 10 μM, SC-51322 relaxed of the 30 nM U-46619-induced tone by about 10% and had no effect at all on 10 nM carbachol-induced tone.

At this point, it was decided to include 100 nM BMS-180291 and 1 μM SC-51322, pre-incubated for 30 min for all agonist or antagonist sequences, to ensure that there was no interference from TP and EP_1 contractile component in the relaxant studies.

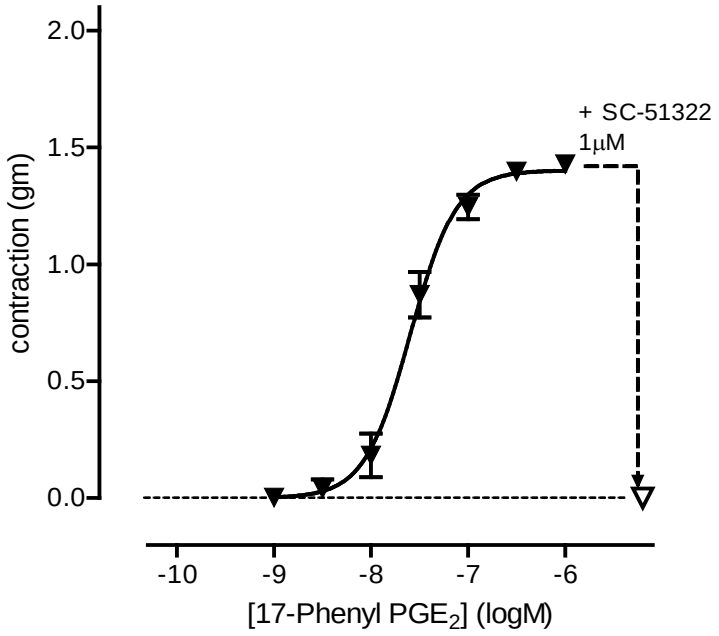

Figure 3.5 Contractile activity of 17-phenyl PGE_2 on guinea-pig trachea. 17-Phenyl PGE_2 (1 nM – 1 μM) was used in the experiment (n = 4). 100 nM BMS-180291 was present. 1 μM SC-51322 completely relaxed the tone.

Table 3.2 The pEC_{50} and maximal response (E_{max}) of the prostanoid agonists in the contractile study.

	pEC_{50}	**E_{max} (g)**
U-46619	7.37 ± 0.07	2.8 ± 0.2
PGE_2	7.76 ± 0.09	1.6 ± 0.1
17-Phenyl PGE_2	7.63 ± 0.09	1.5 ± 0.1
Sulprostone	7.88 ± 0.05	2.3 ± 0.2†

* All the experiments were done in the presence of 1 μM indomethacin and 100 nM BMS-180291 (When U-46619 as the agonist, BMS-180291 was omitted).
† $P < 0.05$, sulprostone vs. PGE_2, 17-phenyl PGE_2.

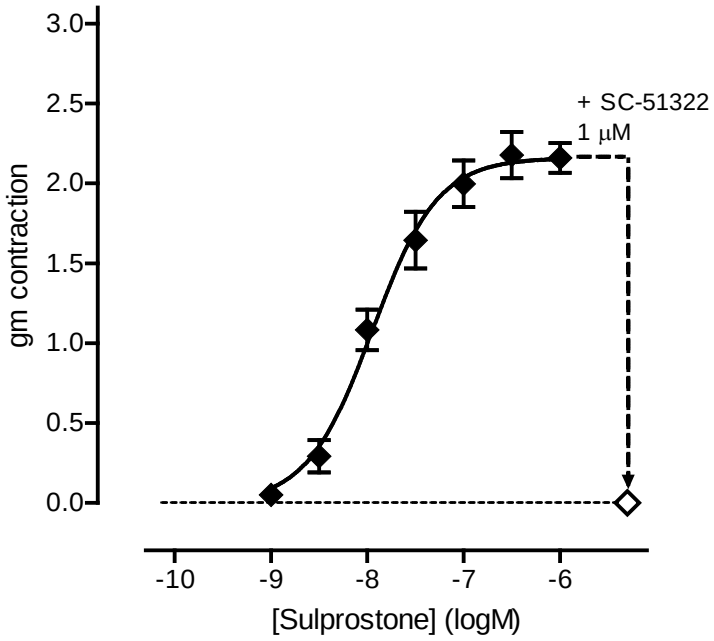

Figure 3.6 Contractile activity of sulprostone on guinea-pig trachea. Sulprostone (1 nM – 1 µM) was used in the experiment (n = 4). 100 nM BMS-180291 was present. 1 µM SC-51322 completely relaxed the tone.

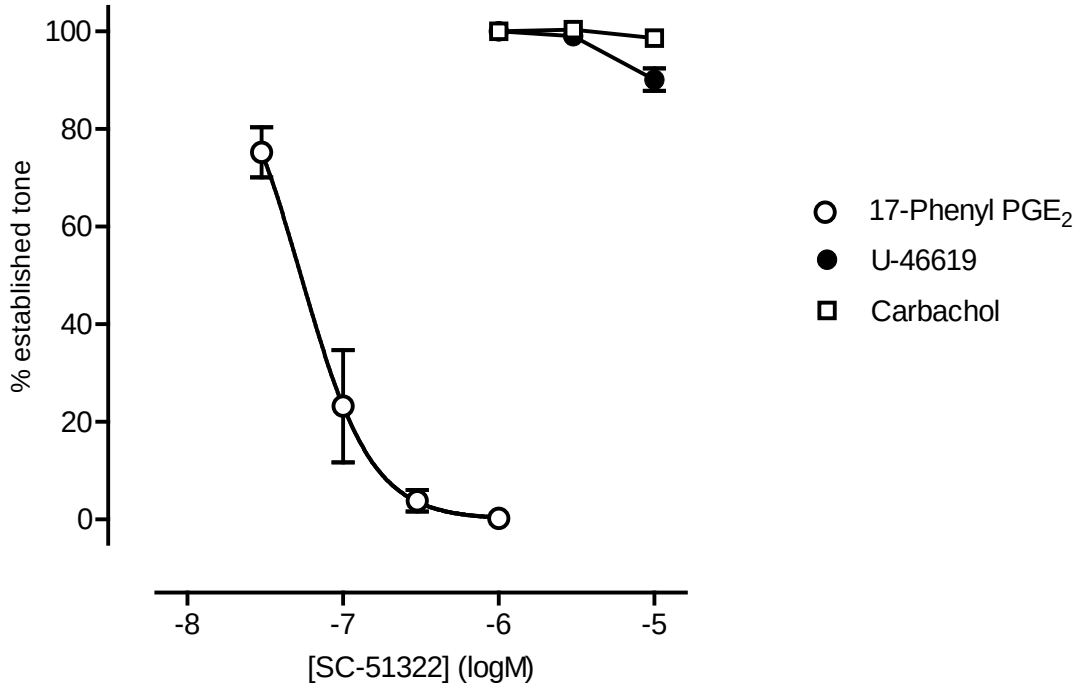

Figure 3.7 Antagonism by SC-51322 of contraction induced by 10 nM 17-phenyl PGE_2, 30 nM U-46619 and 10 nM carbachol in guinea-pig trachea (n = 4, n = 2, n = 3; respectively). 1 µM indomethacin is present.

3.3.3 Effects of PGE_2 and butaprost on precontracted guinea-pig tracheal ring under low tone

Preliminary experiments established that histamine produced a stable contractile response in the GPT. Hence, histamine was chosen as the contractile agent. Once the tone was established, the prostanoid agonist was added cumulatively to construct an inhibition curve (Figure 3.1B).

Initially, GPT was precontracted with histamine 1 μM (representing 30% of maximal histamine contraction). The response to cumulative doses of PGE_2 and the selective EP_2 antagonist, butaprost are shown in Figure 3.8 (n = 4). PGE_2 and butaprost-FA (a selective EP_2 agonist) relaxed the preparation in a concentration-dependent manner. Butaprost-FA was about 6 times less potent than PGE_2. Butaprost-FA is considerably less potent than PGE_2 on EP_4 receptors (Wilson *et al.*, 2004), and therefore at this stage, it was concluded that the relaxation by PGE_2 is most likely mediated by the EP_2 receptor. It is also clear that SC-51322 at 1 μM is sufficient for inhibition of the EP_1 agonist activity of PGE_2, thereby exposing its EP_2 relaxant activity. The other agonists studied were expected to have lower EP_1 agonist potencies than PGE_2.

After further experimentation, it was decided that differences in receptor efficacy on the EP_2 system might be demonstrable if relaxation curves were obtained against a much higher tone level. Histamine concentrations of 1 μM and 100 μM were therefore chosen to contract the tracheal rings, corresponding to about 30 and 80% of the histamine maximum respectively.

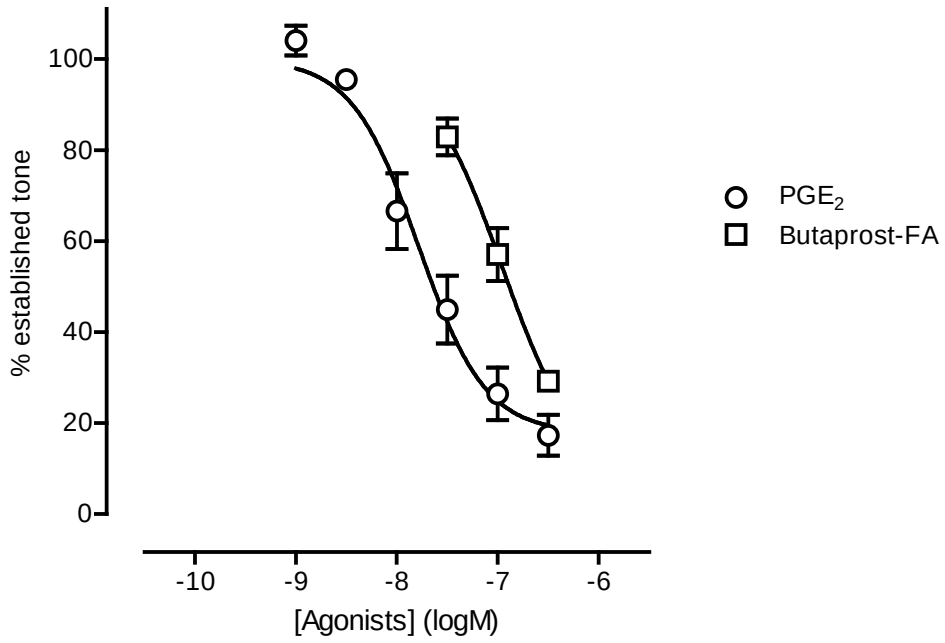

Figure 3.8 Relaxation activity of PGE_2 and butaprost-FA on pre-contracted guinea-pig trachea. GPT was pre-contracted with 1 μM histamine. PGE_2 (1 – 300 nM) and butaprost (30 – 300 nM) were used as agonists (n = 4). 100 nM BMS-180291 and SC-51322 1 μM were present.

3.3.4 Comparison of EP_2 agonists on precontracted guinea-pig tracheal ring under low tone and high tone

Table 3.3 listed the maximal relaxation and pIC_{50} of the EP_2 agonists used in the current study.

PGE_2 induced maximal relaxation of the histamine (1 μM)-contracted tracheal ring at a concentration of 1 μM (Figure 3.9; n = 4). Under higher tone, the relaxation curve to PGE_2 was shifted to the right and only 52% relaxation was found at 1 μM.

From Figures 3.10, 3.11, 3.12, and 3.13 and Table 3.3, it is clear that butaprost-FA, CAY-10399, CP-533536 and AH-13205 showed similar profiles to PGE_2. There were inconsistencies however. Firstly, the slopes of the curves appeared to be different between the agonists. Instead of using the Hill slope (a sigmoidicity measure that is dependent on how the lower asymptote is fixed), the relaxation curves of these EP_2 agonists can be compared as the concentration interval for 20 - 80% relaxation of 1 μM histamine-induced tone as a measurement of slope (Figure 3.14, example on PGE_2 relaxation curve). The log intervals for 20 - 80% relaxation are: PGE_2 1.45; CAY-10399 1.25; Butaprost-FA 1.40; CP-533536 1.10 and AH-13205 1.9. The steeper slope of the CP-533536 curve may be due to its slower onset at concentration $\leq$ 100 nM; it is possible that the corresponding responses have been under-estimated. The shallower slope of the AH-13205 curve appears to be a genuine result.

Table 3.3 Guinea-pig trachea: pIC_{50} values and maximal inhibitions of the prostanoid agonists under two different levels of histamine tone in the relaxant study.

	Histamine 1 µM		Histamine 100 µM
	pIC_{50}	% relaxation	% relaxation
PGE_2	7.30 ± 0.11	100 ± 0	52 ± 5
Butaprost-FA	6.98 ± 0.03	98 ± 1	32 ± 3
CAY-10399	7.64 ± 0.07	100 ± 0	39 ± 1
CP-533536	6.97 ± 0.06	100 ± 0	52 ± 5
AH-13205	6.84 ± 0.06	97 ± 2	53 ± 4

All the experiments were done in the presence of 1 µM indomethacin, 100 nM BMS-180291 and 1 µM SC-51322.

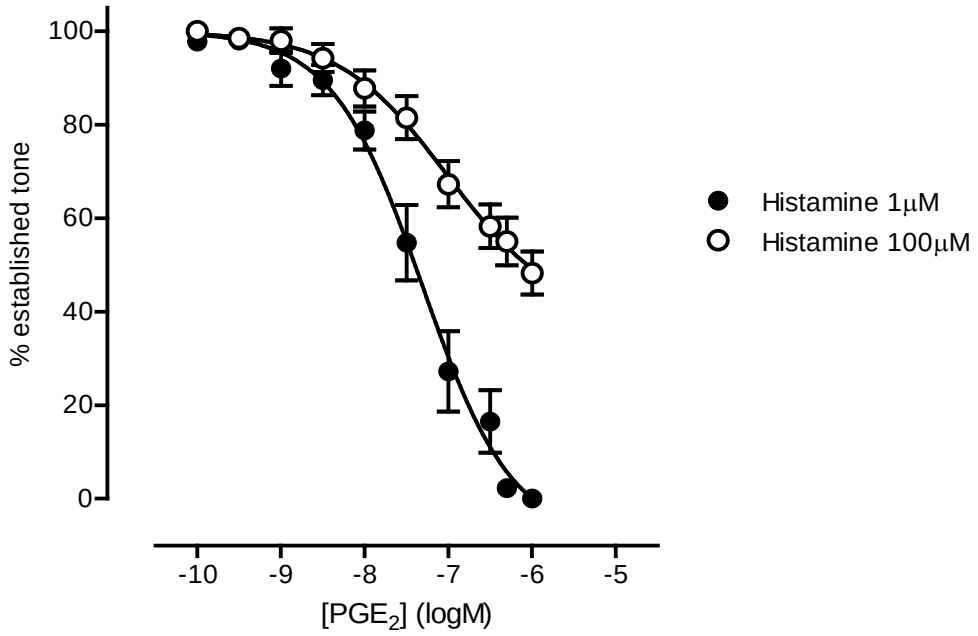

Figure 3.9 Relaxant activity of PGE_2 on pre-contracted guinea-pig trachea. GPT were pre-contracted with histamine 1 µM and 100 µM (n = 4). 100 nM BMS-180291 and 1 µM SC-51322 were present.

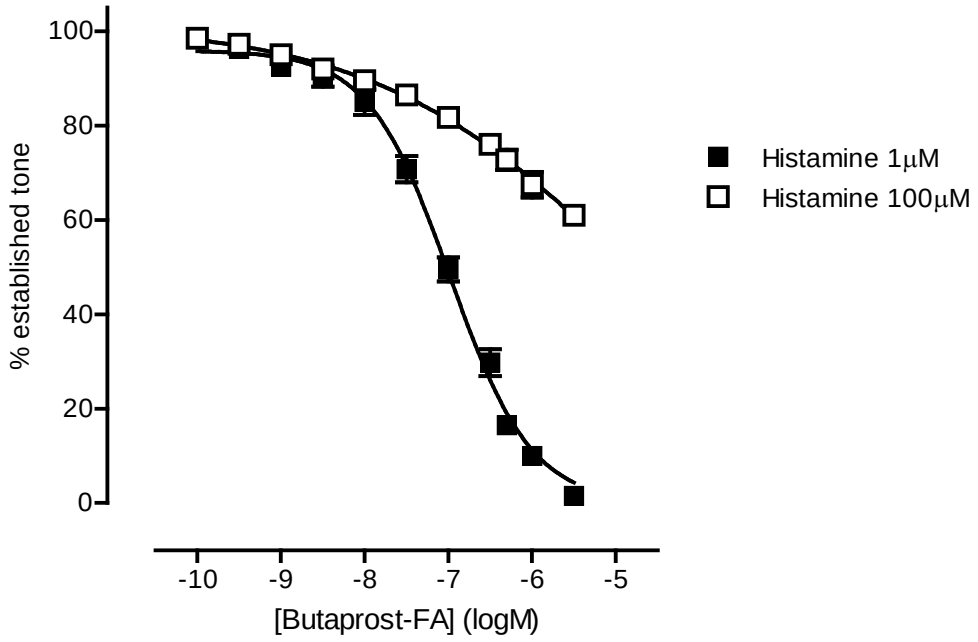

Figure 3.10 Relaxant activity of butaprost-FA on pre-contracted guinea-pig trachea. GPT were pre-contracted with histamine 1 μM and 100 μM (*n* = 4). 100 nM BMS180291 and 1 μM SC51322 were present.

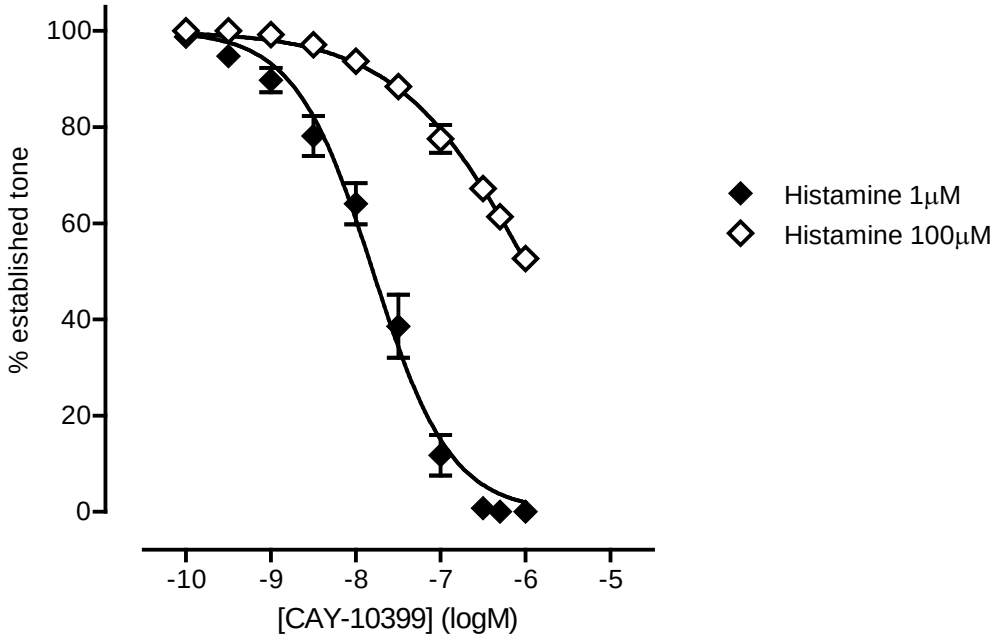

Figure 3.11 Relaxant activity of CAY-10399 on guinea-pig trachea. The trachea was contracted with 1 μM and 100 μM histamine (n = 4). 100 nM BMS-180291 and 1 μM SC-51322 were present.

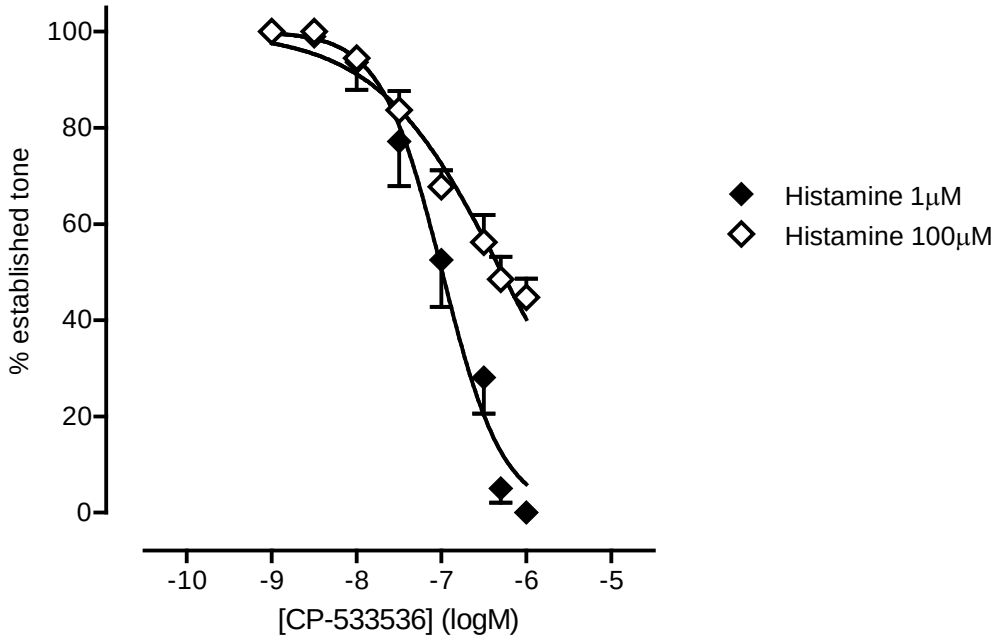

Figure 3.12 Relaxant activity of CP-533536 on guinea-pig trachea. The trachea was contracted with 1 μM and 100 μM histamine (*n* = 4). 100 nM BMS-180291 and 1 μM SC-51322 were present.

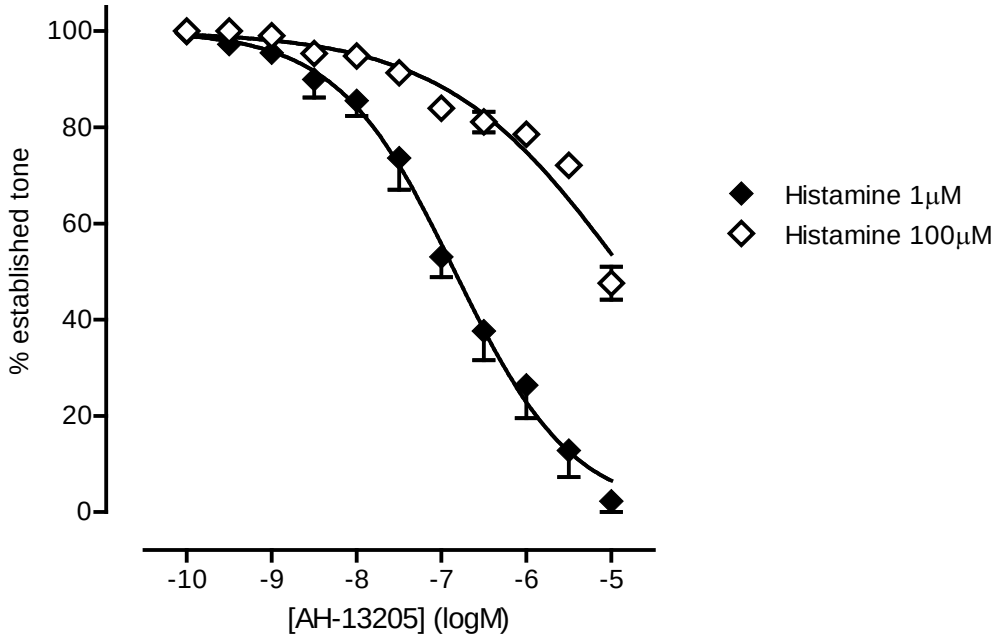

Figure 3.13 Relaxant activity of AH-13205 on guinea-pig trachea. Tone was induced by 1 μM (n = 4) and 100 μM (n = 4) histamine. 100 nM BMS-180291 and 1 μM SC-51322 were present.

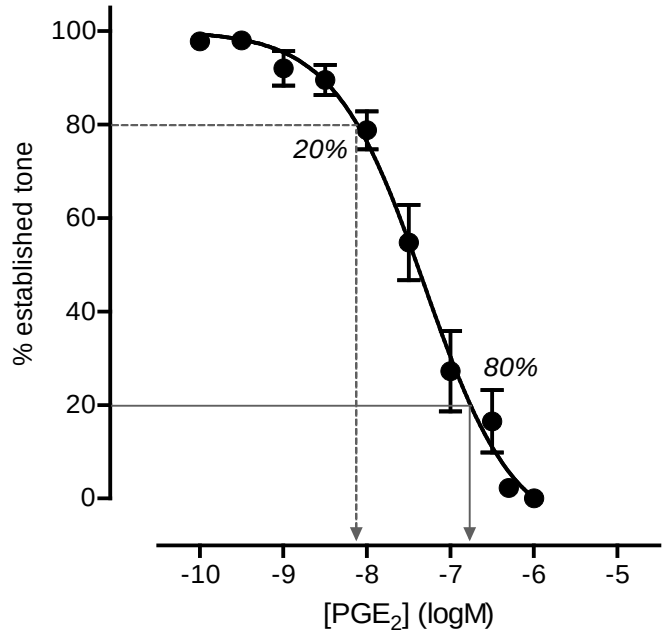

Figure 3.14 The logM interval for 20 - 80% relaxation of 1 μM histamine-induced contraction as an alternative method measurement of curve slope (data from Figure 3.9).

In terms of estimating efficacy, it was decided to compare relaxations under high and low tone for each agonist at the level of 75% relaxation under low tone. The fraction of the 75% relaxation under low tone for the EP_2 agonists are: PGE_2 57%; Butaprost-FA 47%; CAY-10399 43%; CP-533536 73% and AH-13205 44% (Figure 3.15). There were significant differences between CP-533536 in compared to CAY-10399 and AH-13205 (*p = 0.003*). Otherwise, there were no large differences using this procedure.

The log concentration-response curve for AH-13205 under high tone was atypical (Figure 3.13) and it was decided to analyse these data further.

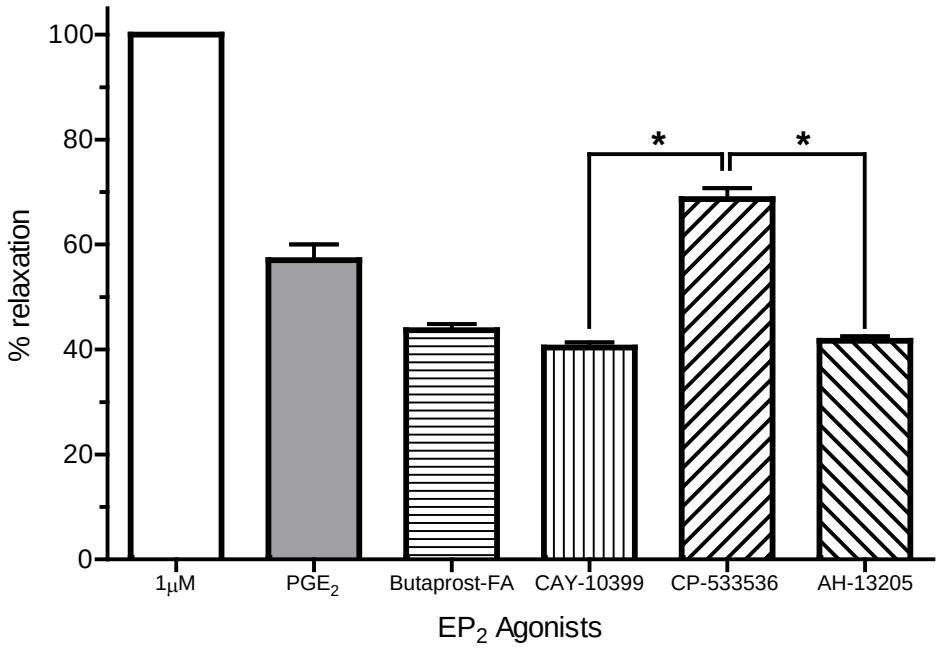

Figure 3.15 Relaxation induced by EP_2 agonists under high tone (histamine 100 μM) corresponding to 75% relaxation under low tone (histamine 1 μM). Values expressed as a percentage of the low tone relaxation. * *P < 0.01*, CP-533536 vs CAY-10399 and AH-13205, using one-factor ANOVA.

3.3.5 Two-site competition model

It appeared that there could be two components to the inhibition-curve for AH-13205 against 100 µM histamine-induced tone, as the data points did not fit the standard sigmoidal curve well (Figure 3.13). Two theoretical curves were fitted to the inhibition data using the two-site competition equation in GraphPad Prism as described in Chapter 2 (Figure 3.16A). The combined curve is shown in Figure 3.16B. The r^2-values were compared as described in Chapter 2. The r^2-value was 0.96 for the two-component fit and 0.91 for the one-component fit.

The best-fit two-site curve has a high affinity site with a pIC_{50} of 7.72 and a low affinity site with pIC_{50} of 4.84. The fraction of high affinity site (the upper curve) is 16%, with 95% confidence intervals of 12 – 19%. The These results are sensible to make a statistical comparison using the modified F test as described in Section 2.5.2. There are 44 data points in the curve (i.e. 4 replicates, with 11 different concentrations; 4 x 11 = 44). Four parameters are fitted by the one-site equation fit: IC_{50}, slope, top and bottom and five parameters fitted for the two-site model: $IC_{50}1$, $IC_{50}2$, top, bottom and common middle-level. Using these data, the calculation is summarized in Table 3.4. The F ratio is 28.78 with 1 (numerator) and 28 (denominator) degrees of freedom (df). With references to the F table (Appendix), the two-site model is significantly better than one-site model ($p < 0.001$).

Table 3.4 The F test of two-site model against one-site model of AH-13205 vs 100 µM histamine.

Model	**SS**	**df**
Null hypothesis (1 site)	862	44
Null hypothesis (2 site)	456	43
Difference	406	1
Fractional difference	0.8904	0.0233
Ratio (F)	**38.21**	

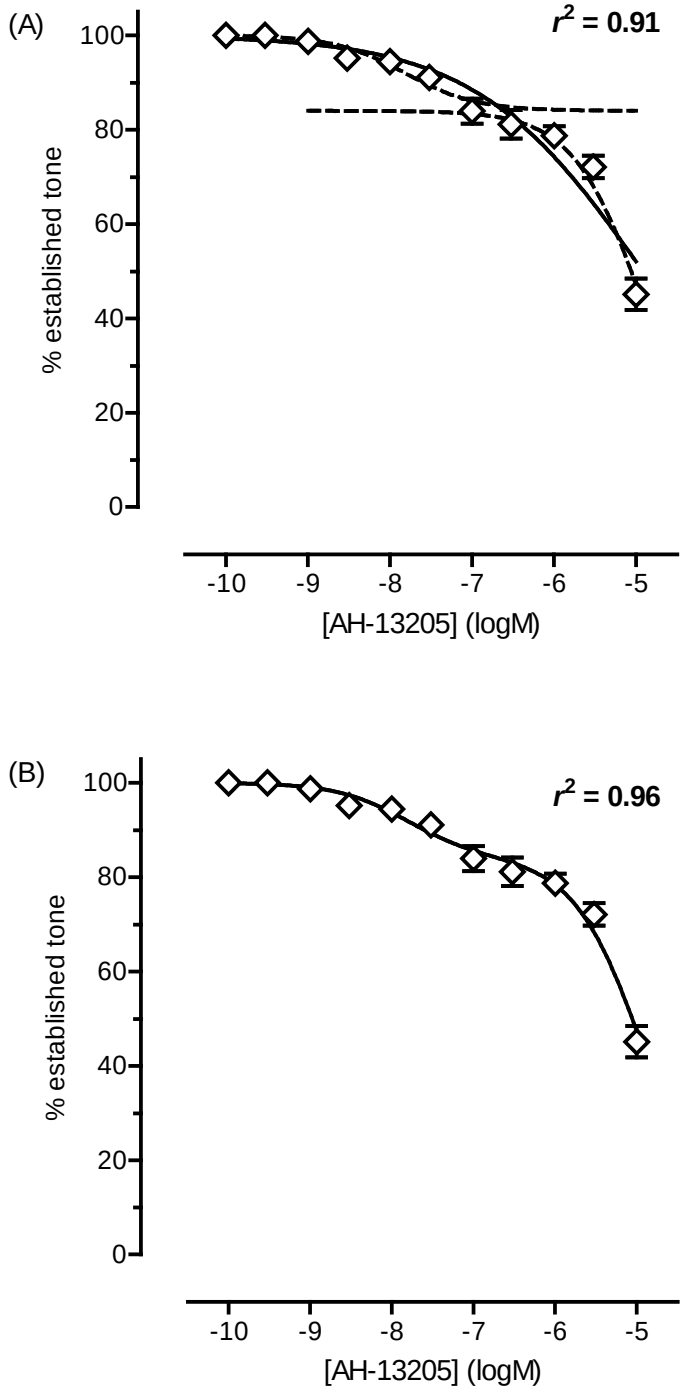

Figure 3.16 An attempt to establish a two-receptor mechanism for AH-13205 in guinea-pig trachea by applying the two-site competition equation to data from Figure 3.13. (A) AH-13205 curve vs. 100 µM histamine, showing the two theoretical curves. (B) The two-site model fitted to the data.

3.4 Discussion

The guinea-pig tracheal ring has been shown to have contractile prostanoid receptors, namely TP and EP_1 (Jones *et al.*, 1982; Coleman and Kennedy, 1985; Eglen and Whiting, 1988; McKenniff *et al.*, 1988), while the relaxant activity of prostanoids has been demonstrated to be mediated by the EP_2 receptor (Eglen and Whiting, 1988). As an established preparation, it was a good point to gain experience of isolated smooth muscle preparations, especially since my data could be compared to previous studies.

3.4.1 The tracheal response to prostanoid agents

Table 3.2 lists the response of GPT to prostanoid agonists in the contractile study. The potent TP agonist, U-46619 (Coleman *et al.*, 1981) produced a contractile effect in the guinea-pig trachea. In the current study, the preparation were slightly less sensitive to the U-46619 (pEC_{50} 7.37) than reported in previous studies (Jones *et al.*, 1982, 7.60; McKenniff *et al.*, 1988, 7.47; Tymkewycz *et al.*, 1991, 7.8). This may be due to difference in source of the animal and the techniques applied among the studies. The complete antagonism of U-46619-induced contraction by 100 nM BMS-180291 is consistent with the presence of TP receptor as demonstrated by previous studies (Jones *et al.*, 1982; Coleman and Kennedy, 1985; Eglen and Whiting, 1988; McKenniff *et al.*, 1988).

PGE_2 is a prostanoid agonist that has affinity to all the EP receptors; in the rank order: $EP_3 = EP_4 > EP_1 > EP_2$ with very low affinity for FP, DP, TP and negligible on IP (> 10,000) (Abramovitz *et al.*, 2000). In the current study, the response of GPT to cumulative addition of PGE_2 was similar to 17-phenyl PGE_2 ($EP_1 > EP_3$, with minimal activity on EP_2; Lawrence *et al.*, 1992).

However, PGE_2-induced contraction is completely antagonised by the EP_1 antagonist SC-51322, while the EP_3 antagonist L798106 has no effect.

Sulprostone is an extremely potent EP_3 agonist, for example on guinea-pig vas deferens (Lawrence *et al.*, 1992) and aorta (Jones *et al.*, 1998). Sulprostone has higher affinity to EP_3 receptor than EP_1 receptor (Lawrence *et al.*, 1992; Abramovitz *et al.*, 2000). In the current study, the pEC_{50} for sulprostone corresponded well to K_i values obtained by radioligand binding using recombinant receptors. Similar to PGE_2, the contractile action of sulprostone was blocked by SC-51322, but not by L-798106. The results indicate that EP_3 receptors are absent from GPT smooth muscle. Collectively, these results agree with the presence of EP_1 receptor in the GPT.

3.4.2 Relaxant response of the trachea to EP_2 agonists

The initial relaxant studies with PGE_2 and butaprost-FA supported the presence of EP_2 receptor as opposed to EP_4 receptor in GPT. All the EP_2 agonists investigated induced a complete or nearly complete relaxation under 1 μM histamine tone (Figure 3.14). In other words, they are considered to be EP_2 full agonists. Using the data for 1 μM histamine, the pIC_{50} values of PGE_2, butaprost-FA, CAY-10399, CP-533536 and AH-13205 were 50, 105, 23, 107 and 145 nM respectively. The corresponding equipotent molar ratios are 1.0, 2.1, 0.46, 2.14 and 2.9. Thus the potency ranking of the EP_2 agonists on GPT demonstrated in the current study was: CAY-10399 > PGE_2 > butaprost-FA = CP-533536 > AH-13205. However, the slopes of the relaxation curves under low tone were different. In the case of CP533536, this may have been due to its slow onset of action. CP-533536 is much more lipophilic than the other agonist studied and this may underlie its slow onset (Jones RL, personal communication).

Under higher tone induced by 100 μM histamine, all the prostanoid agonists were all much less effective relaxants. An agonist with lower efficacy would be expected to elicit relatively less relaxation under the condition of higher tone; this was seen with CP-533536 but not with AH-13205.

3.4.3 Dual receptor activity of AH-13205

The data for AH-13205 against 100 μM histamine seems to be poorly fitted using one-site competition model (Figure 3.13). Using the two-site competition model, two theoretical curves were superimposed on the AH-13205 curve (Figure 3.16A). The curve for two-site competition refitted on the curve using GraphPad Prism is shown in Figure 3.16B. Statistical analysis established that the two-curve fitting was significantly better than the single-curve fitting, indicating that AH-13025 has two components to its relaxation curve.

One explanation of the biphasic relaxant effect of AH-13205 at high tone is activation of two receptors, the EP_2 receptor and another receptor that remain to be determined. AH-13205 has been used as a selective EP_2 agonist (Wheeldon and Vardey, 1993) and has a binding K_i of 240 nM for mouse recombinant EP_2 receptors (Kiriyama *et al.*, 1997; Breyer *et al.*, 2001). However, AH-13205 also has affinity for EP_3 receptor, with K_i of 82 nM (Kiriyama *et al.*, 1997; Breyer *et al.*, 2001). Moreover, in recent experiments on guinea-pig aorta by one of my supervisors, AH-13205 has been shown to be a low-potency EP_3 agonist (Jones RL, unpublished result). However, no EP_3 receptor has been documented in guinea-pig trachea smooth muscle in this and previous studies. Inhibitory EP_3 receptors are present on parasympathetic neurones in the guinea-pig trachea (Spicuzza *et al.*, 1998; Clarke *et al.*, 2004), but it seems unlikely that the contractile action of histamine involves activation of the parasympathetic innervation.

A second explanation relates to the chemical structure of AH-13205. Figure 1.3 shows a wavy line for the hydroxyl group attachment in the ω-chain of AH-13205. This means that the compound is a mixture of isomers, one with the hydroxyl group down from the plane of the paper, the other above the plane. The ratio will be close to 1:1, since they are difficult to separate chromatographically. The other PGE_2 analogues studied all have a single configuration for this hydroxyl. It is usual for one of the two possible hydroxyl isomers to be more active than the other. For example, 15(R)-PGE_2 is 870 times less potent than natural 15(S)-PGE_2 in a recombinant EP_1 receptor-Ca^{2+} flux assay (Ungrin *et al.,* 2001). It is possible that a similar scenario applies to AH-13205.

3.5 Conclusions

The results from the current study are in agreement with the presence of TP, EP_1 and EP_2 receptors in the guinea-pig trachea. The selective EP_2 agonists used in the current study all behaved as full agonists.

In contrast to the other EP_2 agonists, AH-13205 showed a biphasic log concentration-response curve. This profile may be due to activation of the EP_2 receptor and a second receptor that needs to be elucidated. Alternatively, the presence of two isomers in AH-13205 may be responsible.

CHAPTER FOUR

RAT MESENTERIC ARTERY

4.1 Introduction

Essential hypertension (EH) is one of the most important treatable causes of premature death worldwide (Ezzati *et al.*, 2002). It is a major public health problem in many countries due to its high prevalence and its association with coronary heart disease, stroke, renal disease, peripheral vascular disease and other disorders. EH is a heterogenous, multi-factorial disorder. Both genetic and environmental factors influenced the onset and severity of EH (Gong and Hubner, 2006).

Maintenance of normal blood pressure is dependent on a balance between the cardiac output and peripheral vascular resistance. In humans, the elevated blood pressure in EH is associated with a normal cardiac output but raised peripheral resistance (Dustan *et al.*, 1972). Thus, the main contribution to the high blood pressure in EH is the elevation in arterial tone contributed to the changes in peripheral resistance. The smaller arterial resistance vessels (generally less than 200 µm in diameter) are most involved in regulating blood flow and capillary pressure (Christensen and Mulvany, 2001). However, all the peripheral vessels, including aorta contribute to the peripheral resistance to some extent.

In-vitro study on an animal model of hypertension is an ideal method to study the pathophysiology and the effect of treatment in EH. The rat is the most common animal used in hypertension research. Previous work with isolated vessels in hypertensive rats has involved aorta, conductance arteries and resistance vessels. The rat superior mesenteric artery is considered to be a conductance artery having internal diameters greater than 300 µm, but less than 1 mm (Mulvany and Halpern, 1977; Christensen and Mulvany, 2001). Structural abnormality in this conductance artery leading to wall stiffness, is considered to play an important role in the development of hypertension (Korner and Angus, 1997) and to be a predictor of cardiovascular events in essential hypertension (Mathiassen *et al.*, 2007). The contribution of the rat mesenteric bed in hypertension has been investigated using wire-

myography (Mulvany and Halpern, 1977; Garcia-Redondo *et al.*, 2009) and under various conditions of pressure-myography (Coats and Hillier, 1999; Bolla *et al.*, 2004). However, the main trunk of the artery has not frequently been used in previous experiments.

Noradrenaline has been shown to have a strong contractile effect on this artery (Massett *et al.*, 1998; Buus *et al.*, 2000). Phenylephrine also produced a good contractile response in the proximal part of the main trunk (Massett *et al.*, 1998). The superior rat mesenteric artery has been demonstrated to have a marked similarity in control of its vascular tone to the human counterpart (Hutri-Kahonen *et al.*, 1999). However, the scope of the study was limited to endothelium-derived mediators only.

In mesenteric artery preparations from normal male Wistar rats, arachidonic acid (AA) was shown to inhibit established contraction to noradrenaline in the presence and absence of endothelium and the effect was comparable to that of human small subcutaneous arteries (Buus *et al.*, 2000). AA may be converted to PGE_2 and / or PGI_2, which could then activate EP_2 / EP_4 and IP receptors on smooth muscle cells. The same study also demonstrated that increasing the extracellular potassium concentration (more than 7 mM) caused a transient relaxation in rat mesenteric artery, which was absent in human small arteries. In contrast, a transient relaxation response to extracellular potassium was absent in male Sprague-Dawley rats despite the higher concentration of KCl, up to 100 mM (Massett *et al.*, 1998).

The response of the rat mesenteric artery to prostanoid agonists has been demonstrated in several studies. U-46619, a potent TP receptor agonist induced a strong contractile response with concentration ranging from 1 nM to 1 µM (Chauhan *et al.*, 2003). U-46619 also has been used to precontract rat mesenteric artery to study the effect of 17β-estradiol-induced relaxation in the presence of various antagonists (Tsang *et al.*, 2003). In another study, the presence of periadventitial adipose tissue have been demonstrated to have no effect on rat mesenteric artery response to 100 nM U-46619 (Verlohren *et al.*, 2004). Of particular relevance to the current

investigations is the demonstration of strong constriction of perfused second order mesenteric artery vessels from male Wistar-Kyoto rats by PGE_2 in the presence of the TP antagonist SQ-29548 (Bolla *et al.*, 2004).

The rat mesenteric artery was used in the current study to study the role of the prostaglandins in the control on the vascular tone for three reasons. Firstly, the distribution of prostanoid receptors in rat mesenteric artery has never been documented before. Secondly, its wall thickness is small and it was hope that responses to prostanoids would be conveniently faster than those previously seen in more robust preparations such as rabbit and guinea-pig aorta and human pulmonary artery. Thirdly, there is a marked similarity in the function of mesenteric arterial rings of corresponding size *in vitro* between humans and rats (Hutri-Kahonen *et al.*, 1999). Therefore, the rat mesenteric artery is a useful model to study the physiology and pathophysiology of arterial function. The superior rat mesenteric artery has been chosen in the current study due to its easy accessibility and it provided a good and consistent response to prostanoid agonists in preliminary experiments.

In order to classify prostanoid receptors in rat mesenteric artery, the antagonist protocol described in detail in Chapter 2 was used in the current study (Figure 4.1B). Basically, the protocol involved construction of an initial agonist concentration-response curve (CRC) followed by a concentration-inhibition curve for a selective antagonist on established response of the agonist. Prostanoid agonists (selectivity specified) that usually induce smooth muscle contraction include: 17-phenyl PGE_2 ($EP_1 > EP_3$), sulprostone ($EP_3 > EP_1$), ONO-D1-004 (EP_1), ONO-AE-248 (EP_3), $PGF_{2\alpha}$ (FP) and U-46619 (TP). Prostanoid agonists inducing relaxation include: butaprost-FA (EP_2), ONO-AE1-259 (EP_2) and iloprost (IP). A selective EP_4 agonist was not available during the period of the study.

Prostanoid receptor antagonists that were used in the current study include a well-established EP_1 antagonist, SC-51322 (Hallinan *et al.*, 1994). L-798106 was the only selective EP_3 receptor antagonist available for the study. It has been reported to show high selectivity on EP_3 receptors based on ligand binding at recombinant prostanoid receptors (K_i 1.1 nM; Juteau *et al.*, 2001). Previous functional study on EP_3 receptor shows L-798106 blocked the inhibitory action of sulprostone pre-synaptically in guinea-pig vas deferens and trachea with pA_2 values of 7.48 and 7.82, respectively (Clarke *et al.*, 2004). At the time of the current study, there was no other report of L-798106 activity on other isolated tissue or vessel preparation. Recently, L-798106 (CM9) was shown to inhibit the PGE_2-induced Ca^{2+} influx in a rat EP_3 receptor-Ca^{2+} flux assay with pK_i value of 7.12 (Jugus *et al.*, 2009). Another selective EP_3 receptor antagonist, L-826266 also was used in the current study (Clark *et al.*, 2008).

BMS-180291 was used as the selective TP antagonist in the study (Ogletree *et al.*, 1993). Concentrations were chosen to give large rightward shifts of the log concentration-response curves of the appropriate agonists, based on previously published affinity data (Table 4.1).

Table 4.1 Antagonists and concentrations chosen for use in the studies

Antagonists	**Reported pA_2**	**Concentrations used in the current study**	**References**
SC-51322	8.45	1 nM - 1 µM	Hung *et al.*, 2006
BMS-180291	9.5	1 – 300 nM	Zhang *et al.*, 1996
L-798106	7.48, 7.82	1 µM	Clarke *et al.*, 2004
L-826266	8.35	100 nM – 1 µM	Clark *et al.*, 2008

4.2 Methods

The basic methodology used has been described in detail in Chapter 2. Specific methodological points not discussed previously are addressed below.

4.2.1 Setting up of preparations

The superior mesenteric arteries were obtained as described in Chapter 2. The artery was either used the same day or kept overnight at 4 ºC in Krebs solution (viability as demonstrated by McIntyre *et al.*, 1998). The resting tone was set at an optimal tension of 1.0 g, determined from preliminary experiments and documented in previous study (Maggi *et al*., 1988; Schneider *et al*., 2004). In the early part of the study, the resting tone of the rat mesentery artery was erratic. It was found that setting the resting tension in the presence of 100 nM isoprenaline produced more stable preparations. Drugs were added directly to the tissue bath and the concentrations of drugs were the final concentrations in the bath. Thirty minutes after being set up in organ baths, the arterial rings were constricted by 40 mM of potassium chloride to assess the contractility and were then washed several times until baseline tone was restored. Any arterial rings not contracted by more than 0.5 g (representing 50% of normal 40 mM potassium chloride response) were excluded from the study. The vessel rings were then exposed to 10 nM PGE_2 for 10 min followed by a washout period of 15 min and equilibration for 30 – 40 min; increasing agonist concentrations were added cumulatively to construct CRC.

Each preparation was used to obtain a concentration-response curve for one prostanoid only. The selective antagonist was either applied as a single dose before the construction of agonist CRC (Figure 4.1A) or as cumulative doses when the inhibition-curve protocol was utilised (Figure 4.1B).

In inhibition curve studies, the arterial rings were precontracted with agonist (at 80% of maximal response; EC_{80}), followed by cumulative addition of antagonist (Figure 4.1B). Preparation without the antagonist served as a control.

For studies of agonist-induced relaxation, phenylephrine 300 nM (representing 35% of maximal response, EC_{35}) was chosen as the precontractile agent. The selective antagonists for contractile prostanoid receptor were incubated 30 min before the addition of phenylephrine. Once the contraction had stabilised, the agonist was added cumulatively (Figure 4.2). Phenylephrine was used as the precontractile agent in antagonist studies, in the presence of selective antagonist pertaining to the agonist used. Once the phenylephrine tone was established, a cumulative-dose response curve to the particular agonist was constructed.

4.2.2 Antagonist protocol and pA_2 estimation

Antagonist affinity was determined by calculating the pA_2. In this study, the basic inhibition-curve protocol is used. The details have been described in Section 1.7.2. The pA_2 (= $-\log K_b$) is estimated from the equation (Lazareno and Birdsall, 1993b):

$$K_b = \frac{IC_{50}^*}{\frac{[A]}{EC_{50}^*} - 1}$$

and

$$K_b = \frac{[B_i]}{\frac{[A_f]}{[A_i]} - 1}$$

.

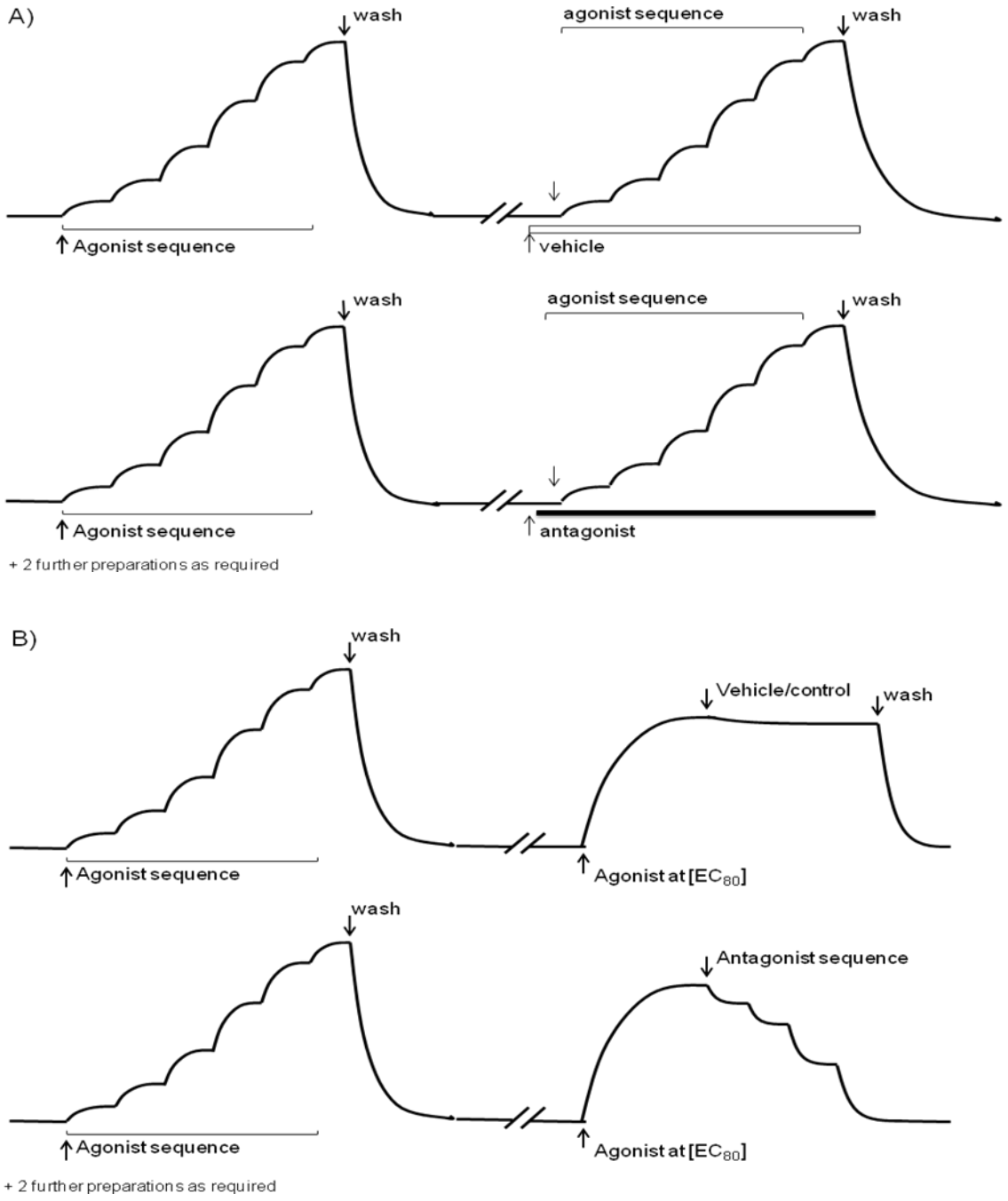

Figure 4.1 Protocols used for rat mesentery artery to determine the profile of an antagonist and where appropriate its affinity constant. A) The basic protocol: antagonist at different concentrations was added before the cumulative addition of prostanoid agonist in the second

sequence. B) The inhibition-curve protocol: an initial agonist sequence followed by cumulative inhibition of the response to an EC_{80} concentration of the same agonist.

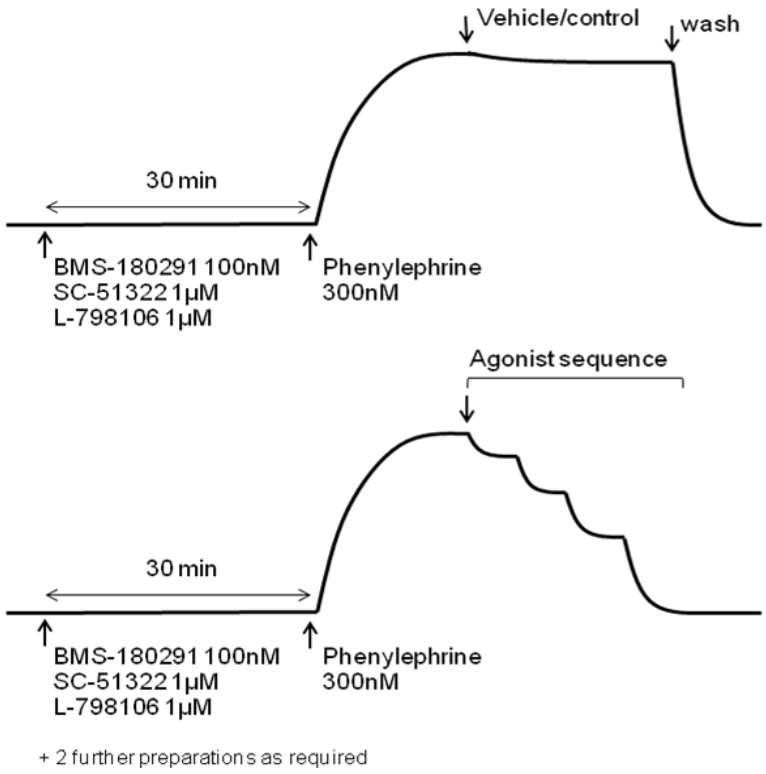

Figure 4.2 Protocol used in rat mesenteric artery to determine the presence of relaxant prostanoid receptor. All three selective antagonists were added 30 min before pre-contraction with phenylephrine 300 nM, followed by the cumulative addition of the agonist.

4.2.3 Statistical analysis

Contractile responses were measured as increases in tension (g) above the resting level. Relaxant responses were expressed as a percentage loss of the initial contractile tone developed to the established tone of the contractile agonist. A variable-slope sigmoidal curve was fitted to log concentration–response data using GraphPad Prism software; the bottom asymptote was constrained to zero for contraction and to 100% for relaxation. Sigmoidal curve parameters were derived from data for individual preparations. Data were further analysed by 1-factor and repeated measures 2-factor ANOVA combined with comparison of selected means by planned (orthogonal) contrasts using SuperANOVA software; all tests were two-tailed and the significance level was set at $p < 0.05$. Where applicable, data were analysed by the two-site competition equation using the modified F test in combination with the r^2-values comparison. All data are presented as mean $\pm$ SEM.

4.3 Results

4.3.1 Initial investigations

All experiments on rat mesenteric artery rings were conducted in the presence of 1 µM indomethacin to suppress prostanoid biosynthesis. Phenylephrine produced a sustained contraction with the maximal response of 0.97 ± 0.04 g and a pEC_{50} of 6.31 ± 0.20 (Figure 4.3, *n* = 5). The contraction was not affected by addition of 100 nM BMS-180291, 1 µM SC-51322 or 1 µM L-798106. Potassium chloride contraction was not sustained and started to fade at concentration of 40 mM and above (Figure 4.4). Histamine up to 10 µM did not contract the ring.

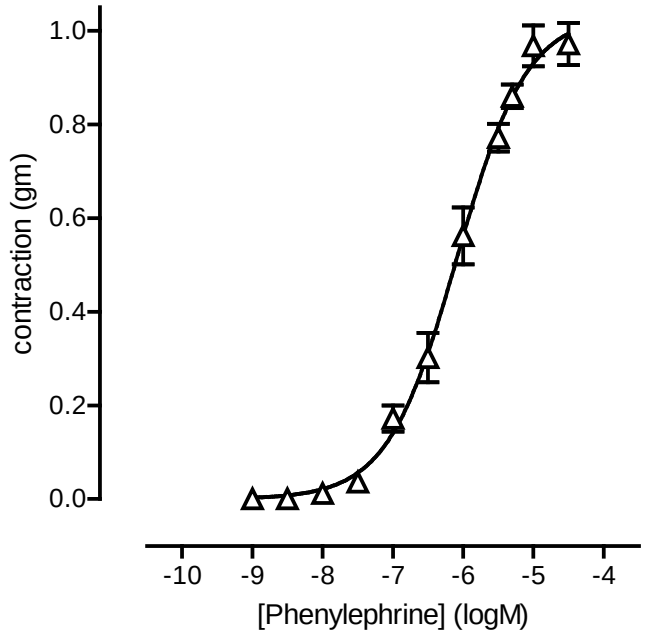

.

Figure 4.3 Contractile activity of phenylephrine in rat mesenteric artery. Phenylephrine (1 nM – 30 µM) contracted the artery in a concentration dependent manner (*n* = 5).

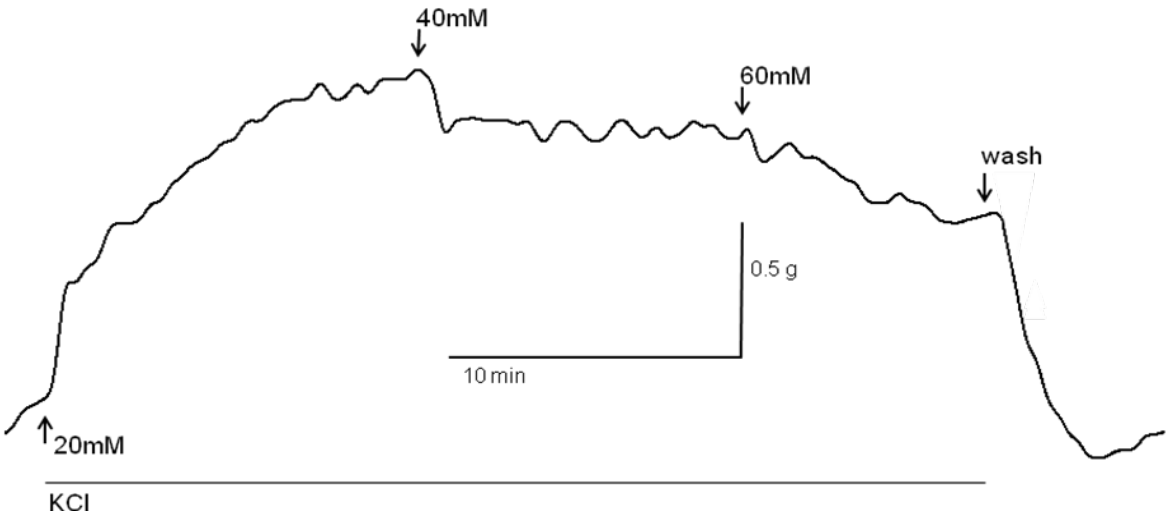

Figure 4.4 Trace illustrating the effect of increasing potassium chloride concentration in the rat mesenteric artery. At concentration of 40 mM and above, the contractile response starts to fade.

Initial experiments showed that three prostanoid agonists, PGE_2, 17-phenyl PGE_2 and sulprostone, produced a contractile response on the arterial rings (Figure 4.5, n = 7). The pEC_{50} values for sulprostone, 17-phenyl PGE_2 and PGE_2 were 7.80, 7.41 and 6.87, affording equi-effective molar ratios (EMR) of 1.0, 2.46 and 8.48, respectively. The sulprostone curve appeared to be parallel to that of 17-phenyl PGE_2. The absolute contractile responses produced by the prostanoid agonists were consistent throughout the study and normalisation was not considered necessary.

$PGF_{2\alpha}$, the natural ligand for the FP receptor was also tested on the rat mesenteric artery. No contraction was observed at concentrations ranging from 1 – 300 nM (Figure 4.5, n = 4).

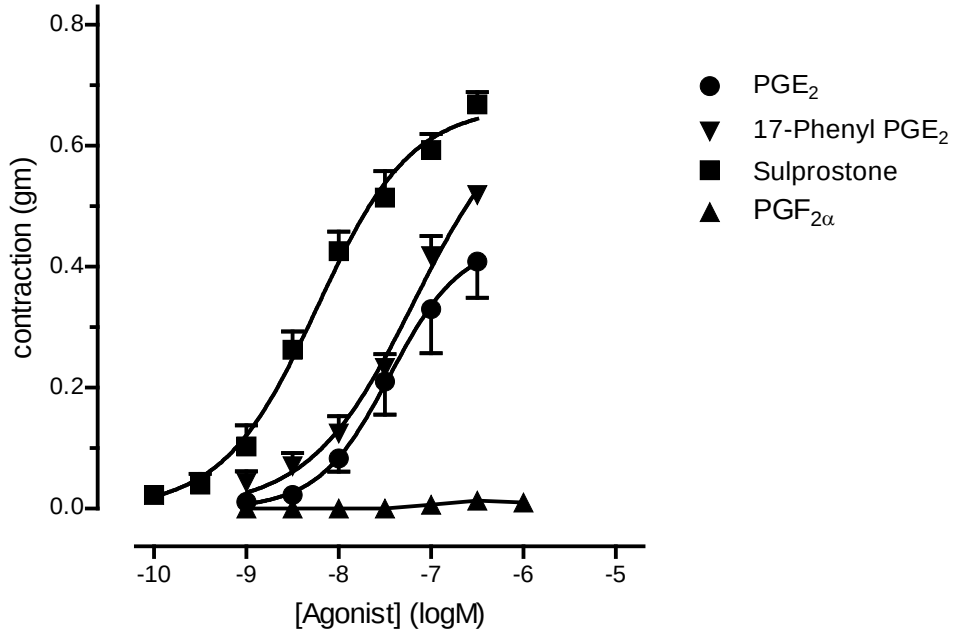

Figure 4.5 Contractile activities of prostanoid agonists in rat mesentery artery. PGE_2, 17-phenyl PGE_2 and sulprostone contracted the artery in a concentration dependent manner with different potency (n = 7). $PGF_{2\alpha}$ (1 nM – 1 μM) did not contract the artery (n = 4). There was no prostanoid antagonist present.

4.3.2 Effects of U-46619 and BMS-180291

As it was still unclear about the distribution of prostanoid receptor in the rat mesentery artery, the next step was to use U-46619 and BMS-180291 to investigate the presence of the TP receptor. U-46619 (selective TP agonist) produced a contractile response with maximal response of 0.81$\pm$ 0.01 g (Figure 4.6; n = 5).

After the period of washout and the preparation had returned to resting tension, the arterial rings were precontracted with 100 nM U-46619, corresponding to EC_{90}. Once the contractile tone was stable and established, BMS-180291 was then added cumulatively (protocol in Figure 4.1B). BMS-180291 started to relax the arterial ring at 1 nM and completed relaxation was achieved at 100 nM (Figure 4.7, n = 5). The antagonism of BMS-180291 on rat mesenteric artery was quick as shown in Figure 4.8. The pIC_{50} for BMS-180291 was 8.31 $\pm$ 0.14; the dose-ratio for this level was 28 affording a pA_2 of 9.83 $\pm$ 0.25. At this stage, it was concluded that TP receptors are present in the rat mesenteric artery. In further experiments, 100 nM BMS-180291 was added 30 min before the cumulative addition of other agonists; the expected dose-ratio is about 680.

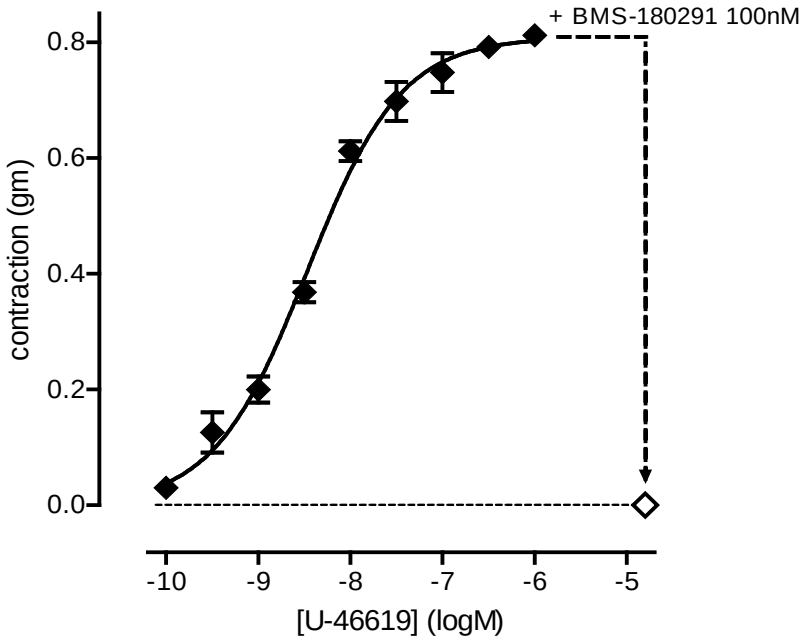

Figure 4.6 Contractile activity of U-46619 in rat mesenteric artery. U-44619 (0.1 nM – 1 µM), a selective TP agonist contracted the artery in concentration dependent manner (*n* = 5). 100 nM BMS-180291 completely antagonised the response.

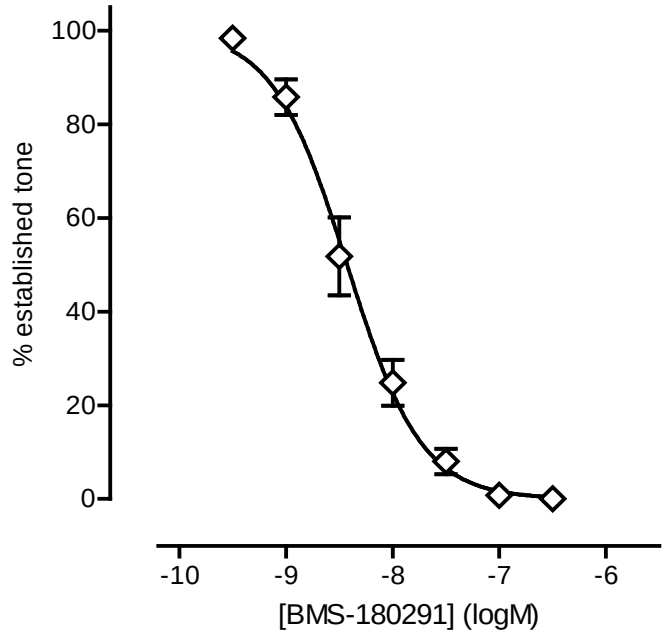

Figure 4.7 Antagonism of 100 nM U-46619-induced contraction by BMS-180291 in rat mesenteric artery (n = 5). After 40 - 45 min agonist contact, BMS-180291 (1 – 300 nM) was added cumulatively.

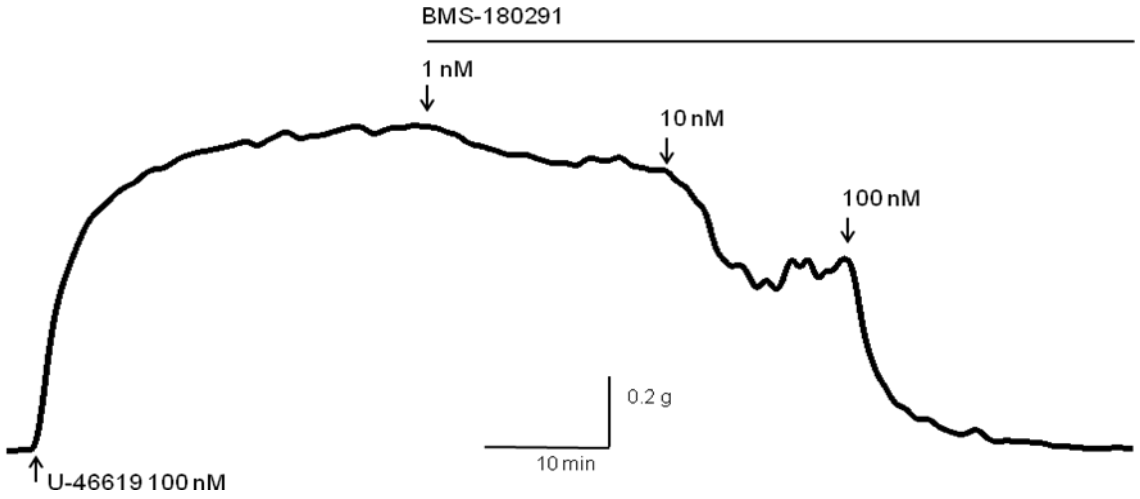

Figure 4.8 Experimental trace illustrating the effect of BMS-180291 on 100 nM U-46619-induced contraction by in rat mesenteric artery. The inhibition by BMS-180291 was quick and at concentration of 100 nM, the response to U-46619 was abolished

4.3.3 Effects of prostaglandin E_2

Initial investigation with PGE_2 in the presence of 100 nM BMS-180291 showed a contractile response in the rat mesenteric artery (Figure 4.9, *n* = 7). The maximal response was 0.60 $\pm$ 0.01 g with pEC_{50} of 7.14 $\pm$ 0.06.

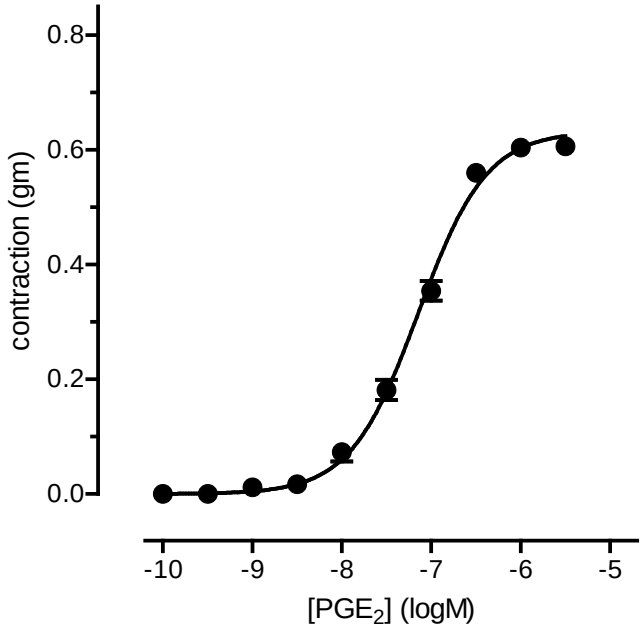

Figure 4.9 Contractile activity of PGE_2 in rat mesenteric artery. PGE_2 (0.1 nM - 3 µM) a non-selective agonist at EP receptors contracted the artery in concentration dependent manner (*n* = 7). 100 nM BMS-180291 was present.

4.3.4 Interaction of L-798106, L-826266 and SC-51322 with sulprostone

In the presence of BMS-180291 (100 nM), the EP_3 receptor antagonist L-798106 and EP_1 receptor antagonist SC-51322 were tested against sulprostone-induced contraction (Figure 4.10). L-798106 at 10 and 300 nM shifted the log concentration-response curve for sulprostone in non-parallel manner (Figure 4.11, n = 4). This result clearly precludes calculation of a meaningful pA_2 value. However, in order to obtain some measure of antagonist affinity, dose-ratios were measured at the 25% response level for each L-798106 concentration, where a predominance of the EP_3 system is expected. The dose-ratios for 10 and 300 nM L-798106 were 3 and 14, giving pA_2 values of 8.30 and 7.65, respectively.

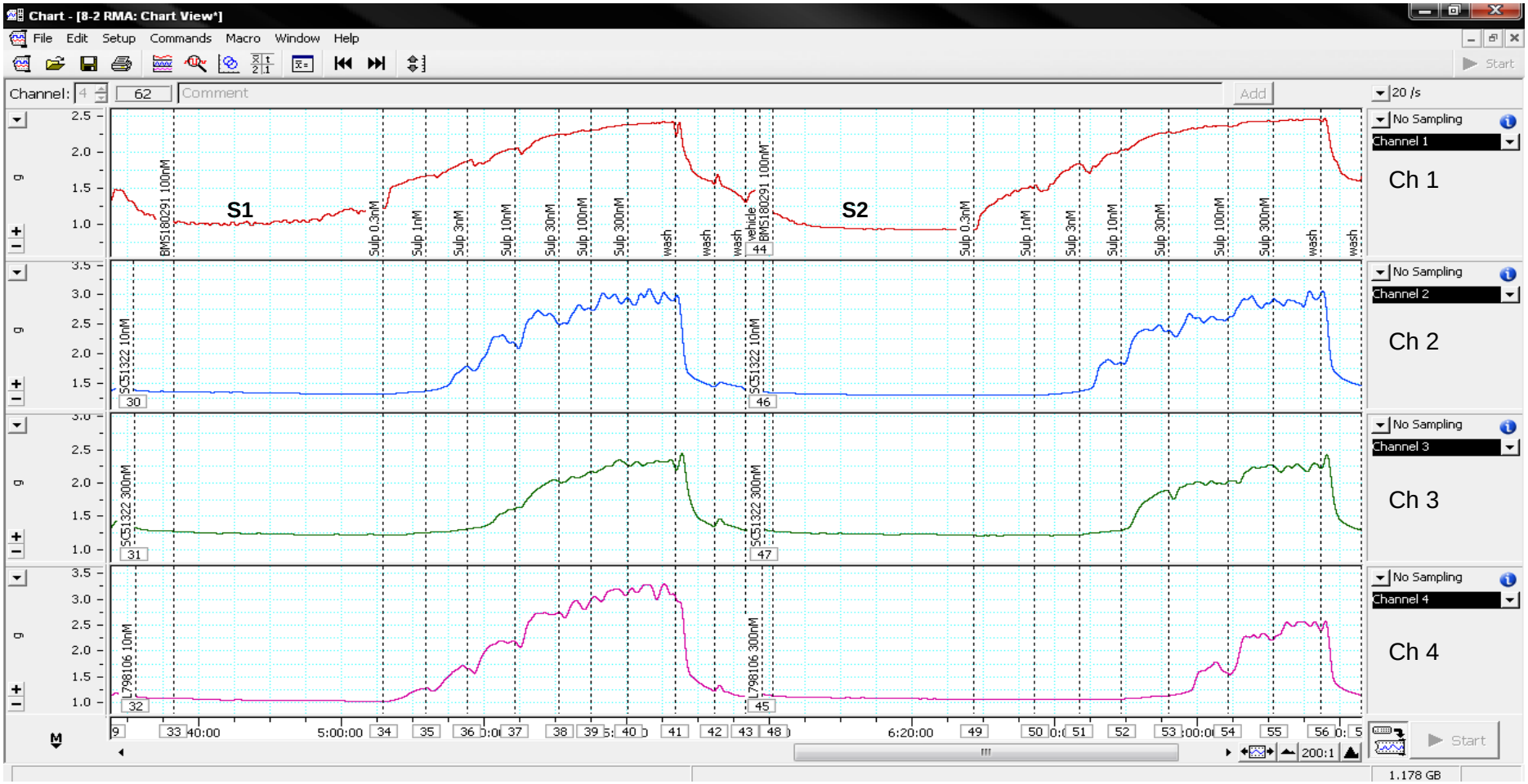

Figure 4.10 Experimental records showing the effects of SC-51322 and L-798106 on sulprostone-induced contractile responses in the rat mesenteric artery. All antagonists were added 30 min before the addition of sulprostone. 100 nM BMS-180291 was present.

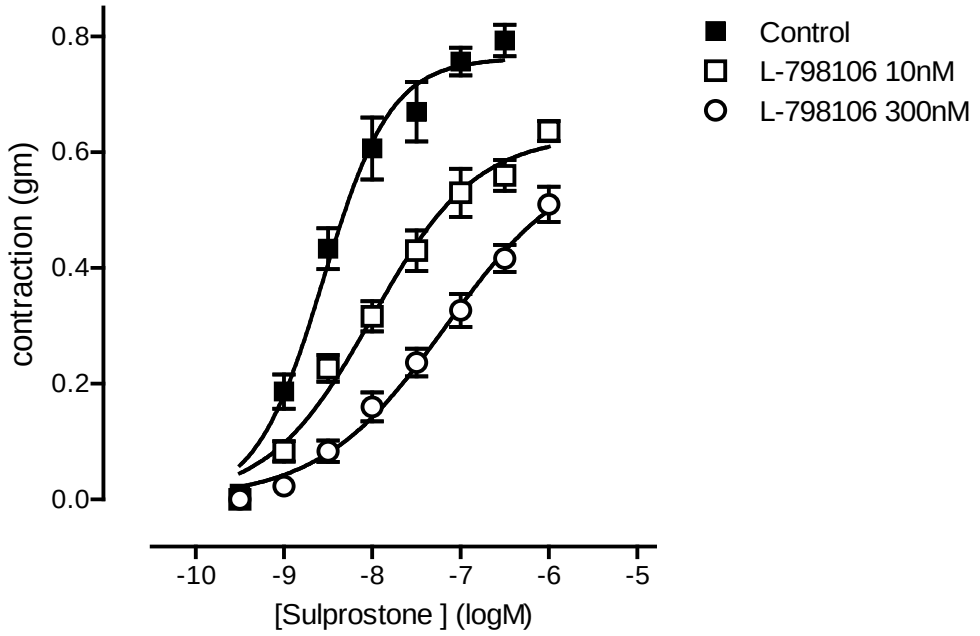

Figure 4.11 Antagonism of sulprostone-induced contraction by L-798106 in rat mesenteric artery. Log concentration-response curves for sulprostone following treatment with 10 nM and 300 nM L-798106 are shown (n = 4).

SC-51322 also shifted the log concentration-response curve of sulprostone in non-parallel manner (Figure 4.12, n = 3). By the same reasoning, dose-ratios for 10 nM and 300 nM SC-51322 measured at the 25% response level were 71 and 148, with the estimated pA_2 of 9.2 and 8.69, respectively.

Inhibition-curve protocols were also utilised to study the antagonist profile of L-798106 and L-826266. The arterial rings started to contract to sulprostone at 0.1 nM (Figure 4.13, n = 6). The maximal response was 0.76 $\pm$ 0.02 g with pEC_{50} of 7.62 $\pm$ 0.09. Established contraction to sulprostone (100 nM, EC_{80}) was inhibited by L-798106 over the concentration range of 10 - 1000 nM. (Figure 4.14, n = 6). However, relaxation was only 56 $\pm$ 9% at 1 µM. Given I am proposing that two receptor systems contribute to the contractile action of sulprostone (see discussion section), the use of the modified Cheng-Prusoff equations (section 4.2.2) to

calculate a pA_2 value from the dose-ratio corresponding to the IC_{50} value for L-798106 seems problematical. However, calculation of a dose-ratio for a modest inhibition (20%) by L-798106 ought to give a rough estimate of its affinity for the EP_3 receptor. Thus, for 100 nM L-798106 in Figure 4.14 the dose-ratio is about 2.8, affording a pA_2 of 7.41, which is comparable with the value from Figure 4.11.

L-826266 at 1 μM also produced a similar partial inhibition of the established contraction to sulprostone. However, antagonism by L-826266 was slower than that for L-798106, with contact time of up to 2 hours required for steady state to be reached (see next section for similar response in 17-phenyl PGE_2).

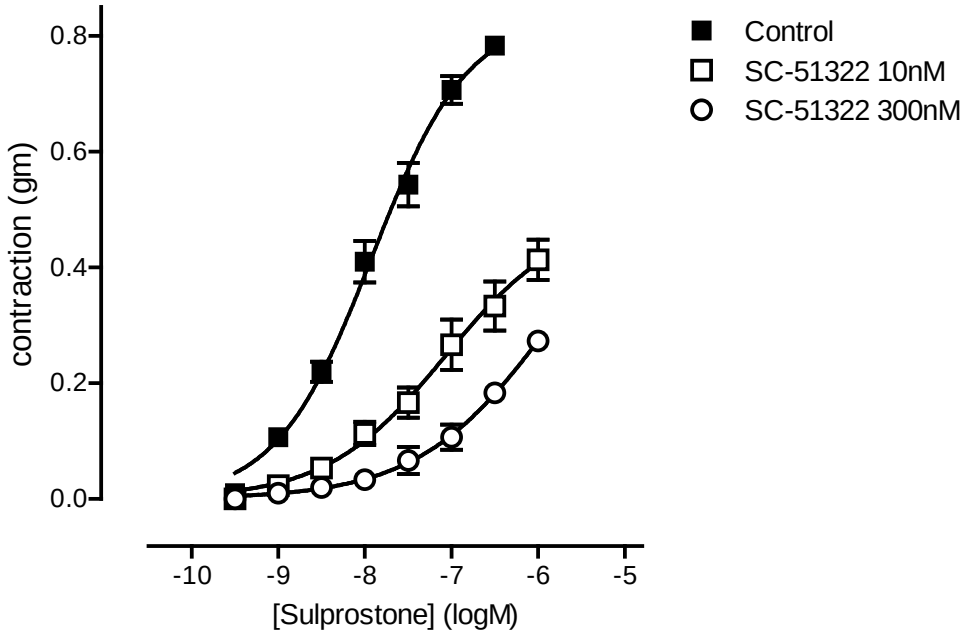

Figure 4.12 Antagonism of sulprostone-induced contraction by SC-51322 in rat mesenteric artery. Log concentration response curves for sulprostone following treatment with 10 nM and 300 nM SC-51322 are shown (n = 3).

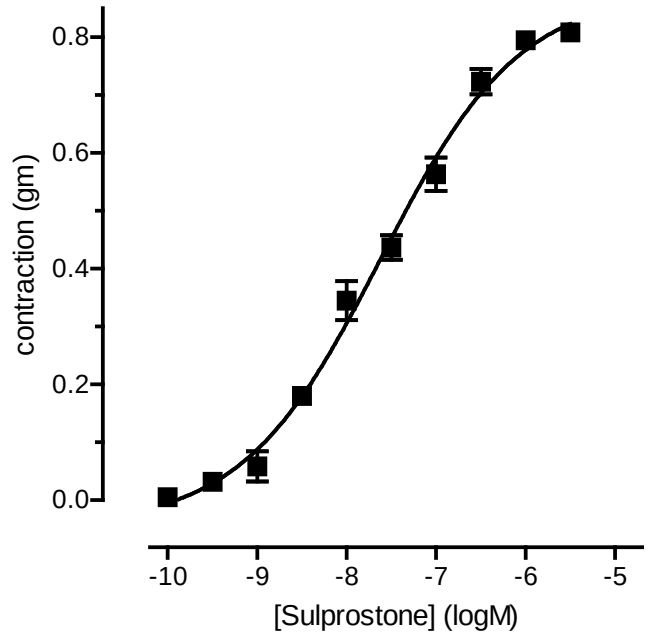

Figure 4.13 Contractile activity of sulprostone on rat mesenteric artery. Sulprostone (0.1 nM - 3 µM) contracted the artery in concentration dependent manner (*n* = 6). 100 nM BMS-180291 was present.

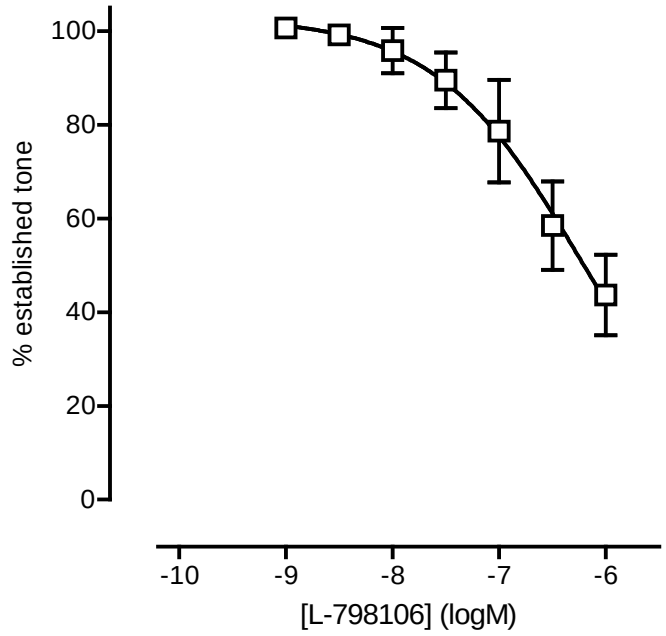

Figure 4.14 Antagonism of sulprostone-induced tone by L-798106 in rat mesenteric artery (*n* = 6). The arterial rings were precontracted with 100 nM sulprostone (EC_{80}). L-798106 (1 nM – 1 µM) was added cumulatively after 40-45 min. 100 nM BMS-180291 was present.

4.3.5 Interaction of 17-phenyl PGE_2 with SC-51322 and L-826266

17-Phenyl PGE_2 (which has moderate EP_1 / EP_3 selectivity) was used in later studies on rat mesenteric artery. The experiments were done in the presence of 100 nM BMS-180291. 17-Phenyl PGE_2 contracted the arterial rings, with E_{max} of 0.71 $\pm$ 0.02 g and pEC_{50} of 7.06 $\pm$ 0.08 (Figure 4.15, n = 5).

Under the inhibition-curve protocol (Figure 4.1B), the arterial rings were contracted with 100 nM of 17-phenyl PGE_2, corresponding to 80% of maximal response (EC_{80}). SC-51322 started to relax the arterial ring at 1 nM (Figure 4.16, n = 5). At 1 µM, the maximal relaxation by SC-51322 was 84 $\pm$ 4%. Similar to sulprostone, the modified Cheng-Prusoff equations cannot be properly utilised in a two-receptor system. With reference to Figure 4.15, the dose-ratio at 25% relaxation was 2.0, affording a pA_2 of 7.80 for SC-51322.

It has been observed that L-826266 was slow to reach equilibrium blockade as demonstrated in Figure 4.17. At 1 µM, L-826266 took approximately two hours to inhibit the established tone of 100 nM 17-phenyl PGE_2. Therefore in inhibition-curve studies, each concentration (0.1, 0.3, 1.0 µM) was allowed 90 - 120 min contact (Figure 4.18, n = 5). L-826266 induced 30.2 $\pm$ 13.3% relaxation at 1 µM. Similarly, the modified Cheng-Prusoff cannot be utilised due to incomplete inhibition. The dose-ratio at 20% relaxation was 1.78, with pA_2 of 6.21 for L-826266.

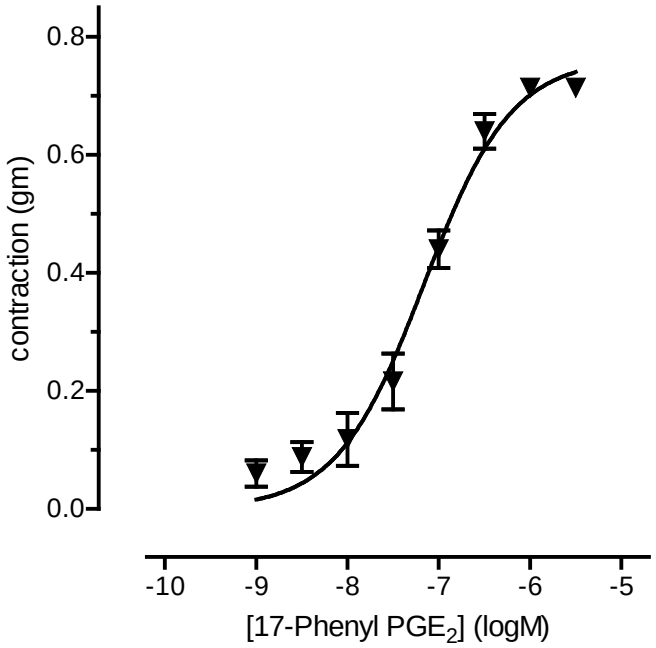

Figure 4.15 Contractile activity of 17-phenyl PGE_2 on rat mesenteric artery (*n* = 5). 17-Phenyl-PGE_2 (1 nM – 3 µM) contracted the artery in concentration dependent manner. 100 nM BMS-180291 was present.

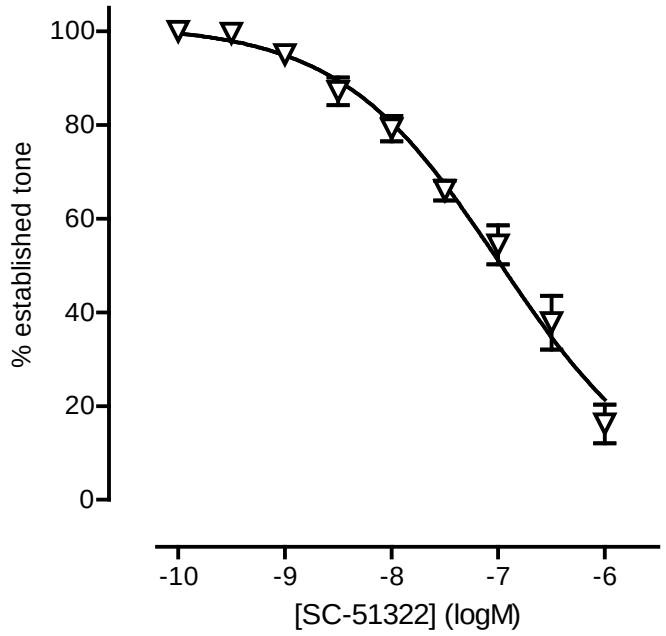

Figure 4.16 Antagonism of 17-phenyl PGE_2-induced contraction by SC-51322 in rat mesenteric artery (n = 5). The artery was contracted with 100 nM of 17-phenyl-PGE_2 (EC_{80}). SC-51322 (1 nM – 1 µM) was added cumulatively after 40 - 45 min. 100 nM BMS-180291 was present.

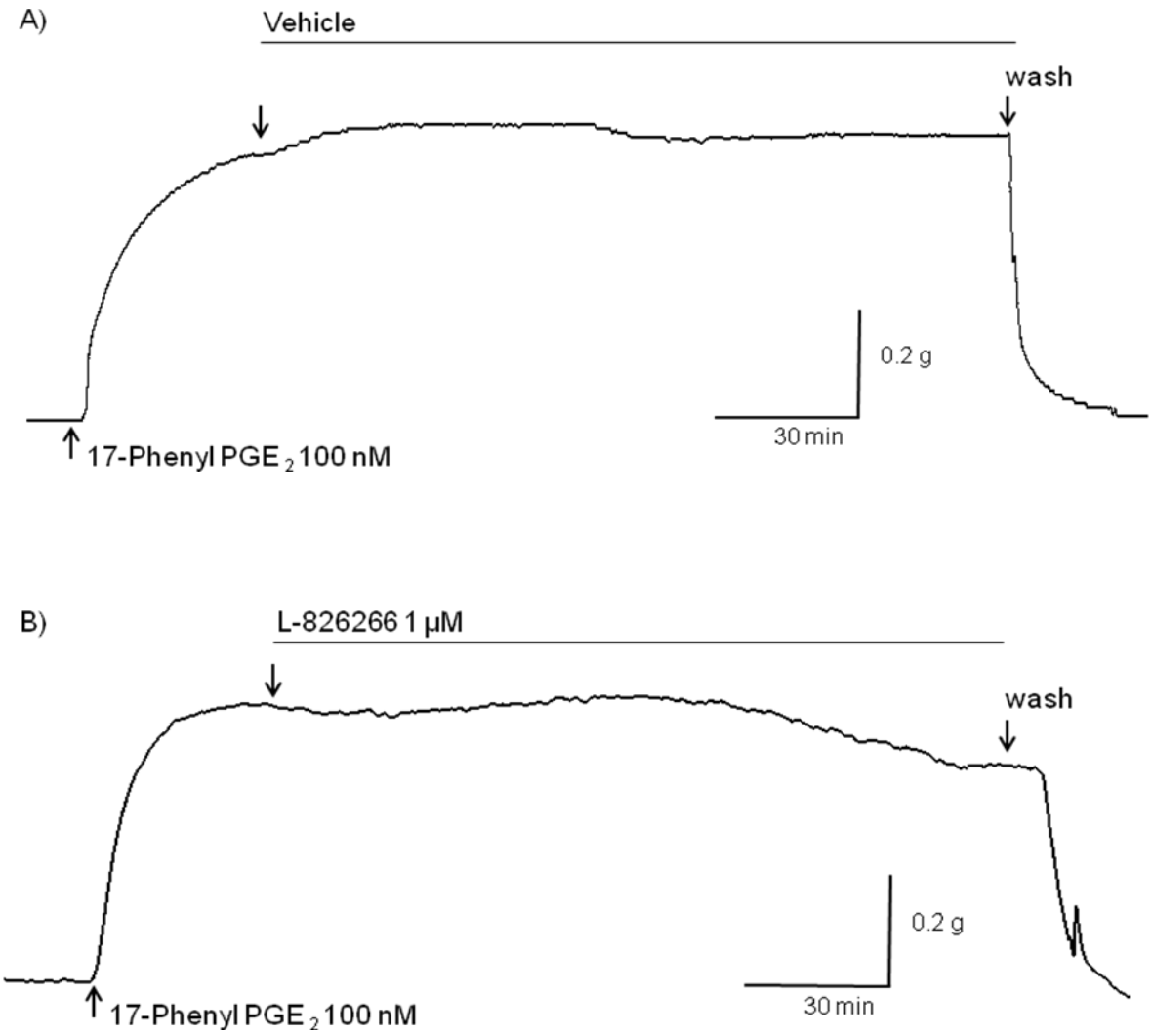

Figure 4.17 Trace illustrating the effect of 1 µM L-826266 on 100 nM 17-phenyl PGE_2 -induced contraction in comparison with control (vehicle). 100 nM BMS-180291 was present.

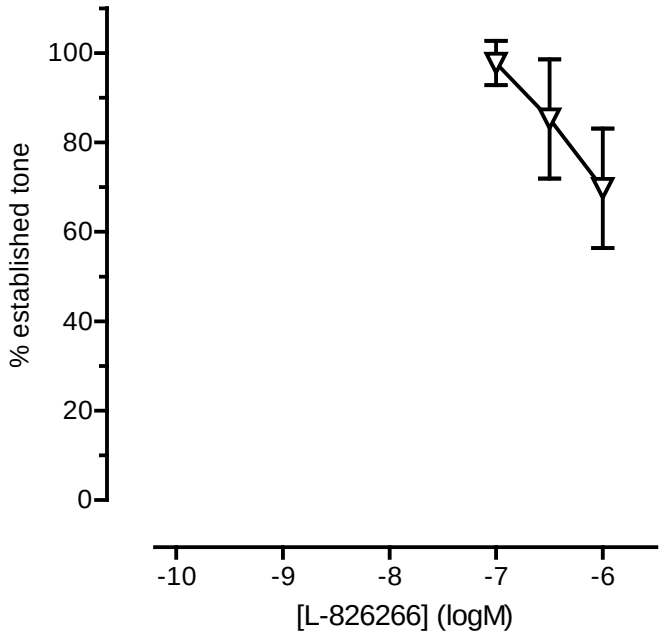

Figure 4.18 Antagonism of 17-phenyl PGE_2-induced tone by L-826266 in rat mesenteric artery (n = 5). The artery was contracted with 100 nM of 17-phenyl-PGE_2 (EC_{80}). Once the tone was established, L-826266 (100 nM – 1 μM) was added cumulatively. 100 nM BMS-180291 was present.

4.3.6 Effects of ONO-D1-004 and ONO-AE-248

ONO-D1-004, a selective EP_1 agonist, was tested on the arterial rings in the presence of 100 nM BMS-180291. A contractile response was seen with maximal response of 0.50 $\pm$ 0.01 g at 3 µM and pEC_{50} of 7.21 $\pm$ 0.23 (Figure 4.19, n = 4). ONO-AE-248, a selective EP_3 agonist, produced a much weaker response; maximal response of 0.21 $\pm$ 0.01 g at 3 µM and pEC_{50} of 7.63 $\pm$ 0.15 (Figure 4.19, n = 4). SC-51322 at 1 µM completely inhibited the contractile response of ONO-D1-004. In the presence of 100 nM BMS-180291, L-798106 at 1 µM did not have any effect on established contraction to ONO-AE-248.

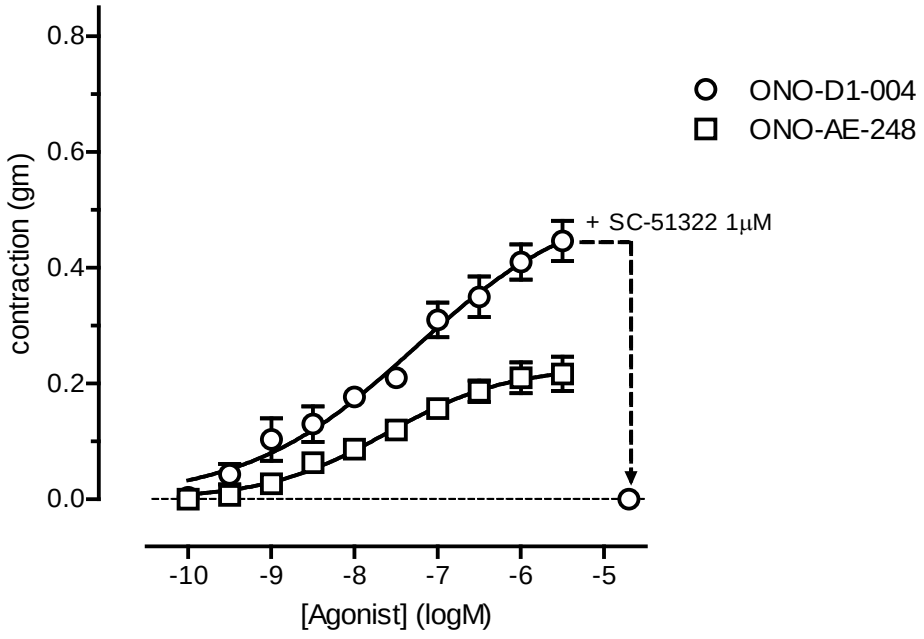

Figure 4.19 Contractile activities of ONO-D1-004 and ONO-AE-248 on rat mesenteric artery (n = 4). 1 µM SC-51322 completely antagonised the response by ONO-D1-004. 100 nM BMS-180291 was present in all tests.

4.3.7 Relaxant studies

The arterial rings were precontracted with 300 nM phenylephrine in the presence of 1 µM SC-51322, 1 µM L-798106 and 100 nM BMS-180291. The selective EP_2 receptor agonist ONO-AE1-259 started to relax the rings at 10 nM (Figure 4.20, *n* = 4). However, the relaxant responses were not significantly different compared with the control and no further relaxation was seen from 100 nM onwards. Butaprost-FA at the same concentration range also did not produce any relaxation (*n* = 4; data not shown).

The IP agonist iloprost (1 – 300 nM) did not relax the arterial rings precontracted with 300 nM phenylephrine (*n* = 4; data not shown).

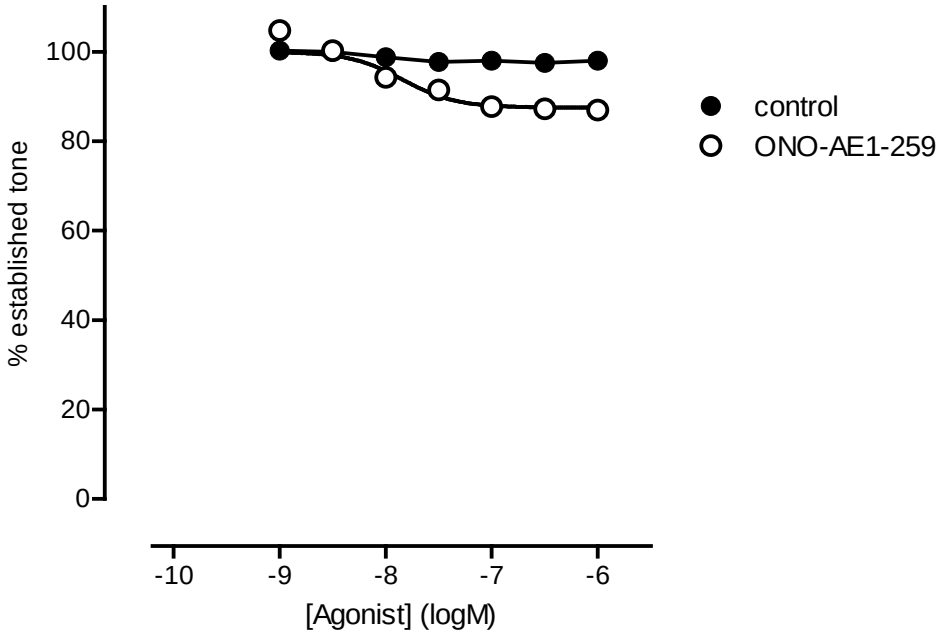

Figure 4.20 Relaxant activity of ONO-AE1-259 (1 nM – 1 µM) in comparison with control in rat mesentery artery (*n* = 4). The artery was precontracted with 300 nM phenylephrine. 100 nM BMS-180291, 1 µM L-798106 and 1 µM SC-51322 were present in all tests.

4.3.8 Two-site competition model

It appeared that there could be two components to the inhibition-curves for SC-51322 against 17-phenyl $PGE_{2,}$ as some of the data seems to deviate from the monotonic curve (Figure 4.16). Two theoretical curves were fitted in the inhibition curve (Figure 4.21A). Using the two-site competition equation in GraphPad Prism, the curve was refitted as described in Section 2.5.2. The data in graph of the two-site fit looks better (Figure 4.21B) than one-site model. The r^2-values were compared as described in Section 2.5.2. The r^2-value for one-site model is 0.92 and for two-site is 0.95.

The best-fit two-site curve has a high affinity site with a pIC_{50} of 8.23 and a low affinity site with pIC_{50} of 6.46 (Figure 4.21B). Based on the two theoretical curves, the fraction of high affinity sites is 33% with a 95% confidence interval that is reasonably narrow (20 – 45%). These results are acceptable; and it makes sense to compare the sum-of-squares of both models using the modified F test.

There are 45 data points to compare in 17-phenyl PGE_2 against SC-51322 curve. There are four parameters are fitted by the one-site equation fit and five parameters fitted for the two-site model. Using these data, the calculation is summarized in Table 4.2. The F ratio is 5.27 with 1 (numerator) and 40 (denominator) degrees of freedom. Using the F tables (see Appendix), the two-site model is significantly better than one-site model ($p < 0.05$).

Despite no big difference between the r^2-values between both models, the F test result concluded that the two-side model fits the data significantly better than one-site model.

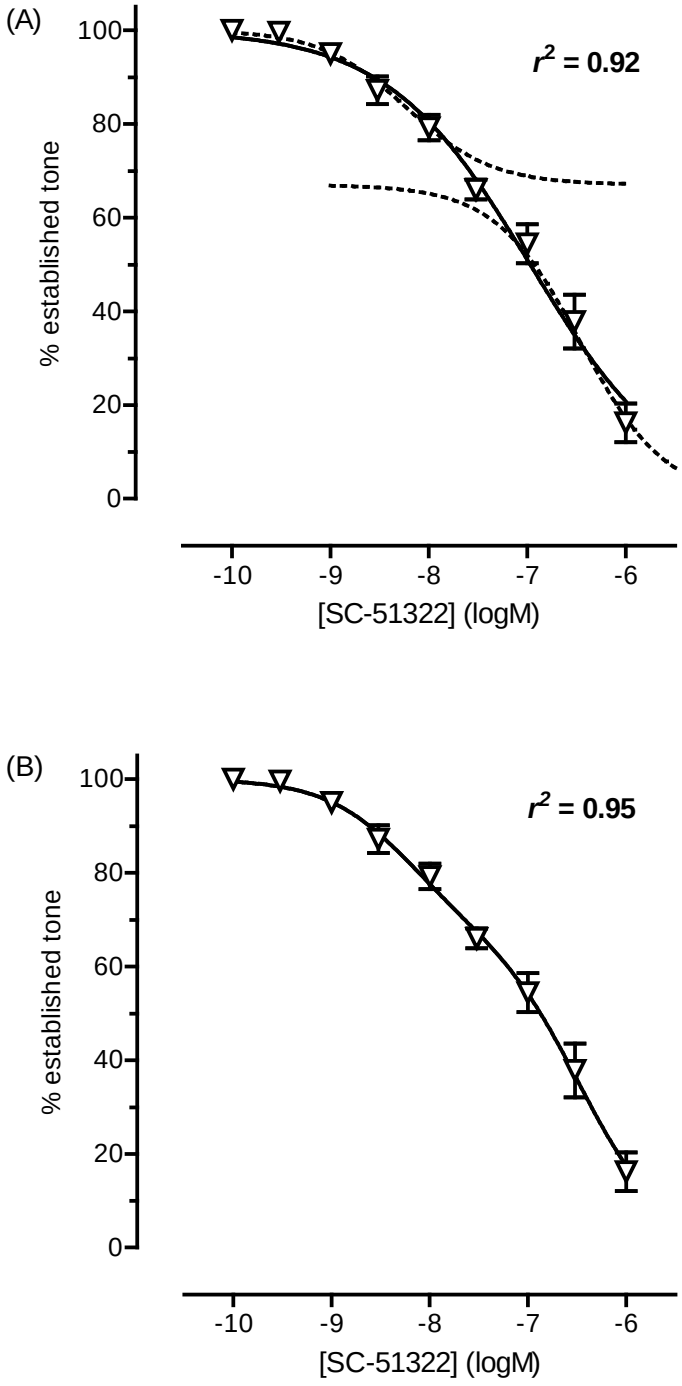

Figure 4.21 The two-site competition model vs one-site model on SC-51322 and 17-phenyl PGE_2 inhibition curve (from data in Figure 4.16) using GraphPad Prism software. A) The one-site model with two theoretical curves superimposed. B) The two-site model fitted to the same data.

Table 4.2 The F test for two-site model against one-site model of 17-phenyl PGE_2 vs. SC-51322.

Model	**SS**	**df**
Null hypothesis (1 site)	2139	41
Null hypothesis (2 sites)	1890	40
Difference	249	1
Fractional difference	0.1317	0.025
Ratio (F)	**5.27**	

4.4 Discussion

The superior rat mesenteric artery is part of a conductance system. Although resistance arteries present the greatest contribution to peripheral resistance, previous study has demonstrated the role of other conductance arteries, the femoral artery (Holloway and Bohr, 1973) and external iliac artery (Hansen and Bohr, 1975) in the control of blood pressure in the rat. The control of vascular tone in rat small artery is markedly similar to control in human artery of similar size (Hutri-Kahonen *et al.*, 1999). Thus, the effects of prostaglandins on the rat mesenteric artery may be relevant to the human artery.

The main interest of this study is to characterize prostanoid receptors that potentially control vascular tone in the rat mesenteric artery. It has been demonstrated that thromboxane A_2 (TXA_2) plays a role in the artery through TP receptor. (Bolla *et al.*, 2004). In agreement, TXA_2 together with PGE_2 and prostacyclin (PGI_2) were released from the pressurised artery in response to noradrenaline infusion (Soma *et al.*, 1996).

4.4.1 Defining optimum conditions for studying prostanoid systems

The rat mesentery exhibits a good viability over duration of the experiment, on average 8 hours. McIntyre *et al.* (2008) demonstrated that storage of the mesenteric artery in physiological salt solution (PSS) at 4º C preserved the artery response to noradrenaline up to two days of storage. In our study, we used the artery on the same day or after overnight storage in Krebs solution at 4 ºC.

The use of isoprenaline in setting the resting tone of a smooth muscle preparation has been described previously for the guinea-pig trachea preparation (Farmer *et al.*, 1974). The guinea-pig trachea tube was exposed to 20 nM of isoprenaline to obtain the maximal relaxation of the preparation, during which time fluid was allowed to flow into the lumen. On re-sealing the system, a consistent level of intraluminal pressure was attained for the remainder of the experiment. Isoprenaline (1 nM – 10 µM) has been demonstrated to relax rat mesentery artery precontracted with KCl, with a maximal relaxation of 66.8 $\pm$ 2.4% (Graves and Poston, 1993). In other studies, the relaxation with isoprenaline (10 nM – 100 µM) relaxed the 40 mM KCl precontracted artery to 80% of initial tone (Hutri-Kahonen *et al.*, 1999). In the current study, the arterial rings were exposed once to 100 nM isoprenaline for 10 min, followed by setting of the resting tone and then washout. Despite the absence of relaxation to isoprenaline in the majority of preparations, the resting tension was more stable and not prone to oscillate.

4.4.2 The artery response to non-prostanoid agents

Buus *et al.* (2000) demonstrated transient relaxation with exogenous KCl in ring preparations from Wistar rats at concentrations above 7 mM. The study was conducted in the presence of L-NOARG and indomethacin. In another study on rat mesenteric artery, KCl induced transient relaxation at concentration of 10 mM and above (Edwards *et al.*, 1998). Ba^{2+} and oubain inhibited this transient relaxation. However, in the current study, transient relaxation

was not seen (only indomethacin 1 μM was present in bath). Instead, the contractile response to exogenous KCl slowly faded at concentrations above 40 mM. An explanation for these different responses of KCl in the rat mesenteric artery is not readily apparent, although Edwards *et al.* (1998) has postulated K^+ may act as an EDHF, through an increase in extracellular concentration of K^+ causing hyperpolarisation and vasorelaxation of the artery. For this reason, KCl was not used as the contractile agent for the relaxant study.

In the current study, phenylephrine was demonstrated to produce a strong and sustained contractile response with a maximal response attained at a concentration of 10 μM. The concentration of 300 nM (representing 35% of maximal response) was chosen to precontract the arterial rings in the relaxant study. Other workers have used 3 μM as the precontractile dose (Edwards *et al.*, 1998).

4.4.3 Defining the prostanoid receptors involved in the contractile response

Table 4.3 listed the maximal responses and pEC_{50} values of the contractile prostanoid agonists examined on the rat mesenteric artery.

The TP analogue, U-46619 produced a concentration-dependent contractile response. This agreed with a previous study where U-46619 produced a stable contractile response and was used as a pre-contractile agent in a study of steroid hormone-induced relaxation on the rat mesenteric artery (Tsang *et al.*, 2003).

The selective TP receptor antagonist, BMS-180291 at 100 nM completely inhibited the U-46619 response in the current study. In previous studies in our laboratory, BMS-180291 in the low nanomolar range had a very slow onset on guinea-pig aorta and a cumulative

inhibition curve could not be obtained (unpublished observation by Jones RL). In comparison, the antagonism of BMS-189291 in rat mesenteric artery on U-46619 has a fast onset even at concentration of 1 nM as demonstrated in Figure 4.8. The difference may be due to the greater wall thickness of the aorta, such that diffusion through the extracellular space is markedly retarded by high affinity binding to TP receptors located on the cell surface (limited diffusion theory, Colquhoun *et al.*, 1972; Colquhoun and Ritchie, 1972).

Under the inhibition-curve protocol, the pA_2 for BMS-180291 against U-46619 was estimated to be 9.83 $\pm$ 0.25 for the rat mesenteric artery, which translates roughly into a dose-ratio of about 700 for 100 nM concentration. This is clearly sufficient to abolish any weak TP agonist activity of the EP agonists under study. The pA_2 estimated is comparable to pA_2 for BMS-180291 against U-46619 in rat aorta, reported as 9.5 (Zhang *et al.*, 1996) and 9.3 (Ogletree *et al.*, 1993). However the pA_2 reported in an early study in human platelets was 8.0 (Webb *et al.*, 1993). Since platelet-rich plasma (PRP) was used and BMS-180291 is a moderately lipophilic ligand, plasma protein binding will tend to reduce the estimate of its affinity.

Table 4.3 pA_2 values for prostanoid receptor antagonists on rat mesenteric artery estimated from the inhibition-curve protocol.

Agonists	**pEC_{50}**	**E_{max} (g)**	**Antagonists**	**pA_2**
U-46619	8.31 $\pm$ 0.14	0.81 $\pm$ 0.01	BMS-180291	9.83 $\pm$ 0.25
Sulprostone	7.62 $\pm$ 0.09	0.76 $\pm$ 0.02	L-798106	7.41†
17-Phenyl PGE_2	7.06 $\pm$ 0.08	0.71 $\pm$ 0.02	SC-51322	7.80†
17-Phenyl PGE_2	7.06 $\pm$ 0.08	0.71 $\pm$ 0.02	L-826266	6.21†

* 100 nM BMS-180291 was present in all experiments except when U-46619 was used as the agonist.
† Incomplete inhibition of established agonist response; pA_2 values are rough estimates from dose-ratios measured at the 20 - 25% inhibition level – see text.

$PGF_{2\alpha}$, a potent FP agonist did not produce any effect on the rat mesenteric artery, indicating the absence of FP receptors.

In initial experiments on the rat mesenteric artery, PGE_2, 17-phenyl PGE_2 and sulprostone contracted the artery in the absence of any prostanoid antagonist. The order of potency was as follows: sulprostone > 17-phenyl PGE_2 = PGE_2, which in the first instance suggests the presence of EP_3 and possibly also EP_1 receptors. Sulprostone is usually about 3 - 5 times more potent than PGE_2 on well established EP_3 preparations (e.g. guinea-pig vas deferens; Lawrence *et al.*, 1992). However, in this experiment, sulprostone was only about 1.5 times potent than PGE_2. As expected, BMS-180291 did not affect the profiles of these three agonists.

Probably the most important observation in relation to the 'two EP receptors proposal' is the inability of the EP_1 antagonist SC-51322 and the EP_3 antagonist L-798106 to completely inhibit submaximal contractions elicited by 17-phenyl PGE_2 and sulprostone respectively. The rough estimate of the pA_2 for L-798106 under the inhibition-curve protocol was 7.41. The study by Clark *et al.* (2004) on EP_3 preparations using sulprostone as agonist, gave a pA_2 value of 7.82 in guinea-pig trachea and 7.42 in vas deferens of the same species. In rat femoral artery, L-798106 caused a parallel displacement of log concentration-response curve by sulprostone (Hung *et al.*, 2006) The pA_2 estimated in this EP_3 preparation was 7.43 - 8.03. Recently, L-798106 has been shown to inhibit PGE_2-induced Ca^{2+} flux in a rat recombinant assay EP_3 receptor, with pK_i of 7.12 $\pm$ 0.04 (Jugus *et al.*, 2009). The pA_2 value obtained in the current study is comparable to the other 'pure' EP_3 preparation and suggests the presence of EP_3 receptor in the rat mesenteric artery.

Against 17-phenyl PGE_2, the pA_2 value for SC-51322 estimated from the experiment was 7.80, which is somewhat lower than corresponding values from Schild protocol studies in EP_1 preparations (guinea-pig trachea, 8.45; Hung *et al.*, 2006). This could be due to species difference or the selectivity of 17-phenyl-PGE_2, which can activate both EP_1 and EP_3 receptors in this case. Despite the high affinity for rat EP_1 receptors (rat hepatocytes, pIC_{50} of

8.0; Kimura *et al.*, 2001), SC-51322 does have measurable affinity for the human recombinant EP_3 receptor (pK_i of 6.16; Abramovitz *et al.*, 2000). Moreover, the slope of the SC-51322 inhibition curve in Figure 4.16 is much less than the slope of the agonist curve for 17-phenyl PGE_2 (Figure 4.15); this is consistent with activation of two receptors by the fixed concentration of 17-phenyl PGE_2 and subsequent inhibition of both receptors by SC-51322, but with considerable difference in affinity. Fitting of the inhibition-curve for SC-51322 against 17-phenyl PGE_2 using the two-site competition equation in GraphPad Prism is shown in Figure 4.22. The Hill slopes of both sigmoidal components are automatically constrained to 1.0. The first phase of inhibition curve gave a pIC_{50} of 8.22 and the second phase a pIC_{50} of 6.45. Whether the two-component fit better than the one-component fit will be discussed in next section.

The slow onset of L-826266 may be attributed to its high lipophilicity, where the predicted *n*-octanol / water partition coefficient (ClogP) for L-826266 is 7.4 (ChemAxon software). In the current study, due to limited availability and slowly developing block of L-826266 (need 2-h contact before the inhibition is observed), only concentrations from 100 nM to 1 µM were used. This slow inhibition against 17-phenyl PGE_2 (used as EP_3 agonist) in guinea-pig aorta, documented by Jones *et al*. (2008), afforded a pA_2 of 7.58 after 3-h contact. In the current study, the estimated pA_2 was 6.21, which is lower than in guinea-pig aorta.

The presence of two contractile EP receptors, EP_1 and EP_3 receptor in a vascular smooth muscle preparation has not often been reported. In large cerebral arteries of the adult pig, the contractile response to the prostanoid agonists used were attributed to the presence of both EP_1 and EP_3 receptors (Jadhav *et al.*, 2004). The EP_1 antagonist AH-6809 at 30 µM and 100 µM attenuated the PGE_2 contraction, with dose-ratios of 2.85 and 7.94 affording pA_2 values of 4.78 and 4.84 respectively. However these values are considerably lower than pA_2 values obtained in authentic EP_1 preparations. For example AH-6809 inhibited the contractile response to PGE_2 at 10 µM in guinea-pig ileum with pA_2 of 7.42 (Eglen and Whiting, 1988). Furthermore, 11-deoxy-16,16-dimethyl PGE_2 (DX-DM PGE_2; a selective EP_2 / EP_3 agonist) has been shown by Jadhav *et al.* (2004) to be a potent contractile agonist in the porcine cerebral artery. The DX-DM PGE_2-induced contraction was not inhibited by AH-6809 (3 –

300 µM), and the EP_3 receptor was concluded to be responsible for the response. However, the antagonist was tested against an established *supra-maximal* contraction to DX-DM PGE_2, which casts doubt on the conclusions drawn.

Guinea-pig ileum also has a mixed EP_1 with other contractile EP receptors (Lawrence *et al.*, 1992). AH-6809 (0.2 - 5 µM) shifted the logCRC of the EP_1 agonist with pA_2 corresponding to its reported EP_1 affinity. The morphine / AH 6809-resistant contractile effect for sulprostone and other EP_3 agonists confirm the existence of a EP_3 receptor on the guinea-pig ileum.

The porcine cerebral artery study has however raised several issues related to ligand selectivity. The contractile response of DX-DM PGE_2 was attributed to EP_3 receptor activation despite no direct evidence documented for the present of functional EP_3 receptor in the artery. At higher concentration of EP receptor antagonists, the inhibition effect may not be specific. Thus, AH-6809 at 300 µM completely blocked (3 of 6 preparations) the sulprostone-induced contractions. Given the rather low specificity of AH-6809 at high concentration (Keery and Lumley, 1988), it is not clear whether EP_1 or EP_3 receptors are involved. Moreover, could DX-DM PGE_2-contraction in the cerebral artery be mediated by EP_1 receptor? DX-DM PGE_2 itself has been shown to have relatively high affinity for the EP_1 receptor in radio-ligand binding studies in HEK cells, with K_i of 3.8, normalised to PGE_2 (Ungrin *et al.*, 2001).

The involvement of EP_1 and EP_3 receptor has not been clearly defined in the functional studies. The coexistence of the two receptors in the porcine cerebral artery was concluded by the positive immunoreactivities and receptor bands in Western blot studies though the findings in the functional studies are not consistent. Thus, DX-DM-PGE_2 induced contractions can be due to other contractile prostanoid receptor despite being shown to have a potent contractile effect on EP_3 receptor in human respiratory tract smooth muscle (Karim *et al.*, 1980).

4.4.4 The two-site competition model versus one-site competition model in relation to EP receptor-mediated contraction

As discussed earlier, the study proposed the existence of two receptors mediating contractions to PGE_2 analogues. The graph of the one site fit model for SC-51322 against 17-phenyl PGE_2 seems to deviate systematically from the data point (Figure 4.16). The possibility of two contractile receptor systems is demonstrated by re-fitting the curve on Figure 4.16 using the two-site model in GraphPad Prism program (Figure 4.21A). The two-site curve-fitting procedure coupled with statistical evaluation by F test supported this proposal. In general, this procedure requires reproducible inhibition curves between individual preparations and a difference in pIC_{50} values for the two components of at least 1.5 log units. In the current case, the difference was 1.77 log units. It would be of value to test another EP_1 antagonist with greater EP_1 / EP_3 selectivity than SC-51322. GW-848687 may serve this purpose; Giblin *et al.* (2007) reported > 400 fold selectivity for EP_1 over other EP receptors in human recombinant receptor assays.

4.4.5 Utility of the novel EP agonists

The specificities of ONO-DI-004 and ONO-AE-248 to the EP_1 and EP_3 receptor respectively, have been demonstrated in a study on intestinal smooth muscle preparations from EP knock-out mice (Okada *et al.*, 2000). However, the sensitivities of the EP_1 and EP_3 systems and the true potencies of these novel agonists in the rat mesenteric artery preparation have never been documented before. The maximal response (comparing at 3 μM) of ONO-D1-004 was significantly higher than ONO-AE-248 on rat mesenteric artery preparation, while their pEC_{50} were similar for, at 7.65 $\pm$ 0.06 and 7.65 $\pm$ 0.01 respectively. On the basis that both compounds are full agonists the EP_1 system would appear to be the marginally dominant system in the rat mesenteric artery. In addition, ONO-D1-004 contractile response in rat mesenteric artery was 71% of the 17-phenyl PGE_2 response at similar maximum concentration (3 μM). Importantly, SC-51322 abolished contraction induced by ONO-DI-004, which argues strongly for ONO-DI-004 contracting the artery by solely activating EP_1

receptors. Conversely, L-798106 (selective EP_3 antagonist) did not block the contraction induced by ONO-AE-248. This raised a question of specificity of ONO-AE-248 on EP_3 receptor. Further studies need to be done to elucidate the true sensitivities of these compounds in the rat mesenteric artery.

The previous study of the selectivity of these ONO compounds has produced a mixed results. The human pulmonary veins have been documented to have a TP and EP_1 contractile system (Walch *et al.,* 2001). ONO-D1-004 activity has been compared with sulprostone in the concentration range of 1 nM – 10 µM in this venous preparation (Norel *et al.,* 2004). However, ONO-D1-004 potency was very low and a pEC_{50} was not calculable, while sulprostone-induced contraction was much more pronounced. Established responses to sulprostone were partially inhibited by the selective EP_1 antagonists, ONO-8711 and ONO-8713 at concentration of 30 µM and 10 µM, respectively. However, from the reported K_i values for these antagonists (1.7 and 0.3 nM respectively; Watanabe *et al.*, 1999) one would have expected abolition of sulprostone action. Finally, the same study also demonstrated the ability of ONO-AE-248 to contract the vein consistent with its moderate affinity for the EP_3 receptor (K_i value of 7.5 – 15 nM; Suzawa *et al.*, 2000). Collectively, these results suggest that the human pulmonary veins contains either an EP_3 system only or EP_1 and EP_3 systems, but not EP_1 system alone as implied by Norel *et al.* (2004).

4.4.6 Relaxant EP and IP receptors

Iloprost, a selective IP receptor agonist did not shown any relaxant effect on phenylephrine contraction. From radio-ligand binding studies, iloprost has some affinity for EP_1 and EP_3 receptors, with K_i of 21 and 22 nM, respectively (Kiriyama *et al.*, 1997). Also functional studies indicate the high agonist potency of iloprost on EP_1 receptors (Dong *et al.*, 1986). However, the influence from both EP receptors has been eliminated, as the respective selective antagonists were added 30 min prior to the phenylephrine pre-contracted sequence (Figure 4.2).

ONO-AE1-259 has been shown to relax the non-pregnant porcine uterus selectively through EP_2 receptor activity (Cao *et al.*, 2002). In rat mesenteric artery, the activity of ONO-AE1-259 was not significantly different from the control. Butaprost-FA did not have any relaxant activity on the artery. Thus, evidence from the current study demonstrated the absence of relaxant EP_2 receptors in the rat mesenteric artery.

4.5 Conclusions

The current evidence has shown that only the contractile prostanoid receptors are present in the rat mesenteric artery. The receptors are TP, EP_1 and EP_3 receptors. Several PGE_2 analogues simultaneously activated both the EP_1 and EP_3 contractile receptor systems. Their inhibition curves could be fitted to a two-component inhibition equation and statistical testing showed that this fitting process was better than the one-component fit. Both receptor systems are likely to contribute to the contractile activity of the natural agonist PGE_2, and activation of either alone appears insufficient to cause maximal contraction of the tissue.

The rank order of potency of EP agonists was sulprostone > 17-phenyl PGE_2 = PGE_2.

CHAPTER FIVE

RAT URINARY BLADDER

5.1 Introduction

The main function of the urinary bladder is to store and periodically release the urine into the urethra. The 'micturition reflex pathway' governs emptying of the bladder, which is voluntary in nature. There are various forms of bladder dysfunction; urgency and frequency are particularly common in older males and usually not controlled satisfactorily by drug administration. The control of the bladder involves interplay of neuronal and chemical factors. There are two main neuronal systems in the control of the bladder; the autonomic nervous system and somatic nerves (de Groat and Yoshimura, 2001; Andersson, 2002). The autonomic nervous system is responsible for the control of the bladder wall smooth muscle, whereas the somatic nerve is responsible for the control of the bladder neck sphincter.

Various chemical factors are involved in the control of the bladder wall, including histamine, neuropeptides and prostaglandins (prostanoids). The role of prostanoids is mainly to modulate the function and to maintain the basal tone of the urinary bladder (Ishizuka *et al.*, 1995; de Groat and Yoshimura, 2001; Schroder *et al.*, 2003). Prostanoids can affect the bladder wall function directly or indirectly. Prostanoids produce a contraction in the bladder directly through activation of prostanoid receptors on the smooth muscle cells. Prostanoids also have a potent stimulating action on sensory fibres (Schroder *et al.*, 2003). This will sensitise the afferent fibres of the bladder to natural stimuli. Intravesical infusion of PGE_2 in the conscious rat increased the levels of neurokinins, which in turn induced the micturition reflex (Ishizuka *et al.*, 1995). The interplay between neuronal and chemical controls of the bladder wall is summarized in Figure 5.1 (modified from Andersson, 2002).

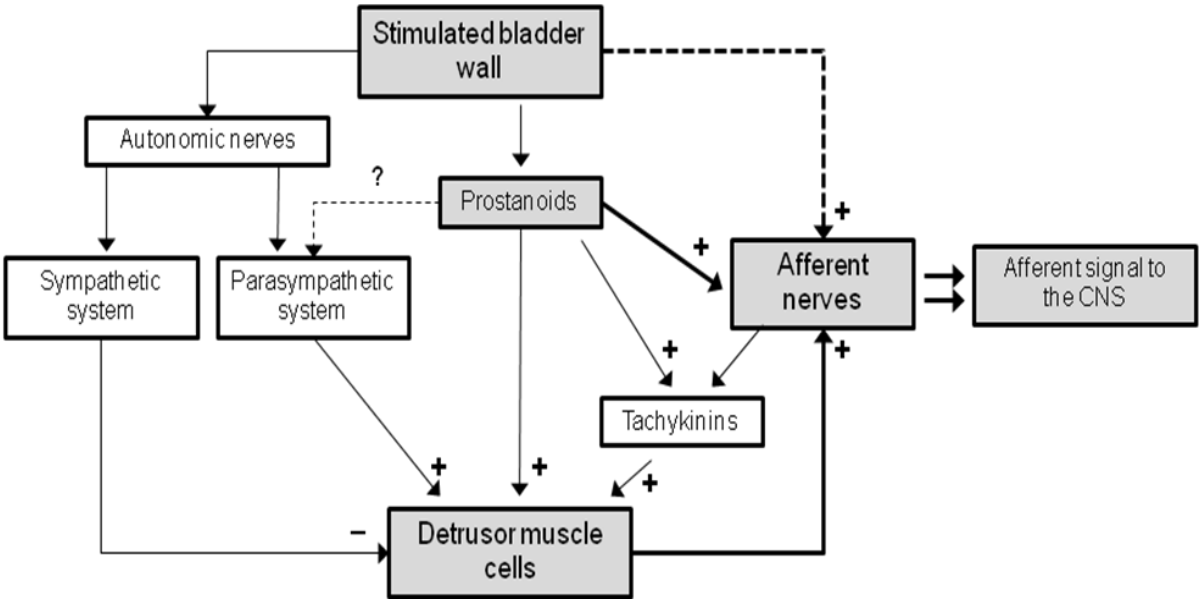

Figure 5.1 The neuronal and chemical controls of the urinary bladder, *CNS* – Central Nervous System (modified from Andersson, 2002).

It has been shown that various stimuli including mechanical stretching, inflammation and injuries to the bladder wall may initiate the synthesis and release of prostaglandins by the bladder wall (Ishizuka *et al.*, 1995; Park *et al.*, 1999; de Groat and Yoshimura, 2001; Wheeler *et al.*, 2001; Schroder *et al.*, 2003). Park *et al.* (1999) demonstrated the over-expression of COX-2 in the bladder smooth muscle cells of the Lewis rat after stretch-induced stimulation. COX-1 basal level remained unchanged. The study also demonstrated that NS-398 (COX-2 specific inhibitor) almost completely attenuated the increase in PGE_2 levels caused by stretching. Non-steroidal anti-inflammatory drugs (NSAIDs) also reduced prostaglandin levels and improved bladder function in the rat (Takagi-Matsumoto *et al.*, 2004).

The type of prostanoids and the relative amounts synthesized and released by the urinary bladder vary between species. In the rat urinary bladder, PGE_2, 6-keto-$PGF_{1\alpha}$ and TXB_2 form the major part of the basal PG activity generated in the tissue (Jeremy *et al.*, 1984; Kasakov and Vlaskovska, 1985). By comparison, PGI_2 (prostacyclin) is the major prostanoid released followed by PGE_2, $PGF_{2\alpha}$ and TXA_2 in the human bladder (Poli *et al.*, 1992; Khan *et al.*, 1998).

To my knowledge, the receptor subtype(s) that mediate the actions of prostanoids on rat bladder have not been well characterized. However, the presence of EP_1 receptor in rat bladder is provided by a study of the selective EP_1 receptor antagonist, SC-19220, which increased bladder capacity in normal rats (Maggi *et al.*, 1988). The amplitude of the micturition contraction was slightly but not significantly decreased by treatment with SC-19220. On isolated strips of rat detrusor muscle, SC-19220 also shifted the log concentration-response curve for PGE_2 to the right affording a pA_2 value of 4.4 ± 0.1, the value that is less than other recognized EP_1 systems.

In a rat model of bladder outlet obstruction (BOO), PGE_2 have been shown to increase bladder capacity, micturition volume and micturition interval without increasing residual urine (Lee *et al.*, 2007). The study also demonstrated that a selective EP_1 antagonist; PF-2907617-02 inhibited this effect of PGE_2 in a dose-dependent manner. In agreement, there

were no changes in bladder parameters after intravesical PGE_2 instillation following EP_1 gene deletion in BOO mice model (Schroder *et al.*, 2004). In contrast, there were significant changes in the micturition pattern in wild type (WT) mice in response to PGE_2. These results suggested that under normal condition, endogenous PGE_2 is not involved in modulating bladder function. In the case of the stimulated bladder, PGE_2 level increased and produced an overactive bladder, mediated by EP_1 receptor.

The existence of the EP_3 receptor in rat urinary bladder was documented by qualitative PCR (Su *et al.*, 2008). The study also showed that the EP_3 receptor antagonist DG-041 inhibited rhythmic bladder contraction, which in-turn reduced the frequency of micturition. By doing so, the visceromotor reflex (VMR) response was prevented. DG-041 and CM9 (L-798106) also increased bladder capacity in the conscious rat (Jugus *et al.*, 2009). The same study also demonstrated that DG-041 and CM9 inhibit the Ca^{2+} influx induced by PGE_2 through the EP_3 receptor with pK_i of 7.57 and 7.12; respectively. In agreement, the study showed that the EP_3 receptor agonist GR-63799X reduced the efficacy of the voiding, with reduction of urine per void. The selectivity effect of GR63799X were demonstrated by work on EP_3 receptor knockout (EP_3 KO) mice (McCafferty *et al.*, 2008). Intravesical administration of GR-63799X produced overactive bladder in wild-type (WT) mice. This effect was absent in EP_3 KO mice. EP_3 KO mice also presented with higher bladder capacity compared with WT mice. This implied the EP_3 receptor is responsible for the bladder overactivity.

PGE_2 and its analogue sulprostone caused a strong urgency sensation and bladder instability in healthy women (Schussler, 1990). However, sulprostone activates both EP_1 and EP_3 prostanoid receptor subtypes and has direct and neuronally-mediated actions on smooth muscle (Coleman *et al.*, 1994b; Narumiya *et al.*, 1999). The instability caused by sulprostone in human bladder could be due to activation of EP_1 receptors alone rather than EP_3 receptors.

Cyclophosphamide treatment in rats induced bladder inflammation and hyperactivity which in turn increased the expression of COX-2 (Chuang *et al.*, 2008). The study also demonstrated the up-regulation of EP_4 expression in the bladder is paralleled with the elevation of COX-2 expression. The increased expression of COX-2 in inflammatory bladder could lead to increased production of PGE_2, which might sensitise peripheral EP_4 receptors and produce bladder hyperactivity. The intravesicular administration of Botulinum toxin A, prevented the release of neurotransmitter and consequently decreased the inflammatory response. Concurrently, the expression of COX-2 and EP_4 receptor also decreased, accompanied by loss of the bladder hyperactivity. However, the exact mechanism by which the EP_4 receptor causes the hypersensitivity in cystitis was not elucidated in the study. It must be borne in mind that the EP_4 system is always inhibitory to smooth muscles, i.e. causes relaxation.

The main aim of the current experiments is to characterize functionally the prostanoid receptor(s) in the rat urinary bladder preparation, using selective agonist and antagonists. Agonists used included PGE_2, 17-phenyl PGE_2 (moderate EP_1 / EP_3 selectivity), sulprostone (moderate EP_3 / EP_1 selectivity), U-46619 (TP-selective), butaprost-FA (EP_2 selective) and latanoprost-FA (FP-selective).

Table 5.1 lists pA_2 values of the selective antagonists used in the rat urinary bladder experiment. Selective receptor antagonists, particularly EP_1 antagonists, are crucial to achieve this aim. SC-51322, a well documented and potent EP_1 antagonist, with pA_2 of 8.45 in the guinea-pig trachea (Hung *et al.*, 2006), was used. In addition, GW-848687, a recently described EP_1 antagonist with higher affinity than previously developed agents was also used (Giblin *et al*., 2007). In recombinant EP_1 receptor study, GW-848687 has been shown to be a competitive antagonist at the EP_1 receptor with pA_2 of 9.1 (Giblin *et al.*, 2007). It also has 30-fold selectivity over the TP receptor and with very low activity on the other prostanoid receptors.

L-798106 was the only EP_3 antagonist available for this study. It shows high selectivity for EP_3 receptors based on ligand binding assays involving recombinant prostanoid receptors (Juteau *et al.*, 2001). In functional studies, it blocked the action of sulprostone with pA_2 values of 7.82 in guinea-pig trachea (Clarke *et al.*, 2004) and 7.43 – 8.03 in rat femoral artery (Hung *et al.*, 2006) (Table 5.1). Recently, L-798106 (CM9) have been shown to inhibit PGE_2-induced Ca^{2+} entry in cells of rat EP_3 receptors, with pK_i value of 7.12 (Jugus *et al.*, 2009). BMS-180291 is the first choice antagonist to block TP receptors, owing to its high selectivity and affinity (pA_2 of 9.3 on rat aorta; Ogletree *et al.*, 1993).

However, during the period of this study, there was no selective agonist or antagonist available to assess the functional EP_4 receptor in the rat urinary bladder.

Table 5.1 Antagonists and concentrations chosen for use in the rat urinary bladder experiments.

Antagonists	**Reported pA_2**	**Concentrations used in the current study**	**References**
GW-848687	9.1	30 – 300 nM	Giblin *et al.*, 2007
SC-51322	8.45	30 nM – 1 µM	Hung *et al.*, 2006
L-798106	7.43 – 8.03	30 nM - 1µM	Juteau *et al.*, 2001; Clarke *et al.*, 2004; Hung *et al.*, 2006
	7.12 (rat)		Jugus *et al.*, 2009
BMS-180291	9.3	100 nM	Ogletree *et al.*, 1993

5.2 Methods

The basic methodology used has been described in detail in Chapter 2. Specific methodological points not discussed previously are addressed below.

5.2.1 Setting up of preparations

The rat urinary bladders were obtained as described in Chapter 2. The resting tone was set at an optimal tension of 1 g, determined from preliminary experiments**.** Previous study also has documented 1 g as the optimal resting tension for this preparation (Maggi *et al*., 1988; Schneider *et al*., 2004). The four preparations were allowed to equilibrate for 1 h, and then exposed twice to 100 nM carbachol to assess the contractile function.

All subsequent sequences were done in the presence of 100 nM BMS-180291, incubated for 30 min before the sequence commenced. The preparations were allowed a further 30 - 40 min to equilibrate before exposure to 30 nM PGE_2 for 10 min (Chan and Jones, 2004). Preliminary experiments established that the response to cumulative addition of prostanoid agonists was improved and more reproducible following exposure to low-dose PGE_2.

After washout, the preparations were allowed to stabilize for at least 30 min. The presence of the prostanoid receptors was assessed by performing the experimental protocol in the presence of various antagonists (Table 5.1). Basically, a concentration-response curve (CRC) was constructed by cumulative addition of the particular agonists. In the immediate sequences, the vehicle (serve as control) or antagonist with different concentration was added at least 30 min before the cumulative addition of the agonist (Figure 5.2A).

For assessment of antagonist potency, an inhibition-curve protocol was utilised as described in Chapter 2. Basically, the first sequence involved the construction of agonist curve in absence of antagonist of interest. After washout and stabilization, the preparation was precontracted with the fixed concentration of agonist at 80% of maximal contraction (EC_{80}). Antagonist was then added cumulatively to the precontracted bladder strips (Figure 5.2B and 5.3). Preparation without the antagonist served as a control.

5.2.2 Antagonist protocol and pA_2 estimation

Antagonist affinity was determined by calculating the pA_2. In this study, the basic inhibition-curve protocol is used. The details have been described in Section 1.7.2. The pA_2 is estimated from the equation (Lazareno and Birdsall, 1993b):

$$K_b = \frac{IC_{50}^*}{\frac{[A]}{EC_{50}^*} - 1}$$

and

$$K_b = \frac{[B_i]}{\frac{[A_f]}{[A_i]} - 1}$$

.

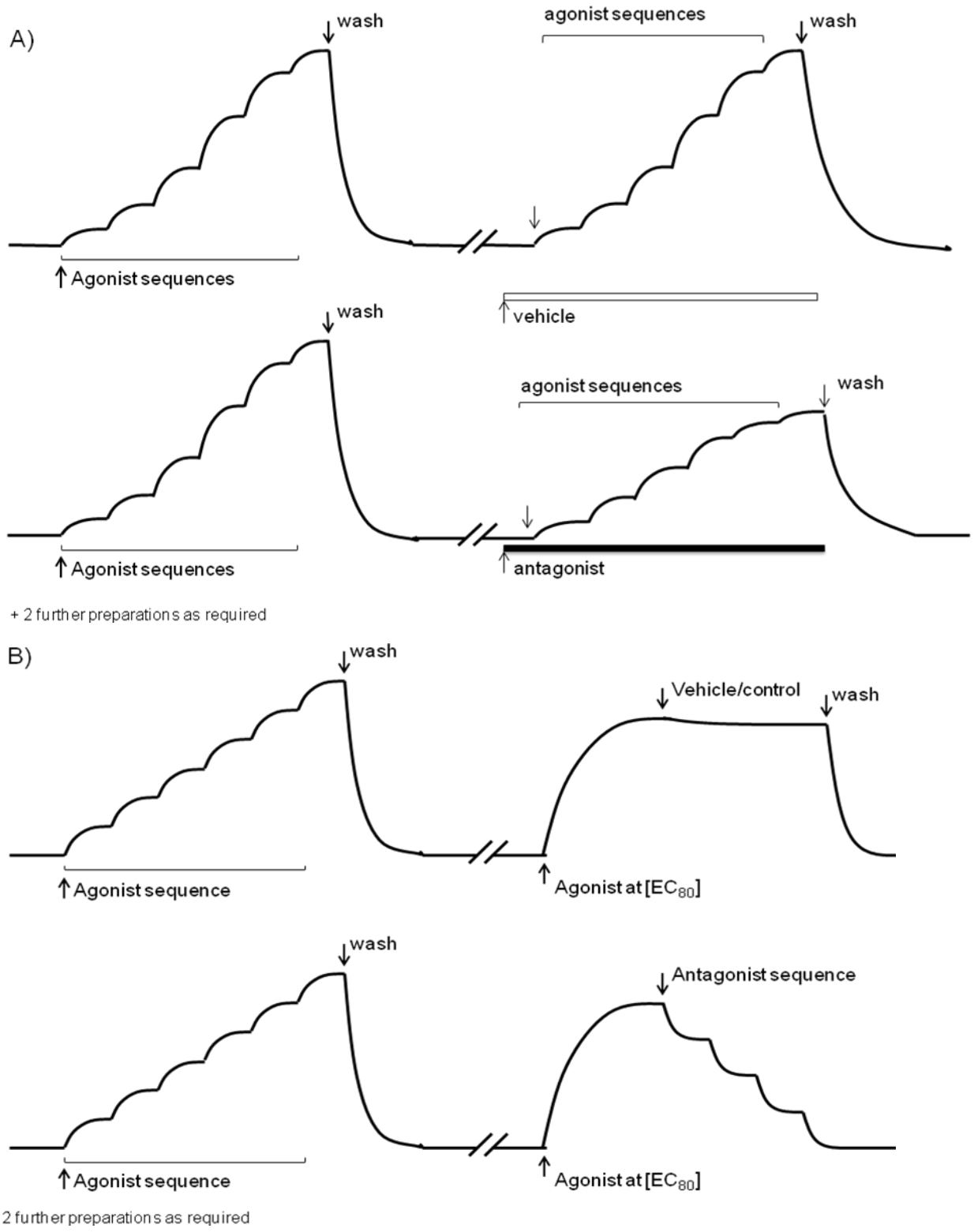

Figure 5.2 Protocols used for rat urinary bladder to determine the profile of an antagonist and where appropriate its affinity constant. A) The basic protocol B) The inhibition-curve protocol.

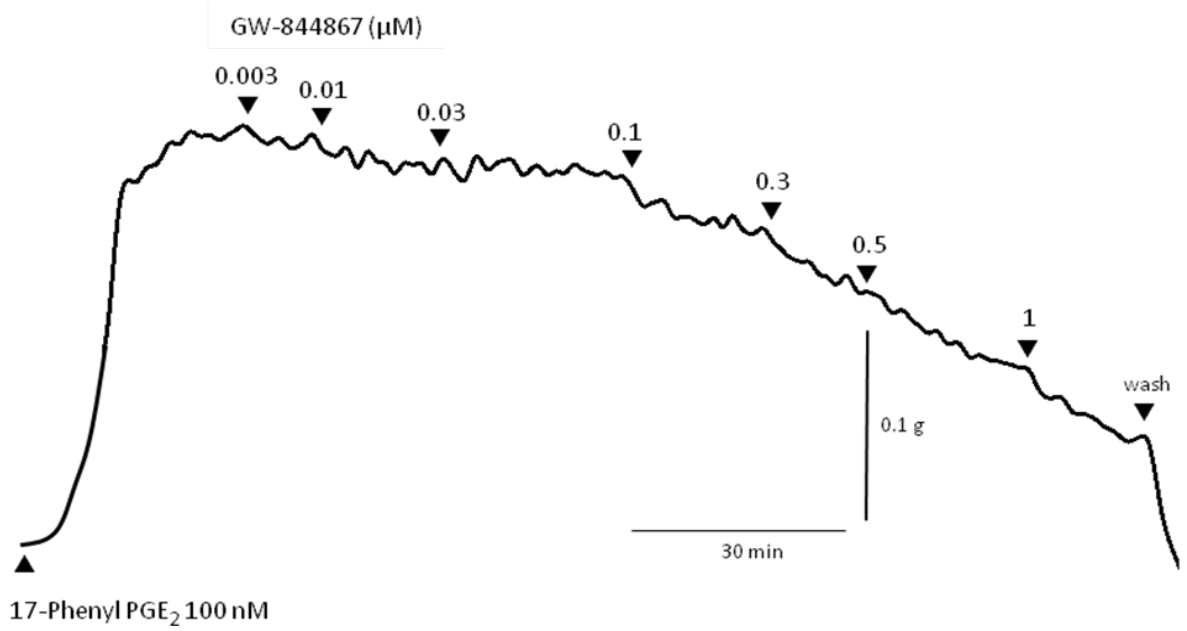

Figure 5.3 An experimental tracing of the effects of increasing concentrations of GW-848687 on the established response to 17-phenyl PGE_2 in rat urinary bladder, part of inhibition curve protocol (Figure 5.2B).

5.2.3 Statistical analysis

Contractile responses were measured as increases in tension (g) above the resting level and normalised to the second 100 nM carbachol response on each bladder preparation. Relaxant responses were expressed as a percentage of the established tone of the contractile agonist. A variable-slope sigmoidal curve was fitted to log concentration–response data using GraphPad Prism software; the bottom asymptote was constrained to zero for contraction and to 100% for relaxation. Sigmoidal curve parameters were derived from data for individual preparations. Data were further analysed by 1-factor and repeated measures 2-factor ANOVA combined with comparison of selected means by planned (orthogonal) contrasts using SuperANOVA software; all tests were two-tailed and the significance level was set at $p < 0.05$. Where applicable, data were analysed by the two-site competition equation using the modified F test in combination with the r^2-values comparison. All data are presented as mean $\pm$ SEM.

5.3 Results

5.3.1 Initial investigations of rat urinary bladder strips

All experiments on rat urinary bladder strips were conducted in the presence of 1 µM indomethacin to suppress prostanoid biosynthesis. Carbachol at 100 nM produced reproducible contractions, which did not fade. Histamine (50 – 100 nM) also contracted the bladder strips, but the response faded quickly. On the other hand, phenylephrine (10 – 500 nM) failed to produce any contractile response in the strips. In subsequent experiments, contractions were normalised to the response to the second 100 nM carbachol response obtained on each preparation.

The responses of the rat urinary bladder to cumulative addition of PGE_2, 17-phenyl PGE_2 and sulprostone are shown in Figure 5.4, with a maximum concentration used of 300 nM (n = 7). All three prostanoid agonists produced dose-dependent contractions. PGE_2 produced a higher response compared to other agonists at the maximal concentration of 300 nM (E_{300nM}: 72 $\pm$ 3%; pEC_{50} of 7.41 $\pm$ 0.08, n = 7), 17-Phenyl PGE_2 and sulprostone induced weaker response compared to PGE_2 (E_{300nM}: 56 $\pm$ 8% and 37 $\pm$ 3%; pEC_{50} of 7.29 $\pm$ 0.08 and 7.13 $\pm$ 0.13, respectively, n = 7). The majority of responses to these contractile prostanoids were quick and sustained; slight fading was seen only in about one-fourth of preparations.

Cumulative addition of the selective TP agonist, U-46619 (1 nM – 1 µM) produced no contractile response (n = 4; data not shown). The addition of 100 nM BMS-180291 was without effect on established contraction to 100 nM PGE_2 (n = 4; data not shown). In subsequent experiments, 100 nM BMS-180921 was routinely present (see Section 1.7.1).

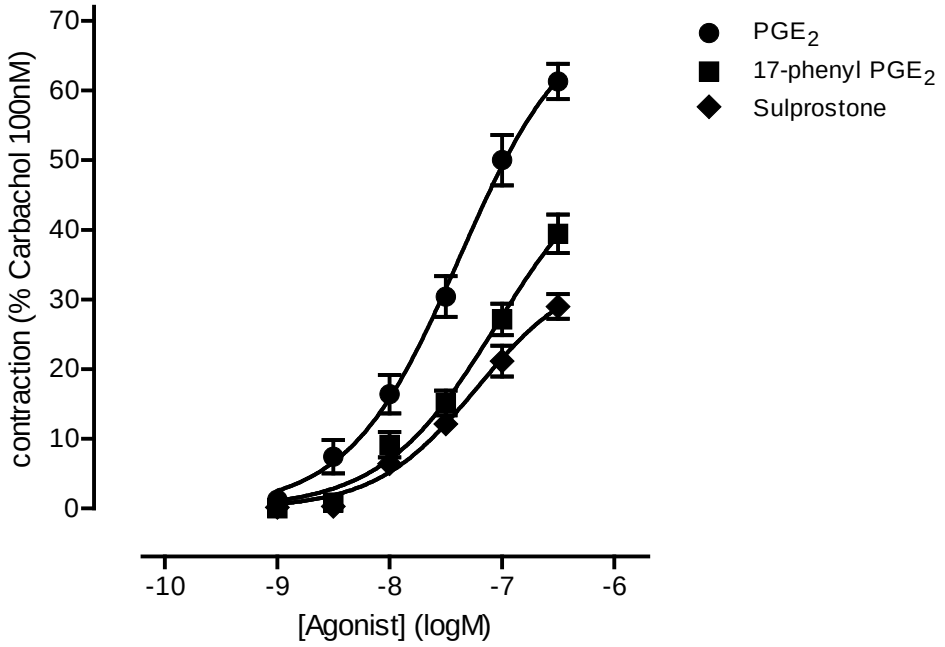

Figure 5.4 Concentration-response curves for PGE_2 and two of its analogues in rat urinary bladder (*n* = 7).

Latanoprost-FA (100–300 nM) (FP selective agonist) failed to produce any response in the muscle strips (*n* = 4, data not shown). Cumulative addition of the selective EP_2 agonist butaprost-FA (100 – 300 nM) had no effect on the preparation precontracted with 80 nM carbachol (corresponding to EC_{60} total response) (*n* = 4, data not shown). PGE_2 (100 - 300 nM) also did not relax the preparation precontracted with 80 nM carbachol (data not shown).

At this stage, it was concluded that relaxant EP_2 receptors, and probably EP_4 receptors, were not present in the rat urinary bladder, and that the contractile responses to prostanoids were only mediated by EP receptors. Further studies were performed to investigate the involvement of EP_1 and EP_3 receptors.

5.3.2 Effects of SC-51322 on contractile effects of prostanoid agonists

Pre-incubation of the bladder with 30 nM SC-51322 resulted in a roughly parallel right-shift of the log concentration-response curve for PGE_2 as shown in Figure 5.5 (n = 3). The log interval of 1.02 (measured at EC_{25}) afforded a pA_2 of 8.5. In contrast, the PGE_2 curve was displaced in a non-parallel manner by SC-51322 300 nM (DR comparison at EC_{30} and EC_{10}; $p = 0.02$ with CI 95% of 7.41 – 40.15). There appeared to be a component of the PGE_2-induced contraction that was (relatively) resistant to antagonism by SC-51322.

The CRC of 17-phenyl PGE_2 was constructed in the presence of SC-51322 at 30 and 300 nM (Figure 5.6, n = 3). The curve was displaced to the right in non-parallel manner by 30 nM and 300 nM SC-51322. However, there was no significant difference between the effect of 30 nM and 300 nM SC-51322 on 17-phenyl PGE_2 curve ($p = 0.65$).

The pre-treatment of SC-51322 (30 and 300 nM) before cumulative addition of sulprostone significantly reduced the maximal contractile response ($p = 0.001$) (Figure 5.7, n = 4). Similarly with PGE_2 and 17-phenyl PGE_2, the CRC for sulprostone is displaced non-parallel to the right. There were significant difference between sulprostone response to 30 nM and 300 nM SC-51322 as compared to control ($p = 0.001$, both). There was also significant difference in effect of pre-treatment with 30 nM and 300 nM SC-51322 ($p = 0.01$).

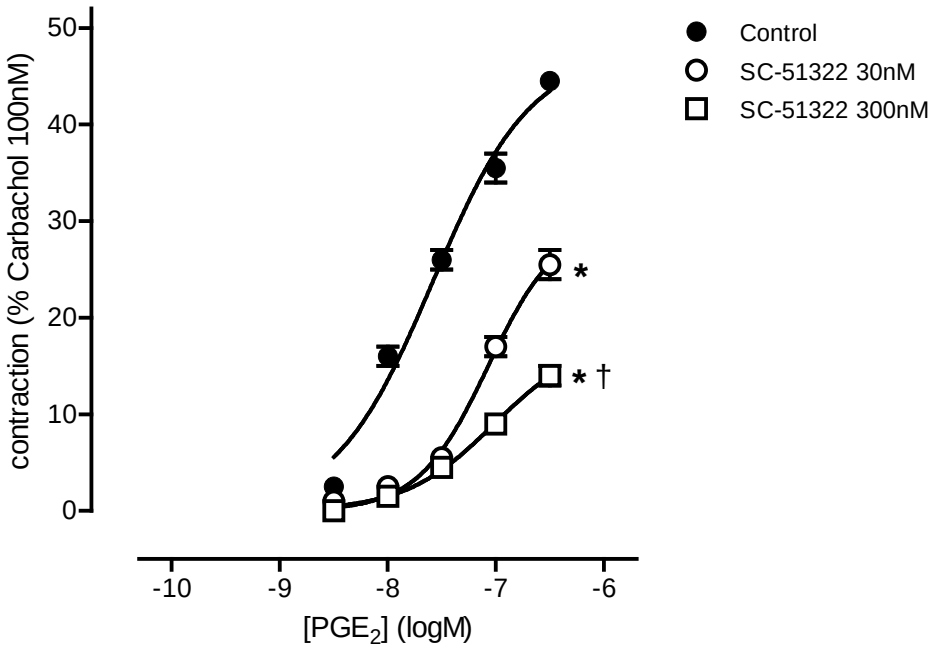

Figure 5.5 Antagonism of PGE_2-induced contraction by SC-51322 in rat urinary bladder. Log concentration-response curves for PGE_2 following treatment with 30 nM and 300 nM SC-51322 are shown (n = 3).*$P < 0.01$ 30 nM and 300 nM SC-51322 vs. control; $^{\dagger}P < 0.01$, 300 nM SC-51322 vs. 30 nM SC-51322, using main effects contrasts.

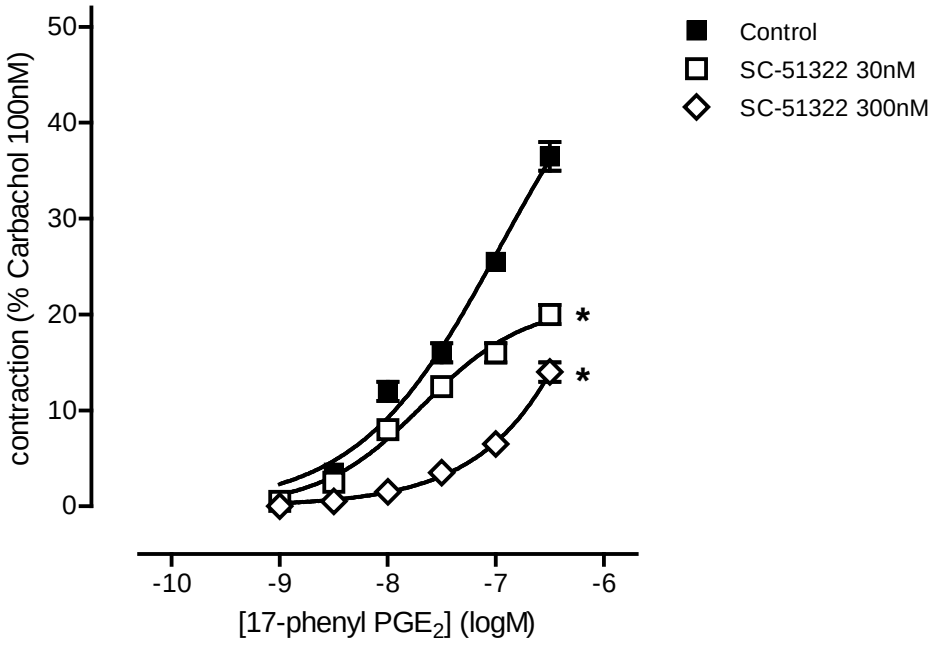

Figure 5.6 Antagonism of 17-phenyl PGE_2-induced contraction by SC-51322 in rat urinary bladder. Log concentration-response curves for 17-phenyl PGE_2 following treatment with 30 nM and 300 nM SC-51322 are shown (n = 3). *$P < 0.01$, 30 nM and 300 nM SC-51322 vs. control, using main effects contrasts.

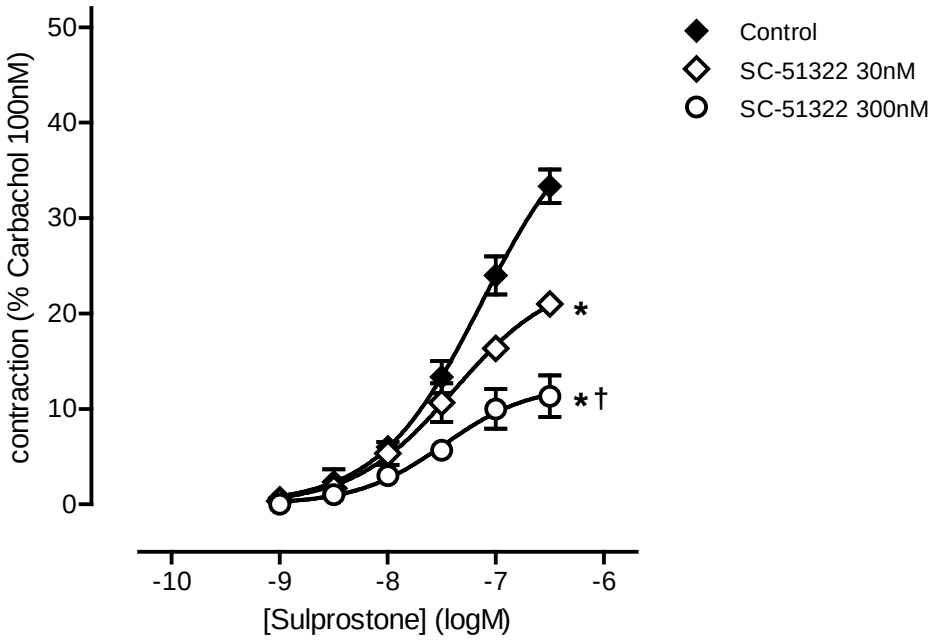

Figure 5.7 Antagonism of sulprostone-induced contraction by SC-51322 in rat urinary bladder. Log concentration-response curves for sulprostone following treatment with 30 nM and 300 nM SC-51322 are shown (n = 4). *$P < 0.01$, 30 nM and 300 nM SC-51322 vs. control; $^{\dagger}P < 0.01$, 300 nM SC-51322 vs. 30 nM SC-51322, using main effects contrasts.

5.3.3 Effects of L-798106 on contractile effects of prostanoid agonists

L-798106 is highly lipophilic and it was decided to make all dilutions from the stock with DMSO to be sure that the compound remained in solution. DMSO (at 14 mM) had no significant effect on the location of the PGE_2 curve, but may have slightly suppressed the maximum response (Figure 5.8, $n = 3$). 1 µM L-798106 significantly depressed the PGE_2 tone in control and in the presence of DMSO ($p = 0.001$, $p = 0.003$; respectively). However, there was no significant displacement of the curves.

1 µM L-798106 significantly reduced the tone produced by 300 nM 17-phenyl PGE_2 ($p = 0.001$) (Figure 5.9, $n = 3$). The curve is displaced in non-parallel manner. The reduction of maximal response by 17-phenyl PGE_2 by 1 µM L-798106 (62%) was similar as for reduction in PGE_2 tone (68%, Figure 5.8).

Pre-incubation of L-798106 at 1 µM produced a significant suppression of maximal response by sulprostone ($p = 0.001$) (Figure 5.10, $n = 4$). The curve was displaced in non-parallel manner.

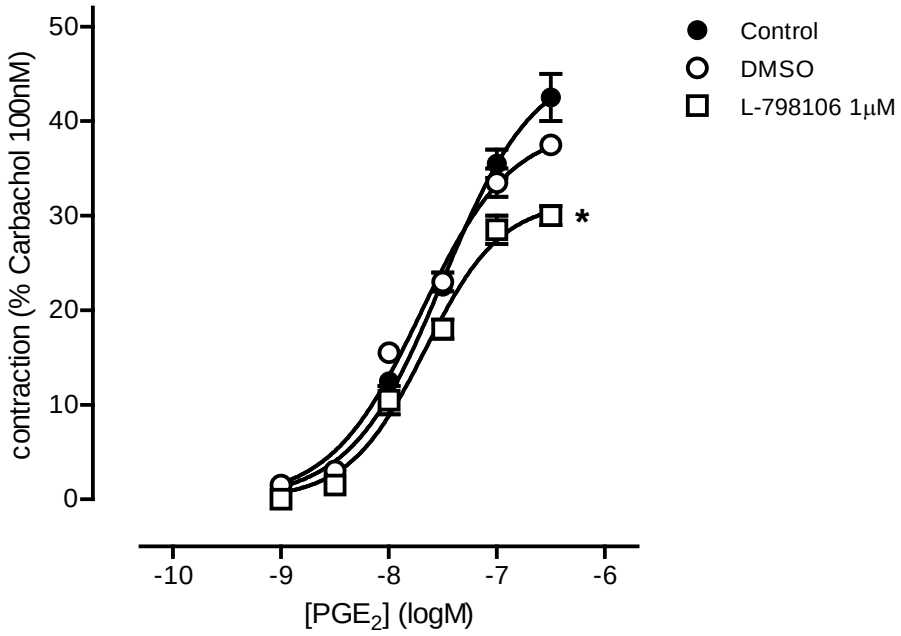

Figure 5.8 Antagonism of PGE_2-induced contraction by L-798106 in rat urinary bladder. Log concentration-response curves for PGE_2 following treatment with 1 μM L-798106 and DMSO are shown (n = 3). *$P < 0.01$, 1 μM L-798106 vs. control and DMSO, using main effects contrasts.

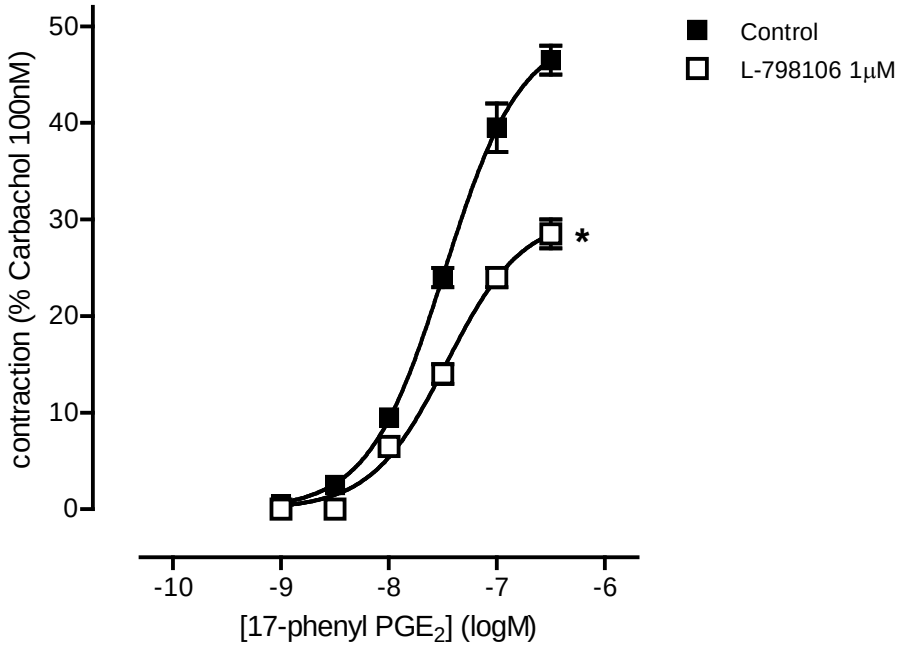

Figure 5.9 Antagonism of 17-phenyl PGE_2-induced contraction by L-798106 in rat urinary bladder. Log concentration-response curve for 17-phenyl PGE_2 following treatment with 1 μM L-798106 is shown (n = 3). *$P < 0.01$, 1 μM L-798106 vs. control, using main effects contrasts.

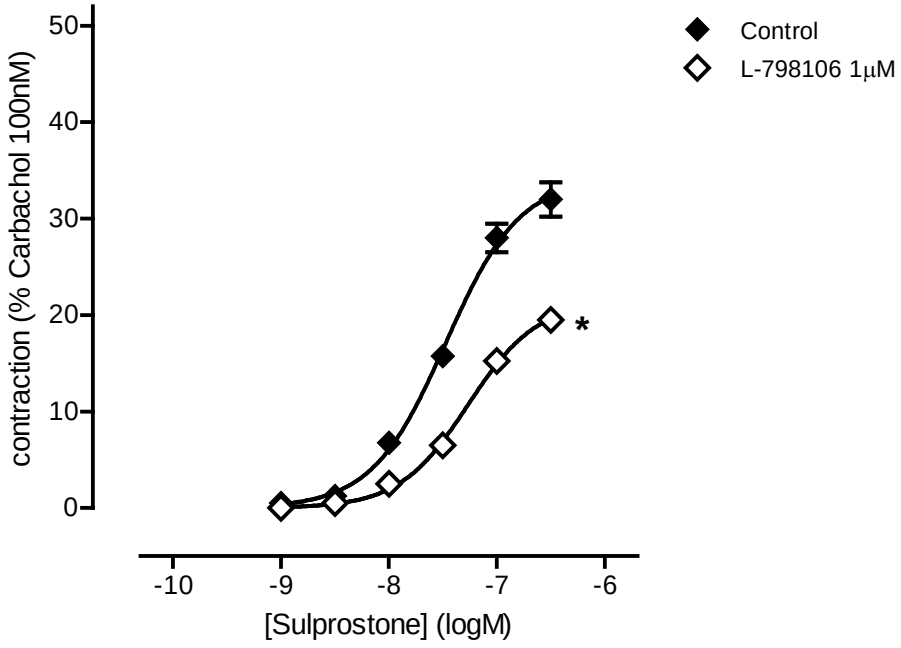

Figure 5.10 Antagonism of sulprostone-induced contraction by L-798106 in rat urinary bladder. Log concentration-response curve for sulprostone following treatment with 1 μM L-798106 is shown (n = 4). *$P < 0.01$, 1 μM L-798106 vs. control, using main effects contrasts.

5.3.4 Effects of a combination, of SC-51322 and L-798106 on contractile effects of prostanoid agonists

It was decided to perform further experiments in which pre-treatment with 300 nM L-798106 was added to 30 nM and 300 nM SC-51322. The combination of both drugs did not produce any significant changes to PGE_2 response in comparison with pre-treatment with SC-51322 alone as demonstrated in Figure 5.11 (n = 3). Main effects analysis gave p values of 0.41 and 0.30 for comparison of 30 nM SC-51322 vs 30 nM SC-51322 / L-798106 and 300 nM SC-51322 vs 300 nM SC-51322 / L-798106 respectively.

For 17-phenyl PGE_2, main effects analysis of 30 and 300 nM SC-51322 in combination with 300 nM L-798106 in comparison with control gave p values of 0.001 (Figure 5.12, n = 3). In comparison to 300 nM SC-51322 alone, the addition of 300 nM L-798106 did not produce any significant changes. However, although the maximum response for 30 nM SC-51322 alone and in the presence of L-798106 was similar, there was a significant rightward displacement of the 17-phenyl PGE_2 curve ($p = 0.001$ *to* 0.004 for cell-cell contrasts for 10, 30, 100 and 300 nM agonist).

Similarly for sulprostone, the antagonist combination produced a similar finding as pre-treatment with SC-51322 alone (Figure 5.13, n = 3). There were no significant changes in the curves between effects of 30 nM SC-51322 vs 30 nM SC-51322 / L-798106 and 300 nM SC-51322 vs 300 nM SC-51322 / L-798106 ($p = 0.65$, $p = 0.50$; respectively).

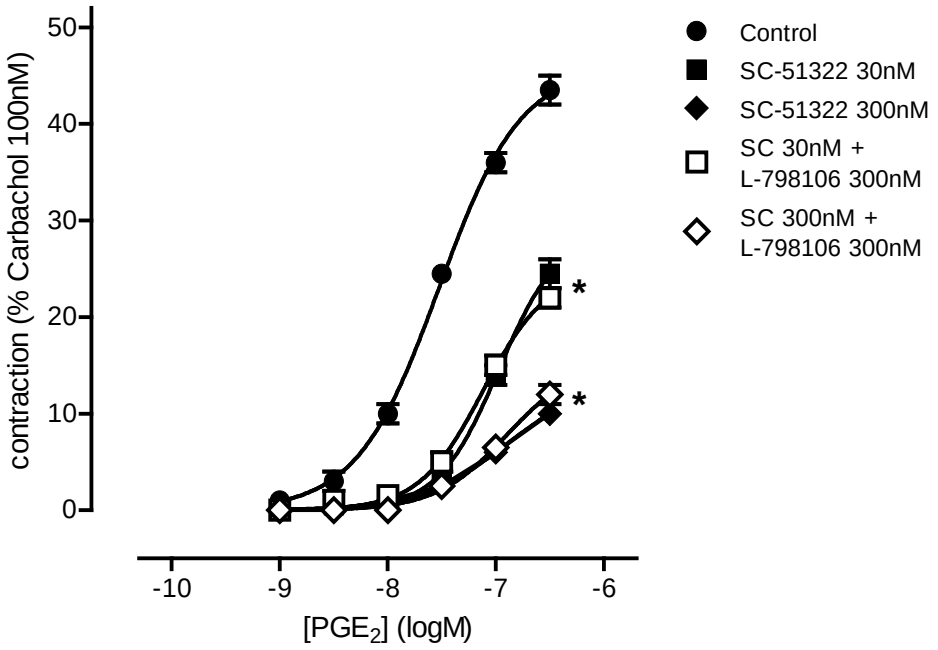

Figure 5.11 Antagonism of PGE_2-induced contraction by SC-51322 and L-798106 in rat urinary bladder. Log concentration-response curves for PGE_2 following treatment with 30 nM and 300 nM SC-51322 in the presence and absence of L-798106 300 nM are shown (n = 3). *$P < 0.01$, 30 nM and 300 nM SC-51322 vs. control, using main effects contrasts.

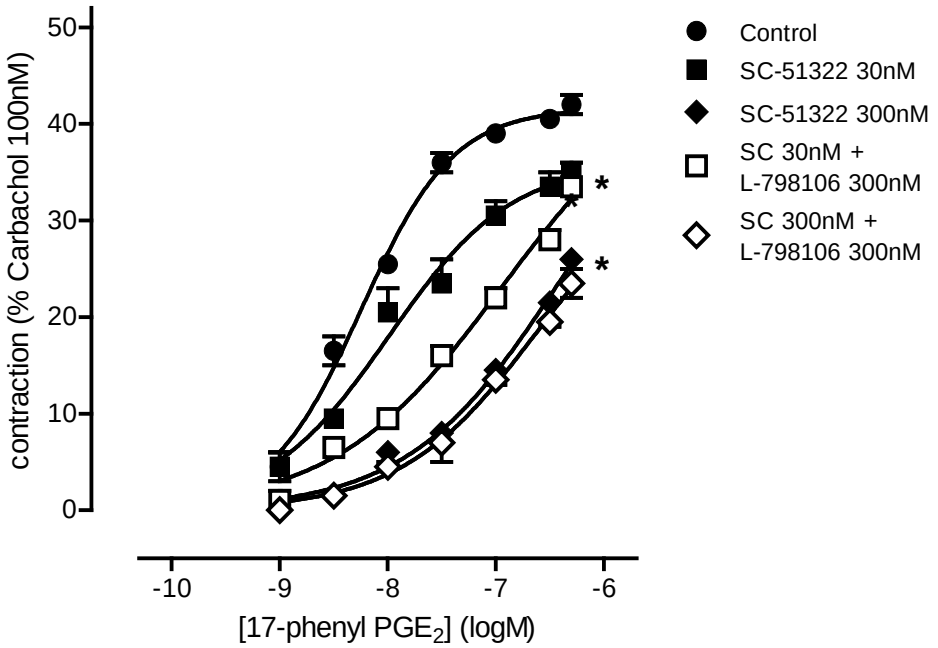

Figure 5.12 Antagonism of 17-phenyl PGE_2-induced contraction by SC-51322 and L-798106 in rat urinary bladder. Log concentration-response curves for 17-phenyl PGE_2 following treatment with 30 nM and 300 nM SC-51322 in the presence and absence of L-798106 300 nM are shown (n = 3). *$P < 0.01$, 30 nM and 300 nM SC-51322 vs. control, using main effects contrasts.

.

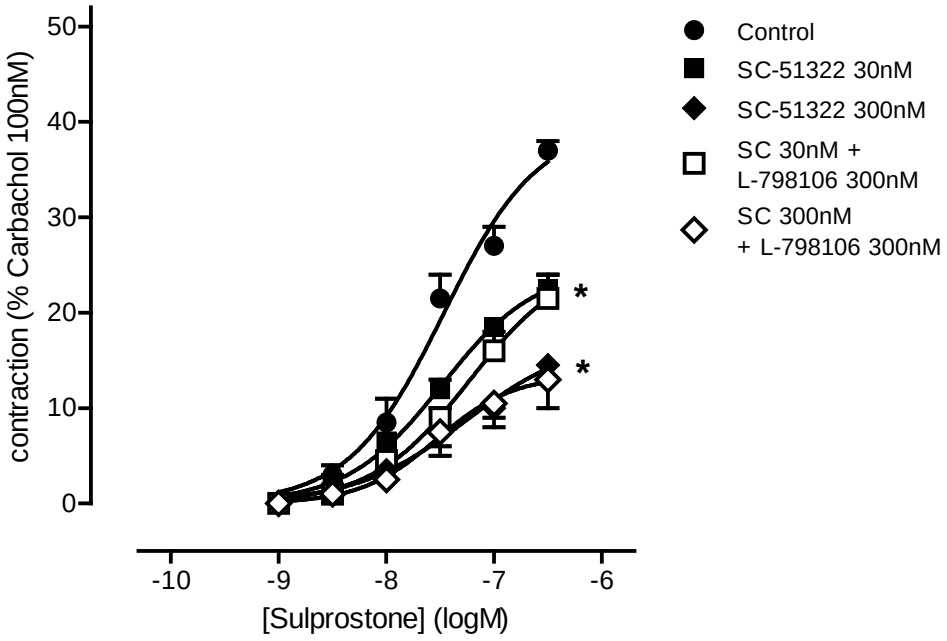

Figure 5.13 Antagonism of sulprostone-induced contraction by SC-51322 and L-798106 in rat urinary bladder. Log concentration-response curves for sulprostone following treatment with 30 nM and 300 nM SC-51322 in the presence and absence of L-798106 300 nM are shown (n = 3). *$P < 0.01$, 30 nM and 300 nM SC-51322 vs. control, using main effects contrasts.

5.3.5 Antagonist potency of L-798106 under inhibition-curve protocol

The CRC of sulprostone was constructed as part of inhibition-curve protocol to assess the potency of L-798106. The pEC_{50}* estimated from the curve was 7.44 $\pm$ 0.06 (Figure 5.14A, *n* = 4). Cumulative addition of L-798106 relaxed the established tone by 100 nM sulprostone in dose-dependent manner; 87% inhibition was found at 300 nM (Figure 5.14B, *n* = 4). L-798106 started to inhibit the tone at 1 nM. The inhibition was slow and took nearly 20 min to be noticeable and another 10 min before addition of the next dose. The pIC_{50}* estimated from the inhibition curve was 8.15 $\pm$ 0.14. Calculated pA_2 for L-798106 on sulprostone in the rat urinary bladder using equation described in section 5.2.4 is 8.35.

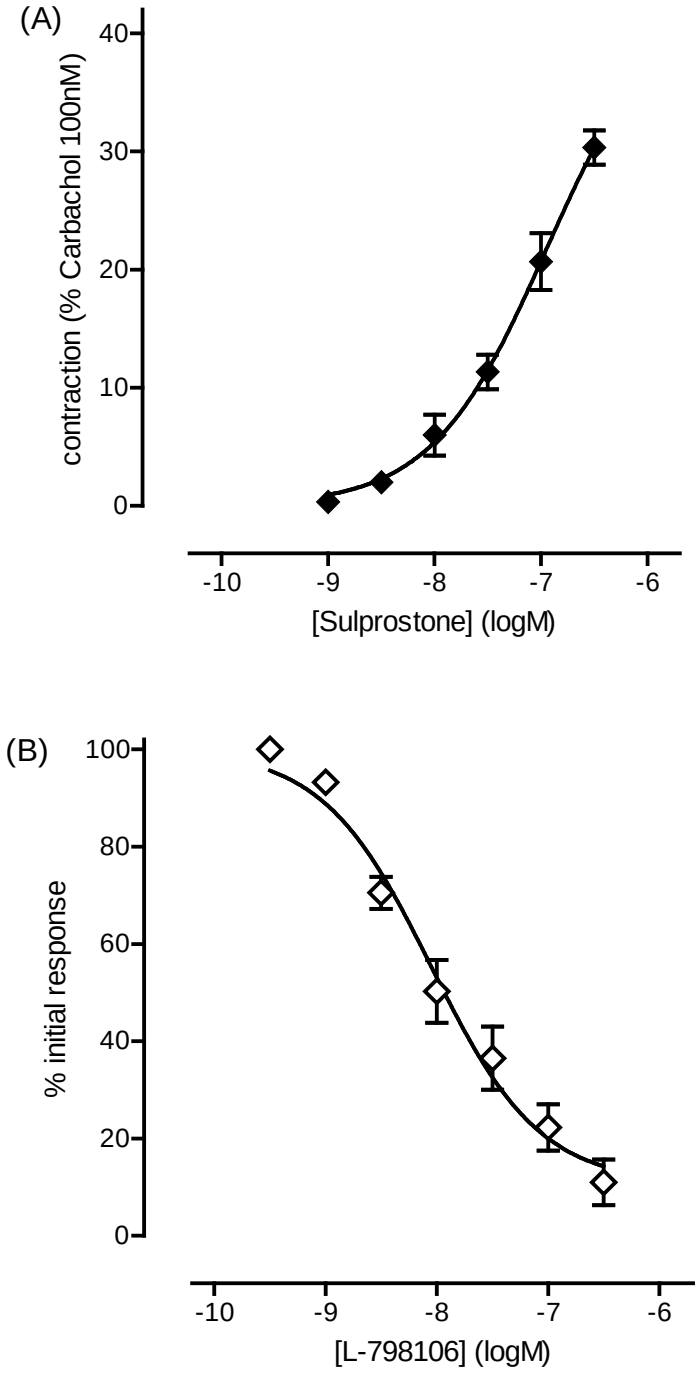

Figure 5.14 The inhibition-curve protocol for sulprostone and L-798106 in the rat urinary bladder. (A) Log concentration curve for sulprostone (n = 4). (B) Log concentration-inhibition curve for L-798106 using 100 nM sulprostone to establish tone (n = 4).

5.3.6 Effects of GW-848687 on contractile effects of prostanoid agonists

Pre-treatment with 300 nM GW-848687 significantly displaced the PGE_2 curve with depression of tone (*p = 0.002)* (Figure 5.15, *n* = 4). 30 nM GW-848687 did not significantly affect the control curve (*p = 0.06).*

The effect of the GW-848687 on 17-phenyl PGE_2-induced contractions is shown in Figure 5.16 (*n* = 4). Pre-incubation with GW-848687 at two different concentrations (30 and 300 nM) before the cumulative addition of 17-phenyl PGE_2 significantly reduced the tone (*p = 0.01,* both). There were also significant displacement in non-parallel manner between control with 30 nM and 300 nM GW-848687 curve (*p = 0.01*).

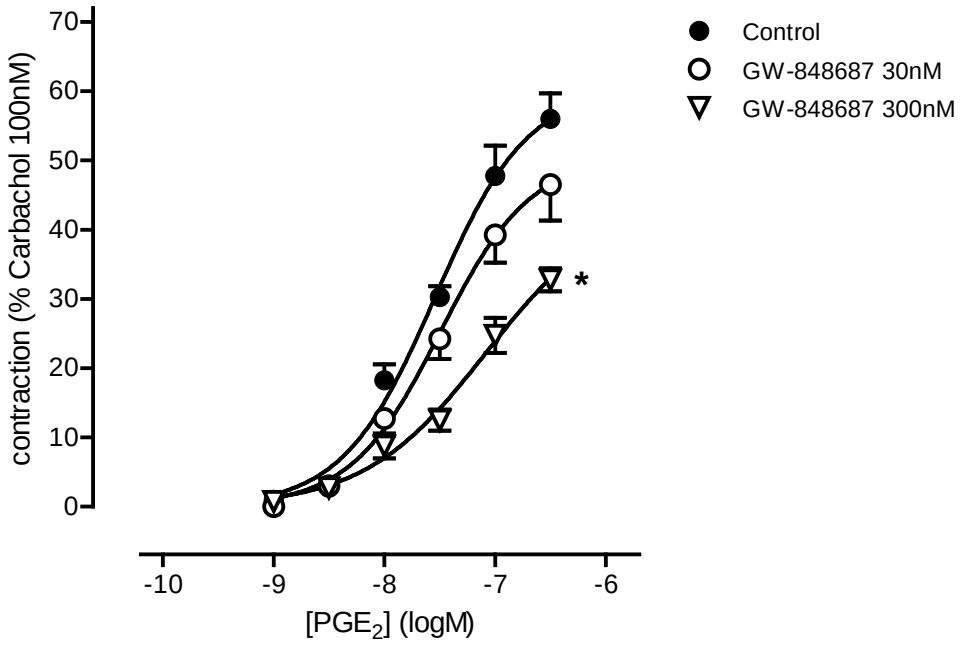

Figure 5.15 Antagonism of PGE_2-induced contraction by GW-848687 in rat urinary bladder. Log concentration-response curves for PGE_2 following treatment with 30 nM and 300 nM GW-848687 are shown (*n* = 4). **P< 0.01*, 300 nM GW-848687 vs. control and 30 nM GW-848687, using main effects contrasts.

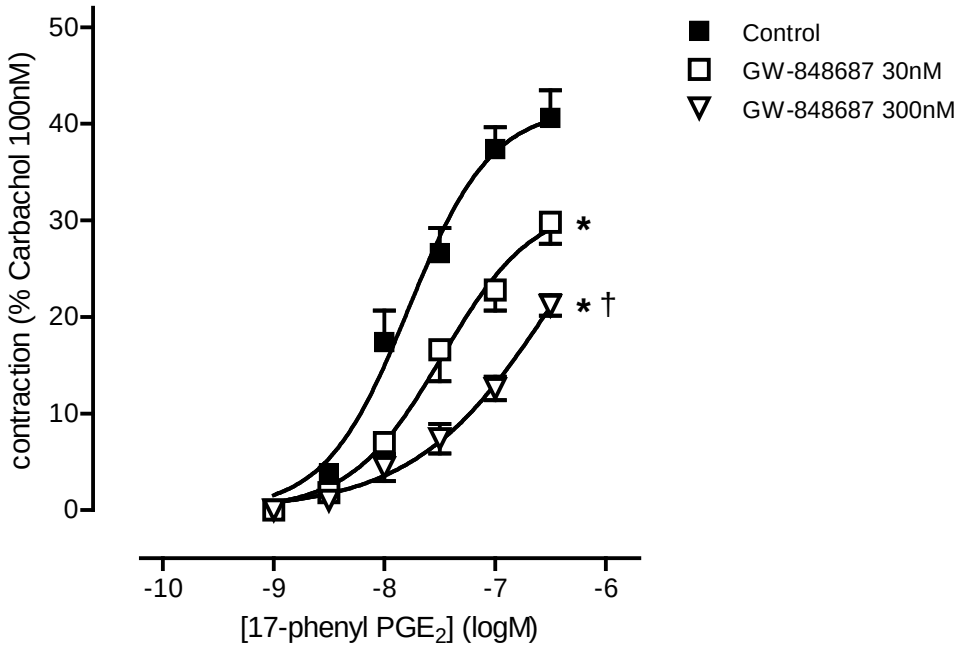

Figure 5.16 Antagonism on 17-phenyl PGE_2-induced contraction by GW-848687 in rat urinary bladder. Log concentration-response curves for 17-phenyl PGE_2 following treatment with 30 nM and 300 nM GW-848687 are shown (n = 4). *$P < 0.01$, 30 nM and 300 nM GW-848687 vs control; $^{\dagger}P < 0.01$, 300 nM GW-848687 vs. 30 nM GW-848687, using main effects contrasts.

5.3.7 Antagonist potency of GW-848687 under inhibition-curve protocol

The antagonist property of GW-848687 was assessed using the inhibition-curve protocol (protocol 5.2B). The response of PGE_2 in the absence of GW-848687 can be shown in Figure 5.17A (n = 5). pEC_{50}* estimated was 7.64 $\pm$ 0.06. The effect of cumulative addition of GW-848687 (0.1 - 300 nM) on established tone to PGE_2 100 nM is demonstrated in Figure 5.17B (n = 5). The inhibition curve pIC_{50}* was estimated to be 7.83 $\pm$ 0.11. The pA_2 estimated from equation described in section 5.2.4 was 8.35.

17-Phenyl PGE_2 curve in the absence of antagonist was constructed as shown in Figure 5.18A (n = 5). pEC_{50}* estimated from the graph was 7.50 $\pm$ 0.11. Inhibition curve of GW-848687 then constructed against the tone established with 100 nM 17-phenyl PGE_2 (Figure 5.18B, n = 5). GW-848687 started to relax the tone at 0.3 nM, and continue to do so with a definitive plateau at each cumulative concentration increment. The pIC_{50}* estimated from the inhibition curve is 7.39 $\pm$ 0.15. Using the equation in Section 5.2.2, calculated pA_2 for GW-848687 against as 7.64.

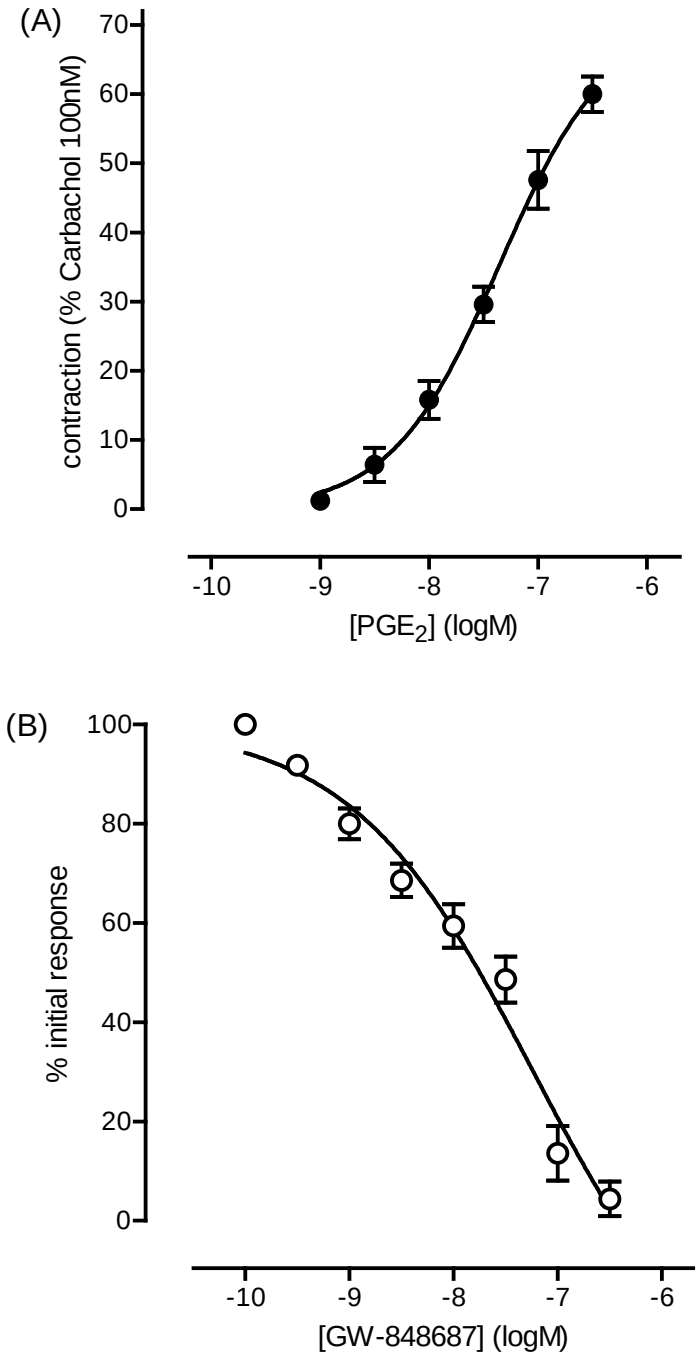

Figure 5.17 The inhibition-curve protocol for GW-848687 versus PGE_2 in rat urinary bladder. (A) Log concentration-response curve for PGE_2 (n = 5). (B) Log concentration-inhibition curve for GW-848687, precontracted with 100 nM PGE_2 (n = 5).

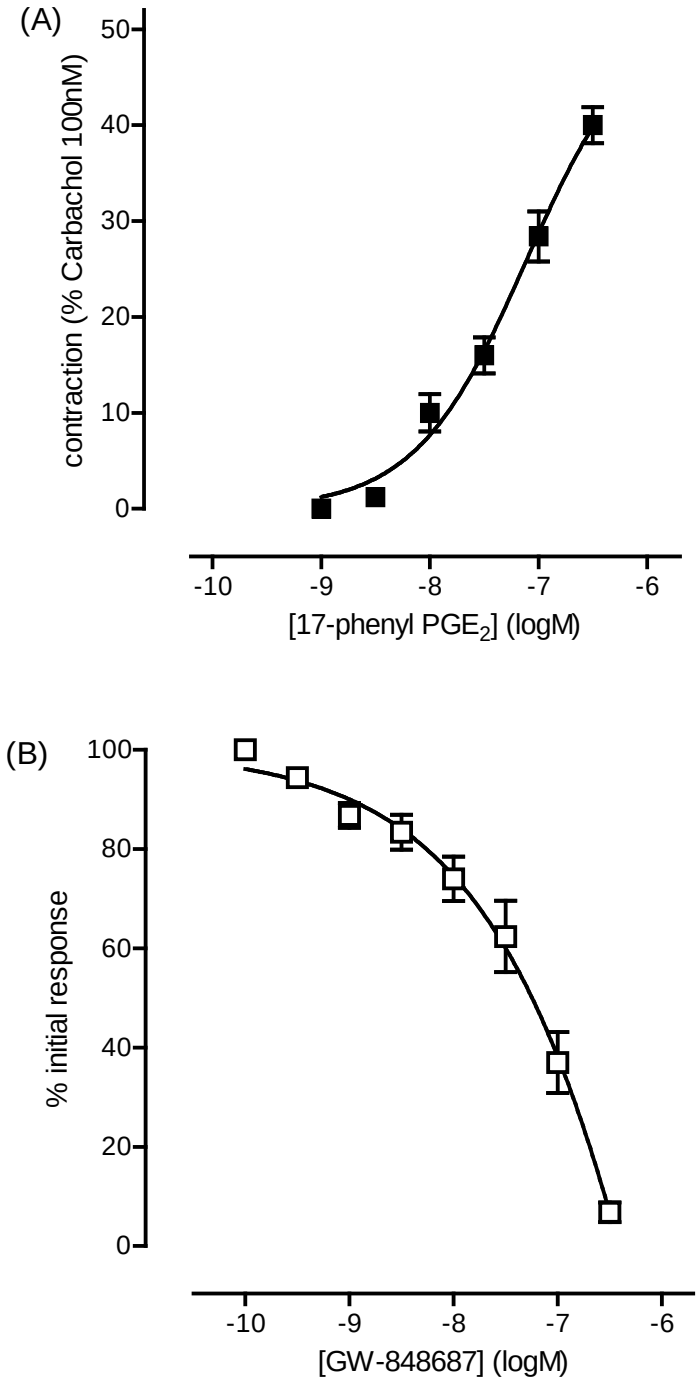

Figure 5.18 The inhibition-curve protocol for GW-848687 versus 17-phenyl PGE_2 in rat urinary bladder. (A) Log concentration-response curve for 17-phenyl PGE_2 (n = 5). (B) Log concentration inhibition curve for GW-848687, against 100 nM 17-phenyl PGE_2 (n = 5).

5.3.8 Two-site competition model

It appeared that there could be two components to the inhibition-curve for GW-8488687 against both PGE_2 (Figure 5.17B) and 17-phenyl PGE_2 (Figure 5.18B). Two theoretical curves can be fitted in each graph (Figure 5.19B, Figure 5.20B). This was pursued using the two-site competition equation in GraphPad Prism. The Hill slopes of both sigmoidal components are automatically constrained to 1.0.

The best-fit two-site curve has a high affinity site with a pEC_{50} of 9.15 comprising 28% of the sites, and a low affinity site with pEC_{50} of 7.40 (Figure 5.19B). These results are certainly scientifically plausible. Confidence interval is also reasonably narrow (12 – 45 %). Because the results are sensible, it makes sense to compare the sum-of-squares statistically as described in Section 2.5.2.

There are forty data points in the inhibition curve in GW-848687 against 100 nM PGE_2. There were four parameters fitted by the one-site equation fit and five parameters fitted for the two-site model. The calculation for the data can be summarized in Table 5.2. The F ratio is 10.08 with 1 (numerator) and 35 (denominator) degrees of freedom. Using the F table (appendix), the two-site model is significantly better than one-site model ($p < 0.05$).

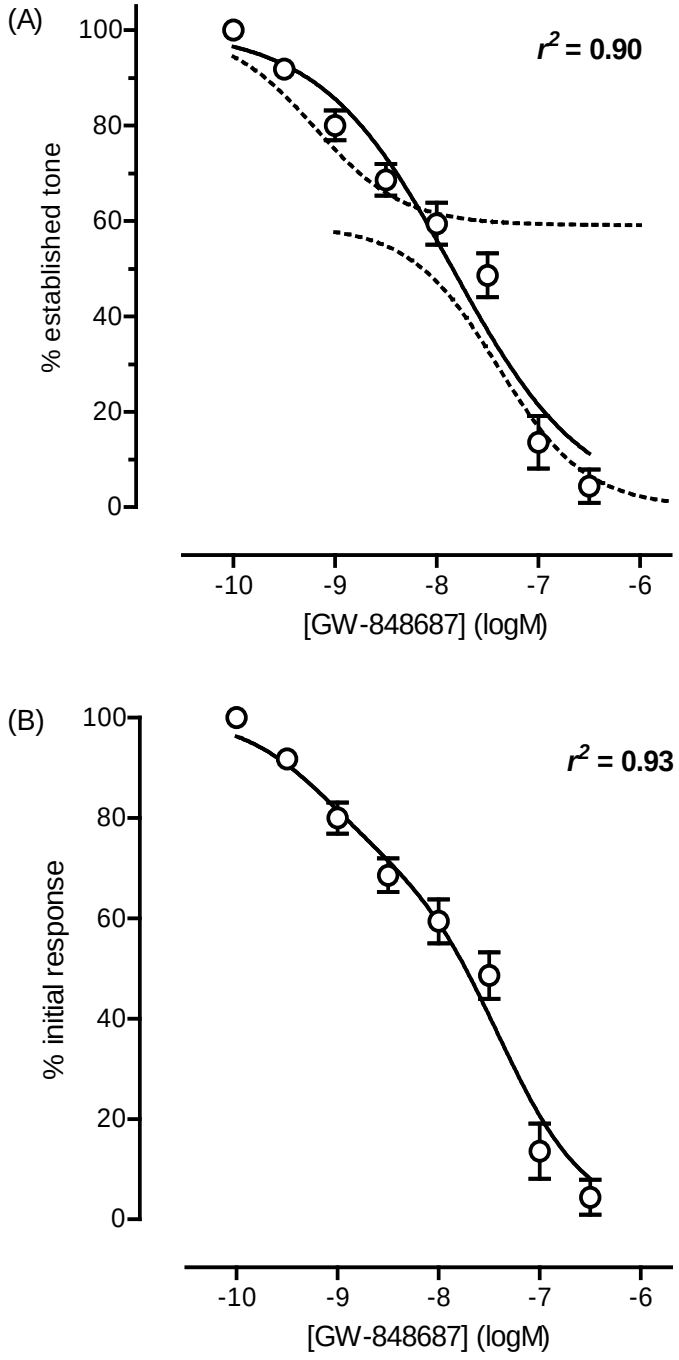

Figure 5.19 The two-site competition model curve re-fitted on GW-848687 – PGE_2 inhibition curve (from data in Figure 5.17B) using GraphPad Prism software. (A) The two theoretical curves superimposed on one-site model fit. (B) The two-site model fitted on similar curve.

Table 5.2 The F test for GW-848687 against 100 nM PGE_2.

Model	**SS**	**df**
Null hypothesis (1 site)	3688	36
Null hypothesis (2 site)	2863	35
Difference	825	1
Fractional difference	0.2882	0.0286
Ratio (F)	**10.08**	

The same applied for GW-848687 inhibition curve against 100 nM 17-phenyl PGE_2 (Figure 5.18B). The data points were not fitted in the curve properly using the one-site model. Using the two-site model, two possible inhibition curves can be fitted in the original curve (Figure 5.20A). The best-fit two-site curve has a high affinity site with a pIC_{50} of 9.32 comprising 14% of the sites, and a low affinity site with pIC_{50} of 7.17 (Figure 5.20B). Even the fraction of high affinity sites is only 14% but 95% confidence interval are reasonably narrow (3 - 26%).

There are forty data points in the inhibition curve in GW-848687 against 100 nM 17-phenyl PGE_2. Similarly, four parameters were fitted in one-site model and five parameters in two-site models. The F test calculation for GW-848687 against 17-phenyl PGE_2 is summarized in Table 5.3. The F ratio is 9.02 with 1 (numerator) and 35 (denominator) degrees of freedom. In reference to F table (appendix), the two-site model fitted is significantly better than one-site model ($p < 0.01$).

The next step is to examine how well is the graph fits, the *w*-values. For GW-848687 against PGE_2, the r^2-value is 0.93 for two-component fit and 0.90 for one-component fit. For GW-848687 against 17-phenyl PGE_2, r^2-value is 0.94 for two-component fit and 0.89 for one-component fit.

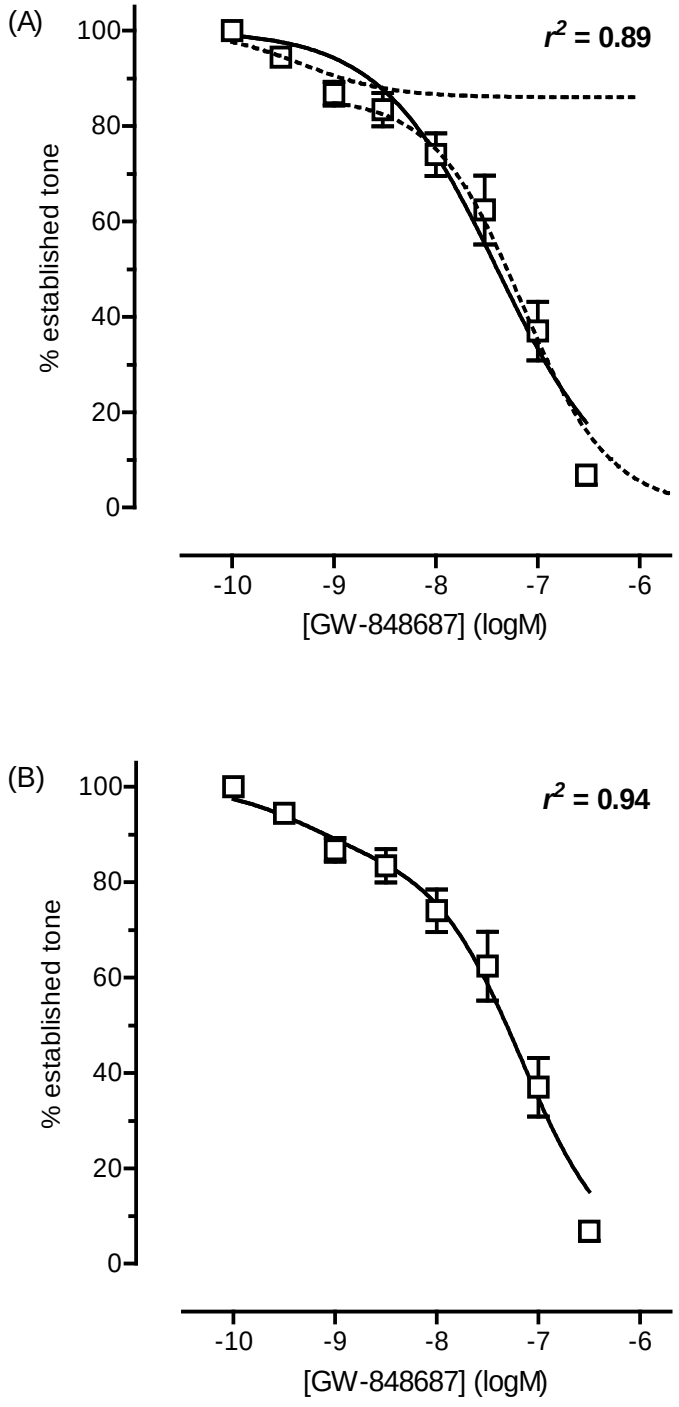

Figure 5.20 The two-site competition model curve re-fitted on GW-848687 – 17-phenyl PGE_2 inhibition curve (from data in Figure 5.18B) using GraphPad Prism software. (A) The two theoretical curves superimposed on one-site model fit. (B) The two-site model fitted on similar curve.

Table 5.3 The F test for GW-848687 against 100 nM 17-phenyl PGE_2.

Model	**SS**	**df**
Null hypothesis (1 site)	4052	36
Null hypothesis (2 site)	3221	35
Difference	831	1
Fractional difference	0.2580	0.0286
Ratio (F)	**9.02**	

5.4 Discussion

5.4.1 General overview

The rat urinary bladder is a useful tool to study functionally prostanoid antagonists due to its ready availability. The anatomical structure of the rat urinary bladder itself is similar to other hollow organs in the body with slight differences in the arrangement of the musculature layer. The muscle is not arranged in layer, instead as bundles (Gabella and Uvelius, 1990). The muscle cells are uninucleated. There is an abundance of collagen in between the muscle bundles, contributing to the high distensibility of the bladder.

The control of the rat urinary bladder involves the interplay of various factors (Figure 5.1). Prostanoids are involved in modulating and maintaining the basal tone of the bladder. Prostanoids exert their effects directly on bladder smooth muscle cells and by sensitising the afferent nerves (Schroder *et al.*, 2003). Indirectly, prostanoids are potent stimuli for neurokinins to be released, which induce the micturition reflex in the rat bladder (Ishizuka *et al.*, 1995). There has been no study documented on the direct interaction between prostanoids and autonomic nervous system on rat bladder function. However, one study has shown an interaction between PGE_2 and parasympathetic system at the level of spinal cord (Miura *et al.*, 2002). Parasympathetic preganglionic neuron in the rat spinal cord regulates the activity of pelvic visceral organs. The stimulation of EP_1 receptor in the spinal cord stimulates the parasympathetic neuron that leads to a hyperexcitability state in the bladder. Otherwise, no study has demonstrated direct interaction between prostanoids and autonomic nervous system in bladder control.

Prostanoids might be released during manipulation and removal of the bladder (Park *et al.*, 1999). In this study, it was noted that the preparation had not settled during the initial set-up of resting tension, which may be attributed to increase in endogenous prostaglandins. This

effects were prevented by the inclusion of 1 µM indomethacin in the organ bath (Schroder *et al.*, 2003). The current study also included a selective TP antagonist (100 nM BMS-180291), which is usually included by many researchers during EP receptor studies and described in Section 1.7.1.

5.4.2 Response to prostanoid agonists

Little is known of the prostanoid receptor characterization in the rat urinary bladder. Earlier functional and qualitative studies mainly concentrated on a particular prostanoid receptor (Maggi *et al.*, 1988; Schroder *et al.*, 2004; Chuang *et al.*, 2008; Su *et al.*, 2008). Therefore, the overall aim of this study was to characterize the prostanoid receptor in the rat urinary bladder.

In the current study, initial results showed that the EP agonists had contractile effects that are rapid in onset. PGE_2 is a prostanoid agonist that can activate all four EP receptor subtypes with different affinity; in the rank order: $EP_3 > EP_4 >> EP_2 > EP_1$ with lower affinity for FP, DP, TP and negligible affinity for IP receptors (> 10,000) (Abramovitz *et al.*, 2000). PGE_2 has been demonstrated to increase bladder pressure in the normal, conscious rat (Ishizuka *et al.*, 1995). In agreement, in the current study, PGE_2 contracted the quiescence preparation. 17-Phenyl PGE_2 ($EP_1 > EP_3$, with minimal activity on EP_2) and sulprostone ($EP_3 > EP_1$, with some activity on FP) also contracted the bladder strips with different potency and maximal response in the presence of indomethacin and the selective TP receptor antagonist (Figure 5.4) (Table 5.4).

Table 5.4 The pEC_{50} and E_{max} for three prostanoid agonist used in the current experiment, at maximal concentration used (300 nM).

Agonists	**pEC_{50}**	**E_{max} (300 nM) (%)**
PGE_2	7.41 $\pm$ 0.08	72 $\pm$ 3
17-Phenyl PGE_2	7.29 $\pm$ 0.08	56 $\pm$ 8
Sulprostone	7.13 $\pm$ 0.13	37 $\pm$ 3

Latanoprost-FA, is an analogue of a prostaglandin F_2 alpha ($PGF_{2\alpha}$) and highly selective to FP receptor with K_i value of 2.8 nM (Abramovitz *et al.*, 2000). In this study, latanoprost-FA (100 - 300 nM) failed to produce any contractile response. The lack of activity of latanoprost-FA suggested the absence of FP receptor in the rat urinary bladder.

The potent TP analogue, U-46619 (Coleman *et al.*, 1981; Abramovitz *et al.*, 2000) did not contract the muscle strips even with the higher dose up to 1 µM. 100 nM BMS-180291 had a weak inhibition (< 10%) effect on 100 nM carbachol, but this unlikely to be due to activation of TP receptor. The involvement of endogenous TXA_2 released by the mechanical stimulation can be ruled out as indomethacin was present in the bath fluid throughout the experiment. It is unlikely that the TP receptor is present in the rat urinary bladder.

Butaprost has a high affinity for the EP_2 receptor with negligible activity on the other EP receptors (Gardiner, 1986; Coleman *et al.*, 1994a; Narumiya *et al.*, 1999; Abramovitz *et al.*, 2000; Wilson *et al.*, 2004). It is assumed that this activity results from hydrolysis of its C1-ester group by non-specific esterases present in most tissues. In the present study, butaprost-free acid (FA) failed to relax carbachol precontracted bladder strips in spite of higher concentration (100-300 nM) used. The possible explanation is there was no EP_2 receptor in the rat urinary bladder. Moreover, butaprost-FA also has been shown to contract the guinea-

pig ileum at concentration as low as 30 nM (Lawrence *et al.*, 1992). The contraction has been attributed to EP_1 receptor in the guinea-pig ileum. It is possible that the absence of relaxation with butaprost-FA in the rat bladder could be due to the presence of highly sensitive EP_1 receptor system.

A study by Chuang *et al.* (2008) has demonstrated the over-expression of EP_4 receptor in parallel to an increase in COX-2 level in the bladder of the rat with cyclophosphamide-induced cystitis. However, the basal level of the EP_4 receptor in the normal rat urinary bladder was not documented. The exact mechanism of the EP_4 receptor causing the hypersensitivity in cystitis was not explained in the study. In general, the EP_4 is inhibitory to smooth muscles, i.e. to cause relaxation. A selective EP_4 antagonist was not available at the time of the current experiment to assess the EP_4 activity in the rat urinary bladder. PGE_2 however, is known to have high affinity for EP_4 receptor with K_i value of 0.79 nM (Abramovitz *et al.*, 2000). In the current experiment, PGE_2 (100 - 300 nM) did not relax the preparation precontracted with 80 nM carbachol. Thus, it is unlikely that the EP_4 receptor involved directly in modulating bladder function in the current experiment. In view of the above results, the next step was to characterize the contractile EP receptor in the rat urinary bladder using the antagonist studies.

5.4.3 The nature of the EP receptor(s) mediating contraction of the rat urinary bladder preparation

The high agonist potency of 17-phenyl PGE_2 and sulprostone on the rat urinary bladder preparation indicated the potential presence of both EP_1 and EP_3 receptors. Both Schild plot and inhibition curve protocols with EP_1 and EP_3 antagonists were used to clarify this situation. Under the Schild protocol, the antagonism profile of SC-51322 and GW-848687 did not conform to classical competitive antagonism at a single receptor site. Thus, the agonist log concentration-response curves (CRCs) under antagonist treatment were not parallel to the vehicle curve and there was some evidence of non-surmountability. In guinea-pig trachea preparations, SC-51322 (Hung *et al.*, 2006) and GW-848687 (Jones RL, personal

communication) produced a parallel right-shifts of the 17-phenyl PGE_2 curve; Schild plot slopes were not significantly different from unity, thereby allowing pA_2 values to be calculated (8.45 and 9.75; respectively). Two explanations appear possible in the first instance: either both EP_1 antagonists behave non-competitively (see later) or two receptors contribute to the contractile activity of the prostaglandin E analogues examined.

In examining the second proposal, the right-shifts of the agonist logCRC caused by SC-51322 and GW-848687 are consistent with their known affinities for the EP_1 receptor. From published data (Hung *et al.,* 2006; Giblin *et al.,* 2007), one would expect selective block of EP_1 receptors at 30 nM of either SC-51322 or GW-848687. The same could be true of 300 nM, but it is a common occurrence for the high selectivity of a novel antagonists reported initially to be subsequently downgraded. Similarly, the right-shifts of the logCRCs for PGE_2, 17-phenyl PGE_2 and sulprostone by 1 μM L-798106 indicate the existence of a functional EP_3 system (Figure 5.8, 5.9 and 5.10).

However, the combination of EP_1 and EP_3 antagonists under the Schild protocol does not support the above findings. Figure 5.13 clearly shows that the addition of L-798106 to SC-51322 pre-treatment did not produce further right-shifts of the sulprostone curve, thereby providing little support for the presence of an EP_3 contractile system.

Turning to inhibition curve protocols, there is statistically sound evidence using SC-51322 and GW-848687 for a two-component contractile system in the rat bladder preparation. Again, the higher sensitivity system is compatible with selective EP_1 antagonism, with GW-848687 at 1 nM showing clear inhibition of PGE_2-induced contraction (Figure 5.19). The lower sensitivity component may represent the EP_3 receptor, but it was expected that GW-848687 would show higher selectivity than the current experiments inform.

There is some discrepancy between the inhibitory potencies of the EP_1 blockers under the Schild and inhibition-curve protocols, with greater potency accorded to the latter. It is unlikely that this is due to fade of the agonist response under the inhibition curve protocol. As shown in Figure 5.21, tension induced by the EP agonist was well maintained for at least 90 min.

The inhibition curve protocol using the L-798106 provided strong evidence for an EP_3 system, with inhibition of sulprostone-induced contraction starting at 1 nM and proceeding monotonically to 87% inhibition at 300 nM (Figure 5.14). However, this large degree of inhibition was unexpected and also clearly disagrees with data in Figure 5.11.

Several issues must be considered in relation to the above discrepancies. In relation to the kinetics properties of the antagonists, had the antagonists reached steady-state at the time of agonist addition? Thirty minutes pre-treatment was allowed for L-798106 in the Schild protocol, while 10 - 15 min was allowed for each concentration increment in the inhibition-curve protocol. It seems unlikely that this is relevant issue given the lower L-798106 concentrations effective in the inhibition-curve protocols. In other words, we would expect to see slower inhibition at the lower concentrations thereby potentially underestimating the potency of the antagonist – this was not the case. The constancy of the contribution of the two contractile components between bladder preparations from different animals needs to be considered also. It is difficult to assess this factor, given that sulprostone and 17-phenyl PGE_2 have both EP_1 and EP_3 agonist activity. Finally, how do the two contractile systems interact when simultaneously activated? In the rat femoral artery, there is synergism between EP_3 agonist and phenylephrine (α_1 agonist), K^+ (depolarizing agent) or U-46619 (TP agonist) (Hung *et al.*, 2006). In guinea-pig aorta, where there is synergism between EP_3 receptor and α_1-adrenoreceptor systems, comprehensive EP_3 antagonism does not completely return established contraction to the level of α_1 agonist alone (Jones RL, personal communication). Could there be synergism between the EP_1 and EP_3 systems in the rat urinary bladder preparation?

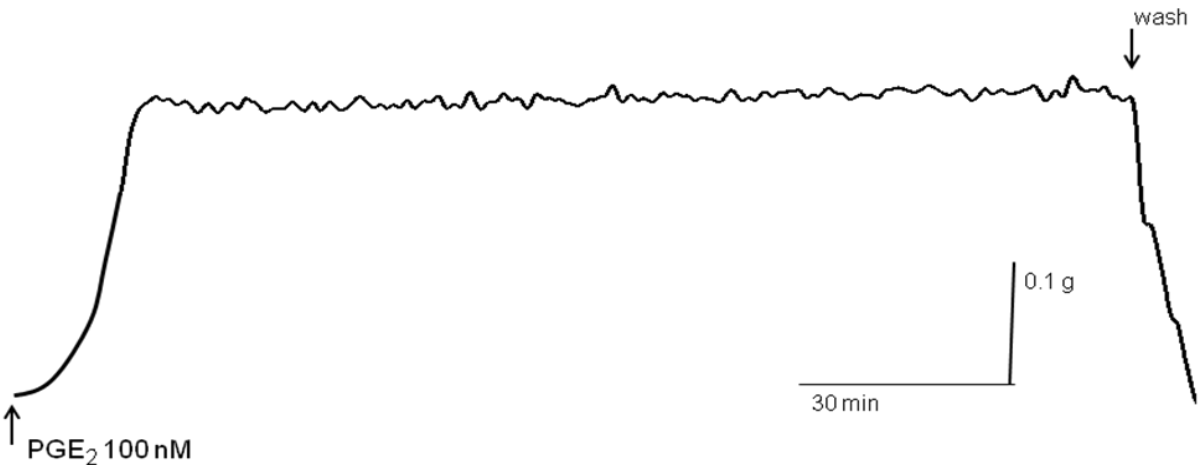

Figure 5.21 Typical tracing of 100 nM PGE_2-induced contraction response in the rat bladder in the absence of antagonists, time-control preparation. The established response was well sustained over the period of more than 90 min.

5.4.4 Two-site competition model versus one-site competition model

The possibility of two contractile receptor systems in the rat urinary bladder can be further examine by refitting the antagonist-inhibition curve as described in details in Section 2.5.2. The non-parallel right displacement by GW-848687 on PGE_2 curves suggested the presence of two receptor systems in the rat bladder, possibly EP_1 and EP_3 receptors. The graph of the one site fit model for GW-848687 against 100 nM PGE_2 seems to deviate systematically from the data point (Figure 5.17B). The possibility of two contractile receptor systems is demonstrated by re-fitting the curve on Figure 5.17B using the two-site model in GraphPad Prism program (Figure 5.19B). The data seems better fitted in two-site model.

Both, the F test and r^2-values comparison results suggested the incomplete inhibition by GW-848687 on tone established by PGE_2 and 17-phenyl PGE_2 could be due to presence of two functional EP-receptors system in the rat urinary bladder.

5.4.5 Insurmountable antagonism and the hemi-equilibrium concept

The depression of maximal agonist response with a relatively small right-shift of the agonist curve is usually termed 'insurmountable antagonism' (Kenakin *et al.*, 2006). Insurmountable antagonism can be due to non-competitive antagonism, whereby the antagonist either binds irreversibly at or close to the agonist binding site or affects receptor function at a site distinct from the agonist binding site. SC-51322 and GW-848687 have been documented to behave as competitive antagonists in functional and / or recombinant receptor studies (Hung *et al.*, 2006; Giblin *et al.*, 2007), but this does not necessarily mean that they behave similarly on the EP_1 receptor system in the rat urinary bladder.

Another possibility involves true competition for the agonist binding site, but a hemi-equilibrium state exists for the antagonist-receptor interaction. In an ideal situation, on addition of agonist to determine the extent of the antagonism, the receptor should fully re-equilibrate with the antagonist and agonist in the receptor compartment. For a low- to moderate-affinity antagonist, the antagonist dissociation rate constant will be relatively large and antagonist will quickly dissociate, thereby allowing agonist to occupy the empty receptors. For a high-affinity antagonist, dissociation will much slower and the agonist response may be measured at a time when the dissociation process is incomplete. An insurmountable antagonist profile may thus occur (Figure 5.22, redrawn from Kenakin *et al.*, 2006). To overcome this hemi-equilibrium situation, the antagonist contact time must be increased, i.e. increase the duration before addition of the consecutive agonist dose.

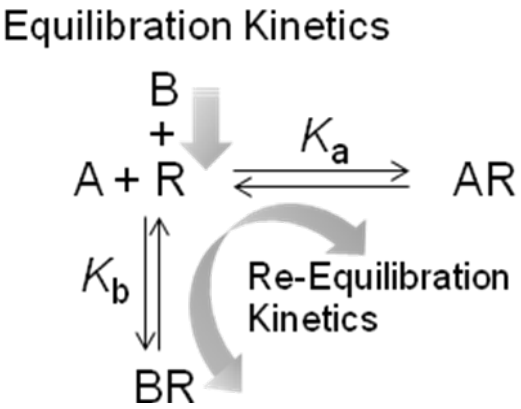

Figure 5.22 The re-equilibration kinetics that contributes to the hemi-equilibration state; A = agonist, B = antagonist, R = receptor (redrawn from Kenakin *et al.*, 2006).

5.4.6 EP_4 receptor

The functional EP_4 receptor in the rat bladder cannot be determined in the current study due to non-availability of selective EP_4 agonist or antagonist. However, the failure of PGE_2 to inhibit the precontracted preparation suggested the absence of EP_4 in the rat urinary bladder. Despite over-expression of EP_4 receptor in rat bladder following cystitis (Chuang *et al.*, 2008) this study failed to show the contribution from EP_4 receptor in bladder function. Nevertheless, the functionality of EP_4 in bladder can be explored once the appropriate receptor agonist or antagonist made available.

5.5 Conclusions

In the present work, it has been shown that the prostanoid agonists produced a contractile effect on the rat urinary bladder. It seems likely that a EP_1 receptor is present. However, there was some doubt as to the identity of the second receptor as an EP_3 receptor. This arose from discrepancies between the degree of antagonism seen a) with combined use of EP_1 and EP_3 antagonists and EP_1 or EP_3 antagonist alone under the Schild protocol, and b) under the Schild and inhibition curve protocols. There was no functional relaxant prostanoid receptor documented in this study.

GW-848687 did not show surmountable antagonism on the bladder preparation. This may be explained on the basis of two contractile EP receptors as alluded to above. Another possibility to consider is that GW-848687 is selective towards the EP_1 receptor, but has a non-competitive mechanism or achieves a hemi-equilibrium state. This situation needs to be resolved before one could fully recommend GW-848687 as a robust tool for characterizing EP_1 receptor systems.

CHAPTER SIX

RAT FEMORAL ARTERY AND DIABETES

6.1 Introduction

Endothelium dysfunction has been reported in diabetic people and experimental animals with diabetes (De Vriese *et al.*, 2000, Schofield *et al.*, 2002). The dysfunction is caused by the high glucose content in tissues, which triggers a cascade of functional and structural alterations in vascular cells, leading to macrovascular and microvascular diseases (Schalkwijk and Stehouwer, 2005). A hallmark of endothelial dysfunction in diabetes is alteration in the biosynthesis of prostaglandins and oxidative stress products and decreased release and / or bioavailability of nitric oxide (NO) (Tesfamariam *et al.*, 1989; Vanhoutte *et al.*, 2005). The hyperglycaemic state in diabetes alone is the stimulation for productions of prostaglandins (Tesfamariam *et al.*, 1990). Endothelial COX, which is upregulated in various pathological conditions including diabetes, is thought to be responsible (Tesfamariam *et al.*, 1989; Ge *et al.*, 1995; Shi *et al.*, 2006; Shi *et al.*, 2007b). In contrast, Peredo *et al.* (2001) showed impairment of prostanoid production in the mesenteric vascular bed of the diabetic rat.

Endogenous prostanoids are likely to exert their constrictor or dilator actions on blood vessels by activating prostanoid receptors located on smooth muscle cells (Narumiya *et al.*, 1999; Breyer *et al.*, 2001). With reference to the diabetic state, the increased levels of vasoconstrictor prostaglandins act mainly through TP receptors in femoral artery from rats with early stage STZ-induced diabetes (Peredo *et al.*, 1999; Shi *et al.*, 2007a) and in aorta from alloxan-diabetic rabbits (Tesfamariam *et al.*, 1989). In contrast, the synthesis of the vasodilator prostacyclin is decreased in STZ-induced diabetic rats (Harrison *et al.*, 1978; Peredo *et al.*, 1999). Moreover, Shi *et al.* (2007a) showed that the TP antagonist, S-18886 partially inhibited the contractile response to A-23187 (calcium ionophore) in 12 weeks STZ-rat femoral artery. S-18886 in combination with SC-19220 (EP_1 antagonist) and AH-6809 (DP_1, EP_1, EP_2 antagonist) abolished the contraction. In support of this picture, there was a mixed production of vasoconstrictor prostaglandins and TXA_2, in rat mesenteric arterial bed (Peredo *et al.*, 1999).

While the vascular action of TXA_2 is straightforward, that of PGE_2 is potentially complicated. Firstly, PGE_2 may cause vasodilatation through activation of EP_2 and / or EP_4 receptors. Secondly, it may activate TP receptors at high concentrations, as shown by Jones *et al.* (1982) in rabbit aorta and by Dorn *et al.* (1992) in rat aorta. Thirdly, PGE_2 may activate an EP receptor, most likely an EP_3 receptor, to cause vessel contraction. Thus, in rat femoral artery, PGE_2 acting alone induced very weak contraction, but showed pronounced synergism with strong contractile agents including K^+, phenylephrine and the TP agonist U-46619 (Figure 6.1) (Hung *et al.*, 2006). One presumes that it would show a similar synergistic interaction with the natural TP agonist TXA_2. However, this EP_3 receptor-driven synergism has not been taken into account when PGE_2 has been implicated in the diabetic state. For example the TP receptor antagonist S-18886 only partially blocked the contractile response to the calcium ionophore, A-23187 in femoral artery from the 12-week STZ diabetic rat (Shi *et al.*, 2007a). The possibility of activation of both TP and EP receptors in the chronic diabetic state was proposed by the authors, but no reference was made to the potential interaction of these two prostanoid systems.

The effect of diabetes in rat can be examined in various models. The Zucker fatty (ZF) rat (Okamoto *et al.*, 2008) and Goto-Kakizaki (GK) rat (Goto *et al.*, 1976) are both developed by cross-breeding and manifest type 2 diabetes. A more convenient model is the streptozotocin (STZ) induced-diabetic rat. STZ is an *N*-nitroso derivative of D-glucosamine that is chemically unstable in saline or distilled water at room temperature and neutral pH. It has been utilised to induce diabetes in a variety of experimental animals and to determine the short and long-term complication of diabetes (Table 6.1). The dose of streptozotocin varies between 25 – 200 $mgkg^{-1}$ in different species. It was further suggested that the intensity of the damage to the β-cells could be graded according to the dosage used (Junod *et al.*, 1969).

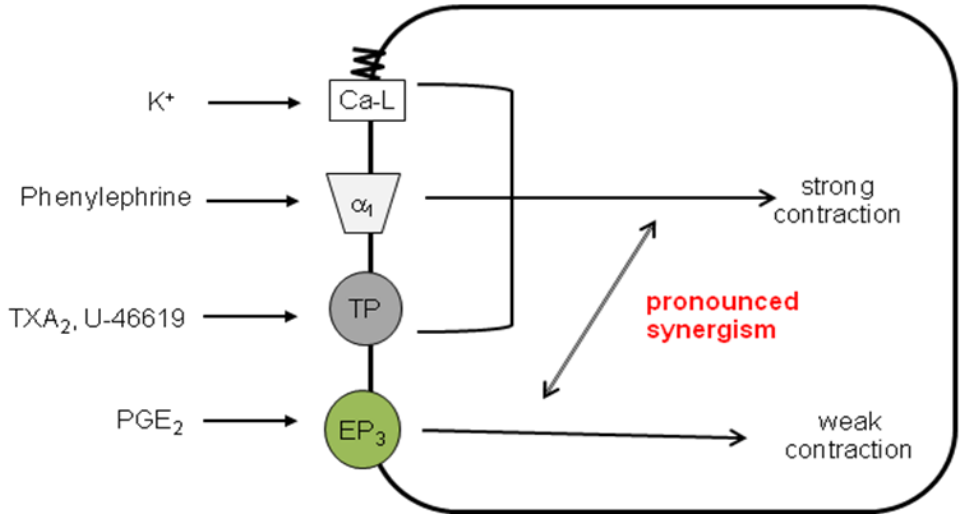

Figure 6.1 Prostanoid pharmacology in rat femoral artery. The synergism between phenylephrine and PGE_2 produced a strong contraction response. *Ca-L*: L-type calcium channel (Hung *et al.*, 2006).

It was shown that the diabetogenic action of streptozotocin results primarily from its highly specific cytotoxic action on insulin producing cells (β-cells of the islets of Langerhans) leading to rapid and irreversible necrosis (Srivastava *et al.*, 1982). The induction of diabetes by streptozotocin causes a triphasic blood-sugar response. Initially, there will be increases in blood sugar level secondary to glycogenolysis or an increase in free fatty acid (FFA). The glucose cannot be utilised properly due to reduction in circulating insulin, thus the body used the glycogen and fat store for the energy, leading to weight loss eventually. In the second phase, there is a profound hypoglycaemic state resulting from augmented endogenous release of insulin from the degenerating β-cells. In the final stage within 24 hours post-injection, an irreversible diabetic state developed (Szkudelski, 2001). The animals will be totally devoid of insulin, resulting in a hyperglycaemic state.

The initial aim of the experiments was to determine which prostanoid receptors are activated in the isolated femoral artery of the STZ-diabetic rat when enhanced endogenous prostaglandin production occurs, and how these prostanoid receptors interact with each other

and with other vaso-active agents. Shi *et al*. (2008) used exogenous hydrogen peroxide (H_2O_2) to generate an oxidative stress environment in rat femoral artery, based on the finding that H_2O_2 produces contraction response in this artery and rat mesenteric artery (Matoba *et al.*, 2000). However, my initial experiments showed minimal or non-sustained contraction with H_2O_2 despite the higher concentration used (more than 10 mM). The focus of the study was therefore switched to examine the role of prostanoids in the associated enhancement of contractile response to α_1-adrenoceptor agonism or K^+-induced depolarization in the diabetic state. The evidence for the involvement of prostanoids in this enhancement derives from the partial inhibition of the contractile responses by the COX inhibitor indomethacin (Shi and Vanhoutte, 2008). Two critical decisions were necessary – which diabetic state to induce and how to differentiate the roles of TP and EP_3 receptors.

In the literature, blood vessels have been harvested at varying intervals (1 – 52 weeks) after STZ injection; these studies are summarized in Table 6.1. Peredo *et al* (1999) have shown the response to noradrenaline in endothelium intact STZ-rat mesenteric bed is similar in all duration of diabetes (2 to 8 weeks), and comparable to control. However, the maximal response was reduced in STZ-rats beyond 8 weeks. The maximal response in denuded STZ-rat femoral artery to U-46619 and 60 mM KCl were also shown to be similar to control at 4 weeks after STZ-induction (Shi *et al.*, 2007a). In contrast, there was significant reduction in response to U-46619 in 12 weeks STZ-rats. Based on these results, it was decided to use the denuded rat femoral artery after 4 weeks of STZ-induction as this is the first experience with STZ-rats model.

Phenylephrine, a selective α_1-adrenoreceptor agonist, has been shown to contract femoral artery in both normal and diabetes rat (Jarajapu *et al.*, 2001; Shi *et al.*, 2006). Its action is mediated via α_1-adrenoceptors, while the post-junctional action of α_2 agonists on rat femoral artery is negligible (Jarajapu *et al.*, 2001). Initial experiments confirmed good reproducibility for contraction of rat femoral artery by phenylephrine, which is essential if the synergism with EP_3 agonist is to be accurately assessed.

Table 6.1 Summary of published studies on effects of vasoactive agents on isolated blood vessels from control and streptozotocin-treated rats

Author, year	STZ dose and route	Induction duration (weeks)	Tissues	Endothelium status	Agents	Responses	Effects of antagonists / inhibitors
Chang and Stevens, 1992	55mg/kg IV	12 52	Rat aorta	Intact and **removed**	Phenylephrine	- increased sensitivity in 52 weeks STZ (increased EC_{50}; E_{max} same) in intact endothelium compared to control - no difference in without endothelium	- not inhibited by indomethacin 5 µM - implicated as diabetes progressed, reduced EDRF due to endothelial dysfunction
Dai *et al.*, 1993	55mg/kg IV	6 16 24	Renal artery	Intact and **removed**	Phenylephrine	- no change in contractile response in both: intact vs. without endothelium control vs. STZ	- as diabetes progressed, increase in endothelial and smooth muscle dysfunction due to increase in free radicals
					Acetylcholine	- as diabetes progressed, reduction in ACh relaxation (intact endothelium)	
					Histamine	- same as Ach	
Mulhern and Docherty, 1989	65mg/kg IP	2-3	Rat aorta	Intact and **removed**	Noradrenaline	- no difference between DM & controls - no difference between with & without endothelium	
					KCl 40mM	- as for noradrenaline	
Peredo *et al.*, 1999	60mg/kg IP	1 2 3 4	Rat mesenteric bed	Intact	Noradrenaline	- contractile response, no difference of maximal response between control / STZ and duration of induction	- all contraction not affected by 10 µM indomethacin, except in 8 weeks animals (STZ / control)

Author, year	STZ dose and route	Induction duration (weeks)	Tissues	Endothelium status	Agents	Responses	Effects of antagonists / inhibitors
		8			KCl 80mM	- no difference between control / STZ and duration	- not affected by indomethacin
Peredo, 2001	100mg/kg IP	18-20	Rat mesenteric bed	Intact and **removed**	Noradrenaline	contractile response - no difference in control & STZ (same in with / without endothelium)	- indomethacin reduced the responses in control but not in STZ (with / without endothelium)
					KCl	- contractile response (as for noradrenaline)	- not affected by indomethacin (with / without endothelium)
Pfaffman *et al.*, 1982	65mg/kg IP	2 – 12	Rat aorta	Intact	Noradrenaline	- significantly decreased E_{max} in STZ but comparable EC_{50}	- the response restored as in control with insulin administration
					KCl	- significantly decreased in STZ (EC_{50} & E_{max})	
Shi and Vanhoutte, 2008	55mg/kg IV	12	Rat femoral artery	Intact	U-46619	- significantly reduced contractile response in STZ - curve shifted to the LEFT (hyper-responsiveness)	- 5 µM indomethacin / 100 nM naproxen– restored the response in STZ compared to control rats
					Phenylephrine	- contractile response reduced in STZ	
					KCl	- comparable between STZ & control	
Shi *et al.*, 2007a	55mg/kg IV	4 12	Rat femoral artery	Intact & **removed**	Phenylephrine	- contraction response, no difference E_{max} between STZ / control - no difference in duration - no differences in with / without endothelium	

Author, year	STZ dose and route	Induction duration (weeks)	Tissues	Endothelium status	Agents	Responses	Effects of antagonists / inhibitors
					A23187	*precontracted by phenylephrine* *4 weeks* - relaxation on lower dose, then contraction on higher dose - **without endothelium**, no relaxation phase on STZ	*4 weeks* - the contraction by Phe inhibited by 5 µM indomethacin and 0.1 µM S-18886
						12 weeks - in control, response same as 4 weeks - in STZ: no relaxation phase in with / without endothelium	*12 weeks* - contraction in STZ inhibited by 5 µM indomethacin and 0.1 µM S-18886
					A23187	*quiescent preparation* *4 weeks* - **without endothelium**: no response in STZ / control - intact endothelium: -contraction, STZ >> control	*4 weeks* - contraction response in intact endothelium in both inhibited by 5 µM indomethacin and 0.1 µM S-18886
						12 weeks - without endothelium: as 4 weeks - intact endothelium: - significant contraction response STZ >>> control STZ >>> 4 weeks	*12 weeks* - contraction in intact endothelium partially inhibited by 5 µM indomethacin and 0.1 µM S-18886 - AH-6809 / SC-19220 / S-18886 completely inhibited the contraction response
					U-46619	- hyper-responsive – shift curve to **LEFT**, and reduced E_{max} in **without endothelium** of 12 weeks STZ (not in 4 weeks, comparable to control)	

Author, year	STZ dose and route	Induction duration (weeks)	Tissues	Endothelium status	Agents	Responses	Effects of antagonists / inhibitors
					KCl 60 mM	-**without endothelium**: significant reduction of contraction in 12 weeks STZ	
Shi *et al.*, 2007b	55mg/kg IV	12	Rat femoral artery	Intact and **removed**	A23187	+ L-NAME - intact endothelium: contraction with higher response in STZ - without endothelium: none	- contraction in intact endothelium inhibited by 5 µM indomethacin and 0.1 µM S-18886
					H_2O_2	- **without endothelium**: contractions; STZ >> control with LEFT shift	-contraction inhibited by 5 µM indomethacin and 0.1 µM S-18886
Taylor *et al.*, 1992	56mg/kg IP	5-6	Rat mesenteric bed	Intact	Noradrenaline	- contraction response, increased in STZ compared to control	- L-NAME increased the response of control nearly as in STZ rats

***** *IP = intraperitoneal; IV = intravenous; KCl = potassium chloride; ACh = acetylcholine; Phe = phenylephrine; S-18886 (TP antagonist)*

BMS-180291 was chosen as the TP antagonist. Its profile is well-documented and it blocked the U-46619 activity in rat aortic rings at pA_2 of 9.3 (Ogletree *et al.*, 1993) (Table 6.2). L-798106 was chosen as the EP_3 antagonist. It shows high selectivity for EP_3 receptors based on ligand binding at recombinant prostanoid receptors (Juteau *et al.*, 2001). In functional studies, it blocked the action of sulprostone with pA_2 values of 7.82 in guinea-pig trachea (Clarke *et al.*, 2004) and 7.43 – 8.03 in rat femoral artery (Hung *et al.*, 2006). In the most recent functional study in rat urinary bladder, L-798106 inhibit the PGE_2-induced Ca^{2+} influx through activation of EP_3 receptor with pK_i of 7.12 (Jugus *et al.*, 2009).

The final aim of the experiment was to examine the effect of endothelium on the response of phenylephrine on STZ-rat femoral artery. Prostaglandins are synthesised by both endothelial and smooth muscle COX (Weksler *et al.*, 1978; Narumiya *et al.*, 1999). This study will establish whether the augmented prostanoids production in diabetes is endothelium dependent or not.

Table 6.2 Antagonists and concentrations chosen for use in the experiment.

Antagonists	**Reported pA_2**	**Concentration used in the current experiment**	**References**
L-798106	7.43 – 8.03	1 µM	Hung *et al.*, 2006; Clarke *et al.*, 2004
BMS-180291	9.3	100 nM	Ogletree *et al.*, 1993
CAY-10441	8.82	1 µM	Clark *et al.*, 2004

6.2 Methods

The basic methodology used has been described in detail in Chapter 2. Specific methodological points not discussed previously are addressed below.

6.2.1 Streptozotocin-induced diabetes

The experiment was carried out on 10 - 12 week old male Sprague-Dawley rats (200 - 250 g). Diabetes was induced with streptozotocin (STZ; 60 $mgkg^{-1}$, i.p) after overnight fasting (Figure 6.2) (Pfaffman *et al.*, 1982; Peredo *et al.*, 1999; Burke *et al.*, 2006). Streptozotocin (20 $mgml^{-1}$) was freshly prepared on the day of induction in 40 mM Na-Citrate buffer solution at pH 4.5 and used within 10 - 15 min. Control rats were injected with corresponding volumes of the STZ vehicle (saline). At 72 hours after STZ injection, a blood sample was taken from the tail artery and the fasting blood glucose level was measured using an Ascensia Breeze 2 glucometer (Bayer HealthCare, UK). Rats were considered diabetic if the blood glucose level was higher than 16 $mmol^{-1}$. Body weight was measured weekly and rats were kept under optimal conditions and given a normal diet.

At 4 weeks after induction, the rats were decapitated. Blood glucose and final weight were measured on the day of death. Control rats with non-fasting blood glucose higher than 11.1 $mmol^{-1}$ were excluded from the study. All procedures and protocols were performed under Home Office Project Licence guidelines (project licence holder: Professor Brian Furman, University of Strathclyde).

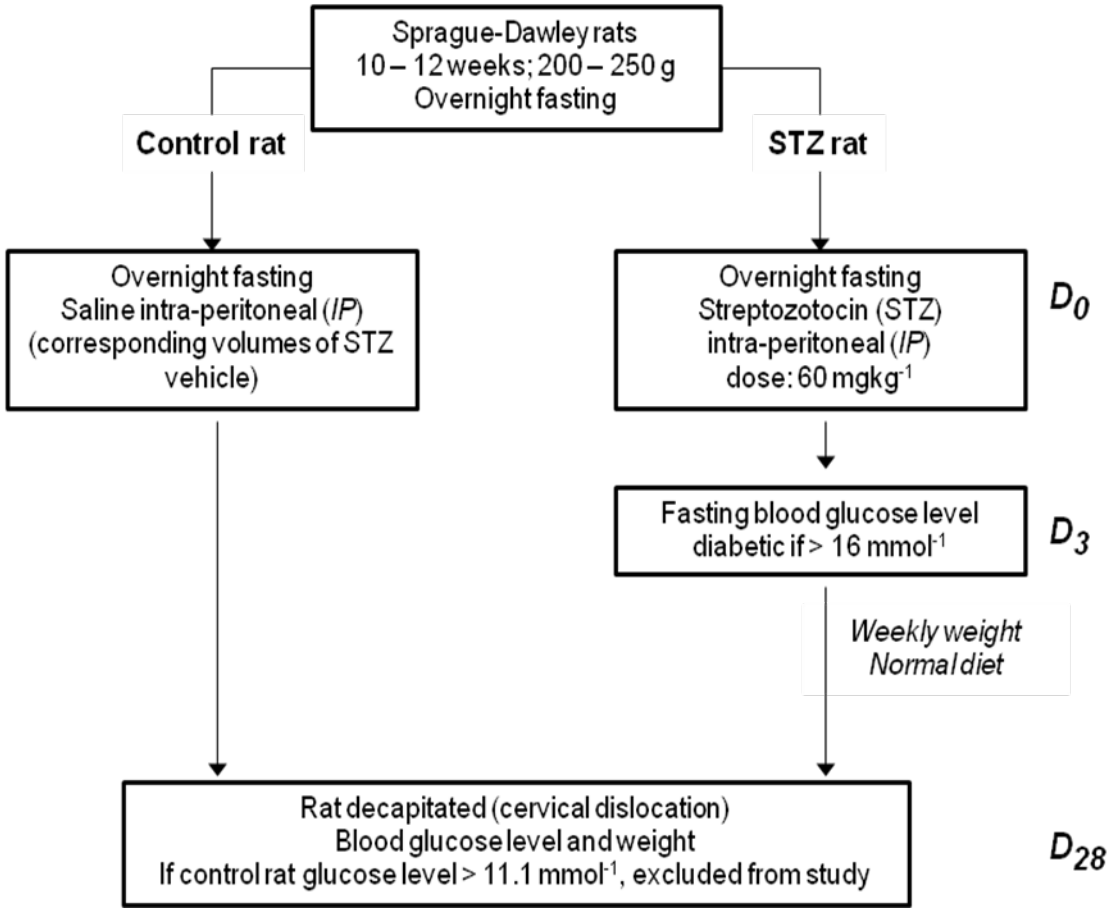

Figure 6.2 The protocol for streptozotocin (STZ)-induced diabetes in rat.

6.2.2 Setting up of preparations

The rat femoral arteries were obtained and mounted in a wire myograph as described in Chapter 2. When indicated, the endothelium was removed mechanically from the artery by rolling the intimal surface against a piece of roughened wire slightly thinner than the lumen of the artery. The resting tone was set at an optimal tension of 1.0 g, determined from preliminary experiments and previous study on the same settings (Shi *et al.*, 2007a; Shi *et al.*, 2007b). Four preparations were used contemporaneously. The preparations were allowed to equilibrate for 1 h, and then exposed twice to KCl at 60 mM for viability assessment. The criteria of exclusion as described in Section 2.2.1.2 were applied.

The artery was contracted with 100 nM phenylephrine (60% maximal response, EC_{60}), followed by cumulative addition of acetylcholine (1, 10, 100 nM) to assess the completeness of endothelium removal (Furchgott and Zawadzki, 1980; Furchgott, 1981). Where applicable, the antagonists used were preincubated for 30 min before cumulative addition of phenylephrine. Repeated concentration response curve to phenylephrine were reproducible and no corrections for time-dependent changes were required.

6.2.3 Antagonist protocol and pA_2 estimation

Antagonist affinity was determined by calculating the pA_2. In this study, the basic inhibition-curve protocol is used. The details have been described in Section 1.7.2. The pA_2 (= $-\log K_b$) is estimated from the equation (Lazareno and Birdsall, 1993b):

$$K_b = \frac{IC_{50}^*}{\frac{[A]}{EC_{50}^*} - 1}$$

and

$$K_b = \frac{[B_i]}{\frac{[A_f]}{[A_i]} - 1}$$

.

6.2.4 Statistical analysis

Contractile responses were measured as increases in tension (g) above the resting level and normalised to the second 60 mM KCl response on each artery preparation. A variable-slope sigmoidal curve was fitted to log concentration–response data using GraphPad Prism software; the bottom asymptote was constrained to zero for contraction. Sigmoidal curve parameters were derived from data for individual preparations. Data were further analysed by 1-factor and repeated measures 2-factor ANOVA combined with comparison of selected means by planned (orthogonal) contrasts using SuperANOVA software. Two means of value ware compared with unpaired Student *t-test.* All tests were two-tailed and the significance level was set at $p < 0.05$. All data are presented as mean $\pm$ SEM.

6.3 Results

6.3.1 General condition of animals

At the beginning of the study, the two groups of rats had a comparable body weight (200 – 250 g). Four weeks later, the control rats had gained weight (*p = 0.003)*, whereas STZ-treated rats exhibited considerable weight loss (*p = 0.009)* (Table 6.3). The STZ-treated rats also had polyuria; the cage bed material had to be changed more frequently compared to control rats. There was a single mortality in the control group, as the animal developed an abdominal cyst at three weeks after saline injection and was terminated under Schedule 1. The femoral arteries from control animals had generous deposits of fats, whereas those from STZ-treated animals looked almost fat-free.

Table 6.3 Comparison of body weight in control and STZ-rats at the start of the study and at four weeks

Time / duration	Control rats (g)	STZ-rats (g)
0 week (start)	218 $\pm$ 13	249 $\pm$ 26
4 weeks	367 $\pm$ 28†	186 $\pm$ 15*

**P < 0.05*, 4 weeks vs 0 weeks STZ-rats
†*P < 0.05*, 4 weeks vs 0 weeks control rats

6.3.2 Effects of endothelium removal on acetylcholine

In preparations with intact endothelium, acetylcholine (1 – 100 µM) produced a graded relaxation of the tone induced by 100 nM phenylephrine (Figure 6.3A). In comparisons, in preparation without endothelium, acetylcholine had no effect (Figure 6.3B).

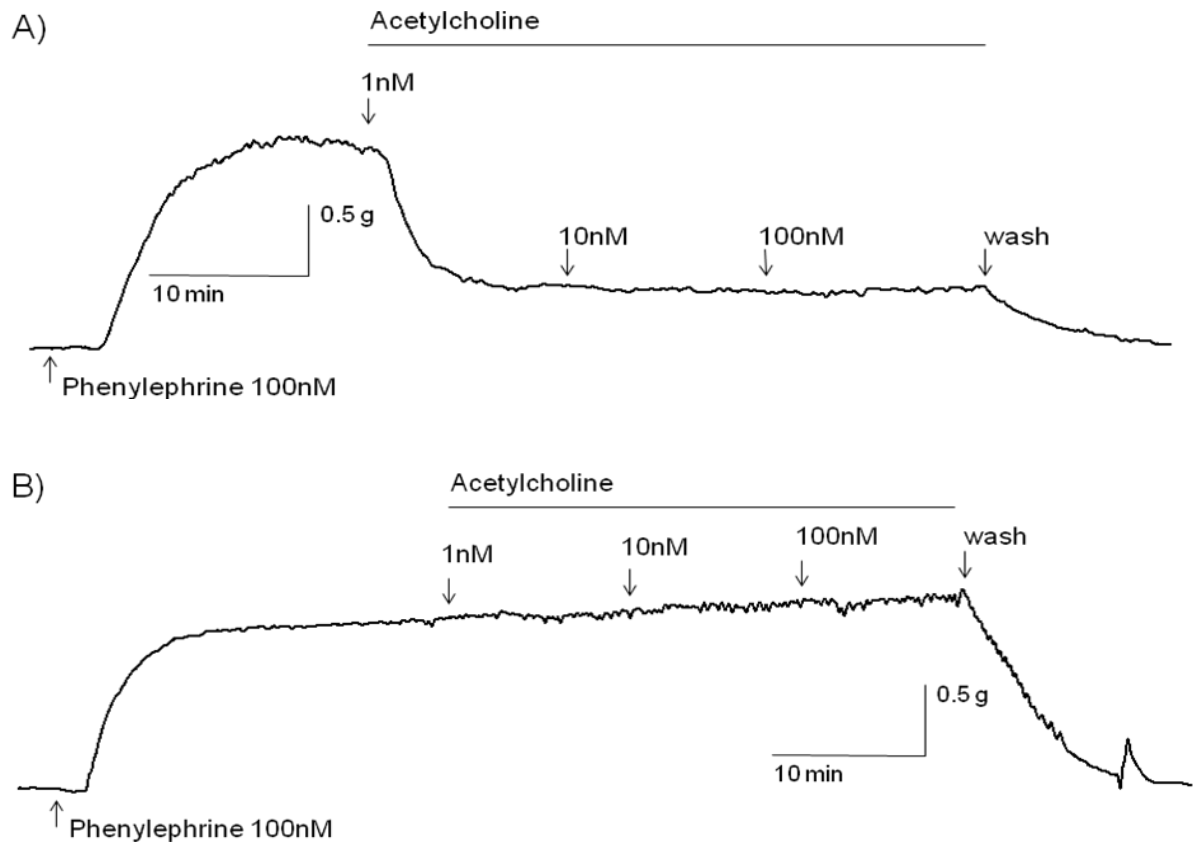

Figure 6.3 The traces from the current study illustrating the relaxant effects of acetylcholine on 100 nM phenylephrine-induced tone on rat femoral artery. (A) The relaxant effect in artery with intact endothelium, (B) the loss of the relaxant response in artery with endothelium removed.

6.3.3 Effects of U-46619 and its block by BMS-180291

U-46619 (1 – 300 nM) potently contracted rat femoral artery preparations. The log concentration-response curves were similar in preparations from control and STZ-rats (E_{max}: 130.6 $\pm$ 2%, 125.6 $\pm$ 5.4%; pEC_{50} = 7.95 $\pm$ 0.03; 7.95 $\pm$ 0.06) (Figure 6.4, n = 4). The main effects contrast for control and STZ treatment were not significantly different ($p = 0.38$). The slope of the two curves was almost the same (control: 1.8; STZ: 1.6).

BMS-180291 at 1 and 10 nM right-shifted the log concentration-response curves for U-46619 in femoral arteries from STZ-rats (Figure 6.5, n = 4). Dose-ratios were 3.16 and 11.2 respectively, affording pA_2 values of 9.33 and 9.01. BMS-180291 at 100 nM abolished the contraction to 100 nM U-46619 (Figure 6.6). After three washouts at 15 min intervals, the preparation had recovered full sensitivity to U-46619.

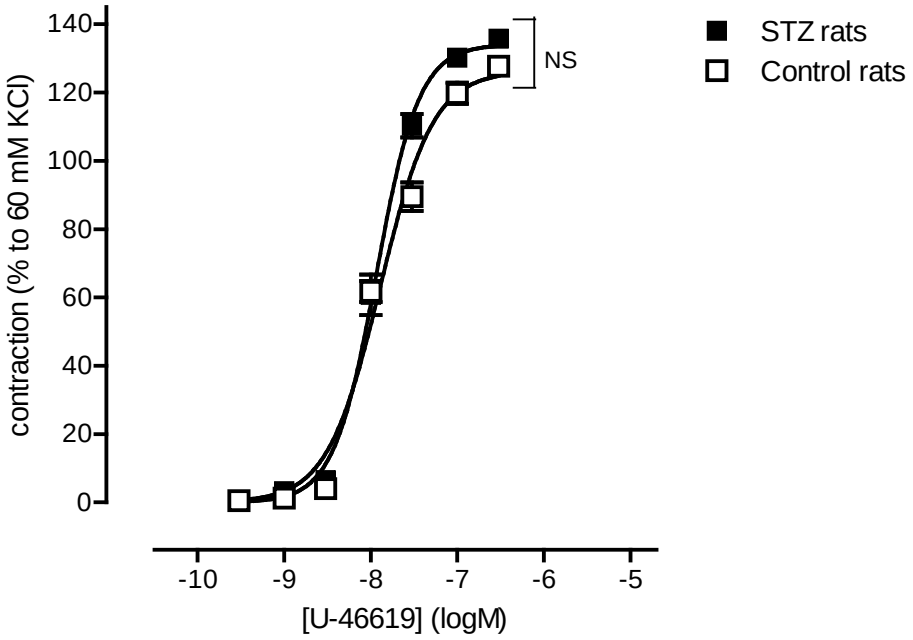

Figure 6.4 Effects of U-46619 on denuded femoral arteries from control and STZ rats (*n* = 4). *NS*, no significant difference between control and STZ-rats, using main effects contrasts.

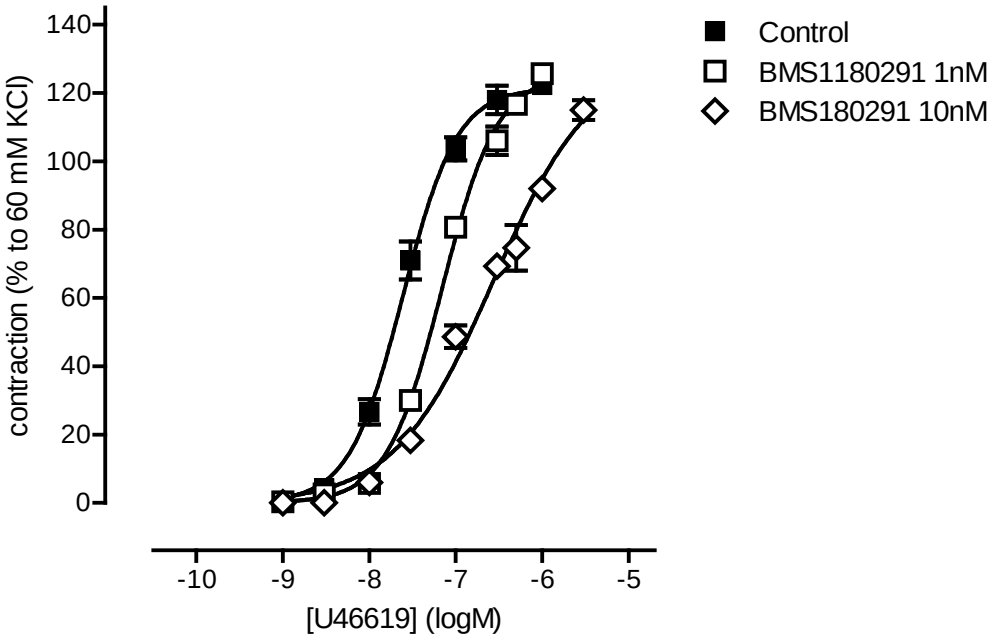

Figure 6.5 Antagonism of U-46619-induced contraction in denuded STZ-rat femoral artery by BMS-180291. Log concentration-response curves for U-46619 following treatment with 1 nM and 10 nM SC-51322 are shown (n = 4).

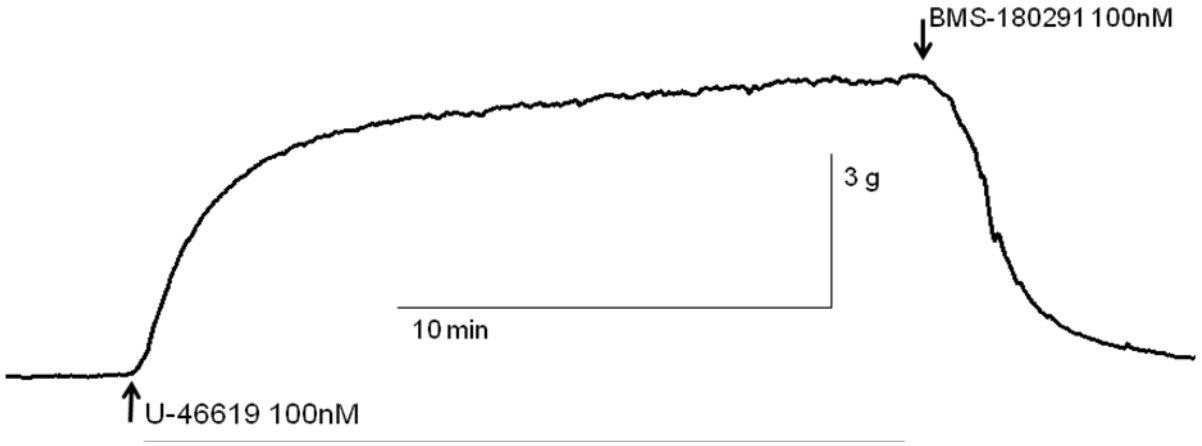

Figure 6.6 Experimental trace illustrating the fast onset and complete inhibition by 100 nM BMS-180291 (TP antagonist) on 100 nM U-46619-induced contraction of endothelium-denuded femoral artery from STZ- rat.

6.3.4 Effects of endothelium on potassium chloride and phenylephrine contraction

The responses to 60 mM KCl for intact and without endothelium preparations were not significantly different in STZ-rats (*p = 0.36*; Figure 6.7, *n* = 5). Similar response was observed in denuded and intact endothelium artery of control rat. Thus, the contractile response in control and STZ-rats were normalised to 60 mM KCl (K^+-standard). Log concentration-response curves for phenylephrine (1 nM – 3 µM) in STZ femoral artery preparations with and without endothelium are shown in Figure 6.8 (*n* = 4). Main effects contrasts for with and without endothelium were not significantly different (*p = 0.67*). (E_{max} values were 92.9 ± 12.0 and 88.3 ± 6.2%; pEC_{50} values were 7.46 ± 0.21 and 7.21 ± 0.10; respectively).

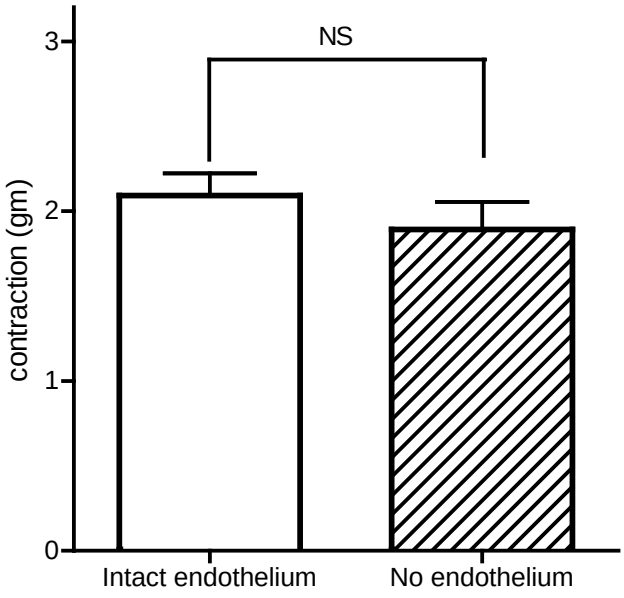

Figure 6.7 Contraction induced by 60 mM KCl in intact endothelium and denuded femoral arteries of STZ-rats (*n* = 5). *NS*, no significant difference using Student *t-test.*

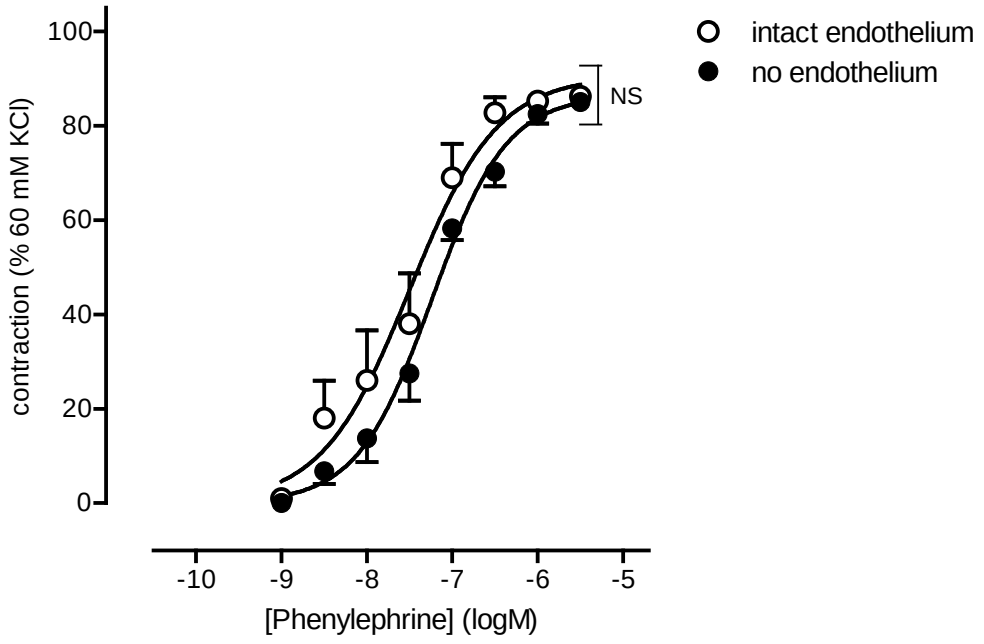

Figure 6.8 Log concentration-response curves for phenylephrine in STZ-rat femoral artery with endothelium and without endothelium (n = 4). *NS*, no significant difference between intact and without endothelium preparation using main effects contrasts.

6.3.5 Effects of phenylephrine on streptozotocin and control arteries

Log concentration-response curves for phenylephrine (1 – 300 nM) in endothelium-denuded femoral artery preparations from STZ and control rats are shown in Figure 6.9 (n = 5). The denuded femoral artery from STZ-rats showed similar contractile responses to phenylephrine (1 – 300 nM) compared to control rats. In arteries from STZ-treated rats, the maximal response to phenylephrine was greater than those from control rats but statistically not significant (E_{max}: 88.8 $\pm$ 2.6% and 75.4 $\pm$ 2.6% respectively, $p = 0.47$). The pEC_{50} values for STZ-rats and control preparations were: 7.39 $\pm$ 0.07 and control: 7.55 $\pm$ 0.08 respectively ($p = 0.98$).

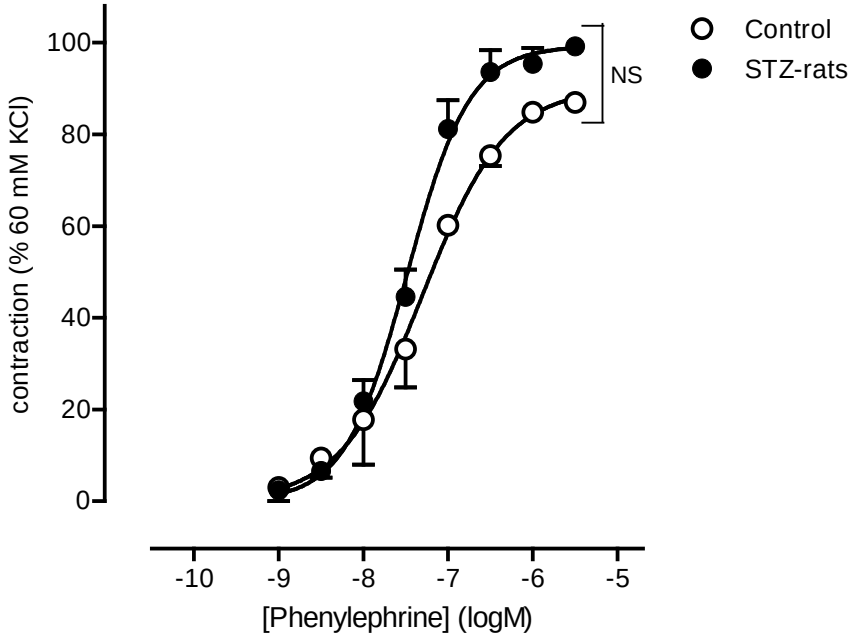

Figure 6.9 Log concentration-response curves for phenylephrine on denuded femoral arteries from control and STZ rats (n = 5). *NS*, no significant difference between control and STZ-rats using main effects contrasts.

6.3.6 Effects of prostanoid antagonists on phenylephrine-induced contraction

The TP receptor antagonist, BMS-180291 at 100 nM did not affect the contractile response to phenylephrine in STZ preparations: E_{max}: vehicle (DMSO) 90.3 ± 11.5%; STZ 92.3 ± 7.3%; *p = 0.63*) (Figure 6.10; *n* = 4). The pEC_{50} values were similar between two groups (Table 6.4). In contrast, the EP_3 receptor antagonist, L-798106 at 1 µM, significantly reduced the maximal response to phenylephrine compared to vehicle (80.3 ± 11.5 *vs.* 52.3 ± 9.8%, *p < 0.05*), with the curve shifted significantly to the right (Table 6.4). The addition of 100 nM BMS-180291 to 1 µM L-798106 produced no significant changes in the two parameters (*p = 0.87*)

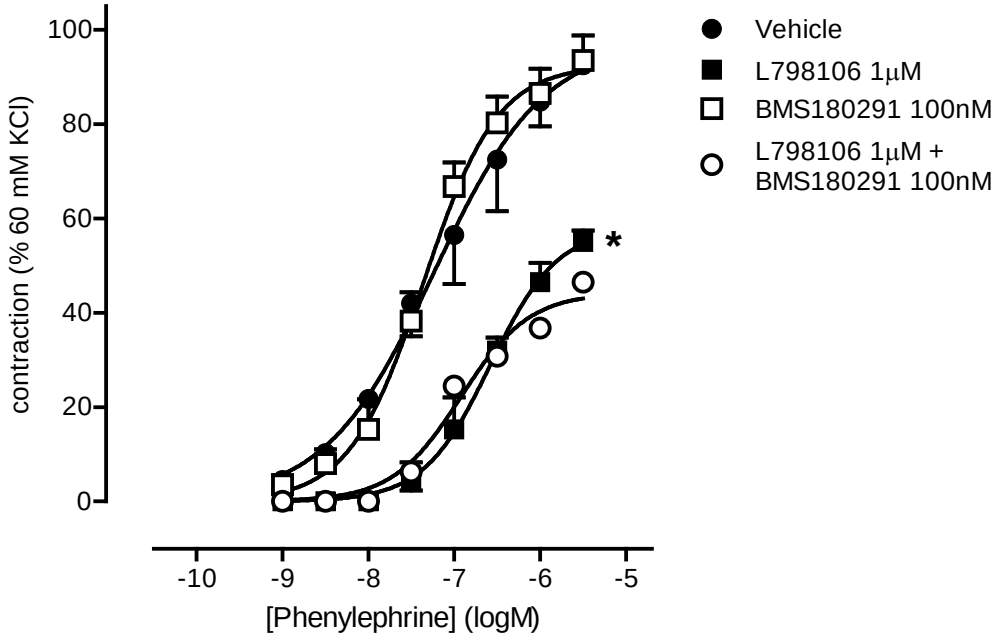

Figure 6.10 Effects of phenylephrine in denuded STZ-rat femoral artery, in the presence of vehicle (DMSO), 1 µM L-798106 and 100 nM BMS-180291 (*n* = 4). *$P < 0.05$, 1 µM L-798106 and vs. vehicle, using main effects contrasts.

Table 6.4 pEC_{50} of phenylephrine response in denuded control and STZ-rats femoral artery, following treatment with L-798106 and BMS-180291.

	pEC_{50}	
	Control	**STZ**
Vehicle	6.44 ± 0.04	7.17 ± 0.16
L-798106 1 µM	6.21 ± 0.09 *****	6.87 ± 0.06 *****
BMS-180291 100 nM	6.91 ± 0.13	7.10 ± 0.31
BMS-180291 100 nM + L-798106 1 µM	6.32 ± 0.08	7.22 ± 0.01

* *P* < *0.05*, L-798106 1 µM vs vehicle (control and STZ-rats)

The antagonist profiles were similar in control rats. Maximal response to phenylephrine in vehicle-treated preparations was no different in the presence of 100 nM BMS-180291 (88.3 ± 8.2%, 90.2 ± 6.3% respectively) (Figure 6.11, n = 4). The pEC_{50} values were also similar (Table 6.4). Similar to STZ-rats, 1 µM L-798106 reduced the phenylephrine maximum and shifted the concentration-response curve to the right in comparison to the control preparation. 100 nM BMS-180291 in combination with 1 µM L-798106 did not produce any significant changes compared with L-798106 alone.

CAY-10441 (IP-antagonist) at 1 µM did not affect the maximal response in diabetic rat femoral artery (Figure 6.12; n = 5).

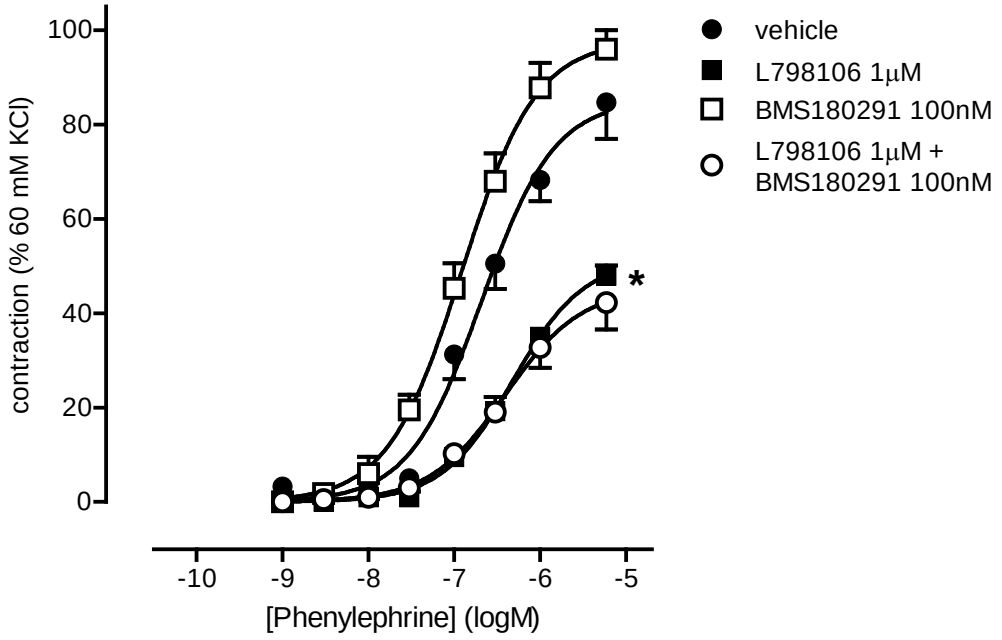

Figure 6.11 Effects of phenylephrine in denuded control rat femoral artery following treatment with vehicle (DMSO), 1 μM L-798106 and 100 nM BMS-180291 (n = 4). *$P < 0.05$, 1 μM L-798106 vs. vehicle, using main effects contrasts.

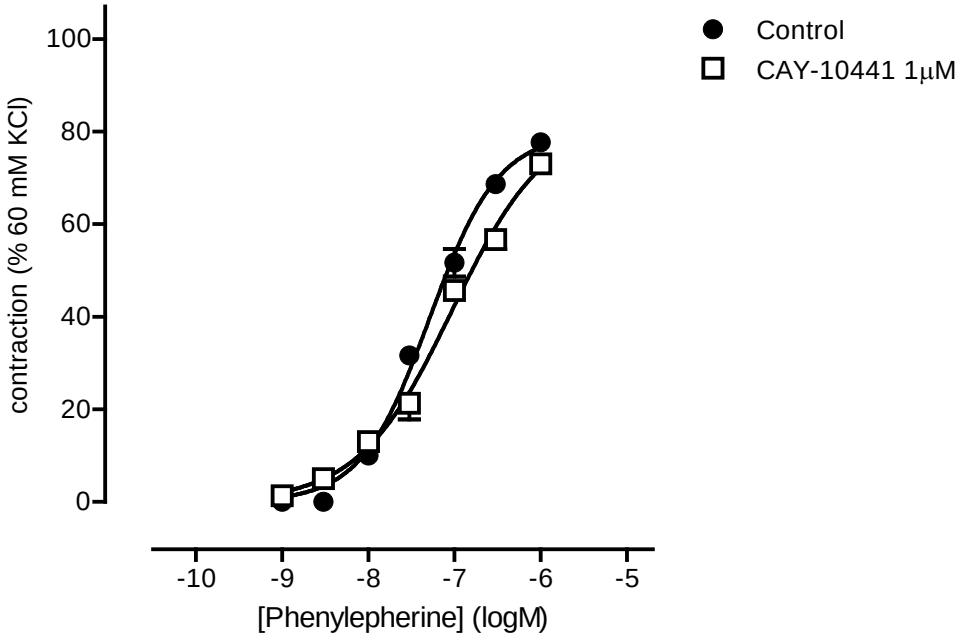

Figure 6.12 Effects of phenylephrine in denuded STZ-rat femoral artery following treatment with 1 μM CAY-10441 (*n = 5*).

6.3.7 Effects of COX-inhibitors on phenylephrine responses

Indomethacin (non-specific COX inhibitors) at 1 and 10 μM did not affect the maximal response produced by phenylephrine in non-endothelium rat femoral artery of STZ-rats (Figure 6.13, *n* = 4). Similar results were found with flurbiprofen at 1 and 10 μM (Figure 6.14, *n* = 4) (Table 6.5). A small increased in spontaneous tone was observed after incubation with flurbiprofen (Figure 6.15).

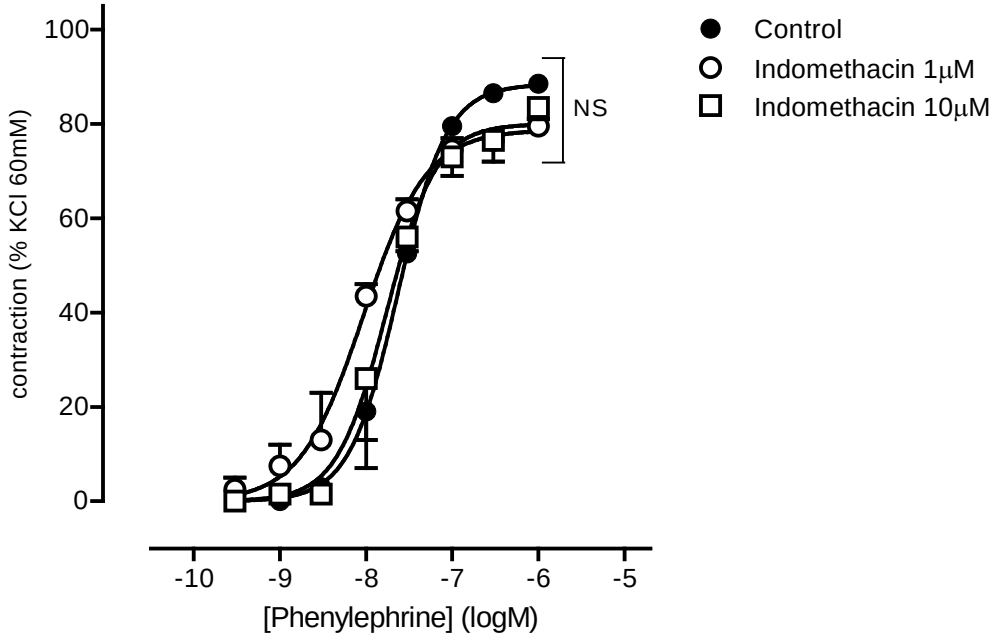

Figure 6.13 Effects of indomethacin on the log-concentration-response curve for phenylephrine in denuded STZ-rat femoral artery (*n* = 4). *NS*, not significant using main effects contrasts.

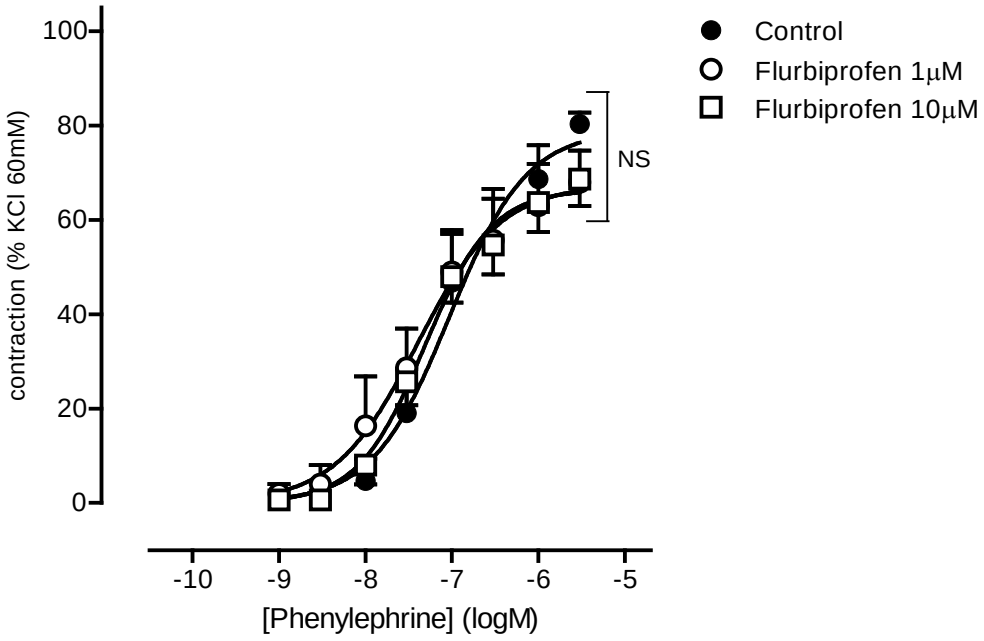

Figure 6.14 Effects of flurbiprofen on the log-concentration-response curve for phenylephrine in denuded STZ-rat femoral artery (n = 4). *NS*, not significant using main effects contrasts.

Table 6.5 pEC_{50} of phenylephrine response in denuded STZ-rat femoral artery, following indomethacin and flurbiprofen.

	pEC_{50}
Vehicle	7.61 ± 0.06
Indomethacin 1 μM	8.03 ± 0.07
Indomethacin 10 μM	7.75 ± 0.08
Vehicle	7.35 ± 0.16
Flurbiprofen 1 μM	7.45 ± 0.21
Flurbiprofen 10 μM	7.31 ± 0.09

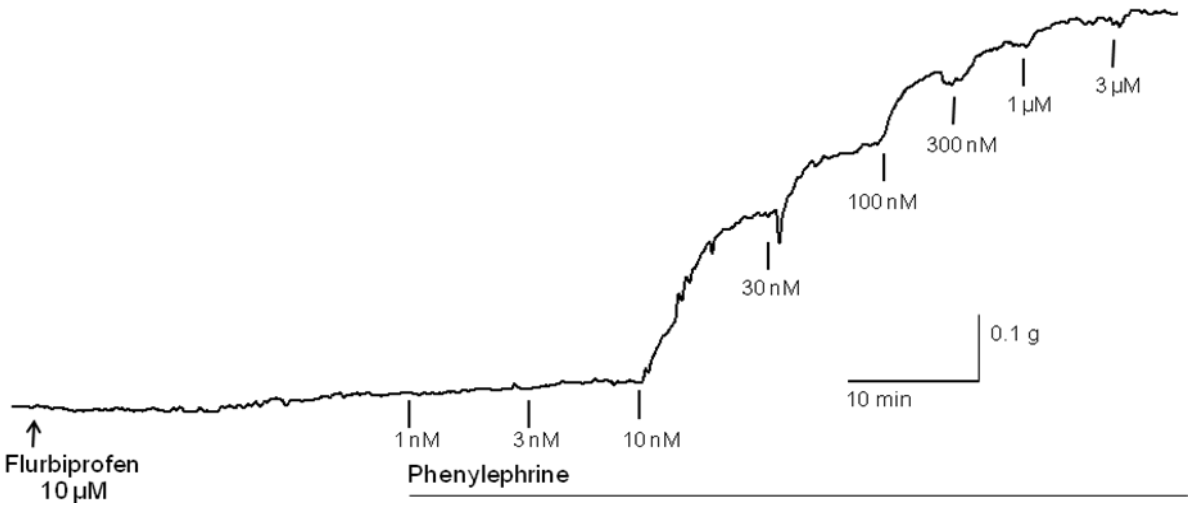

Figure 6.15 Experimental trace illustrating the increased in spontaneous tone induced after addition of 10 µM flurbiprofen on the denuded STZ-rat femoral artery.

6.4 Discussion

6.4.1 General response to streptozotocin

Diabetes mellitus is an endocrine disease characterized by the lack of insulin production (Type 1) or resistance of the target-organ to insulin or insulin resistant (Type 2) (Gale, 2001). In the early stage of diabetes, the subject usually presents with increasing passing out of urine (polyuria) and increase water uptake (polydipsia). Polyuria in STZ-treated rats was evident in the current study as the cage material needed to be change more frequently. Weight loss in the STZ-rats was due to inability of the rat to utilise the carbohydrate due to lack of insulin. Instead, the body fat was utilised for energy. In the current study, the STZ-rats were noticed to be thin and the dissected femoral artery was totally devoid of any connective tissue. The symptoms and signs resemble Type 1 diabetes mellitus in human and are in agreement with previous studies on STZ-induced diabetes in the rat (Harris and MacLeod, 1988; Furman and Sneddon, 1993; Shi *et al.*, 2007a; Shi *et al.*, 2007b; Shi and Vanhoutte, 2008).

6.4.2 Endothelium removal and effects on contractile response

Saponin was used initially in an attempt to remove the endothelium. Saponin is a natural product, obtained from the bark of the South American soap tree, *Quillaja saponaria*. It has been used as a chemical method to remove endothelium in dog femoral artery (Samata *et al.*, 1986) and dog coronary artery (Nakane *et al.*, 1986). Nakane *et al.* (1986) used intraluminal bolus injection of saponin (1 mg) in isolated and perfused dog coronary arteries. In the current study, the arterial rings were incubated with Krebs-Henseleit solution containing 0.3 $mgml^{-1}$ of saponin for 35 min at 37 °C as described earlier by Samata *et al.* (1986). However, responses to KCl and phenylephrine were abolished by this treatment. Instead, the endothelium was mechanically

removed by rubbing roughened myograph wire against the intimal surface of the artery. The method was described previously in a study of acetylcholine mechanism of action in cat cerebral artery (Lee, 1982).

In the current study, contractions to phenylephrine were similar in the presence and absence of endothelium. This agrees with similar studies of the action of noradrenaline on rat mesenteric bed (Fortes *et al.*, 1983; Peredo, 2001) and rat aorta (Fortes *et al.*, 1983; Mulhern and Docherty, 1989). The response is dependent on release of intracellular Ca^{2+} and to lesser extent on entry of extracellular Ca^{2+} (Owen and Carrier, 1980; Hung *et al.*, 2006). In contrast, others have shown that the removal of endothelium increased the maximal response and sensitivity to phenylephrine in comparison to an intact endothelium preparation in STZ-rat aorta (Martin *et al.*, 1986; Alosachie and Godfraind, 1988).

The removal of endothelium had no effect on the response to 60 mM KCl. This agreed with the previous finding in canine femoral artery where removal of endothelium cause slight depression of KCl-induced contraction (De Mey and Vanhoutte, 1981). The response was also similar between denuded artery of control and STZ-rats, in agreement with the earlier work done in diabetic rat aorta where the contractile response to KCl is endothelium independent (Mulhern and Docherty, 1989; Peredo, 2001; Tang *et al.*, 2008).

The present results demonstrated that there were no differences in response to phenylephrine in both denuded femoral artery of control and diabetes rat. This is in consistent with previous work done on rat femoral artery (Dai *et al.*, 1993; Shi *et al.*, 2007a). These results are also similar to work done on denuded diabetic rat aorta (Chang and Stevens, 1992; Tang *et al.*, 2008) and rat mesenteric arteries (Harris and MacLeod, 1988; White and Carrier, 1988; Furman and Sneddon, 1993; Peredo, 2001).

6.4.3 Induction of endogenous prostanoids by diabetes

The induction of endogenous prostanoids varies according the duration of diabetes. In rat mesenteric bed, the vasoconstrictor prostanoid production (TXA_2 / $PGF_{2\alpha}$) were increased up to 100% from basal level in the first week of STZ-induction diabetes, (Peredo *et al.*, 1999). The levels of PGI_2 and PGE_2 were unchanged within the same period. The ratio between the production of PGI_2 and TXA_2 was recovered to reach values similar to those of the controls at four weeks (Peredo *et al.*, 1999; Shi and Vanhoutte, 2008).

There appears to be enhanced activation of the COX enzyme in arteries following induction of diabetes, leading to the production of endogenous contractile factors. In the early stage of the diabetes, the main COX product generated in rat femoral artery is TXA_2 (Shi *et al.*, 2007b). TXA_2 also shown to be increased in diabetic dog mesenteric arteries (Sterin-Borda *et al.*, 1984). TX A_2 mainly activates TP receptors on the smooth muscle cells as shown by the ability of S-18886 (TP receptor antagonist) to inhibit responses to phenylephrine diabetic rat femoral artery (Shi *et al.*, 2007a).

In the current experiment, the TXA_2 mimetic, U-46619 produced a similar contractile profile in femoral arteries from STZ and control rats. These results suggest that in diabetes neither the sensitivity nor the density of the TP receptor is changed. Previous work using radioligand binding studies showed there were no significant differences in the density (B_{max}) or affinity (K_d) of TP receptors on isolated platelets or glomerular membranes between control and STZ-rats (Morinelli *et al.*, 1993). The current results also agreed with the view that the underlying smooth muscle is not affected by STZ diabetes (Chang and Stevens, 1992). However, BMS-180291 at 100 nM did not affect phenylephrine-induced contraction, thus arguing against a facilitatory role for endogenous TXA_2. BMS-180291 (TP antagonist) competitively inhibited U-46619 with pA_2 of 9.33 and 9.01, corresponding to its expected affinity for the TP receptor. Furthermore, 100 nM

BMS-180291 completely antagonised the contractile response to 100 nM U-46619 (~ 60 - 70% maximal response) in the STZ-rats (Figure 6.6). In contrast, Shi *et al* (2007b) showed an increase in sensitivity to U-46619 but decrease in maximal response in STZ-rat femoral artery compared to the control preparation.

In the experiments of Hung *et al.* (2006), PGE_2 alone produced a weak contractile response of the rat femoral artery. However, when the preparation was primed with phenylephrine (10 nM, 10% of maximal response), a strong contractile effect was seen with PGE_2 (1 – 300 nM). 10 nM PGE_2 also enhanced the response to phenylephrine, demonstrating that the synergism is mutual. This synergism was blocked by 1 μM L-798106, with pA_2 of 7.35 – 8.10. These experiments were conducted in the presence of indomethacin, so that endogenous prostanoids did not interfere with the assessment of the exogenous prostanoid.

The current study would tend to support a facilitator role for PGE_2 in the contraction of rat femoral artery. In the absence of COX-inhibition, L-798106 at 1 μM inhibited the response to phenylephrine, with shift of EC_{50} to a higher value and suppression of the maximum response. This profile is compatible with the generation of PGE_2 within the tissue, which then acts on EP_3 receptors on the smooth muscle cells to enhance α_1-adrenoceptor mediated events. This profile was very similar in control and STZ-diabetic rats. However, in the current experiments, indomethacin and flurbiprofen did not affect phenylephrine action in the femoral artery from STZ-rat. This result agreed with work done by Chang *et al.* (1992) where 5 μM indomethacin did not affect the contractile response to phenylephrine in STZ-rat aorta (endothelium removed). In addition, Peredo (2001) showed no effect of 10 μM indomethacin on the contractile response to noradrenaline in STZ-rat mesenteric beds.

A possible explanation for the nil effect of indomethacin on contractile response to phenylephrine is that a non-COX pathway generates the prostaglandin or prostaglandin-like compounds. One group of compounds of interest are the isoprostanes (isoPs), prostaglandin (PG)-like compounds produced by non-enzymatic degradation (lipid peroxidation) of arachidonic acid (Roberts and Morrow, 1995; Dogne *et al.*, 2005). Examples include 8-iso PGE_2 and 8-iso $PGF_{2\alpha}$. This lipid peroxidation is independent of the COX enzyme in human and animals (Figure 6.16). Indeed, isoP levels increased as a consequences of enhanced lipid peroxidation in diabetes (Davi *et al.*, 1999). The plasma level of isoPs was about two-fold higher in 8 weeks STZ-rat than in control rats (Wigg *et al.*, 2004). In response to bolus injection of noradrenaline, the level of isoPs and TXA_2 significantly increased in human umbilical vein (Sametz *et al.*, 2000b). Thus, the same stimulation that enhanced prostaglandin production will also increased the level of isoPs in the tissue.

Previously, radio-ligand binding studies on rat smooth muscle cells have shown receptors for isoprostanes distinct from prostanoid receptors (Fukunaga *et al.*, 1993; Fukunaga *et al.*, 1997). However, in high concentration, there was a cross-activation of TP receptors. Moreover, recent studies on isolated vascular preparation have shown the contractile effect is due to activation on EP and TP receptors with no evidence for distinct isoPs receptors. IsoPs have shown to contract various tissues, including guinea-pig trachea (Clarke *et al.*, 2004), rat gastric fundus, guinea-pig ileum (Sametz *et al.*, 2000a), human umbilical vein (Daray *et al.*, 2003; Daray *et al.*, 2004) and pig pulmonary artery (Janssen and Tazzeo, 2002). The isoPs constrictive effect is also not dependent on intact endothelium as demonstrated earlier on a canine intestine preparation (Elmhurst *et al.*, 1997). In the current experiment, a TP antagonist did not affect the response to phenylephrine. In view of this result, it is most likely in STZ-rat femoral artery isoPs potentially synergise with phenylephrine through EP_3 system in the artery as evidenced by the inhibitory effect of L-798106.

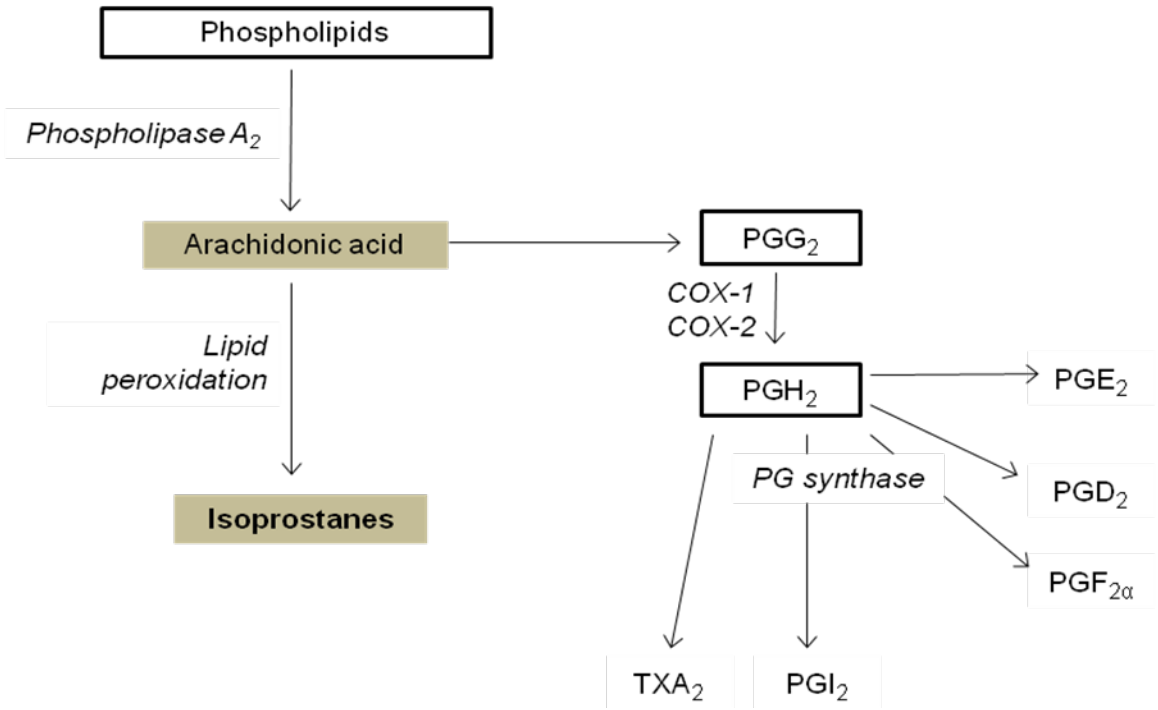

Figure 6.16 Phospholipids are metabolised by phospholipase A_2 to form arachidonic acid in response to various stimuli, like the diabetes process. Oxidation of arachidonic acid via a non-enzymatic pathway (lipid peroxidation) produces a family of isoprostanes (redrawn from Dogne *et al.*, 2005).

Another possibility for the inhibitory effect of L-798106 is a non-specific mechanism. However, it would be difficult to distinguish between, say, block of synergism induced by an endogenous non-prostanoid and a non-specific inhibitory effect since the responses to other contractile agents may be inhibited by L-798106 to the same extent. The alternative method is to use a chemically different EP_3 antagonist that is more selective on the same settings. For example, ONO-AE3-240 is reported to be a highly selective EP_3 antagonist (mouse EP_3 / EP_1 selectivity ratio = 2500; Amano *et al.*, 2003), which significantly suppressed tumor-associated angiogenesis and tumor growth in WT mice; perhaps it would show high selectivity in general.

6.4.4 Roles of prostacyclin

Rat femoral artery is relaxed by prostacyclin analogues (Hung *et al.*, 2006). Prostacyclin (PGI_2) could therefore be part of the prostaglandins released, exerting its relaxant action through IP receptor (Narumiya *et al.*, 1999). The nil effect of the indomethacin and flurbiprofen could then be due to inhibition of the production of both TXA_2 (contractile) and PGI_2 (relaxant). If this is the reason, by blocking the IP receptor, the contractile response to phenylephrine in the preparation should be higher than in the absence of any antagonist. However, the IP antagonist CAY-10441 (pA_2 8.82; Clark *et al.*, 2004) did not affect the maximal response to phenylephrine in the STZ-rats. Interestingly, there is a substantial evidence that in the STZ-induced diabetes rat, the production of PGI_2 is decreased (Harrison *et al.*, 1978; Peredo *et al.*, 1999).

6.5 Conclusions

The evidence for a role of endogenous prostanoid(s) in enhancing the contractility of rat femoral artery is conflicting. In both control and STZ treatment situations, the results with L-798106 suggest that an endogenous EP_3 agonist may enhance α_1-adrenoreceptor-induced contraction. However, the COX-inhibitor data would argue against this proposal. It is possible that the endogenous facilitator could be a product of a non-COX biosynthetic pathway, such as an isoprostane. A co-role for prostacyclin acting as a functional antagonist seems unlikely in view of the lack of effect of the IP antagonist CAY-10441. Additionally, a thorough investigation of the specificity of L-798106 is required. It may be useful to repeat the current experiments using an EP_3 antagonist of a different chemical class.

Nevertheless, the current study has shown that there was no significant difference in response to phenylephrine in control and STZ-induced diabetes rat. The discrepancy between other published works cannot be readily explained. Several possibilities are due to variations between the duration of STZ-induced diabetes, the different tissue preparations, and sources of animal or experimental conditions.

CHAPTER SEVEN

GENERAL DISCUSSION AND CONCLUSION

The present study has used classical organ bath pharmacology and utilised fundamental principles of pharmacology to characterize prostanoid receptors in several isolated vessels or tissues. In the process, the utility of certain novel prostanoid agonists and antagonists has been assessed.

7.1 Functional studies

Organ bath studies were carried out to determine the functional responses of the guinea-pig trachea, rat mesenteric artery, rat urinary bladder and rat femoral artery to prostaglandin analogues. This was used to provide information on the population of key prostanoid receptors within these tissues.

Although Schild antagonism protocols remain the gold standard to determine the affinity constant of an antagonist, the current study has utilised inhibition-curve protocols based on the Cheng-Prusoff relationship. The decision to choose this method was based on the limited availability of prostanoid analogues as the inhibition-curve protocol is operating over a low concentration range. Furthermore, the inhibition protocol provides direct observation of the rate of onset of antagonism in the case of highly potent and / or lipophilic antagonists, which were expected to be slower in onset. The affinity constants estimated for particular antagonists were in agreement with other functional studies using Schild protocols. The inhibition-curve protocol has not been used frequently in previous studies for prostanoid receptor antagonists

In the guinea-pig trachea, the current study findings were consistent with the presence of contractile EP_1 and TP receptors and a relaxant EP_2 receptor. All the EP_2 agonists tested in the GPT study behaved as full agonists. CAY-10399 was shown to be the most potent EP_2 receptor agonist of those studied. The EP_2 receptor agonist AH-13205 appeared to have two relaxant

components. This profile may arise from the existence of another relaxant receptor in the trachea. Alternatively, it is possible that the two isomers present in AH-13205 may be responsible. It should be possible to separate these isomers by high-performance liquid chromatography and study each separately.

In the rat mesenteric artery, the absence of relaxant prostanoid receptors was of considerable assistance in establishing the presence of contractile TP, EP_1 and EP_3 prostanoid receptors. In addition, the use of the potent and selective TP antagonist BMS-180291 was crucial to studying only EP receptor-mediated effects. The presence of these functional receptors was confirmed by the reduction of established contractile response in the presence of the respective selective antagonists. EP_1 and EP_3 receptors were activated simultaneously by PGE_2 analogues such as 17-phenyl PGE_2 and sulprostone. The two-site competition equation fitted the inhibition-curve data significantly better than one-site competition model, as shown by a modified F test. This is the first time that this type of analysis has been used for a prostanoid system. The novel EP_1 agonist, ONO-D1-004 was shown to be a selective on EP_1 receptor. However, the activity of novel EP_3 agonist, ONO-AE-248 on rat mesenteric artery needs to be investigated further due to contradictory results.

In similar situation in the rat urinary bladder, only contractile EP-type receptors were shown to be present functionally. Antagonist studies demonstrated both EP_1 and EP_3 receptors contributed to the contractile response induced by the prostanoid agonists. As in the rat mesenteric artery, inhibition-curve protocols underpinned the finding of two contractile systems. Again, the two-site competition model fitted better than the one-site competition model. Non-parallel right-shifts of EP agonist curves were found with the novel EP_1 antagonist, GW-848687. The profile GW-844687 may be due to presence of two contractile receptors or non-competitive antagonism. In relation to the latter, a state of hemi-equilibrium for the antagonist-agonist interaction needs to be considered.

The current studies were able to characterize the prostanoid receptors by utilising the inhibition curve protocol instead of full Gaddum-Schild protocol. Further studies, in availability of the more selective prostanoid would help to clarify the uncertainty results in this study. Similarly, binding studies on this isolated preparation could be performed to allow identification of the specific receptors that the analogues bind.

The studies reported here were carried out over the same time period as related work on several guinea-pig smooth muscle preparations by one of my supervisors. The guinea-pig trachea (EP_1 and TP preparation) and aorta rings (EP_3 and TP preparation) were used in the experiments in a conventional organ bath. The experiments were often plagued by the slow approach of prostanoid agonists and antagonists to steady state, particularly when the ligands showed high potency or affinity. Thus, inhibition-curve protocols could not be performed satisfactorily. In addition, it is never clear whether the slow onset has affected the absolute potency of the ligand under study. Onset rates of both agonists and antagonists in my experiments were much faster, thereby allowing construction of cumulative relationships within a reasonable time period. This difference may be due to the thinner nature of my tissues, which allows rapid diffusion to centrally situated receptors.

The use of conventional organ bath experiments has declined of late in favour of recombinant receptor studies, usually involving radioligand binding. The transfer of these data to complex *in vivo* functional systems soon follows. The results are often equivocal however. Part of the problem relates to a lack of the sorts of information that isolated tissue studies readily provide. For example: the true potency and selectivity of the agent when a complex functional response is measured and opposing transduction systems are present; the rate of attainment of steady-state when access to the receptor pool is not instantaneous as it is the case for receptors located in the cell membrane of a carrier cell. It is hoped that some of the data contained in this thesis will help to bridge this gap as far as prostanoid systems are concerned.

7.2 Streptozotocin-induced diabetes study

Optimising the diabetic state of the experimental rat is a crucial aspect in determining the effect of the diabetic disease process on the arterial response to prostaglandin analogues. The period of four weeks after the administration of streptozotocin was chosen as the cut-off point in the current experiment, based on previous studies by various authors.

In STZ study, attention has been focused on the TP and EP_3 receptors in rat femoral artery. The rationale for this was that previous studies in the same setting in the diabetic rat only concentrated on the TP receptor / α_1-adrenoceptor interaction and failed to take into account that an EP_3 agonist (e.g. PGE_2 in the *in vivo* situation) can markedly enhance the contractile actions of other agonists (including noradrenaline *in vivo*). The present of TP receptor in the study was demonstrated by complete inhibition of U-46619-induced contraction by the selective TP antagonist BMS-180291. In addition, the study also focused on the effect of the endothelium on the phenylephrine-induced response. The endothelium was removed mechanically, by rolling the intima side of the femoral artery in order to remove the effects of endothelial dysfunction secondary to diabetes. Another method involving chemical removal using saponin proved difficult to achieve.

The current study demonstrated that the contractile response of KCl and phenylephrine in rat femoral artery were endothelium independent, in agreement with other studies. The response to phenylephrine was partially inhibited by the selective EP_3 antagonists L-798106 and L-826266, implying that the tissue continuously generates PGE_2 or a similar endogenous EP_3 agonist . Indeed, it is known that diabetes itself induces the production of the endogenous prostaglandins. However, two COX-inhibitors, indomethacin and flurbiprofen, failed to produce a similar inhibition of the phenylephrine response. *Per se*, this finding does not rule out a role for EP_3 receptors in controlling the sensitivity of the α_1-adrenoceptor (or other) contractile systems.

There is still the possibility that compounds with EP_3 agonist properties are generated through a non-COX pathway. Another possibility, namely that endogenous PGI_2 acting via IP receptors opposes the contractile action of the endogenous EP_3 agonist, was ruled out through the use of a selective IP antagonist.

The time factor was the main limitation of why the duration of four weeks STZ-induction was chosen for the study. In reviewing of the results obtained, there were no significant differences between the contractility of the femoral arteries from control and STZ-induced diabetes rat. Future work should include a longer duration of the diabetes state with increased availability of the STZ-rats. This is necessary to provide greater understanding of the effects of diabetes on prostanoid production and the vascular response to the prolonged diabetes.

REFERENCES

Abe Y, Tatsumi K, Sugito K, Ikeda Y, Kimura H & Kuriyama T (2001). Effects of inhaled prostacyclin analogue on chronic hypoxic pulmonary hypertension. *J Cardiovasc Pharmacol* **37:** 239-51.

Abramovitz M, Adam M, Boie Y, Carriere M, Denis D, Godbout C *et al.* (2000). The utilization of recombinant prostanoid receptors to determine the affinities and selectivities of prostaglandins and related analogs. *Biochim Biophys Acta* **1483:** 285-93.

Abramovitz M, Boie Y, Nguyen T, Rushmore TH, Bayne MA, Metters KM *et al.* (1994). Cloning and expression of a cDNA for the human prostanoid FP receptor. *J Biol Chem* **269:** 2632-6.

Albert PR, Zhou QY, Van Tol HH, Bunzow JR & Civelli O (1990). Cloning, functional expression, and mRNA tissue distribution of the rat 5-hydroxytryptamine1A receptor gene. *J Biol Chem* **265:** 5825-32.

Alexander SP, Mathie A & Peters JA (2008). Guide to Receptors and Channels (GRAC), 3rd edition. *Br J Pharmacol* **153 Suppl 2:** S1-209.

Alosachie I & Godfraind T (1988). The modulatory role of vascular endothelium in the interaction of agonists and antagonists with α-adrenoceptors in the rat aorta. *Br J Pharmacol* **95:** 619-29.

Amano H, Hayashi I, Endo H, Kitasato H, Yamashina S, Maruyama T *et al.* (2003). Host prostaglandin E_2-EP_3 signaling regulates tumor associated angiogenesis and tumor growth. *J Exp Med* **197**: 221–232.

Andersson KE (2002). Bladder activation: afferent mechanisms. *Urology* **59:** 43-50.

Andrade da Costa BL, Kang KD, Rittenhouse KD & Osborne NN (2009). The localization of PGE_2 receptor subtypes in rat retinal cultures and the neuroprotective effect of the EP_2 agonist butaprost. *Neurochem Int* **55:** 199-207.

Angeli V, Staumont D, Charbonnier AS, Hammad H, Gosset P, Pichavant M *et al.* (2004). Activation of the D prostanoid receptor 1 regulates immune and skin allergic responses. *J Immunol* **172:** 3822-9.

Anthony TL, Pierce KL, Stamer WD & Regan JW (1998). Prostaglandin $F_{2\alpha}$ receptors in the human trabecular meshwork. *Invest Ophthalmol Vis Sci* **39:** 315-21.

Arita H, Nakano T & Hanasaki K (1989). Thromboxane A_2: its generation and role in platelet activation. *Prog Lipid Res* **28:** 273-301.

Armstrong RA (1995). Investigation of the inhibitory effects of PGE_2 and selective EP agonists on chemotaxis of human neutrophils. *Br J Pharmacol* **116:** 2903-8.

Armstrong R A, Jones RL, Peesapati V, Will SG & Wilson NH (1985). Competitive antagonism at thromboxane receptors in human platelets. *Br J Pharmacol* **84:** 595-607.

Arunlakshana O & Schild HO (1959). Some quantitative uses of drug antagonists. *Br J Pharmacol Chemother* **14:** 48-58.

Bastien L, Sawyer N, Grygorczyk R, Metters KM & Adam M (1994). Cloning, functional expression, and Characterization of the human prostaglandin E_2 receptor EP_2 subtype. *J Biol Chem* **269:** 11873-7.

Belton O, Byrne D, Kearney D, Leahy A & Fitzgerald DJ (2000). Cyclo-oxygenase-1 and -2-dependent prostacyclin formation in patients with atherosclerosis. *Circulation* **102:** 840-5.

Bewick V, Cheek L & Ball J (2004). Statistics review 9: one-way analysis of variance. *Crit Care* **8:** 130-6.

Bley KR, Bhattacharya A, Daniels DV, Gever J, Jahangir A, O'Yang C *et al.* (2006). RO1138452 and RO3244794: Characterization of structurally distinct, potent and selective IP (prostacyclin) receptor antagonists. *Br J Pharmacol* **147:** 335-45.

Boie Y, Rushmore TH, Darmon-Goodwin A, Grygorczyk R, Slipetz DM, Metters KM *et al.* (1994). Cloning and expression of a cDNA for the human prostanoid IP receptor. *J Biol Chem* **269:** 12173-8.

Boie Y, Sawyer N, Slipetz DM, Metters KM & Abramovitz M (1995). Molecular cloning and Characterization of the human prostanoid DP receptor. *J Biol Chem* **270:** 18910-6.

Boie Y, Stocco R, Sawyer N, Slipetz DM, Ungrin MD, Neuschafer-Rube F *et al.* (1997). Molecular cloning and Characterization of the four rat prostaglandin E_2 prostanoid receptor subtypes. *Eur J Pharmacol* **340:** 227-41.

Bolla M, You D, Loufrani L, Levy BI, Levy-Toledano S, Habib A *et al.* (2004). Cyclo-oxygenase involvement in thromboxane-dependent contraction in rat mesenteric resistance arteries. *Hypertension* **43:** 1264-9.

Bombardier C, Laine L, Reicin A, Shapiro D, Burgos-Vargas R, Davis B *et al.* (2000). Comparison of upper gastrointestinal toxicity of rofecoxib and naproxen in patients with rheumatoid arthritis. VIGOR Study Group. *N Engl J Med* **343:** 1520-8, 2 p following 1528.

Breyer MD & Breyer RM (2001). G protein-coupled prostanoid receptors and the kidney. *Annu Rev Physiol* **63:** 579-605.

Breyer RM, Bagdassarian CK, Myers SA & Breyer MD (2001). Prostanoid receptors: subtypes and signaling. *Annu Rev Pharmacol Toxicol* **41:** 661-90.

Buus NH, Simonsen U, Pilegaard HK & Mulvany MJ (2000). Nitric oxide, prostanoid and non-NO, non-prostanoid involvement in acetylcholine relaxation of isolated human small arteries. *Br J Pharmacol* **129:** 184-92.

Calabresi L, Rossoni G, Gomaraschi M, Sisto F, Berti F & Franceschini G (2003). High-density lipoproteins protect isolated rat hearts from ischemia-reperfusion injury by reducing cardiac tumor necrosis factor-alpha content and enhancing prostaglandin release. *Circ Res* **92:** 330-7.

Cameron KO, Lefker BA, Ke HZ, Li M, Zawistoski MP, Tjoa CM *et al.* (2009). Discovery of CP-533536: an EP_2 receptor selective prostaglandin E_2 (PGE_2) agonist that induces local bone formation. *Bioorg Med Chem Lett* **19:** 2075-8.

Cao J, Shayibuzhati M, Tajima T, Kitazawa T & Taneike T (2002). *In vitro* pharmacological Characterization of the prostanoid receptor population in the non-pregnant porcine myometrium. *Eur J Pharmacol* **442:** 115-23.

Chan KM & Jones RL (2004). Partial agonism of taprostene at prostanoid IP receptors in vascular preparations from guinea-pig, rat, and mouse. *J Cardiovasc Pharmacol* **43:** 795-807.

Chang KS & Stevens WC (1992). Endothelium-dependent increase in vascular sensitivity to phenylephrine in long-term streptozotocin diabetic rat aorta. *Br J Pharmacol* **107:** 983-90.

Chauhan S, Rahman A, Nilsson H, Clapp L, MacAllister R & Ahluwalia A (2003). NO contributes to EDHF-like responses in rat small arteries: a role for NO stores. *Cardiovasc Res* **57:** 207-16.

Cheng Y, Austin SC, Rocca B, Koller BH, Coffman TM, Grosser T *et al.* (2002). Role of prostacyclin in the cardiovascular response to thromboxane A_2. *Science* **296:** 539-41.

Cheng Y & Prusoff WH (1973). Relationship between the inhibition constant (K_i) and the concentration of inhibitor which causes 50 per cent inhibition (I_{50}) of an enzymatic reaction. *Biochem Pharmacol* **22:** 3099-108.

Christensen KL & Mulvany MJ (2001). Location of resistance arteries. *J Vasc Res* **38:** 1-12.

Christman BW, McPherson CD, Newman JH, King GA, Bernard GR, Groves BM *et al.* (1992). An imbalance between the excretion of thromboxane and prostacyclin metabolites in pulmonary hypertension. *N Engl J Med* **327:** 70-5.

Chuang YC, Yoshimura N, Huang CC, Wu M, Chiang PH & Chancellor MB (2008). Intravesical Botulinum Toxin A administration inhibits COX-2 and EP_4 expression and suppresses bladder hyperactivity in cyclophosphamide-induced cystitis in rats. *Eur Urol*.

Cirillo R, Tos EG, Page P, Missotten M, Quattropani A, Scheer A *et al.* (2007). Arrest of preterm labor in rat and mouse by an oral and selective nonprostanoid antagonist of the prostaglandin $F_{2\alpha}$ receptor (FP). *Am J Obstet Gynecol* **197:** 54 e1-9.

Clark P, Rowland SE, Denis D, Mathieu MC, Stocco R, Poirier H *et al.* (2008). MF498 [N-{[4-(5,9-Diethoxy-6-oxo-6,8-dihydro-7H-pyrrolo[3,4-g]quinolin-7-yl)-3-methylbenzyl]sulfo-nyl}-2-(2-methoxyphenyl)acetamide], a selective E prostanoid receptor 4 antagonist, relieves joint inflammation and pain in rodent models of rheumatoid and osteoarthritis. *J Pharmacol Exp Ther* **325:** 425-34.

Clark RD, Jahangir A, Severance D, Salazar R, Chang T, Chang D, *et al.* (2004). Discovery and SAR development of 2-(phenylamino) imidazolines as prostacyclin receptor antagonists [corrected]. *Bioorg Med Chem Lett* **14:** 1053-6.

Clarke DL, Giembycz MA, Patel HJ & Belvisi MG (2004). E-ring 8-isoprostanes inhibit ACh release from parasympathetic nerves innervating guinea-pig trachea through agonism of prostanoid receptors of the EP_3-subtype. *Br J Pharmacol* **141:** 600-9.

Clyman RI, Mauray F, Roman C, Rudolph AM & Heymann MA (1980). Circulating prostaglandin E_2 concentrations and patent ductus arteriosus in fetal and neonatal lambs. *J Pediatr* **97:** 455-61.

Coats P & Hillier C (1999). Determination of an optimal axial-length tension for the study of isolated resistance arteries on a pressure myograph. *Exp Physiol* **84:** 1085-94.

Coleman RA, Grix SP, Head SA, Louttit JB, Mallett A & Sheldrick RL (1994a). A novel inhibitory prostanoid receptor in piglet saphenous vein. *Prostaglandins* **47:** 151-68.

Coleman RA, Humphrey PP, Kennedy I, Levy GP & Lumley P (1981). Comparison of the actions of U-46619, a prostaglandin H_2-analogue, with those of prostaglandin H_2 and thromboxane A_2 on some isolated smooth muscle preparations. *Br J Pharmacol* **73:** 773-8.

Coleman RA & Kennedy I (1985). Characterization of the prostanoid receptors mediating contraction of guinea-pig isolated trachea. *Prostaglandins* **29:** 363-75.

Coleman RA, Smith WL & Narumiya S (1994b). International Union of Pharmacology classification of prostanoid receptors: properties, distribution, and structure of the receptors and their subtypes. *Pharmacol Rev* **46:** 205-29.

Colquhoun D, Henderson R & Ritchie JM (1972). The binding of labelled tetrodotoxin to non-myelinated nerve fibres. *J Physiol* **227:** 95-126.

Colquhoun D & Ritchie JM (1972). The kinetics of the interaction between tetrodotoxin and mammalian nonmyelinated nerve fibers. *Mol Pharmacol* **8:** 285-92.

Craig DA (1993). The Cheng-Prusoff relationship: something lost in the translation. *Trends Pharmacol Sci* **14:** 89-91.

Crowston JG, Lindsey JD, Aihara M & Weinreb RN (2004). Effect of latanoprost on intraocular pressure in mice lacking the prostaglandin FP receptor. *Invest Ophthalmol Vis Sci* **45:** 3555-9.

Dai FX, Diederich A, Skopec J & Diederich D (1993). Diabetes-induced endothelial dysfunction in streptozotocin-treated rats: role of prostaglandin endoperoxides and free radicals. *J Am Soc Nephrol* **4:** 1327-36.

Daray FM, Minvielle AI, Puppo S & Rothlin RP (2003). Pharmacological Characterization of prostanoid receptors mediating vasoconstriction in human umbilical vein. *Br J Pharmacol* **139:** 1409-16.

Daray FM, Minvielle AI, Puppo S & Rothlin RP (2004). Vasoconstrictor effects of 8-iso-prostaglandin E_2 and 8-iso-prostaglandin $F_{2\alpha}$ on human umbilical vein. *Eur J Pharmacol* **499:** 189-95.

Davi G, Ciabattoni G, Consoli A, Mezzetti A, Falco A, Santarone S *et al.* (1999). *In vivo* formation of 8-iso-prostaglandin $F_{2\alpha}$ and platelet activation in diabetes mellitus: effects of improved metabolic control and vitamin E supplementation. *Circulation* **99:** 224-9.

de Groat WC & Yoshimura N (2001). Pharmacology of the lower urinary tract. *Annu Rev Pharmacol Toxicol* **41:** 691-721.

De Mey JG & Vanhoutte,PM (1981). Role of the intima in cholinergic and purinergic relaxation of isolated canine femoral arteries. *J Physiol* **316:** 347-55.

De Vriese AS, Verbeuren TJ, Van de Voorde J, Lameire NH & Vanhoutte PM (2000). Endothelial dysfunction in diabetes. *Br J Pharmacol* **130:** 963-74.

Dogne JM, Hanson J & Pratico D (2005). Thromboxane, prostacyclin and isoprostanes: therapeutic targets in atherogenesis. *Trends Pharmacol Sci* **26:** 639-44.

Dong YJ, Jones RL & Wilson NH (1986). Prostaglandin E receptor subtypes in smooth muscle: agonist activities of stable prostacyclin analogues. *Br J Pharmacol* **87:** 97-107.

Dorn GW, 2nd Becker MW & Davis MG (1992). Dissociation of the contractile and hypertrophic effects of vasoconstrictor prostanoids in vascular smooth muscle. *J Biol Chem* **267:** 24897-905.

Ducharme DW, Weeks JR & Montgomery RG (1968). Studies on the mechanism of the hypertensive effect of prostaglandin $F_{2\alpha}$. *J Pharmacol Exp Ther* **160:** 1-10.

Dustan HP, Tarazi RC & Bravo EL (1972). Physiologic characteristics of hypertension. *Am J Med* **52:** 610-22.

Edwards G, Dora KA, Gardener MJ, Garland CJ & Weston AH (1998). K^+ is an endothelium-derived hyperpolarizing factor in rat arteries. *Nature* **396:** 269-72.

Eglen RM & Whiting RL (1988). The action of prostanoid receptor agonists and antagonists on smooth muscle and platelets. *Br J Pharmacol* **94:** 591-601.

Elmhurst JL, Betti PA & Rangachari PK (1997). Intestinal effects of isoprostanes: evidence for the involvement of prostanoid EP and TP receptors. *J Pharmacol Exp Ther* **282:** 1198-205.

Errasti AE, Luciani LI, Cesio CE, Tramontano J, Boveris D, Daray FM *et al.* (2007). Potentiation of adrenaline vasoconstrictor response by sub-threshold concentrations of U-46619 in human umbilical vein: involvement of smooth muscle prostanoid TP_{α} receptor isoform. *Eur J Pharmacol* **562:** 227-35.

Ezzati M, Lopez AD, Rodgers A, Vander Hoorn S & Murray CJ (2002). Selected major risk factors and global and regional burden of disease. *Lancet* **360:** 1347-60.

Farber HW & Loscalzo J (2004). Pulmonary arterial hypertension. *N Engl J Med* **351:** 1655-65.

Farmer JB, Farrar DG & Wilson J (1974). Antagonism of tone and prostaglandin-mediated responses in a tracheal preparation by indomethacin and SC-19220. *Br J Pharmacol* **52:** 559-65.

Feoktistov I, Breyer RM & Biaggioni I (1997). Prostanoid receptor with a novel pharmacological profile in human erythroleukemia cells. *Biochem Pharmacol* **54:** 917-26.

Fortes ZB, Garcia Leme J & Scivoletto R (1983). Vascular reactivity in diabetes mellitus: role of the endothelial cell. *Br J Pharmacol* **79:** 771-81.

Fujino T, Nakagawa N, Yuhki K, Hara A, Yamada T, Takayama K *et al.* (2004). Decreased susceptibility to renovascular hypertension in mice lacking the prostaglandin I_2 receptor IP. *J Clin Invest* **114:** 805-12.

Fukunaga M, Makita N, Roberts LJ, 2nd, Morrow JD, Takahashi K & Badr KF (1993). Evidence for the existence of F_2-isoprostane receptors on rat vascular smooth muscle cells. *Am J Physiol* **264:** C1619-24.

Fukunaga M, Yura T, Grygorczyk R & Badr KF (1997). Evidence for the distinct nature of F_2-isoprostane receptors from those of thromboxane A_2. *Am J Physiol* **272:** F477-83.

Funk CD, Furci L, FitzGerald GA, Grygorczyk R, Rochette C, Bayne MA *et al.* (1993). Cloning and expression of a cDNA for the human prostaglandin E receptor EP_1 subtype. *J Biol Chem* **268:** 26767-72.

Furchgott RF (1983). Role of endothelium in responses of vascular smooth muscle. *Circ Res* **53:** 557-73.

Furchgott RF & Zawadzki JV (1980). The obligatory role of endothelial cells in the relaxation of arterial smooth muscle by acetylcholine. *Nature* **288:** 373-6.

Furman BL & Sneddon P (1993). Endothelium-dependent vasodilator responses of the isolated mesenteric bed are preserved in long-term streptozotocin diabetic rats. *Eur J Pharmacol* **232:** 29-34.

Gabella G & Uvelius B (1990). Urinary bladder of rat: fine structure of normal and hypertrophic musculature. *Cell Tissue Res* **262:** 67-79.

Gale EA (2001). The discovery of type 1 diabetes. *Diabetes* **50:** 217-26.

Garcia-Redondo AB, Briones AM, Beltran AE, Alonso MJ, Simonsen U & Salaices M (2009). Hypertension increases contractile responses to hydrogen peroxide in resistance arteries through increased thromboxane A_2, Ca^{2+}, and superoxide anion levels. *J Pharmacol Exp Ther* **328:** 19-27.

Gardiner PJ (1986). Characterization of prostanoid relaxant / inhibitory receptors (*psi*) using a highly selective agonist, TR4979. *Br J Pharmacol* **87:** 45-56.

Ge T, Hughes H, Junquero DC, Wu KK, Vanhoutte PM & Boulanger CM (1995). Endothelium-dependent contractions are associated with both augmented expression of prostaglandin H synthase-1 and hypersensitivity to prostaglandin H_2 in the SHR aorta. *Circ Res* **76:** 1003-10.

Giblin GM, Bit RA, Brown SH, Chaignot HM, Chowdhury A, Chessell IP *et al.* (2007). The discovery of 6-[2-(5-chloro-2-{[(2,4-difluorophenyl)methyl]oxy}phenyl)-1-cyclopenten-1-yl]-2-pyridinecarboxylic acid, GW-848687X, a potent and selective prostaglandin EP_1 receptor antagonist for the treatment of inflammatory pain. *Bioorg Med Chem Lett* **17:** 385-9.

Giles H, Leff P, Bolofo ML, Kelly MG & Robertson AD (1989). The classification of prostaglandin DP-receptors in platelets and vasculature using BW-A868C, a novel, selective and potent competitive antagonist. *Br J Pharmacol* **96:** 291-300.

Glass GV & Hopkins KD (1996). Multiple comparisons and trend analysis, in: *Statistical methods in education and psychology*. Boston, Mass. ; London: Allyn and Bacon pp 444-481.

Gong M & Hubner N (2006). Molecular genetics of human hypertension. *Clin Sci (Lond)* **110:** 315-26.

Goto Y, Kakizaki M & Masaki N (1976). Production of spontaneous diabetic rats by repetition of selective breeding. *Tohoku J Exp Med* **119:** 85-90.

Graves J & Poston L (1993). Beta-adrenoceptor agonist mediated relaxation of rat isolated resistance arteries: a role for the endothelium and nitric oxide. *Br J Pharmacol* **108:** 631-7.

Hansen TR & Bohr DF (1975). Hypertension, transmural pressure, and vascular smooth muscle response in rats. *Circ Res* **36:** 590-8.

Harris KH & MacLeod KM (1988). Influence of the endothelium on contractile responses of arteries from diabetic rats. *Eur J Pharmacol* **153:** 55-64.

Harrison HE, Reece AH & Johnson M (1978). Decreased vascular prostacyclin in experimental diabetes. *Life Sci* **23:** 351-5.

Hata AN & Breyer RM (2004). Pharmacology and signaling of prostaglandin receptors: multiple roles in inflammation and immune modulation. *Pharmacol Ther* **103:** 147-66.

Heptinstall S, Espinosa DI, Manolopoulos P, Glenn JR, White AE, Johnson A *et al.* (2008). DG-041 inhibits the EP_3 prostanoid receptor - a new target for inhibition of platelet function in atherothrombotic disease. *Platelets* **19:** 605-13.

Hirai H, Tanaka K, Yoshie O, Ogawa K, Kenmotsu K, Takamori Y *et al.* (2001). Prostaglandin D_2 selectively induces chemotaxis in T helper type 2 cells, eosinophils, and basophils via seven-transmembrane receptor $CRTh_2$. *J Exp Med* **193:** 255-61.

Hirata M, Hayashi Y, Ushikubi F, Yokota Y, Kageyama R, Nakanishi S *et al.* (1991). Cloning and expression of cDNA for a human thromboxane A_2 receptor. *Nature* **349:** 617-20.

Holloway ET & Bohr DF (1973). Reactivity of vascular smooth muscle in hypertensive rats. *Circ Res* **33:** 678-85.

Honda A, Sugimoto Y, Namba T, Watabe A, Irie A, Negishi M *et al.* (1993). Cloning and expression of a cDNA for mouse prostaglandin E receptor EP_2 subtype. *J Biol Chem* **268:** 7759-62.

Hornby EJ, Foster MR, McCabe PJ & Stratton LE (1989). The inhibitory effect of GR-32191, a thromboxane receptor blocking drug, on human platelet aggregation, adhesion and secretion. *Thromb Haemost* **61:** 429-36.

Hung GH, Jones RL, Lam FF, Chan KM, Hidaka H, Suzuki M *et al.* (2006). Investigation of the pronounced synergism between prostaglandin E_2 and other constrictor agents on rat femoral artery. *Prostaglandins Leukot Essent Fatty Acids* **74:** 401-15.

Hutri-Kahonen N, Kahonen M, Jolma P, Wu X, Sand J, Nordback I *et al.* (1999). Control of mesenteric arterial tone in vitro in humans and rats. *Naunyn Schmiedebergs Arch Pharmacol* **359:** 322-30.

Ishizuka O, Mattiasson A & Andersson KE (1995). Prostaglandin E_2-induced bladder hyperactivity in normal, conscious rats: involvement of tachykinins? *J Urol* **153:** 2034-8.

Jadhav V, Jabre A, Lin SZ & Lee TJ (2004). EP_1- and EP_3-receptors mediate prostaglandin E_2-induced constriction of porcine large cerebral arteries. *J Cereb Blood Flow Metab* **24:** 1305-16.

Janssen LJ & Tazzeo T (2002). Involvement of TP and EP_3 receptors in vasoconstrictor responses to isoprostanes in pulmonary vasculature. *J Pharmacol Exp Ther* **301:** 1060-6.

Jarajapu YP, Hillier C & MacDonald A (2001). The α_{1A}-adrenoceptor subtype mediates contraction in rat femoral resistance arteries. *Eur J Pharmacol* **422:** 127-35.

Jensen BL, Mann B, Skott O & Kurtz A (1999). Differential regulation of renal prostaglandin receptor mRNAs by dietary salt intake in the rat. *Kidney Int* **56:** 528-37.

Jensen, BL, Stubbe, J, Hansen, PB, Andreasen, D & Skott, O (2001). Localization of prostaglandin E_2, EP_2 and EP_4 receptors in the rat kidney. *Am J Physiol Renal Physiol* **280:** F1001-9.

Jeremy JY, Mikhailidis DP & Dandona P (1984). The rat urinary bladder produces prostacyclin as well as other prostaglandins. *Prostaglandins Leukot Med* **16:** 235-48.

Jones R, Woodward D, Wang J (2008). Investigation of the slow kineticsof the prostanoid EP_3 receptor antagonists L-798106 and L-826266 on guinea-pig aorta. *Fundam Clin Pharmacol* **22** (Suppl. 2):P078

Jones RL (2004). An update on ligands for prostanoid receptors. *Sigma-RBI Newsletter for Cell Signallng and Neurosci Res* **20**: 1–9. http://www.sigmaaldrich.com/sigma/general %20information/prostanoidreceptors.pdf.

Jones RL & Chan K (2001). Distinction between relaxations induced via prostanoid EP_4 and IP_1 receptors in pig and rabbit blood vessels. *Br J Pharmacol* **134:** 313-24.

Jones RL & Chan KM (2005). nvestigation of the agonist activity of prostacyclin analogues on prostanoid EP_4 receptors using GW-627368 and taprostene: evidence for species differences. *Prostaglandins Leukot Essent Fatty Acids* **72:** 289-99.

Jones RL, Giembycz MA & Woodward DF (2009). Prostanoid receptor antagonists: development strategies and therapeutic applications. *Br J Pharmacol*.

Jones RL, Peesapati V & Wilson NH (1982). Antagonism of the thromboxane-sensitive contractile systems of the rabbit aorta, dog saphenous vein and guinea-pig trachea. *Br J Pharmacol* **76:** 423-38.

Jones RL, Qian YM, Chan KM & Yim AP (1998). Characterization of a prostanoid EP_3-receptor in guinea-pig aorta: partial agonist action of the non-prostanoid ONO-AP-324. *Br J Pharmacol* **125:** 1288-96.

Jugus M, Jaworski JP, Patra P, Jin J, Morrow DM, Laping NJ, *et al.* (2009). Dual modulation of urinary bladder activity and urine flow by prostanoid EP receptors in the conscious rat. *Br J Pharmacol*.

Junod A, Lambert AE, Stauffacher W & Renold AE (1969). Diabetogenic action of streptozotocin: relationship of dose to metabolic response. *J Clin Invest* **48:** 2129-39.

Juteau H, Gareau Y, Labelle M, Sturino CF, Sawyer N, Tremblay N, *et al.* (2001). Structure-activity relationship of cinnamic acylsulfonamide analogues on the human EP_3 prostanoid receptor. *Bioorg Med Chem* **9:** 1977-84.

Karim SM, Adaikan PG & Kottegoda SR (1980). Prostaglandins and human respiratory tract smooth muscle: structure activity relationship. *Adv Prostaglandin Thromboxane Res* **7:** 969-80.

Kasakov LN & Vlaskovska MV (1985). Profile of prostaglandins generated in the detrusor muscle of rat urinary bladder: effects of adenosine triphosphate and adenosine. *Eur J Pharmacol* **113:** 431-6.

Keery RJ & Lumley P (1988). AH6809, a prostaglandin DP-receptor blocking drug on human platelets. *Br J Pharmacol* **94:** 745-54.

Kenakin T, Jenkinson S & Watson C (2006). Determining the potency and molecular mechanism of action of insurmountable antagonists. *J Pharmacol Exp Ther* **319:** 710-23.

Kennedy CR, Zhang Y, Brandon S, Guan Y, Coffee K, Funk CD *et al.* (1999). Salt-sensitive hypertension and reduced fertility in mice lacking the prostaglandin EP_2 receptor. *Nat Med* **5:** 217-20.

Kennedy I, Coleman RA, Humphrey PP, Levy GP & Lumley P (1982). Studies on the Characterization of prostanoid receptors: a proposed classification. *Prostaglandins* **24:** 667-89.

Khan MA, Thompson CS, Mumtaz FH, Jeremy JY, Morgan RJ & Mikhailidis DP (1998). Role of prostaglandins in the urinary bladder: an update. *Prostaglandins Leukot Essent Fatty Acids* **59:** 415-22.

Kimura M, Osumi S & Ogihara M (2001). Prostaglandin E_2 EP_1 receptor agonist-induced DNA synthesis and proliferation in primary cultures of adult rat hepatocytes: the involvement of TGF_{α}. *Endocrinology* **142:** 4428-40.

Kiriyama M, Ushikubi F, Kobayashi T, Hirata M, Sugimoto Y & Narumiya S (1997). Ligand binding specificities of the eight types and subtypes of the mouse prostanoid receptors expressed in Chinese hamster ovary cells. *Br J Pharmacol* **122:** 217-24.

Kobayashi T, Tahara Y, Matsumoto M, Iguchi M, Sano H, Murayama T *et al.* (2004). Roles of thromboxane A_2 and prostacyclin in the development of atherosclerosis in apoE-deficient mice. *J Clin Invest* **114:** 784-94.

Korner PI & Angus JA (1997). Vascular remodeling. *Hypertension* **29:** 1065-6.

Lawrence RA, Jones RL & Wilson NH (1992). Characterization of receptors involved in the direct and indirect actions of prostaglandins E and I on the guinea-pig ileum. *Br J Pharmacol* **105:** 271-8.

Lazareno S & Birdsall NJ (1993a). Estimation of antagonist K_b from inhibition curves in functional experiments: alternatives to the Cheng-Prusoff equation. *Trends Pharmacol Sci* **14:** 237-9.

Lazareno S & Birdsall NJ (1993b). Estimation of competitive antagonist affinity from functional inhibition curves using the Gaddum, Schild and Cheng-Prusoff equations. *Br J Pharmacol* **109:** 1110-9.

Lee T, Hedlund P, Newgreen D & Andersson KE (2007). Urodynamic effects of a novel EP_1 receptor antagonist in normal rats and rats with bladder outlet obstruction. *J Urol* **177:** 1562-7.

Lee TJ (1982). Cholinergic mechanism in the large cat cerebral artery. *Circ Res* **50:** 870-9.

Leff P & Dougall IG (1993). Further concerns over Cheng-Prusoff analysis. *Trends Pharmacol Sci* **14:** 110-2.

Lydford SJ & McKechnie K (1994). Characterization of the prostaglandin E_2 sensitive (EP)-receptor in the rat isolated trachea. *Br J Pharmacol* **112:** 133-6.

Lydford SJ, McKechnie KC & Leff P (1996). Interaction of BW-A868C, a prostanoid DP-receptor antagonist, with two receptor subtypes in the rabbit isolated saphenous vein. *Prostaglandins* **52:** 125-39.

Ma H, Hara A, Xiao CY, Okada Y, Takahata O, Nakaya K *et al.* (2001). Increased bleeding tendency and decreased susceptibility to thromboembolism in mice lacking the prostaglandin E receptor subtype EP_3. *Circulation* **104:** 1176-80.

Maggi CA, Giuliani S, Patacchini R, Conte B, Furio M, Santicioli P *et al.* (1988). The effect of SC-19220, a prostaglandin antagonist, on the micturition reflex in rats. *Eur J Pharmacol* **152:** 273-9.

Martin W, Furchgott RF, Villani GM & Jothianandan D (1986). Depression of contractile responses in rat aorta by spontaneously released endothelium-derived relaxing factor. *J Pharmacol Exp Ther* **237:** 529-38.

Massett MP, Lewis SJ, Bates JN & Kregel KC (1998). Effect of heating on vascular reactivity in rat mesenteric arteries. *J Appl Physiol* **85:** 701-8.

Mathiassen ON, Buus NH, Sihm I, Thybo NK, Morn B, Schroeder AP *et al.* (2007). Small artery structure is an independent predictor of cardiovascular events in essential hypertension. *J Hypertens* **25:** 1021-6.

Matias I, Chen J, De Petrocellis L, Bisogno T, Ligresti A, Fezza F *et al.* (2004). Prostaglandin ethanolamides (prostamides): in vitro pharmacology and metabolism. *J Pharmacol Exp Ther* **309:** 745-57.

Matoba T, Shimokawa H, Nakashima M, Hirakawa Y, Mukai Y, Hirano K *et al.* (2000). Hydrogen peroxide is an endothelium-derived hyperpolarizing factor in mice. *J Clin Invest* **106:** 1521-30.

Matsuoka T, Hirata M, Tanaka H, Takahashi Y, Murata T, Kabashima K *et al.* (2000). Prostaglandin D_2 as a mediator of allergic asthma. *Science* **287:** 2013-7.

Matthews JS & Jones RL (1993). Potentiation of aggregation and inhibition of adenylate cyclase in human platelets by prostaglandin E analogues. *Br J Pharmacol* **108:** 363-9.

McCafferty GP, Misajet BA, Laping NJ, Edwards RM & Thorneloe KS (2008). Enhanced bladder capacity and reduced prostaglandin E_2-mediated bladder hyperactivity in EP_3 receptor knockout mice. *Am J Physiol Renal Physiol* **295:** F507-14.

McIntyre CA, Williams BC, Lindsay RM, McKnight JA & Hadoke PW (1998). Preservation of vascular function in rat mesenteric resistance arteries following cold storage, studied by small vessel myography. *Br J Pharmacol* **123:** 1555-60.

McKenniff M, Rodger IW, Norman P & Gardiner PJ (1988). Characterization of receptors mediating the contractile effects of prostanoids in guinea-pig and human airways. *Eur J Pharmacol* **153:** 149-59.

Miggin SM, Lawler OA & Kinsella BT (2002). Investigation of a functional requirement for isoprenylation by the human prostacyclin receptor. *Eur J Biochem* **269:** 1714-25.

Miura A, Kawatani M, Maruyama T & de Groat WC (2002). Effect of prostaglandins on parasympathetic neurons in the rat lumbosacral spinal cord. *Neuroreport* **13:** 1557-62.

Morinelli TA, Tempel GE, Jaffa AA, Silva RH, Naka M, Folger W *et al.* (1993). Thromboxane A_2 / prostaglandin H_2 receptors in streptozotocin-induced diabetes: effects of insulin therapy in the rat. *Prostaglandins* **45:** 427-38.

Motulsky H & Christopoulos A (2004). Comparison models using the extra sum-of-squares F test, in: *Fitting models to biological data using linear and nonlinear regression : a practical guide to curve fitting*. Oxford: Oxford University Press pp 138 - 142.

Mukherjee D, Nissen SE & Topol EJ (2001). Risk of cardiovascular events associated with selective COX-2 inhibitors. *Jama* **286:** 954-9.

Mulhern M & Docherty JR (1989). Effects of experimental diabetes on the responsiveness of rat aorta. *Br J Pharmacol* **97:** 1007-12.

Mulvany MJ & Halpern W (1977). Contractile properties of small arterial resistance vessels in spontaneously hypertensive and normotensive rats. *Circ Res* **41:** 19-26.

Murata T, Ushikubi F, Matsuoka T, Hirata M, Yamasaki A, Sugimoto Y *et al.* (1997). Altered pain perception and inflammatory response in mice lacking prostacyclin receptor. *Nature* **388:** 678-82.

Nagata K, Tanaka K, Ogawa K, Kemmotsu K, Imai T, Yoshie O *et al.* (1999). Selective expression of a novel surface molecule by human Th2 cells in vivo. *J Immunol* **162:** 1278-86.

Nakane T, Itoh N & Chiba S (1986). Responses of isolated and perfused dog coronary arteries to acetylcholine, norepinephrine, KCl, and diltiazem before and after removal of the endothelial cells by saponin. *Heart Vessels* **2:** 221-7.

Narumiya S, Sugimoto Y & Ushikubi F (1999). Prostanoid receptors: structures, properties, and functions. *Physiol Rev* **79:** 1193-226.

Nasrallah R & Hebert RL (2005). Prostacyclin signaling in the kidney: implications for health and disease. *Am J Physiol Renal Physiol* **289:** F235-46.

Nasrallah R & Hebert RL (2004). Reduced IP receptors in STZ-induced diabetic rat kidneys and high-glucose-treated mesangial cells. *Am J Physiol Renal Physiol* **287:** F673-81.

Ndukwu IM, White SR, Leff AR & Mitchell RW (1997). EP_1 receptor blockade attenuates both spontaneous tone and PGE_2-elicited contraction in guinea-pig trachealis. *Am J Physiol* **273:** L626-33.

Negishi M, Sugimoto Y & Ichikawa A (1995). Molecular mechanisms of diverse actions of prostanoid receptors. *Biochim Biophys Acta* **1259:** 109-19.

Neubig RR, Spedding M, Kenakin T & Christopoulos A (2003). International Union of Pharmacology Committee on Receptor Nomenclature and Drug Classification. XXXVIII. Update on terms and symbols in quantitative pharmacology. *Pharmacol Rev* **55:** 597-606.

Nguyen M, Camenisch T, Snouwaert JN, Hicks E, Coffman TM, Anderson PA *et al.* (1997). The prostaglandin receptor EP_4 triggers remodelling of the cardiovascular system at birth. *Nature* **390:** 78-81.

Nilsson SF, Drecoll E, Lutjen-Drecoll E, Toris C B, Krauss A. H, Kharlamb A *et al.* (2006). The prostanoid EP_2 receptor agonist butaprost increases uveoscleral outflow in the cynomolgus monkey. *Invest Ophthalmol Vis Sci* **47:** 4042-9.

Norel X, de Montpreville V & Brink C (2004). Vasoconstriction induced by activation of EP_1 and EP_3 receptors in human lung: effects of ONO-AE-248, ONO-DI-004, ONO-8711 or ONO-8713. *Prostaglandins Other Lipid Mediat* **74:** 101-12.

Ogletree ML, Harris DN, Schumacher WA, Webb ML & Misra RN (1993). Pharmacological profile of BMS-180291: a potent, long-acting, orally active thromboxane A_2 / prostaglandin endoperoxide receptor antagonist. *J Pharmacol Exp Ther* **264:** 570-8.

Okada Y, Hara A, Ma H, Xiao CY, Takahata O, Kohgo Y *et al.* (2000). Characterization of prostanoid receptors mediating contraction of the gastric fundus and ileum: studies using mice deficient in prostanoid receptors. *Br J Pharmacol* **131:** 745-55.

Okamoto T, Kanemoto N, Ohbuchi Y, Okano M, Fukui H & Sudo T (2008). Characterization of STZ-Induced Type 2 Diabetes in Zucker Fatty Rats. *Exp Anim* **57:** 335-45.

Olschewski H, Rose F, Grunig E, Ghofrani HA, Walmrath D, Schulz R *et al.* (2001). Cellular pathophysiology and therapy of pulmonary hypertension. *J Lab Clin Med* **138:** 367-77.

Ota T, Aihara M, Saeki T, Narumiya S & Araie M (2007). The IOP-lowering effects and mechanism of action of tafluprost in prostanoid receptor-deficient mice. *Br J Ophthalmol* **91:** 673-6.

Owen MP & Carrier GO (1980). Calcium dependence of norepinephrine-induced vascular contraction in experimental diabetes. *J Pharmacol Exp Ther* **212:** 253-8.

Paller MS & Manivel JC (1992). Prostaglandins protect kidneys against ischemic and toxic injury by a cellular effect. *Kidney Int* **42:** 1345-54.

Paralkar VM, Borovecki F, Ke HZ, Cameron KO, Lefker B, Grasser WA *et al.* (2003). An EP_2 receptor-selective prostaglandin E_2 agonist induces bone healing. *Proc Natl Acad Sci U S A* **100:** 6736-40.

Park JM, Yang T, Arend LJ, Schnermann JB, Peters CA, Freeman MR *et al.* (1999). Obstruction stimulates COX-2 expression in bladder smooth muscle cells via increased mechanical stretch. *Am J Physiol* **276:** F129-36.

Peredo HA (2001). Prostanoid release and constrictor responses to noradrenaline in the rat mesenteric vascular bed in non-insulin-dependent diabetes mellitus. *J Auton Pharmacol* **21:** 131-7.

Peredo HA, Feleder EC & Adler-Graschinsky E (1999). Time-course of the alterations in prostanoid production and in contractile responses of mesenteric beds isolated from streptozotocin diabetic rats. *Prostaglandins Leukot Essent Fatty Acids* **60:** 269-74.

Pfaffman MA, Ball CR, Darby A & Hilman R (1982). Insulin reversal of diabetes-induced inhibition of vascular contractility in the rat. *Am J Physiol* **242:** H490-5.

Poeschmann RP, Doesburg WH & Eskes TK (1991). A randomized comparison of oxytocin, sulprostone and placebo in the management of the third stage of labour. *Br J Obstet Gynaecol* **98:** 528-30.

Poli E, Macaluso G & Pozzoli C (1992). Actions of two novel prostaglandin analogs, SC-29169 and SC-31391, on guinea pig and human isolated urinary bladder. *Gen Pharmacol* **23:** 805-9.

Poyser NL (1995). The control of prostaglandin production by the endometrium in relation to luteolysis and menstruation. *Prostaglandins Leukot Essent Fatty Acids* **53:** 147-95.

Prasanna G, Fortner J, Xiang C, Zhang E, Carreiro S, Anderson S *et al.* (2009). Ocular pharmacokinetics and hypotensive activity of PF-04475270, an EP_4 prostaglandin agonist in preclinical models. *Exp Eye Res*.

Qian YM, Jones RL, Chan KM, Stock AI & Ho JK (1994). Potent contractile actions of prostanoid EP_3-receptor agonists on human isolated pulmonary artery. *Br J Pharmacol* **113:** 369-74.

Raychowdhury MK, Yukawa M, Collins LJ, McGrail SH, Kent KC & Ware JA (1994). Alternative splicing produces a divergent cytoplasmic tail in the human endothelial thromboxane A_2 receptor. *J Biol Chem* **269:** 19256-61.

Regan JW, Bailey TJ, Pepperl DJ, Pierce KL, Bogardus AM, Donello JE *et al.* (1994). Cloning of a novel human prostaglandin receptor with characteristics of the pharmacologically defined EP_2 subtype. *Mol Pharmacol* **46:** 213-20.

Roberts LJ, 2nd & Morrow JD (1995). The isoprostanes: novel markers of lipid peroxidation and potential mediators of oxidant injury. *Adv Prostaglandin Thromboxane Leukot Res* **23:** 219-24.

Ross R (1999). Atherosclerosis is an inflammatory disease. *Am Heart J* **138:** S419-20.

Samata K, Kimura T, Satoh S & Watanabe H (1986). Chemical removal of the endothelium by saponin in the isolated dog femoral artery. *Eur J Pharmacol* **128:** 85-91.

Sametz W, Hennerbichler S, Glaser S, Wintersteiger R & Juan H (2000a). Characterization of prostanoid receptors mediating actions of the isoprostanes, 8-iso-PGE_2 and 8-iso-$PGF_{2\alpha}$, in some isolated smooth muscle preparations. *Br J Pharmacol* **130:** 1903-10.

Sametz W, Hummer K, Butter M, Wintersteiger R & Juan H (2000b). Formation of 8-iso-$PGF_{2\alpha}$ and thromboxane A_2 by stimulation with several activators of phospholipase A_2 in the isolated human umbilical vein. *Br J Pharmacol* **131:** 145-51.

Sanner JH (1969). Antagonism of prostaglandin E_2 by 1-acetyl-2-(8-chloro-10,11-dihydrodibenz (b,f) (1,4) oxazepine-10-carbonyl) hydrazine (SC-19220). *Arch Int Pharmacodyn Ther* **180:** 46-56.

Schalkwijk CG & Stehouwer CD (2005). Vascular complications in diabetes mellitus: the role of endothelial dysfunction. *Clin Sci (Lond)* **109:** 143-59.

Schlemper V, Medeiros R, Ferreira J, Campos MM & Calixto JB (2005). Mechanisms underlying the relaxation response induced by bradykinin in the epithelium-intact guinea-pig trachea in vitro. In *Br J Pharmacol*. pp. 740-50.

Schneider T, Hein P & Michel MC (2004). Signal transduction underlying carbachol-induced contraction of rat urinary bladder. I. Phospholipases and Ca^{2+} sources. *J Pharmacol Exp Ther* **308:** 47-53.

Schofield I, Malik R, Izzard A, Austin C & Heagerty A (2002). Vascular structural and functional changes in type 2 diabetes mellitus: evidence for the roles of abnormal myogenic responsiveness and dyslipidemia. *Circulation* **106:** 3037-43.

Scholz H (2003). Prostaglandins. *Am J Physiol Regul Integr Comp Physiol* **285:** R512-4.

Schroder A, Newgreen D & Andersson KE (2004). Detrusor responses to prostaglandin E_2 and bladder outlet obstruction in wild-type and EP_1 receptor knockout mice. *J Urol* **172:** 1166-70.

Schroder A, Uvelius B, Newgreen D & Andersson KE (2003). Bladder overactivity in mice after 1 week of outlet obstruction. Mainly afferent dysfunction? *J Urol* **170:** 1017-21.

Schussler B (1990). Comparison of the mode of action of prostaglandin E_2 (PGE_2) and sulprostone, a PGE_2-derivative, on the lower urinary tract in healthy women. A urodynamic study. *Urol Res* **18:** 349-52.

Segi E, Sugimoto Y, Yamasaki A, Aze Y, Oida H, Nishimura T, *et al.* (1998). Patent ductus arteriosus and neonatal death in prostaglandin receptor EP_4-deficient mice. *Biochem Biophys Res Commun* **246:** 7-12.

Sharif NA, Kelly CR & Williams GW (2003). Bimatoprost (Lumigan®) is an agonist at the cloned human ocular FP prostaglandin receptor: real-time FLIPR-based intracellular Ca^{2+} mobilization studies. *Prostaglandins Leukot Essent Fatty Acids* **68:** 27-33.

Shi Y, Feletou M, Ku DD, Man RY & Vanhoutte PM (2007a). The calcium ionophore A-23187 induces endothelium-dependent contractions in femoral arteries from rats with streptozotocin-induced diabetes. *Br J Pharmacol* **150:** 624-32.

Shi Y, Ku DD, Man, RY & Vanhoutte PM (2006). Augmented endothelium-derived hyperpolarizing factor-mediated relaxations attenuate endothelial dysfunction in femoral and mesenteric, but not in carotid arteries from type I diabetic rats. *J Pharmacol Exp Ther* **318:** 276-81.

Shi Y, So KF, Man RY & Vanhoutte PM (2007b). Oxygen-derived free radicals mediate endothelium-dependent contractions in femoral arteries of rats with streptozotocin-induced diabetes. *Br J Pharmacol* **152:** 1033-41.

Shi Y & Vanhoutte PM (2008). Oxidative stress and COX cause hyper-responsiveness in vascular smooth muscle of the femoral artery from diabetic rats. *Br J Pharmacol* **154:** 639-51.

Silverstein FE, Faich G, Goldstein JL, Simon LS, Pincus T, Whelton, A *et al.* (2000). Gastrointestinal toxicity with celecoxib vs nonsteroidal anti-inflammatory drugs for osteoarthritis and rheumatoid arthritis: the CLASS study: A randomized controlled trial. Celecoxib Long-term Arthritis Safety Study. *Jama* **284:** 1247-55.

Smith GC (1998). The pharmacology of the ductus arteriosus. *Pharmacol Rev* **50:** 35-58.

Smith GC, Coleman RA & McGrath JC (1994). Characterization of dilator prostanoid receptors in the fetal rabbit ductus arteriosus. *J Pharmacol Exp Ther* **271:** 390-6.

Soma M, Izumi Y, Watanabe Y & Kanmatsuse K (1996). A nitric oxide synthesis inhibitor decreased prostaglandin production in rat mesenteric vasculature. *Prostaglandins* **51:** 225-32.

Sotnikova R, Skalska S, Okruhlicova L, Navarova J, Kyselova Z, Zurova J *et al.* (2006). Changes in the function and ultrastructure of vessels in the rat model of multiple low dose streptozotocin-induced diabetes. *Gen Physiol Biophys* **25:** 289-302.

Spicuzza L, Giembycz MA, Barnes PJ & Belvisi MG (1998). Prostaglandin E_2 suppression of acetylcholine release from parasympathetic nerves innervating guinea-pig trachea by interacting with prostanoid receptors of the EP_3-subtype. *Br J Pharmacol* **123:** 1246-52.

Sterin-Borda LJ, Franchi AM, Borda ES, del Castillo E, Gimeno MF & Gimeno AL (1984). Prostacyclin, its fatty acid precursor and its metabolites on the inotropic function of and on the prostanoid generation by diabetic arteries. *Biomed Biochim Acta* **43:** S257-64.

Stock A, Jones R, Chung T & Fung HY (1995). Pulmonary edema in association with an intravenous infusion of sulprostone. *Acta Obstet Gynecol Scand* **74:** 156-8.

Su X, Lashinger ES, Leon LA, Hoffman BE, Hieble JP, Gardner SD *et al.* (2008). An excitatory role for peripheral EP_3 receptors in bladder afferent function. *Am J Physiol Renal Physiol* **295:** F585-94.

Sugimoto Y, Hasumoto K, Namba T, Irie A, Katsuyama M, Negishi M *et al.* (1994). Cloning and expression of a cDNA for mouse prostaglandin F receptor. *J Biol Chem* **269:** 1356-60.

Sugiyama H, Kashihara N, Makino H, Yamasaki Y & Ota A (1996). Apoptosis in glomerular sclerosis. *Kidney Int* **49:** 103-11.

Suzawa,T, Miyaura C, Inada M, Maruyama T, Sugimoto Y, Ushikubi F *et al.* (2000). The role of prostaglandin E receptor subtypes (EP_1, EP_2, EP_3, and EP_4) in bone resorption: an analysis using specific agonists for the respective EPs. *Endocrinology* **141:** 1554-9.

Szkudelski T (2001). The mechanism of alloxan and streptozotocin action in β cells of the rat pancreas. *Physiol Res* **50:** 537-46.

Takagi-Matsumoto H, Ng B, Tsukimi Y & Tajimi M (2004). Effects of NSAIDs on bladder function in normal and cystitis rats: a comparison study of aspirin, indomethacin, and ketoprofen. *J Pharmacol Sci* **95:** 458-65.

Takahashi Y, Tokuoka S, Masuda T, Hirano Y, Nagao M, Tanaka H *et al.* (2002). Augmentation of allergic inflammation in prostanoid IP receptor deficient mice. *Br J Pharmacol* **137:** 315-22.

Takayama K, Garcia-Cardena G, Sukhova GK, Comander J, Gimbrone MA, Jr. & Libby P (2002). Prostaglandin E_2 suppresses chemokine production in human macrophages through the EP_4 receptor. *J Biol Chem* **277:** 44147-54.

Tang EH, Jensen BL, Skott O, Leung GP, Feletou M, Man RY *et al.* (2008). The role of prostaglandin E and thromboxane-prostanoid receptors in the response to prostaglandin E_2 in the aorta of Wistar Kyoto rats and spontaneously hypertensive rats. *Cardiovasc Res* **78:** 130-8.

Tani K, Naganawa A, Ishida A, Egashira H, Sagawa K, Harada H *et al.* (2001). Design and synthesis of a highly selective EP_2-receptor agonist. *Bioorg Med Chem Lett* **11:** 2025-8.

Taylor PD, McCarthy AL, Thomas CR & Poston L (1992). Endothelium-dependent relaxation and noradrenaline sensitivity in mesenteric resistance arteries of streptozotocin-induced diabetic rats. *Br J Pharmacol* **107:** 393-9.

Tesfamariam B, Brown ML, Deykin D & Cohen RA (1990). Elevated glucose promotes generation of endothelium-derived vasoconstrictor prostanoids in rabbit aorta. *J Clin Invest* **85:** 929-32.

Tesfamariam B, Jakubowski JA & Cohen RA (1989). Contraction of diabetic rabbit aorta caused by endothelium-derived PGH_2-TXA_2. *Am J Physiol* **257:** H1327-33.

Thomas DW, Mannon RB, Mannon PJ, Latour A, Oliver JA, Hoffman M *et al.* (1998). Coagulation defects and altered hemodynamic responses in mice lacking receptors for thromboxane A_2. *J Clin Invest* **102:** 1994-2001.

Toh H, Ichikawa A & Narumiya S (1995). Molecular evolution of receptors for eicosanoids. *FEBS Lett* **361:** 17-21.

Tokuyama Y, Sturis J, DePaoli AM, Takeda J, Stoffel M, Tang J *et al.* (1995). Evolution of β-cell dysfunction in the male Zucker diabetic fatty rat. *Diabetes* **44:** 1447-57.

Tsang SY, Yao X, Chan HY, Wong CM, Chen ZY, Au CL *et al.* (2003). Contribution of K^+ channels to relaxation induced by 17β-estradiol but not by progesterone in isolated rat mesenteric artery rings. *J Cardiovasc Pharmacol* **41:** 4-13.

Tsuboi K, Sugimoto Y & Ichikawa A (2002). Prostanoid receptor subtypes. *Prostaglandins Other Lipid Mediat* **68-69:** 535-56.

Tuder RM, Cool CD, Geraci MW, Wang J, Abman SH, Wright L *et al.* (1999). Prostacyclin synthase expression is decreased in lungs from patients with severe pulmonary hypertension. *Am J Respir Crit Care Med* **159:** 1925-32.

Tymkewycz PM, Jones RL, Wilson NH & Marr CG (1991). Heterogeneity of thromboxane A_2 (TP-) receptors: evidence from antagonist but not agonist potency measurements. *Br J Pharmacol* **102:** 607-14.

Undem BJ & Adams GK, 3rd (1988). An analysis of the functional interactions of selected contractile agonists in the guinea pig isolated trachea. *J Pharmacol Exp Ther* **246:** 47-53.

Ungrin MD, Carriere MC, Denis D, Lamontagne S, Sawyer N, Stocco R *et al.* (2001). Key structural features of prostaglandin E_2 and prostanoid analogs involved in binding and activation of the human EP_1 prostanoid receptor. *Mol Pharmacol* **59:** 1446-56.

Ushikubi F, Segi E, Sugimoto Y, Murata T, Matsuoka T, Kobayashi T *et al.* (1998). Impaired febrile response in mice lacking the prostaglandin E receptor subtype EP_3. *Nature* **395:** 281-4.

Vanhoutte PM, Feletou M & Taddei S (2005). Endothelium-dependent contractions in hypertension. *Br J Pharmacol* **144:** 449-58.

Verlohren S, Dubrovska G, Tsang SY, Essin K, Luft FC, Huang Y *et al.* (2004). Visceral periadventitial adipose tissue regulates arterial tone of mesenteric arteries. *Hypertension* **44:** 271-6.

Walch L, de Montpreville V, Brink C & Norel X (2001). Prostanoid EP_1- and TP-receptors involved in the contraction of human pulmonary veins. *Br J Pharmacol* **134:** 1671-8.

Walch L, Labat C, Gascard JP, de Montpreville V, Brink C & Norel X (1999). Prostanoid receptors involved in the relaxation of human pulmonary vessels. *Br J Pharmacol* **126:** 859-66.

Walsh MT & Kinsella BT (2000). Regulation of the human prostanoid TP_α and TP_β receptor isoforms mediated through activation of the EP_1 and IP receptors. *Br J Pharmacol* **131:** 601-9.

Watanabe K, Kawamori T, Nakatsugi S, Ohta T, Ohuchida S, Yamamoto H *et al.* (1999). Role of the prostaglandin E receptor subtype EP_1 in colon carcinogenesis. *Cancer Res* **59:** 5093-6.

Waterbury LD, Eglen RM, Faurot GF & Cooper GF (1990). EP_3, but not EP_2, FP, or TP prostanoid-receptor stimulation may reduce intraocular pressure. *Invest Ophthalmol Vis Sci* **31:** 2560-7.

Webb ML, Liu EC, Monshizadegan H, Hedberg A, Misra RN, Goldenberg H *et al.* (1993). Binding and function of a potent new thromboxane receptor antagonist, BMS-180291, in human platelets. *J Pharmacol Exp Ther* **264:** 1387-94.

Weksler BB, Ley CW & Jaffe EA (1978). Stimulation of endothelial cell prostacyclin production by thrombin, trypsin, and the ionophore A-23187. *J Clin Invest* **62:** 923-30.

Wheeldon A & Vardey CJ (1993) Characterization of the inhibitory prostanoid receptors on human neutrophils. *Br J Pharmacol* **108:** 1051-4.

Wheeler MA, Yoon JH, Olsson LE & Weiss RM (2001). Cyclo-oxygenase-2 protein and prostaglandin E_2 production are up-regulated in a rat bladder inflammation model. *Eur J Pharmacol* **417:** 239-48.

White RE & Carrier GO (1988). Enhanced vascular alpha-adrenergic neuroeffector system in diabetes: importance of calcium. *Am J Physiol* **255:** H1036-42.

Whittle BJ, Moncada S & Vane JR (1978). Comparison of the effects of prostacyclin (PGI_2), prostaglandin E_1 and D_2 on platelet aggregation in different species. *Prostaglandins* **16:** 373-88.

Wigg SJ, Tare M, Forbes J, Cooper ME, Thomas MC, Coleman HA *et al.* (2004). Early vitamin E supplementation attenuates diabetes-associated vascular dysfunction and the rise in

protein kinase C-β in mesenteric artery and ameliorates wall stiffness in femoral artery of Wistar rats. *Diabetologia* **47:** 1038-46.

Wilson RJ, Rhodes SA, Wood RL, Shield VJ, Noel LS, Gray DW *et al.* (2004). Functional pharmacology of human prostanoid EP_2 and EP_4 receptors. *Eur J Pharmacol* **501:** 49-58.

Wise H & Jones RL, III (2000). *Prostacyclin and its receptors*. New York ; London: Kluwer Academic / Plenum Publishers.

Woodward DF, Bogardus AM, Donello JE, Fairbairn CE, Gil DW, Kedzie KM *et al.* (1995). Molecular characterization and ocular hypotensive properties of the prostanoid EP_2 receptor. *J Ocul Pharmacol Ther* **11:** 447-54.

Woodward DF, Krauss AH, Wang JW, Protzman CE, Nieves AL, Liang Y *et al.* (2007). Identification of an antagonist that selectively blocks the activity of prostamides (prostaglandin-ethanolamides) in the feline iris. *Br J Pharmacol* **150:** 342-52.

Woodward DF, Lawrence RA, Fairbairn CE, Shan T & Williams LS (1993). Intraocular pressure effects of selective prostanoid receptor agonists involve different receptor subtypes according to radioligand binding studies. *J Lipid Mediat* **6:** 545-53.

Worth NF, Berry CL, Thomas AC & Campbell JH (2005). S-18886, a selective TP receptor antagonist, inhibits development of atherosclerosis in rabbits. *Atherosclerosis* **183:** 65-73.

Wright DH, Abran D, Bhattacharya M, Hou X, Bernier SG, Bouayad A *et al.* (2001). Prostanoid receptors: ontogeny and implications in vascular physiology. *Am J Physiol Regul Integr Comp Physiol* **281:** R1343-60.

Xiao CY, Hara A, Yuhki K, Fujino T, Ma H, Okada Y *et al.* (2001). Roles of prostaglandin I_2 and thromboxane A_2 in cardiac ischemia-reperfusion injury: a study using mice lacking their respective receptors. *Circulation* **104:** 2210-5.

Xiao CY, Yuhki K, Hara A, Fujino T, Kuriyama S, Yamada T *et al.* (2004). Prostaglandin E_2 protects the heart from ischemia-reperfusion injury via its receptor subtype EP_4. *Circulation* **109:** 2462-8.

Zhang R, Ogletree ML & Moreland S (1996). Characterization of thromboxane A_2 / prostaglandin endoperoxide receptors in aorta. *Eur J Pharmacol* **317:** 91-6.

APPENDIX

Table of F-statistics *P = 0.05*

df2\df1	1	2	3	4	5	6	7	8	9	10	11	12	13	14	15	16	17	18	19	20	22	24	26	28	30	35
3	10.13	9.55	9.28	9.12	9.01	8.94	8.89	8.85	8.81	8.79	8.76	8.74	8.73	8.71	8.70	8.69	8.68	8.67	8.67	8.66	8.65	8.64	8.63	8.62	8.62	8.60
4	7.71	6.94	6.59	6.39	6.26	6.16	6.09	6.04	6.00	5.96	5.94	5.91	5.89	5.87	5.86	5.84	5.83	5.82	5.81	5.80	5.79	5.77	5.76	5.75	5.75	5.73
5	6.61	5.79	5.41	5.19	5.05	4.95	4.88	4.82	4.77	4.74	4.70	4.68	4.66	4.64	4.62	4.60	4.59	4.58	4.57	4.56	4.54	4.53	4.52	4.50	4.50	4.48
6	5.99	5.14	4.76	4.53	4.39	4.28	4.21	4.15	4.10	4.06	4.03	4.00	3.98	3.96	3.94	3.92	3.91	3.90	3.88	3.87	3.86	3.84	3.83	3.82	3.81	3.79
7	5.59	4.74	4.35	4.12	3.97	3.87	3.79	3.73	3.68	3.64	3.60	3.57	3.55	3.53	3.51	3.49	3.48	3.47	3.46	3.44	3.43	3.41	3.40	3.39	3.38	3.36
8	5.32	4.46	4.07	3.84	3.69	3.58	3.50	3.44	3.39	3.35	3.31	3.28	3.26	3.24	3.22	3.20	3.19	3.17	3.16	3.15	3.13	3.12	3.10	3.09	3.08	3.06
9	5.12	4.26	3.86	3.63	3.48	3.37	3.29	3.23	3.18	3.14	3.10	3.07	3.05	3.03	3.01	2.99	2.97	2.96	2.95	2.94	2.92	2.90	2.89	2.87	2.86	2.84
10	4.96	4.10	3.71	3.48	3.33	3.22	3.14	3.07	3.02	2.98	2.94	2.91	2.89	2.86	2.85	2.83	2.81	2.80	2.79	2.77	2.75	2.74	2.72	2.71	2.70	2.68
11	4.84	3.98	3.59	3.36	3.20	3.09	3.01	2.95	2.90	2.85	2.82	2.79	2.76	2.74	2.72	2.70	2.69	2.67	2.66	2.65	2.63	2.61	2.59	2.58	2.57	2.55
12	4.75	3.89	3.49	3.26	3.11	3.00	2.91	2.85	2.80	2.75	2.72	2.69	2.66	2.64	2.62	2.60	2.58	2.57	2.56	2.54	2.52	2.51	2.49	2.48	2.47	2.44
13	4.67	3.81	3.41	3.18	3.03	2.92	2.83	2.77	2.71	2.67	2.63	2.60	2.58	2.55	2.53	2.51	2.50	2.48	2.47	2.46	2.44	2.42	2.41	2.39	2.38	2.36
14	4.60	3.74	3.34	3.11	2.96	2.85	2.76	2.70	2.65	2.60	2.57	2.53	2.51	2.48	2.46	2.44	2.43	2.41	2.40	2.39	2.37	2.35	2.33	2.32	2.31	2.28
15	4.54	3.68	3.29	3.06	2.90	2.79	2.71	2.64	2.59	2.54	2.51	2.48	2.45	2.42	2.40	2.38	2.37	2.35	2.34	2.33	2.31	2.29	2.27	2.26	2.25	2.22
16	4.49	3.63	3.24	3.01	2.85	2.74	2.66	2.59	2.54	2.49	2.46	2.42	2.40	2.37	2.35	2.33	2.32	2.30	2.29	2.28	2.25	2.24	2.22	2.21	2.19	2.17
17	4.45	3.59	3.20	2.96	2.81	2.70	2.61	2.55	2.49	2.45	2.41	2.38	2.35	2.33	2.31	2.29	2.27	2.26	2.24	2.23	2.21	2.19	2.17	2.16	2.15	2.12
18	4.41	3.55	3.16	2.93	2.77	2.66	2.58	2.51	2.46	2.41	2.37	2.34	2.31	2.29	2.27	2.25	2.23	2.22	2.20	2.19	2.17	2.15	2.13	2.12	2.11	2.08
19	4.38	3.52	3.13	2.90	2.74	2.63	2.54	2.48	2.42	2.38	2.34	2.31	2.28	2.26	2.23	2.21	2.20	2.18	2.17	2.16	2.13	2.11	2.10	2.08	2.07	2.05
20	4.35	3.49	3.10	2.87	2.71	2.60	2.51	2.45	2.39	2.35	2.31	2.28	2.25	2.23	2.20	2.18	2.17	2.15	2.14	2.12	2.10	2.08	2.07	2.05	2.04	2.01
22	4.30	3.44	3.05	2.82	2.66	2.55	2.46	2.40	2.34	2.30	2.26	2.23	2.20	2.17	2.15	2.13	2.11	2.10	2.08	2.07	2.05	2.03	2.01	2.00	1.98	1.96
24	4.26	3.40	3.01	2.78	2.62	2.51	2.42	2.36	2.30	2.25	2.22	2.18	2.15	2.13	2.11	2.09	2.07	2.05	2.04	2.03	2.00	1.98	1.97	1.95	1.94	1.91
26	4.23	3.37	2.98	2.74	2.59	2.47	2.39	2.32	2.27	2.22	2.18	2.15	2.12	2.09	2.07	2.05	2.03	2.02	2.00	1.99	1.97	1.95	1.93	1.91	1.90	1.87
28	4.20	3.34	2.95	2.71	2.56	2.45	2.36	2.29	2.24	2.19	2.15	2.12	2.09	2.06	2.04	2.02	2.00	1.99	1.97	1.96	1.93	1.91	1.90	1.88	1.87	1.84
30	4.17	3.32	2.92	2.69	2.53	2.42	2.33	2.27	2.21	2.16	2.13	2.09	2.06	2.04	2.01	1.99	1.98	1.96	1.95	1.93	1.91	1.89	1.87	1.85	1.84	1.81
35	4.12	3.27	2.87	2.64	2.49	2.37	2.29	2.22	2.16	2.11	2.08	2.04	2.01	1.99	1.96	1.94	1.92	1.91	1.89	1.88	1.85	1.83	1.82	1.80	1.79	1.76
40	4.08	3.23	2.84	2.61	2.45	2.34	2.25	2.18	2.12	2.08	2.04	2.00	1.97	1.95	1.92	1.90	1.89	1.87	1.85	1.84	1.81	1.79	1.77	1.76	1.74	1.72
45	4.06	3.20	2.81	2.58	2.42	2.31	2.22	2.15	2.10	2.05	2.01	1.97	1.94	1.92	1.89	1.87	1.86	1.84	1.82	1.81	1.78	1.76	1.74	1.73	1.71	1.68
50	4.03	3.18	2.79	2.56	2.40	2.29	2.20	2.13	2.07	2.03	1.99	1.95	1.92	1.89	1.87	1.85	1.83	1.81	1.80	1.78	1.76	1.74	1.72	1.70	1.69	1.66
60	4.00	3.15	2.76	2.53	2.37	2.25	2.17	2.10	2.04	1.99	1.95	1.92	1.89	1.86	1.84	1.82	1.80	1.78	1.76	1.75	1.72	1.70	1.68	1.66	1.65	1.62
70	3.98	3.13	2.74	2.50	2.35	2.23	2.14	2.07	2.02	1.97	1.93	1.89	1.86	1.84	1.81	1.79	1.77	1.75	1.74	1.72	1.70	1.67	1.65	1.64	1.62	1.59
80	3.96	3.11	2.72	2.49	2.33	2.21	2.13	2.06	2.00	1.95	1.91	1.88	1.84	1.82	1.79	1.77	1.75	1.73	1.72	1.70	1.68	1.65	1.63	1.62	1.60	1.57
100	3.94	3.09	2.70	2.46	2.31	2.19	2.10	2.03	1.97	1.93	1.89	1.85	1.82	1.79	1.77	1.75	1.73	1.71	1.69	1.68	1.65	1.63	1.61	1.59	1.57	1.54
200	3.89	3.04	2.65	2.42	2.26	2.14	2.06	1.98	1.93	1.88	1.84	1.80	1.77	1.74	1.72	1.69	1.67	1.66	1.64	1.62	1.60	1.57	1.55	1.53	1.52	1.48
500	3.86	3.01	2.62	2.39	2.23	2.12	2.03	1.96	1.90	1.85	1.81	1.77	1.74	1.71	1.69	1.66	1.64	1.62	1.61	1.59	1.56	1.54	1.52	1.50	1.48	1.45
1000	3.85	3.00	2.61	2.38	2.22	2.11	2.02	1.95	1.89	1.84	1.80	1.76	1.73	1.70	1.68	1.65	1.63	1.61	1.60	1.58	1.55	1.53	1.51	1.49	1.47	1.43
>1000	1.04	3.00	2.61	2.37	2.21	2.10	2.01	1.94	1.88	1.83	1.79	1.75	1.72	1.69	1.67	1.64	1.62	1.61	1.59	1.57	1.54	1.52	1.50	1.48	1.46	1.42
df2/df1	1	2	3	4	5	6	7	8	9	10	11	12	13	14	15	16	17	18	19	20	22	24	26	28	30	35

Table of F-statistics *P = 0.01*

df2\df1	1	2	3	4	5	6	7	8	9	10	11	12	13	14	15	16	17	18	19	20	22	24	26	28	30	35
3	34.12	30.82	29.46	28.71	28.24	27.91	27.67	27.49	27.35	27.23	27.13	27.05	26.98	26.92	26.87	26.83	26.79	26.75	26.72	26.69	26.64	26.60	26.56	26.53	26.50	26.45
4	21.20	18.00	16.69	15.98	15.52	15.21	14.98	14.80	14.66	14.55	14.45	14.37	14.31	14.25	14.20	14.15	14.11	14.08	14.05	14.02	13.97	13.93	13.89	13.86	13.84	13.79
5	16.26	13.27	12.06	11.39	10.97	10.67	10.46	10.29	10.16	10.05	9.96	9.89	9.82	9.77	9.72	9.68	9.64	9.61	9.58	9.55	9.51	9.47	9.43	9.40	9.38	9.33
6	13.75	10.92	9.78	9.15	8.75	8.47	8.26	8.10	7.98	7.87	7.79	7.72	7.66	7.61	7.56	7.52	7.48	7.45	7.42	7.40	7.35	7.31	7.28	7.25	7.23	7.18
7	12.25	9.55	8.45	7.85	7.46	7.19	6.99	6.84	6.72	6.62	6.54	6.47	6.41	6.36	6.31	6.28	6.24	6.21	6.18	6.16	6.11	6.07	6.04	6.02	5.99	5.94
8	11.26	8.65	7.59	7.01	6.63	6.37	6.18	6.03	5.91	5.81	5.73	5.67	5.61	5.56	5.52	5.48	5.44	5.41	5.38	5.36	5.32	5.28	5.25	5.22	5.20	5.15
9	10.56	8.02	6.99	6.42	6.06	5.80	5.61	5.47	5.35	5.26	5.18	5.11	5.05	5.01	4.96	4.92	4.89	4.86	4.83	4.81	4.77	4.73	4.70	4.67	4.65	4.60
10	10.04	7.56	6.55	5.99	5.64	5.39	5.20	5.06	4.94	4.85	4.77	4.71	4.65	4.60	4.56	4.52	4.49	4.46	4.43	4.41	4.36	4.33	4.30	4.27	4.25	4.20
11	9.65	7.21	6.22	5.67	5.32	5.07	4.89	4.74	4.63	4.54	4.46	4.40	4.34	4.29	4.25	4.21	4.18	4.15	4.12	4.10	4.06	4.02	3.99	3.96	3.94	3.89
12	9.33	6.93	5.95	5.41	5.06	4.82	4.64	4.50	4.39	4.30	4.22	4.16	4.10	4.05	4.01	3.97	3.94	3.91	3.88	3.86	3.82	3.78	3.75	3.72	3.70	3.65
13	9.07	6.70	5.74	5.21	4.86	4.62	4.44	4.30	4.19	4.10	4.02	3.96	3.91	3.86	3.82	3.78	3.75	3.72	3.69	3.66	3.62	3.59	3.56	3.53	3.51	3.46
14	8.86	6.51	5.56	5.04	4.70	4.46	4.28	4.14	4.03	3.94	3.86	3.80	3.75	3.70	3.66	3.62	3.59	3.56	3.53	3.51	3.46	3.43	3.40	3.37	3.35	3.30
15	8.68	6.36	5.42	4.89	4.56	4.32	4.14	4.00	3.89	3.80	3.73	3.67	3.61	3.56	3.52	3.49	3.45	3.42	3.40	3.37	3.33	3.29	3.26	3.24	3.21	3.17
16	8.53	6.23	5.29	4.77	4.44	4.20	4.03	3.89	3.78	3.69	3.62	3.55	3.50	3.45	3.41	3.37	3.34	3.31	3.28	3.26	3.22	3.18	3.15	3.12	3.10	3.05
17	8.40	6.11	5.19	4.67	4.34	4.10	3.93	3.79	3.68	3.59	3.52	3.46	3.40	3.35	3.31	3.27	3.24	3.21	3.19	3.16	3.12	3.08	3.05	3.03	3.00	2.96
18	8.29	6.01	5.09	4.58	4.25	4.01	3.84	3.71	3.60	3.51	3.43	3.37	3.32	3.27	3.23	3.19	3.16	3.13	3.10	3.08	3.03	3.00	2.97	2.94	2.92	2.87
19	8.19	5.93	5.01	4.50	4.17	3.94	3.77	3.63	3.52	3.43	3.36	3.30	3.24	3.19	3.15	3.12	3.08	3.05	3.03	3.00	2.96	2.92	2.89	2.87	2.84	2.80
20	8.10	5.85	4.94	4.43	4.10	3.87	3.70	3.56	3.46	3.37	3.29	3.23	3.18	3.13	3.09	3.05	3.02	2.99	2.96	2.94	2.90	2.86	2.83	2.80	2.78	2.73
22	7.95	5.72	4.82	4.31	3.99	3.76	3.59	3.45	3.35	3.26	3.18	3.12	3.07	3.02	2.98	2.94	2.91	2.88	2.85	2.83	2.78	2.75	2.72	2.69	2.67	2.62
24	7.82	5.61	4.72	4.22	3.90	3.67	3.50	3.36	3.26	3.17	3.09	3.03	2.98	2.93	2.89	2.85	2.82	2.79	2.76	2.74	2.70	2.66	2.63	2.60	2.58	2.53
26	7.72	5.53	4.64	4.14	3.82	3.59	3.42	3.29	3.18	3.09	3.02	2.96	2.90	2.86	2.82	2.78	2.75	2.72	2.69	2.66	2.62	2.58	2.55	2.53	2.50	2.45
28	7.64	5.45	4.57	4.07	3.75	3.53	3.36	3.23	3.12	3.03	2.96	2.90	2.84	2.79	2.75	2.72	2.68	2.65	2.63	2.60	2.56	2.52	2.49	2.46	2.44	2.39
30	7.56	5.39	4.51	4.02	3.70	3.47	3.30	3.17	3.07	2.98	2.91	2.84	2.79	2.74	2.70	2.66	2.63	2.60	2.57	2.55	2.51	2.47	2.44	2.41	2.39	2.34
35	7.42	5.27	4.40	3.91	3.59	3.37	3.20	3.07	2.96	2.88	2.80	2.74	2.69	2.64	2.60	2.56	2.53	2.50	2.47	2.44	2.40	2.36	2.33	2.31	2.28	2.23
40	7.31	5.18	4.31	3.83	3.51	3.29	3.12	2.99	2.89	2.80	2.73	2.66	2.61	2.56	2.52	2.48	2.45	2.42	2.39	2.37	2.33	2.29	2.26	2.23	2.20	2.15
45	7.23	5.11	4.25	3.77	3.45	3.23	3.07	2.94	2.83	2.74	2.67	2.61	2.55	2.51	2.46	2.43	2.39	2.36	2.34	2.31	2.27	2.23	2.20	2.17	2.14	2.09
50	7.17	5.06	4.20	3.72	3.41	3.19	3.02	2.89	2.79	2.70	2.63	2.56	2.51	2.46	2.42	2.38	2.35	2.32	2.29	2.27	2.22	2.18	2.15	2.12	2.10	2.05
60	7.08	4.98	4.13	3.65	3.34	3.12	2.95	2.82	2.72	2.63	2.56	2.50	2.44	2.39	2.35	2.31	2.28	2.25	2.22	2.20	2.15	2.12	2.08	2.05	2.03	1.98
70	7.01	4.92	4.07	3.60	3.29	3.07	2.91	2.78	2.67	2.59	2.51	2.45	2.40	2.35	2.31	2.27	2.23	2.20	2.18	2.15	2.11	2.07	2.03	2.01	1.98	1.93
80	6.96	4.88	4.04	3.56	3.26	3.04	2.87	2.74	2.64	2.55	2.48	2.42	2.36	2.31	2.27	2.23	2.20	2.17	2.14	2.12	2.07	2.03	2.00	1.97	1.94	1.89
100	6.90	4.82	3.98	3.51	3.21	2.99	2.82	2.69	2.59	2.50	2.43	2.37	2.31	2.27	2.22	2.19	2.15	2.12	2.09	2.07	2.02	1.98	1.95	1.92	1.89	1.84
200	6.76	4.71	3.88	3.41	3.11	2.89	2.73	2.60	2.50	2.41	2.34	2.27	2.22	2.17	2.13	2.09	2.06	2.03	2.00	1.97	1.93	1.89	1.85	1.82	1.79	1.74
500	6.69	4.65	3.82	3.36	3.05	2.84	2.68	2.55	2.44	2.36	2.28	2.22	2.17	2.12	2.07	2.04	2.00	1.97	1.94	1.92	1.87	1.83	1.79	1.76	1.74	1.68
1000	6.66	4.63	3.80	3.34	3.04	2.82	2.66	2.53	2.43	2.34	2.27	2.20	2.15	2.10	2.06	2.02	1.98	1.95	1.92	1.90	1.85	1.81	1.77	1.74	1.72	1.66
>1000	1.04	4.61	3.78	3.32	3.02	2.80	2.64	2.51	2.41	2.32	2.25	2.19	2.13	2.08	2.04	2.00	1.97	1.94	1.91	1.88	1.83	1.79	1.76	1.73	1.70	1.64
df2/df1	1	2	3	4	5	6	7	8	9	10	11	12	13	14	15	16	17	18	19	20	22	24	26	28	30	35

Table of F-statistics *P = 0.001*

df2\df1	1	2	3	4	5	6	7	8	9	10	11	12	13	14	15	16	17	18	19	20	22	24	26	28	30	35
3	167.03	148.50	141.11	137.10	134.58	132.85	131.59	130.62	129.86	129.25	128.74	128.32	127.96	127.65	127.38	127.14	126.93	126.74	126.57	126.42	126.16	125.94	125.75	125.59	125.45	125.17
4	74.14	61.25	56.18	53.44	51.71	50.53	49.66	49.00	48.48	48.05	47.71	47.41	47.16	46.95	46.76	46.60	46.45	46.32	46.21	46.10	45.92	45.77	45.64	45.53	45.43	45.24
5	47.18	37.12	33.20	31.09	29.75	28.84	28.16	27.65	27.25	26.92	26.65	26.42	26.22	26.06	25.91	25.78	25.67	25.57	25.48	25.40	25.25	25.13	25.03	24.95	24.87	24.72
6	35.51	27.00	23.70	21.92	20.80	20.03	19.46	19.03	18.69	18.41	18.18	17.99	17.83	17.68	17.56	17.45	17.35	17.27	17.19	17.12	17.00	16.90	16.81	16.74	16.67	16.54
7	29.25	21.69	18.77	17.20	16.21	15.52	15.02	14.63	14.33	14.08	13.88	13.71	13.56	13.43	13.32	13.23	13.14	13.06	12.99	12.93	12.82	12.73	12.66	12.59	12.53	12.41
8	25.42	18.49	15.83	14.39	13.49	12.86	12.40	12.05	11.77	11.54	11.35	11.20	11.06	10.94	10.84	10.75	10.67	10.60	10.54	10.48	10.38	10.30	10.22	10.16	10.11	10.00
9	22.86	16.39	13.90	12.56	11.71	11.13	10.70	10.37	10.11	9.89	9.72	9.57	9.44	9.33	9.24	9.15	9.08	9.01	8.95	8.90	8.80	8.72	8.66	8.60	8.55	8.45
10	21.04	14.91	12.55	11.28	10.48	9.93	9.52	9.20	8.96	8.75	8.59	8.45	8.33	8.22	8.13	8.05	7.98	7.91	7.86	7.80	7.71	7.64	7.57	7.52	7.47	7.37
11	19.69	13.81	11.56	10.35	9.58	9.05	8.66	8.36	8.12	7.92	7.76	7.63	7.51	7.41	7.32	7.24	7.18	7.11	7.06	7.01	6.92	6.85	6.79	6.73	6.68	6.59
12	18.64	12.97	10.80	9.63	8.89	8.38	8.00	7.71	7.48	7.29	7.14	7.01	6.89	6.79	6.71	6.63	6.57	6.51	6.45	6.41	6.32	6.25	6.19	6.14	6.09	6.00
13	17.82	12.31	10.21	9.07	8.35	7.86	7.49	7.21	6.98	6.80	6.65	6.52	6.41	6.31	6.23	6.16	6.09	6.03	5.98	5.93	5.85	5.78	5.72	5.67	5.63	5.54
14	17.14	11.78	9.73	8.62	7.92	7.44	7.08	6.80	6.58	6.40	6.26	6.13	6.02	5.93	5.85	5.78	5.71	5.66	5.60	5.56	5.48	5.41	5.35	5.30	5.25	5.17
15	16.59	11.34	9.34	8.25	7.57	7.09	6.74	6.47	6.26	6.08	5.94	5.81	5.71	5.62	5.54	5.46	5.40	5.35	5.29	5.25	5.17	5.10	5.04	4.99	4.95	4.86
16	16.12	10.97	9.01	7.94	7.27	6.81	6.46	6.20	5.98	5.81	5.67	5.55	5.44	5.35	5.27	5.21	5.14	5.09	5.04	4.99	4.91	4.85	4.79	4.74	4.70	4.61
17	15.72	10.66	8.73	7.68	7.02	6.56	6.22	5.96	5.75	5.58	5.44	5.32	5.22	5.13	5.05	4.99	4.92	4.87	4.82	4.78	4.70	4.63	4.58	4.53	4.48	4.40
18	15.38	10.39	8.49	7.46	6.81	6.36	6.02	5.76	5.56	5.39	5.25	5.13	5.03	4.94	4.87	4.80	4.74	4.68	4.63	4.59	4.51	4.45	4.39	4.34	4.30	4.22
19	15.08	10.16	8.28	7.27	6.62	6.18	5.85	5.59	5.39	5.22	5.08	4.97	4.87	4.78	4.70	4.64	4.58	4.52	4.47	4.43	4.35	4.29	4.23	4.19	4.14	4.06
20	14.82	9.95	8.10	7.10	6.46	6.02	5.69	5.44	5.24	5.08	4.94	4.82	4.72	4.64	4.56	4.50	4.44	4.38	4.33	4.29	4.21	4.15	4.09	4.05	4.01	3.92
22	14.38	9.61	7.80	6.81	6.19	5.76	5.44	5.19	4.99	4.83	4.70	4.58	4.49	4.40	4.33	4.26	4.20	4.15	4.10	4.06	3.98	3.92	3.86	3.82	3.78	3.69
24	14.03	9.34	7.55	6.59	5.98	5.55	5.24	4.99	4.80	4.64	4.51	4.39	4.30	4.21	4.14	4.07	4.02	3.96	3.92	3.87	3.80	3.74	3.68	3.63	3.59	3.51
26	13.74	9.12	7.36	6.41	5.80	5.38	5.07	4.83	4.64	4.48	4.35	4.24	4.14	4.06	3.99	3.92	3.86	3.81	3.77	3.72	3.65	3.59	3.53	3.49	3.45	3.36
28	13.50	8.93	7.19	6.25	5.66	5.24	4.93	4.70	4.51	4.35	4.22	4.11	4.01	3.93	3.86	3.80	3.74	3.69	3.64	3.60	3.52	3.46	3.41	3.36	3.32	3.24
30	13.29	8.77	7.05	6.13	5.53	5.12	4.82	4.58	4.39	4.24	4.11	4.00	3.91	3.83	3.75	3.69	3.63	3.58	3.54	3.49	3.42	3.36	3.30	3.26	3.22	3.14
35	12.90	8.47	6.79	5.88	5.30	4.89	4.60	4.36	4.18	4.03	3.90	3.79	3.70	3.62	3.55	3.48	3.43	3.38	3.33	3.29	3.22	3.16	3.10	3.06	3.02	2.93
40	12.61	8.25	6.60	5.70	5.13	4.73	4.44	4.21	4.02	3.87	3.75	3.64	3.55	3.47	3.40	3.34	3.28	3.23	3.19	3.15	3.07	3.01	2.96	2.91	2.87	2.79
45	12.39	8.09	6.45	5.56	5.00	4.61	4.32	4.09	3.91	3.76	3.64	3.53	3.44	3.36	3.29	3.23	3.17	3.12	3.08	3.04	2.96	2.90	2.85	2.80	2.76	2.68
50	12.22	7.96	6.34	5.46	4.90	4.51	4.22	4.00	3.82	3.67	3.55	3.44	3.35	3.27	3.20	3.14	3.09	3.04	2.99	2.95	2.88	2.82	2.77	2.72	2.68	2.60
60	11.97	7.77	6.17	5.31	4.76	4.37	4.09	3.87	3.69	3.54	3.42	3.32	3.23	3.15	3.08	3.02	2.96	2.91	2.87	2.83	2.76	2.69	2.64	2.60	2.56	2.47
70	11.80	7.64	6.06	5.20	4.66	4.28	3.99	3.77	3.60	3.45	3.33	3.23	3.14	3.06	2.99	2.93	2.88	2.83	2.78	2.74	2.67	2.61	2.56	2.51	2.47	2.39
80	11.67	7.54	5.97	5.12	4.58	4.20	3.92	3.71	3.53	3.39	3.27	3.16	3.07	3.00	2.93	2.87	2.81	2.76	2.72	2.68	2.61	2.55	2.49	2.45	2.41	2.32
100	11.50	7.41	5.86	5.02	4.48	4.11	3.83	3.61	3.44	3.30	3.18	3.07	2.99	2.91	2.84	2.78	2.73	2.68	2.63	2.59	2.52	2.46	2.41	2.36	2.32	2.24
200	11.16	7.15	5.63	4.81	4.29	3.92	3.65	3.43	3.26	3.12	3.01	2.90	2.82	2.74	2.67	2.61	2.56	2.51	2.47	2.42	2.35	2.29	2.24	2.19	2.15	2.07
500	10.96	7.00	5.51	4.69	4.18	3.81	3.54	3.33	3.16	3.02	2.91	2.81	2.72	2.64	2.58	2.52	2.46	2.41	2.37	2.33	2.26	2.20	2.14	2.10	2.05	1.97
1000	10.89	6.96	5.46	4.66	4.14	3.78	3.51	3.30	3.13	2.99	2.87	2.77	2.69	2.61	2.54	2.48	2.43	2.38	2.34	2.30	2.23	2.16	2.11	2.06	2.02	1.94
>1000	1.04	6.92	5.43	4.62	4.11	3.75	3.48	3.27	3.10	2.96	2.85	2.75	2.66	2.58	2.52	2.46	2.40	2.35	2.31	2.27	2.20	2.14	2.08	2.04	1.99	1.91
df2/df1	1	2	3	4	5	6	7	8	9	10	11	12	13	14	15	16	17	18	19	20	22	24	26	28	30	35